



The
University
Of
Sheffield.

*Exploiting the Role of Coke in
Catalytic Transformations*

Ali Raad Al-Shathr

A thesis submitted in partial fulfilment of the requirements for the
degree of Doctor of Philosophy

The University of Sheffield
Faculty of Engineering
Chemical and Biological Engineering Department

April 2019

Declaration

The work summarised in this thesis was carried out in the Department of Chemical and Biological Engineering, University of Sheffield, over the period from October 2014 to December 2018. I would like to declare that this thesis is the result of my own research except where specifically stated in the text.

No part of the thesis has been submitted in support of an application for another degree or qualification at Sheffield or any other university or other institute of learning. This Thesis contains less than 65,000 words and has less than 150 figures.

Ali Raad Al-Shathr

Dedication

I would like to dedicate this work to my lovely, wonderful, sophisticated and fabulous wife, Safa Aal-Kaeb, for providing me with infinite support and encouragement throughout my life and especially during the critical moments. I will be indebted evermore for you and I cannot imagine my life without you by my side.

Also, I would like to dedicate the present work with huge thanks for my two elegant, gorgeous and brilliant children, Taim and Yazan, who are my source of optimism in this life.

I would like to express my very warmest appreciation, admiration and thanks to my amazing and superb parents and my stunning sister for everything they have done for me. I could not have made it here without you and your continued support; you have been sympathetic and supportive and the greatest family I could have wished for.

Loyalty; I would like to dedicate this thesis to the soul of my paternal grandmother '*Mandoba Al-Qaisy*' (May God have mercy upon your soul).

I promise, I will never ever forget you.

Acknowledgments

First and foremost, I would like to express my deepest gratitude to my supervisor, Dr. James McGregor, for his continued guidance, encouragement, effort and assistance during my PhD studies. This thesis would not have been possible without his distinguished advice, constructive critiques, insightful questions, and his remarkable patience.

I would like to thank Dr. Bashir Al-Zaidi (Chemical Engineering Department / University of Technology) for providing me with direction, support, fruitful information and motivation and helping me to manage my time.

Also, I am grateful to Dr. Zaidoon Shakoor (Chemical Engineering Department / University of Technology) for all his help, direction and assistance with the kinetic study.

My sincere thanks go to Prof Siddharth Patwardhan, Dr. Denis Cumming, Dr. Alan Dunbar (Chemical and Biological Engineering Department / University of Sheffield) and Dr Nik Reeves-McLaren (Department of Materials Science and Engineering / University of Sheffield) for providing me with access to their labs.

I wish also to acknowledge Dr. Amal Shehab, Dr. Laura Gómez, Dr. Richard Archer and Mr Joseph Manning (Chemical and Biological Engineering / University of Sheffield), Dr. Muhannad Al-Saedy and Dr. Ahmed Hsskia (Department of Chemistry / University of Sheffield) and Dr. Mohammed Shaybani (Department of Materials Science and Engineering / University of Sheffield) for their contributions to this research work.

Many thanks to all technical staff of the Chemical and Biological Engineering department at the University of Sheffield; Duncan Schofield, James Grinham, Mark Jones, Keith Penny, Adrian Lumby, Andy Patrick, Usman Younis, Glynn Reynolds, Mark McIntosh, Oz McFarlane and David Wengraf.

I would like also to thank my colleagues in the Catalysis group for their help. Special thanks are owed to Ali Hameed, Duaa Al-aaraj, Righdan Mohsen, Cynthia Kartey, Ibrahim Yakub and Nur Atiqah Nasir for their assistance. I would like to thank Joshua Green and Catherine Collett for proofreading this work.

My sincere thanks go to my sponsor, The Ministry of Higher Education and Scientific Research in the Republic of Iraq, for their full financial support and unlimited technical support throughout my studies. I would like also to give my biggest thanks to the Chemical Engineering Department at the University of Technology for the unlimited support that I have received from them during my PhD studies. I would also like to thank the Iraqi Cultural Attaché for their support during my studies.

Abstract

Global population growth over recent decades has played a crucial role in the increase in demand for hydrocarbon derivatives. The alkylation of aromatics with olefins over zeolite catalysts is applied extensively in the chemical industry, particularly in the production of detergents. However, during this catalytic transformation, carbonaceous residues are formed and accumulate in and/or on the zeolite pores. This complex carbonaceous product is called 'coke' and is the primary reason for catalyst deactivation. Several economic problems occur as a result of coke formation because it is costly to replace or regenerate the zeolite catalyst due to the need to shut down the process which results in the loss of time and money. In addition to the predominate role of coke as a deactivating agent, number of recent studies have focused on the positive role of coke in enhancing catalytic performance in reactions such as alkylation and isomerisation. The overall aim of this thesis is to understand the role of coke that is formed during the catalytic alkylation of toluene with 1-heptene through studying the influence of controlled pre-coking modifications on 2-heptyltoluene selectivity and investigating the kinetics of toluene alkylation with 1-heptene over HY5.1 ($\text{SiO}_2/\text{Al}_2\text{O}_3$ mole ratio: 5.1:1).

Several approaches have been investigated with the aim of limiting coke formation through the modification of a range of zeolites. These include the formation mesopores; reduction in acidity; covering the external acid sites with bulky molecules; and controlled pre-coking of active sites. Desilication causes the formation of mesopores in the catalyst structure; these are larger than micropores, and hence are able to collect more coke. This contributed to enhancing the selectivity to 2-heptyltoluene from ~33 % to ~39 %. The reaction over dealuminated HY30 ($\text{SiO}_2/\text{Al}_2\text{O}_3$ mole ratio is 30:1) illustrated an improvement in 2-heptyltoluene selectivity from ~31 % to ~36 % with slightly decreased carbon deposits. Toluene alkylation over silylated HY5.1 and HY30 showed a significant enhancement in 2-heptyltoluene selectivity from ~27 % to ~34 % for HY5.1 and from ~31 % to ~35 % for HY30 concomitant with a reasonable reduction in the percentage of coke.

Toluene and 1-heptene are employed as model coke pre-cursors for toluene alkylation with 1-heptene. The results obtained from thermal characterisation techniques showed that the structure of carbonaceous deposits that are formed from toluene pre-coking are graphitic-like. Toluene pre-coked HY zeolite showed enhanced selectivity to 2-heptyltoluene (from ~26 % to ~33 % and from ~33 % to ~39 % for HY5.1 and HY30 respectively) with a significant decrease in the amount of coke formed.

A kinetic study investigated 1-heptene isomerisation and toluene alkylation over fresh HY5.1 zeolite. This revealed that the activation energies of the alkylation reaction step 25-30 kJ mol^{-1} are higher than those of the isomerisation steps 15- 20 kJ mol^{-1} . Moreover, the higher reaction temperature 90 °C and higher contact time 7.04 g min mol^{-1} resulted in a slight decrease in the amount of coke alongside increasing in 1-heptene conversion from ~60 % to ~98 % and an increase in selectivity to 2-heptyltoluene from ~12 % to ~28 %.

In summary, pre-coking treatment could be considered for implementation in industrial operations because it is a useful method to enhance the selectivity and yield of monoheptyltoluene through toluene alkylation with 1-heptene and also because it decreases the amount of coke deposited during the reaction.

Contents

Declaration	I
Dedication	II
Acknowledgments	III
Abstract	V
Contents	VI
List of Figures	XII
List of Tables.....	XXVII
Chapter 1	1
Introduction	1
1.1 Background	2
1.2 Objective	4
1.3 Thesis outline	5
Chapter 2	6
Literature Survey.....	6
2.1 Introduction	7
2.1.1 Catalysis.....	7
2.2 Zeolites	9
2.2.1 History of zeolites	9
2.2.2 Application and Uses of Zeolites.....	10
2.2.3 Structures of Zeolites	10
2.2.4 Zeolite Type Y	12
2.2.5 Mordenite.....	13
2.2.6 Zeolite Beta.....	14
2.2.7 Water in Zeolites.....	15
2.2.8 Zeolites Classification.....	16
2.2.9 Zeolites properties.....	17
2.2.9.1 Acidity of zeolites and aluminium content	17
2.2.9.2 Shape selectivity.....	19
2.3 Zeolite modification.....	21
2.3.1 Dealumination.....	21
2.3.2 Desilication	23
2.3.3 Silylation.....	25

2.3.4 Modification through pre-coked	27
2.4 Alkylation reaction	31
2.4.1 Mechanism of alkylation reaction.....	37
2.5 Coke and deactivation	38
2.5.1 Effect of pore structure	39
2.5.2 Role of mesopores	39
2.5.3 Effect of acid sites.....	40
2.5.4 Effect of operation conditions.....	40
2.5.4.1 Temperature	40
2.5.4.2 Time-On-Stream (TOS)	40
2.5.5 Coke and deactivation classification.....	41
2.5.6 Coke characterisation.....	42
2.5.7 Benefits of coke	43
2.5.8 Catalyst deactivation modes	43
2.5.8.1 Acid site poisoning.....	44
2.5.8.2 Pore blockage	45
2.5.8.3 Pore mouth catalysis	46
Chapter 3	48
Characterisation techniques	48
3.1 Introduction	49
3.2 X-ray diffraction.....	49
3.3 Scanning electron microscope (SEM).....	53
3.4 Energy dispersive X-ray spectroscopy (EDX).....	54
3.5 X-ray fluorescence spectrometry.....	55
3.6 Temperature-programmed desorption (TPD).....	56
3.7 Nitrogen adsorption.....	58
3.8 Thermogravimetric Analysis (TGA)	62
3.9 Temperature programmed oxidation (TPO).....	64
3.10 Elemental analysis	65
3.11 Fourier-transform infrared spectroscopy (FTIR).....	67
Chapter 4	69
Materials, experimental work and methodology.....	69
4.1 Introduction	70
4.2 Materials	70
4.2.1 Gases and liquids	70

4.2.2 Catalysts.....	70
4.3 Experimental set-up and operating procedures	71
4.3.1 Batch reactor (BR)	71
4.3.2 Fixed bed reactor (FBR)	72
4.3.3 Water removing	75
4.4 Gas Chromatography.....	76
4.4.1 GC-MS analysis	79
4.4.2 GC-FID analysis.....	80
4.5 Zeolite modification	81
4.5.1 Dealumination technique using hydrochloric acid aqueous solution	81
4.5.2 Desilication technique by using sodium hydroxide aqueous solution.....	81
4.5.3 Silylation technique by employing tetraethoxysilane	82
4.5.4 Pre-coking technique by employing the individual reactant species toluene and 1-heptene	82
4.6 Calculations	83
4.6.1 Volumetric flowrate	83
4.6.2 1-Heptene calibration according to GC-FID	83
4.6.3 Weight hourly space velocity (WHSV)	85
4.6.4 Conversion	85
4.6.5 Selectivity	85
4.6.4 Experimental error	87
.....	88
Chapter 5	88
Role of coke deposits during the toluene alkylation with 1-heptene over fresh and modified zeolites	88
5.1 Introduction	89
5.2 Materials and methods.....	92
5.3 Results and Discussion	93
5.3.1 Zeolite catalyst characterisation.....	93
5.3.1.1 XRD	93
5.3.1.2 SEM	95
5.3.1.3 XRF and EDX results.....	97
5.3.1.4 Nitrogen adsorption-desorption results	97
5.3.1.5 TPD	101
5.4 Catalytic activity measurements.....	106

5.4.1 Impact of zeolite structure and coke formation on the activity and selectivity	107
5.4.1.1 Batch reactor	107
5.4.1.2 Fixed bed reactor	111
5.4.1.2.1 Influence of reaction temperature	112
5.4.1.2.2 Effect of TOS	114
5.4.2.2.3 Impact of zeolite amount	115
5.4.1.2.4 Influence of Si/Al mole ratio of HY zeolite	116
5.5 Zeolite modifications	119
5.5.1 Dealumination modification	119
5.5.2 Desilication modification	125
5.6 Coke characterisations	131
5.6.1 Nitrogen sorption results of post-reaction samples	131
5.6.2 TGA	133
5.6.3 Elemental analysis	137
5.6.4 TPO	138
5.6.5 FTIR	143
5.7 Conclusions	149
Chapter 6	151
Tailored carbon deposition of several zeolites for toluene alkylation with 1-heptene	151
.....	151
.....	151
6.1 Introduction	152
6.2 Experimental	154
6.2.1 Catalysts	154
6.2.2 Silylation modification	155
6.2.3 Pre-coking procedure	155
6.2.4 Catalytic activity measurements	155
6.3 Results and discussion	156
6.3.1 Characterisation techniques	156
6.3.1.1 XRF and EDX results	156
6.3.1.2 TPD results	156
6.3.1.3 Nitrogen sorption results	161
6.3.1.4 TGA results for zeolite pre-coked	164

6.3.1.5 Elemental analysis for zeolite pre-coked	165
6.3.1.6 TPO results of pre-coked zeolite.....	166
6.3.1.7 FTIR results.....	167
6.3.2 Catalytic activity measurements	169
6.3.2.1 Silylation treatment	169
6.3.2.2 Pre-coking modification.....	175
6.4 Coke characterisation	183
6.4.1 Nitrogen adsorption-desorption results of post-reaction samples.....	183
6.4.2 TGA results for the spent samples	186
6.4.3 Elemental analysis results for post-reaction samples	189
6.4.4 TPO results for the spent samples.....	190
6.4.5 FTIR spectroscopy results for the post-reaction samples	196
6.5 Conclusions	202
.....	204
Chapter 7	204
Theoretical study: reaction kinetic in fixed bed reactor.....	204
7.1 Introduction	205
7.2 Optimisation and Genetic algorithms.....	210
7.3 Experimental work	213
7.4 Activity measurements of zeolite catalyst.....	213
7.5 Kinetic study.....	223
7.6 Conclusions	229
Chapter 8	230
Conclusions and future works.....	230
8.1 Introduction	231
8.2 Conclusions	231
8.2.1 Toluene alkylation with 1-heptene over fresh zeolite catalysts.....	231
8.2.2 Toluene alkylation with 1-heptene over dealuminated and desilicated zeolite catalysts	232
8.2.3 Toluene alkylation with 1-heptene over silylated and pre-coked zeolite catalysts.....	233
8.2.4 Kinetics study of toluene alkylation with 1-heptene over fresh HY5.1 zeolite catalyst.....	235
8.3 Recommendations for future work.....	236
References	239
Appendices.....	263

Appendix A	264
TPD calculation	264
Appendix B	266
Calculation the molarity of acid leaching.....	266
Appendix C	267
Calculation the molarity of base leaching	267
Appendix D	268
D.1 Steps of determining of kinetic parameters	268
D.2 Sample of calculation of pseudo-first order reaction.....	271
Appendix E	274
Conference presentations	274
Oral presentations	274
Poster presentations	274

List of Figures

Figure 2.1: Schematic showing the alternative energetic pathway provided by a catalyst, which effects an increase in the rate of reactions (Boomeria, 2015).	7
Figure 2.2. Mechanism steps of a heterogeneously catalysed reaction (Hagen, 2006).	9
Figure 2.3. Tetrahedral units for the structure of zeolite, adapted from (Margeta et al., 2013).	11
Figure 2.4. The structure of zeolite Y, adapted from (Weitkamp, 2000).....	13
Figure 2.5. The structure of zeolite mordenite (Simoncic and Armbruster, 2004)... ..	13
Figure 2.6. The structure of zeolite Beta (Busca, 2014).	14
Figure 2.7. The interaction between water and cations (Byrappa and Yoshimura, 2001).	15
Figure 2.8. The hydroxyl bridge in the zeolite (van Bekkum et al., 2001).	17
Figure 2.9. Formation of Brønsted and Lewis acid sites, adapted from (CIEC, 2015).	18
Figure 2.10. Reactant selectivity (Bellussi and Millini, 2007).	19
Figure 2.11. Product selectivity (Bellussi and Millini, 2007).	20
Figure 2.12. Restricted transition state selectivity (Bellussi and Millini, 2007).....	20
Figure 2.13. The generation of defect pores which are result from the acid leaching, adapted from (Figueiredo et al., 2008).....	22
Figure 2.14. Schematic diagram shows the influence of Al content on the desilication of MFI zeolites in NaOH solution (Groen et al., 2006, Zheng et al., 2002).	24
Figure 2.15. Silaytion modification method.	25

Figure 2.16. Model of coke formation on external surface of HY-zeolite, reproduced from (Tsai et al., 1999).....	29
Figure 2.17. Production of monoheptyltoluene by alkylation of toluene with 1-heptene (Magnoux et al., 1997).....	37
Figure 3.1. X-ray diffractometer parts adapted from (Connolly, 2007).	49
Figure 3.2. The essential features of the X-ray diffraction (van Bekkum et al., 2001).	52
Figure 3.3. Schematic of a SEM adapted from (Bradbury et al., 2018).....	53
Figure 3.4. The interaction between the primary X-ray and an atom (Nummi, 2016).	56
Figure 3.5. IUPAC classification of adsorption-desorption isotherm adapted from (Kaneko, 1994).....	61
Figure 3.6. Schematic of TGA adapted from (Price, 2006).....	63
Figure 3.7. Principle of the CHNS elemental analysis adapted from (Thompson, 2008).	66
Figure 4.1. Scheme of the batch reactor.....	71
Figure 4.2. Scheme of the fixed bed reactor.	73
Figure 4.3. The calibration of mass flow controller using a) nitrogen and b) air.	74
Figure 4.4. Schematic diagram of a Gas Chromatography (GC) instrument reproduced from (Chromacademy, 2015).....	77
Figure 4.5. Calibration curve of 1-heptene using GC-FID; A) Run 1; B) Run 2 and C) Average	84

Figure 4.6. GC/FID Chromatogram for reaction products of toluene alkylation with 1-heptene at 90 °C, atmospheric pressure, 0.25 g HY5.1 zeolite, reaction time of 360 min, T: H ratio is 3: 1 and using BR.	86
Figure 5.1. The XRD patterns of HY5.1 dealuminated with different molarities of acid solution.....	93
Figure 5.2. The XRD patterns of fresh and modified a) HY5.1; b) HY30 zeolite catalyts.....	94
Figure 5.3. The SEM image of fresh HY30.	96
Figure 5.4. The SEM image of HY30 dealuminated zeolite in 0.025 M of HCl solution.	96
Figure 5.5. The SEM image of HY30 desilicated zeolite in 0.05 M of NaOH solution.	96
Figure 5.6. Nitrogen sorption isotherms of fresh HY5.1 (powder), HY5.1 (pellet) and HY30 (pellet) zeolite catalyts.	98
Figure 5.7. Nitrogen sorption isotherms of fresh HY30, dealuminated HY30 and desilicated HY30 zeolite catalyts.	99
Figure 5.8. NH ₃ -TPD profile of fresh HY5.1 and HY30 zeolite catalyts.....	101
Figure 5.9. Experimental and deconvoluted NH ₃ -TPD curves of a) fresh HY5.1, b) HY5.1 dealuminated, c) HY5.1 desilicated, d) fresh HY30, e) HY30 dealuminated and f) HY30 desilicated zeolite samples (refer to Table 5.3).	103
Figure 5.10. Conversion of 1-heptene (■), selectivity of 2-heptyltoluene (■), selectivity of 3-heptyltoluene (■), selectivity of 4-heptyltoluene (■), selectivity of 2- heptene (■), selectivity of 3-heptene (■) and selectivity of coke (■) during toluene alkylation with 1-heptene at 90 °C, atmospheric pressure, 0.25 g HY5.1 zeolite, reaction time of 20, 120 and 360 min, T: H ratio is 3: 1 and using BR.	108

Figure 5.11. Conversion of 1-heptene (■), selectivity of 2-heptyltoluene (■), selectivity of 3-heptyltoluene (■), selectivity of 4-heptyltoluene (■), selectivity of 2-heptene (■), selectivity of 3-heptene (■) and selectivity of coke (■) during toluene alkylation with 1-heptene at 90 °C, atmospheric pressure, 0.25 g H-mordenite zeolite, reaction time of 20, 120 and 360 min, T: H ratio is 3: 1 and using BR. 108

Figure 5.12. Conversion of 1-heptene (■), selectivity of 2-heptyltoluene (■), selectivity of 3-heptyltoluene (■), selectivity of 4-heptyltoluene (■), selectivity of 2-heptene (■), selectivity of 3-heptene (■) and selectivity of coke (■) during toluene alkylation with 1-heptene at 90 °C, atmospheric pressure, 0.25 g H-Beta zeolite, reaction time of 20, 120 and 360 min, T: H ratio is 3: 1 and using BR. 109

Figure 5.13. Effect of reaction temperature on 1-heptene conversion during toluene alkylation with 1-heptene at 80 °C (●) and 90 °C (■), atmospheric pressure, 0.5 g HY5.1 zeolite, TOS of 240 min, T: H ratio is 8: 1, WHSV of 17 h⁻¹, 30 ml min⁻¹ of N₂ flowrate and using FBR. 112

Figure 5.14. Effect of reaction temperature on selectivity of 2-heptyltoluene at 80 °C (●) and 90 °C (■) and 3-heptyltoluene at 80 °C (◆) and 90 °C (▲) during toluene alkylation with 1-heptene at atmospheric pressure, 0.5 g HY5.1 zeolite, TOS of 240 min, T: H ratio is 8: 1, WHSV of 17 h⁻¹, 30 ml min⁻¹ of N₂ flowrate and using FBR. 113

Figure 5.15. Effect of reaction temperature on selectivity of coke during toluene alkylation with 1-heptene at 80 °C (●) and 90 °C (■), atmospheric pressure, 0.5 g HY5.1 zeolite, TOS of 240 min, T: H ratio is 8: 1, WHSV of 17 h⁻¹, 30 ml min⁻¹ of N₂ flowrate and using FBR. 114

Figure 5.16. Influence of TOS on 1-heptene conversion (■), 2-heptyltoluene selectivity (●), 2-heptene selectivity (▲) and coke selectivity (◆) during toluene alkylation with 1-heptene at 90 °C, atmospheric pressure, 0.5 g HY5.1 zeolite, TOS of 720 min, T: H ratio is 8: 1, WHSV of 17 h⁻¹, 30 ml min⁻¹ of N₂ flowrate and using FBR. 115

Figure 5.17. Effect of zeolite catalyst loading on 1-heptene conversion during toluene alkylation with 1-heptene at 90 °C, atmospheric pressure, 0.5 (■), 0.75 (●) and 1 (▲) g HY5.1 zeolite, TOS of 240 min, T: H ratio is 8: 1, WHSV of 17 h⁻¹, 30 ml min⁻¹ of N₂ flowrate and using FBR. 116

Figure 5.18. Effect of TOS on 1-heptene conversion during toluene alkylation with 1-heptene at 90 °C, atmospheric pressure, 0.5 g HY5.1 (■) and HY30 (●) zeolite, TOS of 240 min, T: H ratio is 8: 1, WHSV of 17 h⁻¹, 30 ml min⁻¹ of N₂ flowrate and using FBR. 117

Figure 5.19. Influence of TOS on 2-heptyltoluene selectivity using HY5.1 (■) and HY30 (●) zeolite and 3-heptyltoluene selectivity using HY5.1 (▲) and HY30 (◆) zeolite during toluene alkylation with 1-heptene at 90 °C, atmospheric pressure, 0.5 g, TOS of 240 min, T: H ratio is 8: 1, WHSV of 17 h⁻¹, 30 ml min⁻¹ of N₂ flowrate and using FBR. 118

Figure 5.20. Effect of TOS on selectivity of coke during toluene alkylation with 1-heptene at 90 °C, atmospheric pressure, 0.5 g HY5.1 (■) and HY30 (●) zeolite, TOS of 240 min, T: H ratio is 8: 1, WHSV of 17 h⁻¹, 30 ml min⁻¹ of N₂ flowrate and using FBR. 119

Figure 5.21. Conversion of 1-hepten and selectivity to various reaction products during toluene alkylation with 1-heptene at 90 °C, atmospheric pressure, 0.25 g HY5.1 and HY5.1 dealuminated zeolite, reaction time of 120 min, T: H ratio is 3: 1 and using BR. 120

Figure 5.22. Influence of TOS on 1-heptene conversion during toluene alkylation with 1-heptene at 90 °C, atmospheric pressure, 0.5 g HY5.1 (■) and HY5.1 dealuminated (●) zeolite, TOS of 240 min, T: H ratio is 8: 1, WHSV of 17 h⁻¹, 30 ml min⁻¹ of N₂ flowrate and using FBR. 121

Figure 5.23. Influence of TOS on selectivity of 2-heptyltoluene during toluene alkylation with 1-heptene at 90 °C, atmospheric pressure, 0.5 g HY5.1 (■) and HY5.1 dealuminated (●) zeolite, TOS of 240 min, T: H ratio is 8: 1, WHSV of 17 h⁻¹, 30 ml min⁻¹ of N₂ flowrate and using FBR. 122

Figure 5.24. Influence of TOS on selectivity of coke during toluene alkylation with 1-heptene at 90 °C, atmospheric pressure, 0.5 g HY5.1 (■) and HY5.1 dealuminated (●) zeolite, TOS of 240 min, T: H ratio is 8: 1, WHSV of 17 h⁻¹, 30 ml min⁻¹ of N₂ flowrate and using FBR. 122

Figure 5.25. Influence of TOS on 1-heptene conversion during toluene alkylation with 1-heptene at 90 °C, atmospheric pressure, 0.5 g HY30 (■) and HY30 dealuminated (●) zeolite, TOS of 240 min, T: H ratio is 8: 1, WHSV of 17 h⁻¹, 30 ml min⁻¹ of N₂ flowrate and using FBR. 123

Figure 5.26. Influence of TOS on selectivity of 2-heptyltoluene during toluene alkylation with 1-heptene at 90 °C, atmospheric pressure, 0.5 g HY30 (■) and HY30 dealuminated (●) zeolite, TOS of 240 min, T: H ratio is 8: 1, WHSV of 17 h⁻¹, 30 ml min⁻¹ of N₂ flowrate and using FBR. 124

Figure 5.27. Influence of TOS on selectivity of coke during toluene alkylation with 1-heptene at 90 °C, atmospheric pressure, 0.5 g HY30 (■) and HY30 dealuminated (●) zeolite, TOS of 240 min, T: H ratio is 8: 1, WHSV of 17 h⁻¹, 30 ml min⁻¹ of N₂ flowrate and using FBR..... 125

Figure 5.28. Conversion of 1-hepten and selectivity to various reaction products during toluene alkylation with 1-heptene at 90 °C, atmospheric pressure, 0.25 g HY5.1 and HY5.1 desilicated zeolite, reaction time of 120 min, T: H ratio is 3: 1 and using BR. 126

Figure 5.29. Influence of TOS on 1-heptene conversion during toluene alkylation with 1-heptene at 90 °C, atmospheric pressure, 0.5 g HY5.1 (■) and HY5.1 desilicated (●) zeolite, TOS of 240 min, T: H ratio is 8: 1, WHSV of 17 h⁻¹, 30 ml min⁻¹ of N₂ flowrate and using FBR..... 127

Figure 5.30. Influence of TOS on 1selectivity of 2-heptyltoluene during toluene alkylation with 1-heptene at 90 °C, atmospheric pressure, 0.5 g HY5.1 (■) and HY5.1 desilicated (●) zeolite, TOS of 240 min, T: H ratio is 8: 1, WHSV of 17 h⁻¹, 30 ml min⁻¹ of N₂ flowrate and using FBR. 127

Figure 5.31. Influence of TOS on selectivity of coke during toluene alkylation with 1-heptene at 90 °C, atmospheric pressure, 0.5 g HY5.1 (■) and HY5.1 desilicated (●) zeolite, TOS of 240 min, T: H ratio is 8: 1, WHSV of 17 h⁻¹, 30 ml min⁻¹ of N₂ flowrate and using FBR..... 128

Figure 5.32. Conversion of 1-hepten and selectivity to various reaction products during toluene alkylation with 1-heptene at 90 °C, atmospheric pressure, 0.25 g HY30 and HY30 desilicated zeolite, reaction time of 120 min, T: H ratio is 3: 1 and using BR. 129

Figure 5.33. Influence of TOS on 1-heptene conversion during toluene alkylation with 1-heptene at 90 °C, atmospheric pressure, 0.5 g HY30 (■) and HY30 desilicated (●) zeolite, TOS of 240 min, T: H ratio is 8: 1, WHSV of 17 h⁻¹, 30 ml min⁻¹ of N₂ flowrate and using FBR..... 130

Figure 5.34. Influence of TOS on selectivity of 2-heptyltoluene during toluene alkylation with 1-heptene at 90 °C, atmospheric pressure, 0.5 g HY30 (■) and HY30 desilicated (●) zeolite, TOS of 240 min, T: H ratio is 8: 1, WHSV of 17 h⁻¹, 30 ml min⁻¹ of N₂ flowrate and using FBR..... 130

Figure 5.35. Influence of TOS on selectivity of coke during toluene alkylation with 1-heptene at 90 °C, atmospheric pressure, 0.5 g HY30 (■) and HY30 desilicated (●) zeolite, TOS of 240 min, T: H ratio is 8: 1, WHSV of 17 h ⁻¹ , 30 ml min ⁻¹ of N ₂ flowrate and using FBR.....	131
Figure 5.36. TGA showing the coke % of fresh HY5.1 (■); dealuminated HY5.1 (●) and desilicated HY5.1 (▲) during toluene alkylation with 1-heptene at 90 °C, atmospheric pressure, 0.25 g zeolite, reaction time of 120 min, T: H ratio is 3: 1 and using BR.....	134
Figure 5.37. Soft coke (■) and hard coke (■) % of fresh HY5.1 post-reaction at different TOS 240 and 720 min during toluene alkylation with 1-heptene at 90 °C, atmospheric pressure, 0.5 g zeolite, TOS of 240 min, T: H ratio is 8: 1, WHSV of 17 h ⁻¹ , 30 ml min ⁻¹ of N ₂ flowrate and using FBR.....	134
Figure 5.38. TGA and dTG profiles for a) HY5.1, b) HY5.1 dealuminated and c) HY5.1 desilicated during toluene alkylation with 1-heptene at 90 °C, atmospheric pressure, 0.5 g zeolite, TOS of 240 min, T: H ratio is 8: 1, WHSV of 17 h ⁻¹ , 30 ml min ⁻¹ of N ₂ flowrate and using FBR.....	136
Figure 5.39. TPO profiles of the HY5.1 and HY30 post-reaction during toluene alkylation with 1-heptene at 90 °C, atmospheric pressure, 0.5 g zeolite, TOS of 240 min, T: H ratio is 8: 1, WHSV of 17 h ⁻¹ , 30 ml min ⁻¹ of N ₂ flowrate and using FBR.....	138
Figure 5.40. Peak deconvolution of TPO spectrum for spent HY5.1 during toluene alkylation with 1-heptene at 90 °C, atmospheric pressure, 0.5 g zeolite, TOS of 240 min, T: H ratio is 8: 1, WHSV of 17 h ⁻¹ , 30 ml min ⁻¹ of N ₂ flowrate and using FBR.....	139
Figure 5.41. Peak deconvolution of TPO spectrum for spent HY30 during toluene alkylation with 1-heptene at 90 °C, atmospheric pressure, 0.5 g zeolite, TOS of 240 min, T: H ratio is 8: 1, WHSV of 17 h ⁻¹ , 30 ml min ⁻¹ of N ₂ flowrate and using FBR.....	140
Figure 5.42. TPO profiles of the spent HY30 and its modified zeolite samples during toluene alkylation with 1-heptene at 90 °C, atmospheric pressure, 0.25 g zeolite, TOS of 240 min, T: H ratio is 8: 1, WHSV of 17 h ⁻¹ , 30 ml min ⁻¹ of N ₂ flowrate and using FBR.....	141

Figure 5.43. Peak deconvolution of TPO spectrum for spent HY30 dealuminated during toluene alkylation with 1-heptene at 90 °C, atmospheric pressure, 0.5 g zeolite, TOS of 240 min, T: H ratio is 8: 1, WHSV of 17 h ⁻¹ , 30 ml min ⁻¹ of N ₂ flowrate and using FBR.	141
Figure 5.44. Peak deconvolution of TPO spectrum for spent HY30 desilicated during toluene alkylation with 1-heptene at 90 °C, atmospheric pressure, 0.5 g zeolite, TOS of 240 min, T: H ratio is 8: 1, WHSV of 17 h ⁻¹ , 30 ml min ⁻¹ of N ₂ flowrate and using FBR.	142
Figure 5.45. The FTIR spectra in the $\nu(\text{CH})$ region for fresh and post-reaction zeolite catalysts of a) HY5.1 (powder); b) HY30 (powder); c) HY5.1 (pellet); d) HY30 (pellet); e) HY30 dealuminated (pellet); f) HY30 desilicated (powder) and g) HY30 desilicated (pellet).	145
Figure 5.46. Peak deconvolution of FTIR spectra in the $\nu(\text{CH})$ region for fresh and spent zeolite catalysts of a) HY5.1 (powder); b) HY30 (powder); c) HY5.1 (pellet); d) HY30 (pellet); e) HY30 dealuminated (pellet); f) HY30 desilicated (powder) and g) HY30 desilicated (pellet).	148
Figure 6.1. Experimental and deconvoluted NH ₃ -TPD curves of A) silylated HY5.1, B) silylated HY30, C) HY5.1 pre-coked with toluene, and D) HY30 pre-coked with toluene samples (refer to Table 6.2).....	158
Figure 6.2. NH ₃ -TPD profile of fresh, silylated and toluene pre-coked HY5.1 zeolite catalyst.....	160
Figure 6.3. NH ₃ -TPD profile of fresh, silylated and toluene pre-coked HY30 zeolite catalyst.....	161
Figure 6.4. Nitrogen sorption isotherms of fresh and silylated HY5.1 (powder), HY5.1 (pellet) and HY30 (pellet) zeolite catalysts.....	161
Figure 6.5. Differences of pore size distribution using Horvath-Kawazoe method for a) HY5.1 powder; b) HY5.1 pellet and c) HY30 pellet zeolite catalysts before and after silylation and pre-coking modifications.....	164
Figure 6.6. TPO profiles after toluene and 1-heptene pre-coking treatments over 0.5 gm of HY5.1 zeolite at 90 °C (toluene) and 80 °C (1-heptene) for 2 and 1 h, respectively.	166

Figure 6.7. TPO profiles after toluene pre-coking treatments over 0.5 gm of HY30 zeolite at 90 °C for 2 h.	167
Figure 6.8. The FTIR spectra in the $\nu(\text{CH})$ region for fresh and silylated HY5.1 zeolite catalysts at a) 4000-400 cm^{-1} ; b) 2950-2800 cm^{-1} and c) 920-860 cm^{-1}	168
Figure 6.9. Peak deconvolution of FTIR spectra in the $\nu(\text{CH})$ region for zeolite catalysts of a) HY5.1 and b) HY5.1 silylated.	169
Figure 6.10. Conversion of 1-heptene and selectivity to various reaction products during toluene alkylation with 1-heptene at 90 °C, atmospheric pressure, 0.25 g HY5.1 and silylated HY5.1 zeolite, reaction time of 120 min, T: H ratio is 3: 1 and using BR.	171
Figure 6.11. Influence of TOS on 1-heptene conversion during toluene alkylation with 1-heptene at 90 °C, atmospheric pressure, 0.5 g HY5.1 (■) and silylated HY5.1 (●) zeolite, TOS of 240 min, T: H ratio is 8: 1, WHSV of 17 h^{-1} , 30 ml min^{-1} of N_2 flowrate and using FBR.	172
Figure 6.12. Influence of TOS on 1-heptene conversion during toluene alkylation with 1-heptene at 90 °C, atmospheric pressure, 0.5 g HY30 (■) and silylated HY30 (●) zeolite, TOS of 240 min, T: H ratio is 8: 1, WHSV of 17 h^{-1} , 30 ml min^{-1} of N_2 flowrate and using FBR.	172
Figure 6.13. Influence of TOS on selectivity of 2-heptyltoluene during toluene alkylation with 1-heptene at 90 °C, atmospheric pressure, 0.5 g HY5.1 (■) and silylated HY5.1 (●) zeolite, TOS of 240 min, T: H ratio is 8: 1, WHSV of 17 h^{-1} , 30 ml min^{-1} of N_2 flowrate and using FBR.	173
Figure 6.14. Influence of TOS on selectivity of 2-heptyltoluene during toluene alkylation with 1-heptene at 90 °C, atmospheric pressure, 0.5 g HY30 (■) and silylated HY30 (●) zeolite, TOS of 240 min, T: H ratio is 8: 1, WHSV of 17 h^{-1} , 30 ml min^{-1} of N_2 flowrate and using FBR.	173
Figure 6.15. Influence of TOS on selectivity of coke during toluene alkylation with 1-heptene at 90 °C, atmospheric pressure, 0.5 g HY5.1 (■) and silylated HY5.1 (●) zeolite, TOS of 240 min, T: H ratio is 8: 1, WHSV of 17 h^{-1} , 30 ml min^{-1} of N_2 flowrate and using FBR.	174

Figure 6.16. Influence of TOS on selectivity of coke during toluene alkylation with 1-heptene at 90 °C, atmospheric pressure, 0.5 g HY30 (■) and silylated HY30 (●) zeolite, TOS of 240 min, T: H ratio is 8: 1, WHSV of 17 h⁻¹, 30 ml min⁻¹ of N₂ flowrate and using FBR..... 175

Figure 6.17. Effect of TOS on 1-heptene conversion during toluene alkylation with 1-heptene at 90 °C, atmospheric pressure, 0.5 g fresh HY5.1 (■), HY5.1 pre-coked with toluene (●) and HY5.1 pre-coked with 1-heptene (▲), TOS of 240 min, T: H ratio is 8: 1, WHSV of 17 h⁻¹, 30 ml min⁻¹ of N₂ flowrate and using FBR..... 176

Figure 6.18. Influence of TOS on 1-heptene conversion during toluene alkylation with 1-heptene at 90 °C, atmospheric pressure, 0.5 g fresh HY30 (■) and HY30 pre-coked with toluene (●), TOS of 240 min, T: H ratio is 8: 1, WHSV of 17 h⁻¹, 30 ml min⁻¹ of N₂ flowrate and using FBR. 177

Figure 6.19. Effect of TOS on selectivity of 2-heptyltoluene during toluene alkylation with 1-heptene at 90 °C, atmospheric pressure, 0.5 g fresh HY5.1 (■), HY5.1 pre-coked with toluene (●) and HY5.1 pre-coked with 1-heptene (▲), TOS of 240 min, T: H ratio is 8: 1, WHSV of 17 h⁻¹, 30 ml min⁻¹ of N₂ flowrate and using FBR..... 178

Figure 6.20. Influence of TOS on selectivity of 2-heptyltoluene during toluene alkylation with 1-heptene at 90 °C, atmospheric pressure, 0.5 g fresh HY30 (■) and HY30 pre-coked with toluene (●), TOS of 240 min, T: H ratio is 8: 1, WHSV of 17 h⁻¹, 30 ml min⁻¹ of N₂ flowrate and using FBR..... 179

Figure 6.21. Effect of TOS on selectivity of 3-heptyltoluene during toluene alkylation with 1-heptene at 90 °C, atmospheric pressure, 0.5 g fresh HY5.1 (■) and HY5.1 pre-coked with toluene (●), TOS of 240 min, T: H ratio is 8: 1, WHSV of 17 h⁻¹, 30 ml min⁻¹ of N₂ flowrate and using FBR..... 179

Figure 6.22. Influence of TOS on selectivity of 3-heptyltoluene during toluene alkylation with 1-heptene at 90 °C, atmospheric pressure, 0.5 g fresh HY30 (■) and HY30 pre-coked with toluene (●), TOS of 240 min, T: H ratio is 8: 1, WHSV of 17 h⁻¹, 30 ml min⁻¹ of N₂ flowrate and using FBR..... 180

Figure 6.23. Effect of TOS on selectivity of coke during toluene alkylation with 1-heptene at 90 °C, atmospheric pressure, 0.5 g fresh HY5.1 (■), HY5.1 pre-coked with toluene (●) and HY5.1 pre-coked with 1-heptene (▲), TOS of 240 min, T: H ratio is 8: 1, WHSV of 17 h⁻¹, 30 ml min⁻¹ of N₂ flowrate and using FBR..... 182

Figure 6.24. Influence of TOS on selectivity of coke during toluene alkylation with 1-heptene at 90 °C, atmospheric pressure, 0.5 g fresh HY30 (■) and HY30 pre-coked with toluene (●), TOS of 240 min, T: H ratio is 8: 1, WHSV of 17 h ⁻¹ , 30 ml min ⁻¹ of N ₂ flowrate and using FBR.	182
Figure 6.25. Nitrogen sorption isotherms of a) silylated and silylated spent HY5.1 using BR, b) silylated and silylated spent HY5.1 using FBR and c) silylated and silylated spent HY30 using FBR.	184
Figure 6.26. Nitrogen sorption isotherms of toluene pre-coked and toluene pre-coked spent HY5.1.	184
Figure 6.27. Nitrogen sorption isotherms of toluene pre-coked and toluene pre-coked spent HY30.	186
Figure 6.28. TGA and dTG profiles for HY5.1 silylated during toluene alkylation with 1-heptene at 90 °C, atmospheric pressure, 0.5 g zeolite, TOS of 240 min, T: H ratio is 8: 1, WHSV of 17 h ⁻¹ , 30 ml min ⁻¹ of N ₂ flowrate and using FBR.	187
Figure 6.29. TGA and dTG profiles for a) HY5.1 toluene pre-coked at 90 °C and b) post-reaction HY5.1 toluene pre-coked during toluene alkylation with 1-heptene at 90 °C, atmospheric pressure, 0.5 g zeolite, TOS of 240 min, T: H ratio is 8: 1, WHSV of 17 h ⁻¹ , 30 ml min ⁻¹ of N ₂ flowrate and using FBR.	188
Figure 6.30. The H/C mass ratio obtained by the elemental analysis after silylation treatment of HY5.1 and HY30 zeolite catalysts during toluene alkylation with 1- heptene using BR and FBR.	190
Figure 6.31. TPO profiles of the spent HY5.1 and its silylated during toluene alkylation with 1-heptene at 90 °C, atmospheric pressure, 0.5 g zeolite, TOS of 240 min, T: H ratio is 8: 1, WHSV of 17 h ⁻¹ , 30 ml min ⁻¹ of N ₂ flowrate and using FBR.	191
Figure 6.32. TPO profiles of the spent HY30 and its silylated during toluene alkylation with 1-heptene at 90 °C, atmospheric pressure, 0.5 g zeolite, TOS of 240 min, T: H ratio is 8: 1, WHSV of 17 h ⁻¹ , 30 ml min ⁻¹ of N ₂ flowrate and using FBR.	191
Figure 6.33. TPO profiles of the spent HY5.1, toluene pre-coked HY5.1 and toluene pre-coked HY5.1 post reaction during toluene alkylation with 1-heptene at 90 °C, atmospheric pressure, 0.5 g zeolite, TOS of 240 min, T: H ratio is 8: 1, WHSV of 17 h ⁻¹ , 30 ml min ⁻¹ of N ₂ flowrate and using FBR.	192

Figure 6.34. Peak deconvolution of TPO spectrum for spent HY5.1 during toluene alkylation with 1-heptene at 90 °C, atmospheric pressure, 0.5 g zeolite, TOS of 240 min, T: H ratio is 8: 1, WHSV of 17 h ⁻¹ , 30 ml min ⁻¹ of N ₂ flowrate and using FBR.	193
Figure 6.35. Peak deconvolution of TPO spectrum for toluene pre-coked of HY5.1 at 90 °C, atmospheric pressure, 0.5 g zeolite, TOS of 120 min, WHSV of 17 h ⁻¹ , 30 ml min ⁻¹ of N ₂ flowrate and using FBR.	193
Figure 6.36. Peak deconvolution of TPO spectrum for spent toluene pre-coked of HY5.1 during toluene alkylation with 1-heptene at 90 °C, atmospheric pressure, 0.5 g zeolite, TOS of 240 min, T: H ratio is 8: 1, WHSV of 17 h ⁻¹ , 30 ml min ⁻¹ of N ₂ flowrate and using FBR.	194
Figure 6.37. TPO and dTG profiles for HY5.1 post-reaction during toluene alkylation with 1-heptene at 90 °C, atmospheric pressure, 0.5 g zeolite, TOS of 240 min, T: H ratio is 8: 1, WHSV of 17 h ⁻¹ , 30 ml min ⁻¹ of N ₂ flowrate and using FBR.	195
Figure 6.38. TPO and dTG profiles for toluene pre-coked HY5.1 during toluene alkylation with 1-heptene at 90 °C, atmospheric pressure, 0.5 g zeolite, TOS of 240 min, T: H ratio is 8: 1, WHSV of 17 h ⁻¹ , 30 ml min ⁻¹ of N ₂ flowrate and using FBR.	196
Figure 6.39. TPO and dTG profiles for toluene pre-coked HY5.1 post-reaction during toluene alkylation with 1-heptene at 90 °C, atmospheric pressure, 0.5 g zeolite, TOS of 240 min, T: H ratio is 8: 1, WHSV of 17 h ⁻¹ , 30 ml min ⁻¹ of N ₂ flowrate and using FBR.	196
Figure 6.40. The FTIR spectra in the ν(CH) region for silylated and silylated post-reaction zeolite catalysts of a) HY5.1 (powder); b) HY5.1 (pellet) and c) HY30 (pellet).	198
Figure 6.41. The FTIR spectra in the ν(CH) region for fresh, toluene pre-coked and toluene pre-coked post-reaction zeolite catalysts of a) HY5.1 (pellet) and b) HY30 (pellet).	199
Figure 6.42. Peak deconvolution of FTIR spectra in the ν(CH) region for silylated spent zeolite catalysts of a) HY5.1 (powder); b) HY5.1 (pellet) and c) HY30 (pellet).	200

Figure 6.43. Peak deconvolution of FTIR spectra in the $\nu(\text{CH})$ region for toluene pre-coked post-reaction zeolite catalysts of a) HY5.1 (pellet) and b) HY30 (pellet).....201

Figure 6.44. The fit peak areas of deconvoluted peaks of FTIR spectra in the $\nu(\text{CH})$ region for fresh, silylated and toluene pre-coked of HY5.1 (powder); HY5.1 (pellet) and HY30 (pellet).....201

Figure 7.1. The main steps of Genetic optimisation algorithm to calculate Arrhenius constant, activation energy and rate constant.....212

Figure 7.2. Impact of temperature and contact time (W/F) on 1-heptene conversion and selectivity of MHT and 2-heptyltoluene during toluene alkylation with 1-heptene at various temperatures 60 °C (■), 70 °C (■), 80 °C (■) and 90 °C (■) atmospheric pressure, 0.5 g of fresh HY5.1 zeolite, TOS of 30 min, T: H ratio is 8: 1, 30 ml min⁻¹ of N₂ flowrate and using FBR.215

Figure 7.3. Contact time (W/F) effect on 1-heptene conversion during toluene alkylation with 1-heptene at various temperatures 60 °C (■), 70 °C (●), 80 °C (▲) and 90 °C (◆), atmospheric pressure, 0.5 g of fresh HY5.1 zeolite, TOS of 30 min, T: H ratio is 8: 1, 30 ml min⁻¹ of N₂ flowrate and using FBR.216

Figure 7.4. Contact time (W/F) effect on 2-heptyltoluene (■), 3-heptyltoluene (■) and 4-heptyltoluene (■) selectivity during toluene alkylation with 1-heptene at 60 °C, atmospheric pressure, 0.5 g of fresh HY5.1 zeolite, TOS of 30 min, T: H ratio is 8:1, 30 ml min⁻¹ of N₂ flowrate and using FBR.217

Figure 7.5. Contact time (W/F) effect on 2-heptyltoluene (■), 3-heptyltoluene (■) and 4-heptyltoluene (■) selectivity during toluene alkylation with 1-heptene at 70 °C, atmospheric pressure, 0.5 g of fresh HY5.1 zeolite, TOS of 30 min, T: H ratio is 8:1, 30 ml min⁻¹ of N₂ flowrate and using FBR.218

Figure 7.6. Contact time (W/F) effect on 2-heptyltoluene (■), 3-heptyltoluene (■) and 4-heptyltoluene (■) selectivity during toluene alkylation with 1-heptene at 80 °C, atmospheric pressure, 0.5 g of fresh HY5.1 zeolite, TOS of 30 min, T: H ratio is 8:1, 30 ml min⁻¹ of N₂ flowrate and using FBR.218

Figure 7.7. Contact time (W/F) effect on 2-heptyltoluene (■), 3-heptyltoluene (■) and 4-heptyltoluene (■) selectivity during toluene alkylation with 1-heptene at 90 °C, atmospheric pressure, 0.5 g of fresh HY5.1 zeolite, TOS of 30 min, T: H ratio is 8:1, 30 ml min⁻¹ of N₂ flowrate and using FBR.219

Figure 7.8. Contact time (W/F) effect on selectivity of 2-heptene (■) and 3-heptene (■) isomers during toluene alkylation with 1-heptene at 60 °C, atmospheric pressure, 0.5 g of fresh HY5.1 zeolite, TOS of 30 min, T: H ratio is 8: 1, 30 ml min⁻¹ of N₂ flowrate and using FBR.220

Figure 7.9. Contact time (W/F) effect on selectivity of 2-heptene (■) and 3-heptene (■) isomers during toluene alkylation with 1-heptene at 70 °C, atmospheric pressure, 0.5 g of fresh HY5.1 zeolite, TOS of 30 min, T: H ratio is 8: 1, 30 ml min⁻¹ of N₂ flowrate and using FBR.220

Figure 7.10. Contact time (W/F) effect on selectivity of 2-heptene (■) and 3-heptene (■) isomers during toluene alkylation with 1-heptene at 80 °C, atmospheric pressure, 0.5 g of fresh HY5.1 zeolite, TOS of 30 min, T: H ratio is 8: 1, 30 ml min⁻¹ of N₂ flowrate and using FBR.221

Figure 7.11. Contact time (W/F) effect on selectivity of 2-heptene (■) and 3-heptene (■) isomers during toluene alkylation with 1-heptene at 90 °C, atmospheric pressure, 0.5 g of fresh HY5.1 zeolite, TOS of 30 min, T: H ratio is 8: 1, 30 ml min⁻¹ of N₂ flowrate and using FBR.221

Figure 7.12. Influence of contact time (W/F) on coke selectivity during toluene alkylation with 1-heptene at various reaction temperature 60 °C (■), 70 °C (●), 80 °C (▲) and 90 °C (◆), atmospheric pressure, 0.5 g of fresh HY5.1 zeolite, TOS of 30 min, T: H ratio is 8: 1, 30 ml min⁻¹ of N₂ flowrate and using FBR.....222

Figure 7.13. Coke % of fresh HY5.1 post-reaction during toluene alkylation with 1-heptene at atmospheric pressure, 0.5 g of fresh HY5.1 zeolite, TOS of 30 min, T: H ratio is 8: 1, 30 ml min⁻¹ of N₂ flowrate and using FBR.222

Figure 7.14. Kinetic comparison plot of experimental and predicted concentration of 1-heptene using Eley-Rideal kinetic model during toluene alkylation with 1-heptene at various W/F values and reaction temperatures, atmospheric pressure, 0.5 g of fresh HY5.1 zeolite, TOS of 30 min, T: H ratio is 8: 1, 30 ml min⁻¹ of N₂ flowrate, and using FBR.224

Figure 7.15. Kinetic comparison plot of experimental and predicted concentration of 1-heptene using Eley-Rideal kinetic model during toluene alkylation with 2-heptene at various W/F values and reaction temperatures, atmospheric pressure, 0.5 g of fresh HY5.1 zeolite, TOS of 30 min, T: H ratio is 8: 1, 30 ml min⁻¹ of N₂ flowrate, and using FBR.224

Figure 7.16. Kinetic comparison plot of experimental and predicted concentration of 3-heptene using Eley-Rideal kinetic model during toluene alkylation with 1-heptene at various W/F values and reaction temperatures, atmospheric pressure, 0.5 g of fresh HY5.1 zeolite, TOS of 30 min, T: H ratio is 8: 1, 30 ml min⁻¹ of N₂ flowrate, and using FBR.225

Figure 7.17. Kinetic comparison plot of experimental and predicted concentration of 2-heptyltoluene using Eley-Rideal kinetic model during toluene alkylation with 1-heptene at various W/F values and reaction temperatures, atmospheric pressure, 0.5 g of fresh HY5.1 zeolite, TOS of 30 min, T: H ratio is 8: 1, 30 ml min⁻¹ of N₂ flowrate, and using FBR.225

Figure 7.18. Kinetic comparison plot of experimental and predicted concentration of 3-heptyltoluene using Eley-Rideal kinetic model during toluene alkylation with 1-heptene at various W/F values and reaction temperatures, atmospheric pressure, 0.5 g of fresh HY5.1 zeolite, TOS of 30 min, T: H ratio is 8: 1, 30 ml min⁻¹ of N₂ flowrate, and using FBR.226

Figure 7.19. Kinetic comparison plot of experimental and predicted concentration of 4-heptyltoluene using Eley-Rideal kinetic model during toluene alkylation with 1-heptene at various W/F values and reaction temperatures, atmospheric pressure, 0.5 g of fresh HY5.1 zeolite, TOS of 30 min, T: H ratio is 8: 1, 30 ml min⁻¹ of N₂ flowrate, and using FBR.226

List of Tables

Table 2.1. The properties of the most important zeolite framework types (Busca, 2014, Baerlocher et al., 2007).	12
Table 3.1. XRD-data for typical faujasite with Cu K α radiation; $\lambda = 1.5418 \text{ \AA}$, and $a_0 \approx 24.7 \text{ \AA}$ (Treacy and Higgins, 2007).	51
Table 3.2. The operation conditions of X-ray diffraction.	52
Table 3.3. The main definitions of terms relating to porous solids, adapted from (Rouquerol et al., 1999, Kaneko, 1994).	60
Table 3.4. FTIR bands which formed as a result of coke deposits, adapted from (Ibáñez et al., 2016, Bauer and Karge, 2007, Querini, 2004).	68
Table 4.1. Properties of chromatographic method as used for the analysis of the samples.	79
Table 4.2. Properties of the chromatographic method employed for the analysis of the samples.	80
Table 4.3. 1-Heptene calibration standard.	83
Table 5.1. The results of Si/Al mole ratio using XRF and EDX for fresh and modified zeolite catalysts.	97
Table 5.2. The results of surface area of parent and modified zeolite catalysts.	100
Table 5.3. Fresh and modified acid properties of HY5.1 and HY30 zeolite catalysts.	105
Table 5.4. The results of surface area of fresh and spent zeolite catalysts.	132
Table 5.5. The coke % after dealumination and desilication treatments of HY5.1 and HY30 zeolite catalysts during toluene alkylation with 1-heptene at 90 °C, atmospheric pressure, 0.5 g zeolite, TOS of 240 min, T: H ratio is 8: 1, WHSV of 17 h ⁻¹ , 30 ml min ⁻¹ of N ₂ flowrate and using FBR.	136

Table 5.6. The H/C mass ratio obtained by the elemental analysis after dealumination and desilication treatments of HY5.1 and HY30 zeolite catalysts during toluene alkylation with 1-heptene at 90 °C, atmospheric pressure, 0.5 g zeolite, TOS of 240 min, T: H ratio is 8: 1, WHSV of 17 h ⁻¹ , 30 ml min ⁻¹ of N ₂ flowrate and using FBR.	137
Table 5.7. The fit peak areas and maximum temperature deconvoluted peaks for spent HY5.1 and HY30 during toluene alkylation with 1-heptene at 90 °C, atmospheric pressure, 0.5 g zeolite, TOS of 240 min, T: H ratio is 8: 1, WHSV of 17 h ⁻¹ , 30 ml min ⁻¹ of N ₂ flowrate and using FBR.....	140
Table 5.8. The fit peak areas and maximum temperature deconvoluted peaks for spent HY30, HY30 dealuminated and HY30 desilicated during toluene alkylation with 1-heptene at 90 °C, atmospheric pressure, 0.5 g zeolite, TOS of 240 min, T: H ratio is 8: 1, WHSV of 17 h ⁻¹ , 30 ml min ⁻¹ of N ₂ flowrate and using FBR.....	143
Table 5.9. The fit peak areas of deconvoluted peaks of FTIR spectra in the ν(CH) region for fresh and used of a) HY5.1 (powder); b) HY30 (powder); c) HY5.1 (pellet); d) HY30 (pellet); e) HY30 dealuminated (pellet); f) HY30 desilicated (powder) and g) HY30 desilicated (pellet).	149
Table 6.1. The results of Si/Al mole ratio using XRF and EDX for fresh and silylated zeolite catalysts.	156
Table 6.2. Fresh and modified acid properties of HY5.1 and HY30 zeolite catalysts.	159
Table 6.3. The results of surface area of parent and modified zeolite catalysts.	162
Table 6.4. The coke % after pre-coking <i>via</i> toluene and 1-heptene over 0.5 g of HY5.1 and HY30 zeolites at 90 °C (toluene) and 80 °C (1-heptene) for 2 and 1 h, respectively.	165
Table 6.5. The H/C mass ratio obtained by the elemental analysis after toluene and 1-heptene pre-coking treatments over 0.5 g of HY5.1 zeolite at 90 °C (toluene) and 80 °C (1-heptene) for 2 and 1 h, respectively.	165
Table 6.6. The results of surface area of parent and modified zeolite catalysts.	185

Table 6.7. The coke % of fresh and silylated post-reaction HY5.1 zeolite catalysts during toluene alkylation with 1-heptene at 90 °C, atmospheric pressure, 0.25 g zeolite, reaction time of 120 min, T: H ratio is 3: 1 and using BR.	186
Table 6.8. The percentage of coke content of fresh and silylated post-reaction HY5.1 and HY30 zeolite catalysts during toluene alkylation with 1-heptene at 90 °C, atmospheric pressure, 0.5 g zeolite, TOS of 240 min, T: H ratio is 8: 1, WHSV of 17 h ⁻¹ , 30 ml min ⁻¹ of N ₂ flowrate and using FBR.	187
Table 6.9. TGA showing the coke % after pre-coking <i>via</i> toluene and 1-heptene over 0.5 gm of HY5.1 and HY30 zeolites at 90 °C (toluene) and 80 °C (1-heptene) for 2 and 1 h respectively.....	189
Table 6.10. The fit peak areas and maximum temperature deconvoluted peaks for spent HY5.1, toluene pre-coked HY5.1 and toluene pre-coked HY5.1 post-reaction during toluene alkylation with 1-heptene at 90 °C, atmospheric pressure, 0.5 g zeolite, TOS of 240 min, T: H ratio is 8: 1, WHSV of 17 h ⁻¹ , 30 ml min ⁻¹ of N ₂ flowrate and using FBR.	195
Table 7.1. Experimental data conducted for kinetic study of toluene alkylation with 1-heptene over HY5.1 zeolite by employing the FBR.	214
Table 7.2. Estimated Arrhenius (min ⁻¹) constant and activation energy (kJ mol ⁻¹) for each elementary step during the toluene alkylation with 1-heptene.	227

Chapter 1

Introduction

1.1 Background

Alkylation is the process where an alkyl group is transferred from one molecule to another Encyclopædia Britannica (2015). Several factors influence the use of this reaction, such as market demand, availability of raw materials, cost of feedstock and equipment and legislation such as environmental laws. Alkylation of aromatics is a commercial process and commonly used on a large scale, worldwide (Guisnet and Gilson, 2002). The interest in aromatics is high because they are employed in many manufacturing processes, including the chemical and petrochemical industries. They are considered an important raw material for production of intermediate substances which are used in detergent, plastic and polyester production (Tsai et al., 1999). There are several alkylating agents in the alkylation of aromatics, such as: alkenes, alcohols and esters. Several products can be produced using the alkylation process, such as: ethylbenzene, linear heptyl-methylbenzene, styrene, isopropylbenzene, linear alkylbenzene, alkali benzene sulphonates and alkyl-naphthalene.

Linear alkyl-methylbenzene is usually produced by alkylation of benzene or toluene with α -alkene with zeolite as a catalyst; it has high biodegradability and is cost-effective (Yadav and Doshi, 2002, Liang et al., 1995). The process which produces linear alkyl-methylbenzene is the dehydrogenation of alkanes to alkenes and then aromatic alkylation (Kocal et al., 2001, Mériaudeau et al., 1997). Sodium alkylbenzene sulphonation has been used in the production of soaps since the 1940s (Kocal et al., 2001). This way of synthesis has significant features, such as: detergency characteristics, economically used and it is used widely.

Linear alkyl-methylbenzene replaced dodecylbenzene in the 1960s in the production of detergents because dodecylbenzene had a low rate of biodegradability (Kocal et al., 2001). Nowadays, linear alkyl-methylbenzene is used widely to produce alkylbenzene sulphonates (Kocal et al., 2001, Mériaudeau et al., 1997).

An increase in the demand for household detergents has contributed to the increase in the production of alkylaromatics and alkylaromaticsulfonate. The estimated production of linear alkyl-methylbenzene in 2015 was ~4 million tonnes (AOCS, 2015). Additionally, approximately 98% of linear alkylbenzene production is used to produce linear alkylbenzenesulfonate, which is the most interesting

biodegradable surfactant in the detergents. There are other uses of linear alkyl-methylbenzene, such as ink production, solvents and the paint industry (AOCS, 2015).

Zeolites are an important type of acid catalyst that are employed in aromatic alkylation reactions (Guisnet and Pinard, 2018). These porous materials have reasonable space for the bulky product molecules to form and modify inside the pores of the zeolites. For instance, the HY zeolite which was used in the present study has a large cage diameter of $\sim 13 \text{ \AA}$ and a pore opening of $\sim 7.4 \text{ \AA}$. This zeolite will be used in the alkylation of toluene with 1-heptene. The kinetic diameters of the raw materials and products are: toluene $\sim 5.85 \text{ \AA}$, 1-heptene $\sim 6.47 \text{ \AA}$ and monoheptyltoluene is $\sim 7 \text{ \AA}$ (Jae et al., 2011).

Zeolite catalysts in alkylation reactions suffer from coke build-up and deactivation. Coke is a complex mixture formed from an accumulation of carbonaceous compounds and usually leads to deactivation of the zeolite catalyst. However, in addition to the coke deposits having a negative impact, they can also have beneficial effects (Collett and McGregor, 2015).

The present work focuses on:

- Studying experimentally the influence of catalyst structure as well as the role of catalyst properties (acidity and shape selectivity) at different times on both the conversion of 1-heptene and the selectivity for monoheptyltoluene.
- Understanding the role of coke that accumulated during the liquid phase toluene alkylation with C_7 linear alkenes (does it work positively to enhance the selectivity, or negatively to deactivate the catalyst?)
- Investigating the effect of zeolite modifications (dealumination, desilication, silylation and pre-coking) on 1-heptene conversion and the selectivity for monoheptyltoluene.
- Dealumination and desilication modifications of the zeolite have been used to improve the catalytic performance by altering acid site properties and/or texture features.
- Understanding silylation and pre-coking are the effective methods to modify the catalyst surface. They are considered as economical investigations when they enhance the catalytic activity and selectivity by formation deactivate the non-selective acid sites for silylation treatment or acts as 'active coke' for the pre-

coked samples as a result of incorporation the carbonaceous deposits and the zeolite structure.

- Investigating the role of temperature, contact time and coke deposition on the reaction kinetics through determining the activation energy of both alkylation and isomerisation reactions.

1.2 Objective

The present study is focused on enhancing the catalytic activity of HY zeolite catalysts for toluene alkylation with 1-heptene through post synthesis treatment. The main objectives of the present research are as follows:

- To study experimentally the influence of catalyst structure and the role of catalyst properties (acidity and shape selectivity) at different operating conditions on the catalytic performance of fresh and modified zeolite catalysts by acid leaching (dealumination) and base leaching (desilication) in toluene alkylation with 1- heptene.
- To enhance the catalytic activity *via* silylation (surface modification) of HY5.1 and HY30 zeolite catalysts by employing bulky molecules which cannot penetrate through the zeolite pores and study a controlled pre-coking modification by adsorbing two reactant molecules (toluene and 1-heptene) as a coke pre-cursor of HY5.1 and HY30 zeolite catalysts by using the fixed bed reactor.
- To understand the role of carbonaceous materials and investigate the amount, structure and nature of coke formed after the toluene alkylation with 1-heptene over fresh and treated HY5.1 and HY30 zeolite catalysts on the catalytic performance.
- To examine the impact of carbon deposits from the pre-coking modification and their effect on the catalytic performance during the alkylation reaction over HY zeolite catalysts which allows differentiation between the benefits and drawbacks of the coke formed and evaluate the influence of coke deposits from the pre-coking on the catalytic activity by finding out the main reactant that is responsible for the coke formation and thereby the deactivation.
- To study the kinetics of liquid phase alkylation of toluene with 1-heptene over HY5.1 zeolite catalyst.

1.3 Thesis outline

The present thesis is organised into eight chapters. Chapter 1 contains background information about the alkylation reaction, linear alkyl-methylbenzene, zeolite modification and coke formation. Chapter 2 includes a literature review of zeolite catalysts, zeolite modifications, the alkylation reaction and its modification and the theoretical role of coke deposits during the toluene alkylation with olefin. Chapter 3 encompasses the description for all characterisation techniques that are employed during the present work. This comprises XRD, SEM, EDX, XRF, N₂ sorption, TPD, TGA, TPO, CHNS elemental analysis and FTIR. The experimental set up, methodology and calculation of catalytic activity are described in Chapter 4. In Chapter 5, toluene alkylation with 1-heptene over fresh, dealuminated and desilicated zeolite catalyst using a BR and a FBR is investigated. This chapter also includes an evaluation of the role of coke deposits on both the fresh and modified zeolite catalysts. Chapter 6 studies the effect of surface modification (pre-coking and silylation) on the catalytic activity improvements and investigates the reactant material that is responsible for the zeolite deactivation. In addition, Chapter 6 also assesses the effect of coke accumulated in/on the zeolite pores to determine if this coke is deactivating acid sites or is having a beneficial effect. Chapter 7 includes a mathematical study of the reaction kinetics of toluene alkylation with 1-heptene as well as determining the values of the activation energy and Arrhenius constant. Chapter 8 explains the main conclusions along with the main recommendations for any future studies.

Chapter 2

Literature Survey

2.1 Introduction

2.1.1 Catalysis

Berzelius in 1835 coined the expression ‘catalysis’ from the Greek word *καταλειν*, which means to loosen or dissolve (Figueiredo et al., 2008, Busca, 2014, Armor, 2011). A catalyst can be defined as a material that acts to accelerate a reaction by diminishing its activation energy (E_a), as shown in Figure 2.1 (Figueiredo et al., 2008).

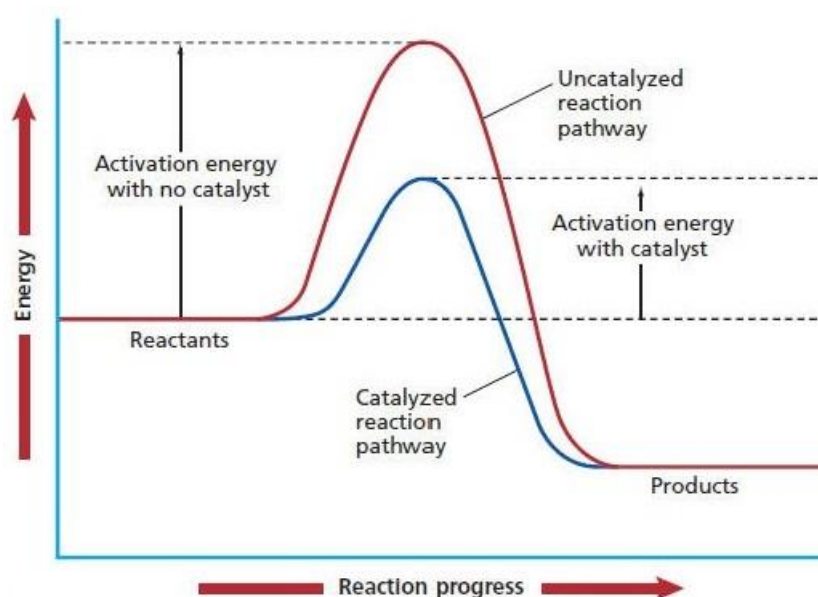


Figure 2.1: Schematic showing the alternative energetic pathway provided by a catalyst, which effects an increase in the rate of reactions (Boomeria, 2015).

Indeed, the interest in catalysts increased during the last century; nowadays, catalytic technology plays a role in 80-90% of the industrialisation process, and represents (Guisnet and Pinard, 2018). Catalysts can be divided into two groups: the first includes heterogeneous and homogeneous catalysts, the second consists of enzymatic catalysts (bio-catalysts) (Hagen, 2006). Busca (2014) defined the heterogeneous catalyst as ‘a keystone in industrial chemistry.’ For this reason, the importance of this type of catalyst increased. Additionally, the chosen type of catalyst is crucial because it effects the conversion, selectivity and yield of the desired product.

Several reasons led to use the heterogeneous catalysts in the industrial field, including (Busca, 2014, Armor, 2011, Hagen, 2006):

- They act to speed up the desired reaction.
- They are easier to separate from the liquid reactants compared with liquid catalysts.
- They are more environmentally friendly than homogeneous catalysts because they can be re-used several times whereas homogeneous catalysts must be disposed after each use.
- They are safer than liquid catalysts because they decrease problems associated with corrosion.
- In the case of endothermic reaction, the catalyst helps the reaction to continue in spite of the high temperature. Conversely, in the case of exothermic reactions, the reaction continues in spite of the temperature getting low.

The heterogeneous catalytic reaction throughout the surface of a catalyst consists of seven sequential steps, as shown in Figure 2.2 (Hagen, 2006, Figueiredo et al., 2008). These steps are:

- 1- Transport of starting materials (i.e. gaseous or liquid) through the layers of the catalyst surface;
- 2- Diffusion of reactant materials from the pore mouth to internal active sites of the catalyst;
- 3- Adsorption of these reactant materials on specific active sites;
- 4- Chemical reaction occurs over the surface of the catalyst and at the active sites;
- 5- Desorption of the products from the surface of the catalyst;
- 6- Diffusion of the products from the internal surface to the external surface of the particle;
- 7- Transport of the products from the outer surface into the homogenous fluid media.

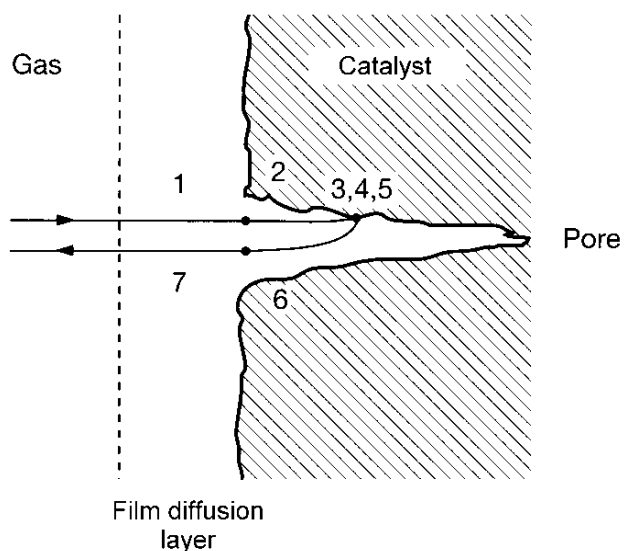


Figure 2.2. Mechanism steps of a heterogeneously catalysed reaction (Hagen, 2006).

2.2 Zeolites

2.2.1 History of zeolites

Zeolites are crucial materials in almost all chemical industries and especially in catalytic reactions and oil refineries because of their role in catalysis science (Sandoval-Díaz et al., 2015). Alex Cronstedt was a Swedish mineralogist who discovered the first zeolite mineral and described it as “an unknown kind” in 1756 (van Bekkum et al., 2001). He coined the name “zeolite” depending on the two Greek words (“Zeo” which means to boil) and (“lithos” which means rock). Barrer in 1945 put the first categorisation for the zeolite depending on the size and rate absorbed, and in 1948 he defined the synthetic zeolite (Barrer, 1978, Kulprathipanja, 2010). Union Carbide in 1959 announced the sale of Y zeolite as an isomerisation catalyst (Milton, 1989). Moreover, zeolites have been used in ion-exchange separations and the first one was at Union Carbide in 1977 (Barrer, 1978, Kulprathipanja, 2010). The 1980s have witnessed a major evolution in the zeolite production by discovering a new kind of molecular sieve with different structure and compositions (Kulprathipanja, 2010). Furthermore, at the end of 20th century the secondary synthesis modification of zeolites was developed.

2.2.2 Application and Uses of Zeolites

There are many uses and applications of zeolites whether they are natural or synthetic zeolites. The main uses of zeolites are as catalysts in many industries such as petroleum refining, petrochemical production and the production of synfuels (van Bekkum et al., 2001, Weitkamp, 2000, Weckhuysen and Yu, 2015).

In the petroleum refining part, the most popular types used in fluid catalytic cracking (FCC), hydrocracking and isomerisation are Y, ZSM-5, Mordenite (van Bekkum et al., 2001, Lenntech, 2015). Moreover, zeolites are important in the petrochemical industry for example in the alkylation process; the well-known types in this process are Y, mordenite and Beta (van Bekkum et al., 2001, Weitkamp, 2000, Hornáček et al., 2013).

There are many other uses of zeolites such as working as absorbents in purification, clean up and drying of gases (van Bekkum et al., 2001, Čejka et al., 2007). In addition, they can be used in separation process, for example the separation of *n*- paraffin from *i*- paraffin (van Bekkum et al., 2001). Similarly, it can be used as a sort of desiccant in the treatment operation of waste water. Finally, it can be used for ion-exchange for instance in the production of detergents and soap (Čejka et al., 2007, Lenntech, 2015).

2.2.3 Structures of Zeolites

Zeolites can be defined as crystalline aluminosilicate minerals, which can be formed from a connection between silica (SiO_4) and alumina (AlO_4) tetrahedral frameworks by the sharing of oxygen atoms (Weckhuysen and Yu, 2015, Kulprathipanja, 2010, Woodford, 2009). The zeolite framework structure consists of a set of secondary building units (SBUs) which are formed from combining primary building units (PBUs) (Busca, 2014). The last are established by either Al or Si atoms which are connected by four atoms of oxygen as shown in Figure 2.3.

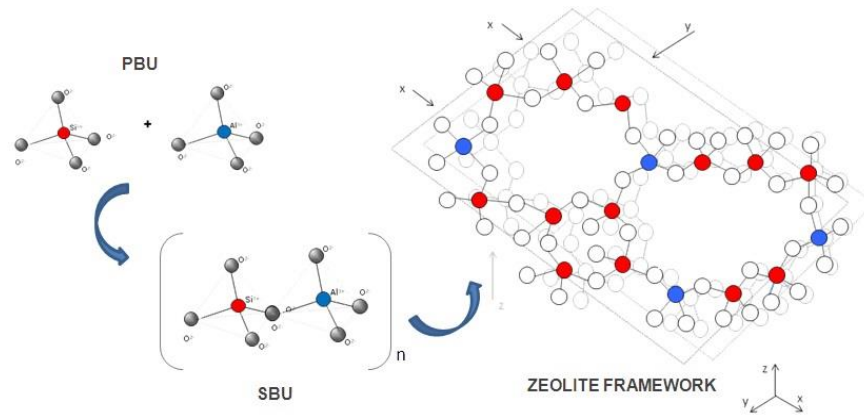


Figure 2.3. Tetrahedral units for the structure of zeolite, adapted from (Margeta et al., 2013).

In fact, the valence of silicon is four while the valence of aluminium is three, so the AlO_4 will possess a negative charge (Barrer, 1978, Barrer, 1982). Therefore, the best way to balance this negative charge, is by the addition of a positive cation like (Na^+ , K^+ and Ca^{2+}) (Weitkamp, 2000). The connection between the T-atoms happens due to the oxygen atoms; this connection is a straight line and it is symbolised by the T-O-T bridges (where T is Si or Al), and the result of this connection is rings (Weitkamp, 2000, Dann et al., 1996).

The rule of Löwenstein explains the connection method of Si and Al with oxygen; it shows the aluminium atom can be connected with four silicon atoms while the silicon is linked up to four aluminium atoms (Barrer, 1978, Weitkamp, 2000). Furthermore, the common rings have 8, 10 or 12 tetrahedra. Cages, cavities and channels are the result of the collection of SBUs depending on the number of tetrahedra atoms in the rings (Kulprathipanja, 2010). The size of the pores and the channels dimensions are necessary to illustrate the structure of zeolite (Barrer, 1982).

The International Zeolite Association (IZA) abbreviates any zeolite by a three letter code (Kulprathipanja, 2010, Busca, 2014). At the beginning of 2014, IZA increased the number of frameworks to 218 (Busca, 2014). Zeolites are a kind of microporous material according to the IUPAC classification, depending on the pore diameter (d_p):

- A- Microporous: $20 \text{ \AA} \geq d_p$,
- B- Mesoporous: $20 \text{ \AA} < d_p \leq 500 \text{ \AA}$ and
- C- Macroporous: $d_p > 500 \text{ \AA}$

Table 2.1 shows the channel size, structure, number of rings and the ratio between Si/Al mole ratio of common frameworks of zeolites (Baerlocher et al., 2007, Aguado and Serrano, 1999).

Table 2.1. The properties of the most important zeolite framework types (Busca, 2014, Baerlocher et al., 2007).

Type of Zeolite	Structure	Number of T-members in ring	Channel Size \AA	Si/Al Molar Ratio
ZSM-5	MFI	10	5.1 x 5.5, 5.3 x 5.6	10 – 1000
Beta	BEA	12	5.5 x 5.5 (tortuous) 7.6 x 6.4 (straight)	8 - 1000
Mordenite	MOR	12 (8)	6.5 x 7 (5.7 x 2.6) and (3.4 x 4.8) (elliptical)	10
Faujasite (Linde X and Y)	FAU	12	7.4 x 7.4	1 – 1.5, 1.5 - 3

2.2.4 Zeolite Type Y

Zeolite Y is one of the most important types of zeolites. It has a similar three-dimensional structure to faujasite (FAU) (Weitkamp, 2000). Lutz (2014) reported the first synthesis of zeolite Y had been made in 1964 by Breck. It can be formed by connection of small sodalite cages through 6-rings, this connection is known as a hexagonal prisms (Kulprathipanja, 2010, Busca, 2014). The result of the connection is large cages with diameter of about 13 Å which are called ‘Supercages’, accessible by three dimensional. The diameter of apertures is around 7.4 Å, consists of 12- member oxygen rings as shown in Figure 2.4.

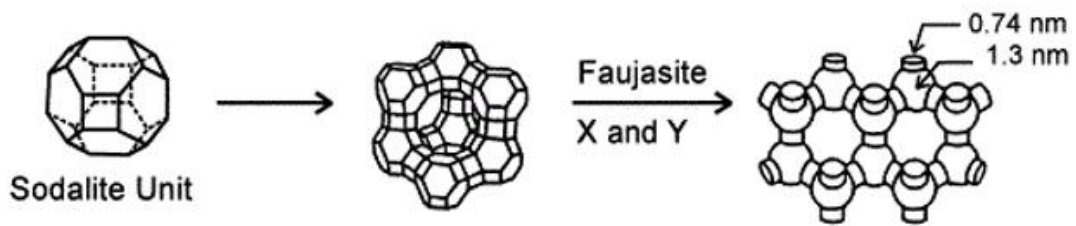


Figure 2.4. The structure of zeolite Y, adapted from (Weitkamp, 2000).

The Si/Al ratio in the Y zeolite is more than 2, and the form of Y which is preferred is a protonic form (HY), because its stability is high (Busca, 2014). There is another kind of zeolite Y which is known as Ultra Stable Y (USY); it is hydrothermally more stable and the Si/Al ratio is more than 30. Furthermore, water is a vital part in the structure of zeolites which have a high aluminium content like zeolite Y in order to increase the stability (Byrappa and Yoshimura, 2001).

2.2.5 Mordenite

Mordenite zeolite is considered as one of the most siliceous types of zeolite which has an orthorhombic zeolite structure (Busca, 2014, Simoncic and Armbruster, 2004). It comprises of one-dimensional straight channels which are created by either 12-membered rings (MR) with an opening diameter of about $6.5 \times 7 \text{ \AA}$ or 8-MR (side pockets) which have elliptical aperture diameters, approximately 8MR parallel to c direction: $5.7 \times 2.6 \text{ \AA}$ or 8MR parallel to b direction: $3.4 \times 4.8 \text{ \AA}$ as shown in Figure 2.5. Moreover, it is considered as a microporous zeolite, and the Si/Al ratio is about 10.

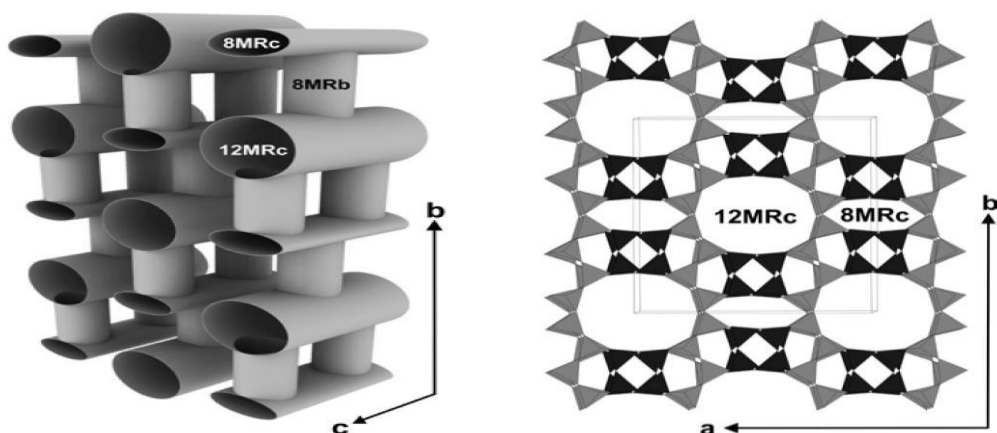


Figure 2.5. The structure of zeolite mordenite (Simoncic and Armbruster, 2004).

Mordenite is synthesised in huge amounts because it is the second one in terms of importance and is used in alkylation reactions because of its high stability and the porous structure (Horňáček et al., 2013, Čejka et al., 2007). Furthermore, zeolites with high silicon contents like mordenite are inherently less hydrophilic, therefore the stability of their structure can be improved through interaction with organic molecules (Byrappa and Yoshimura, 2001). Mordenite has many applications, such as in alkylation and dealkylation reactions, isomerisation processes and aromatic transalkylations (Busca, 2014).

2.2.6 Zeolite Beta

The family of zeolite Beta is classified as a high-silica framework (Kulprathipanja, 2010, Borade and Clearfield, 1996). It was discovered by Wadlinger and his co-workers in 1967. It has a fragile and disordered structure. Furthermore, it comprises of two various channel kinds, and their structures consist of three dimensional 12-rings for each of them, but their pore openings are different (medium and large) pores (Busca, 2014, Liu et al., 1991). The medium pore diameter is (5.5 x 5.5 Å) and the large is (7.6 x 6.4 Å) as shown in Figure 2.6.

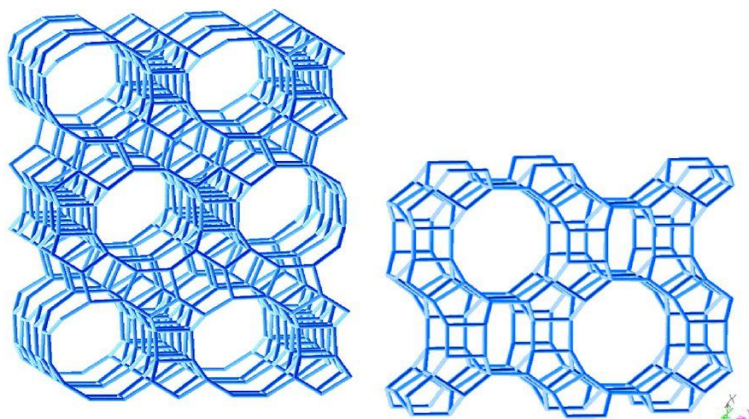


Figure 2.6. The structure of zeolite Beta (Busca, 2014).

Though the Si/Al ratio ranges between 5 and infinity, the typical ratio of Si/Al is more than 10 because zeolite Beta that has an Si/Al ratio under about ten is not crystalline (Busca, 2014, Borade and Clearfield, 1996). The zeolite Beta possesses two advantages: it is highly siliceous and its pores are large, and so there are several uses of this zeolite, for example it is used in aromatic transalkylation, alkylation, hydroisomerisation and cracking (Liu et al., 1991, Busca, 2014). Moreover, the

thermal stability increases with increased Si/Al ratio, thus the stability of zeolite beta is an interesting feature that require when it is used in the industrial field. Additionally, zeolite Beta in H-form has a large channel which permits aromatic materials to diffuse through it (Busca, 2014).

2.2.7 Water in Zeolites

One of the important features of the zeolite structure is the existence of OH⁻ molecules which are easily connected with the cation framework as shown in Figure 2.7 (Byrappa and Yoshimura, 2001).

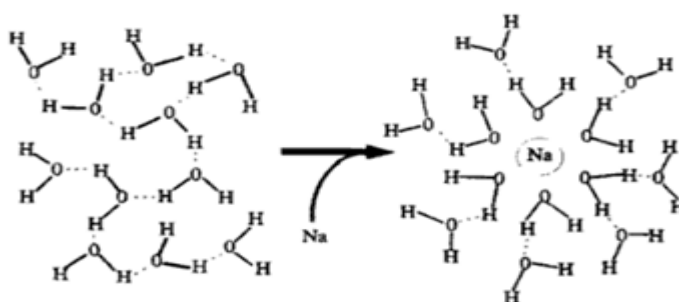


Figure 2.7. The interaction between water and cations (Byrappa and Yoshimura, 2001).

This connection is necessary because it affects the stability of the pore structure by filling the cavities of pore and as a method of hydration (Byrappa and Yoshimura, 2001). Generally, cavities and channels in zeolites are comprised of two sorts of water: chemisorbed and physisorbed water (Weitkamp and Puppe, 1999). The variance between these types is dependent on the strength of the interaction between the water and the cations. So, if the interaction is strong this results in chemisorbed water, whereas if the reverse is true, the physisorbed water is weakly bonded to the pore structure. Furthermore, the presence of physisorbed water in the zeolite structure is not desirable, so, the removal of H₂O in dehydration processes is important to increase the stability of zeolites.

2.2.8 Zeolites Classification

Zeolites are classified according to many criteria (Busca, 2014, van Bekkum et al., 2001, Guisnet and Gilson, 2002):

- 1- The first criteria have a classification based on the difference in the pore apertures:
 - A- Small pore: the pore apertures of this type are about 4 Å and contain 8- rings.
 - B- Micropores: the pore diameters are around 5-6 Å and include 10-rings.
 - C- Large pore: the pore apertures are approximately 7 Å and consist of 12- rings.
 - D- Extra-large pore: the pore diameters are larger than 7 Å and are comprised of more than 12-rings.
- 2- According to the shape of the pores: some zeolites have the same number of tetrahedra but the shape is different, the effect of the shape appears when the pores start to adsorb molecules.
- 3- Depending upon the dimension and arrangement of the channels, therefore the zeolite structure consists of one, two or three dimensions' pore system.
- 4- Other categories divide the zeolite into two types: hydrophilic and hydrophobic.
- 5- Finally, according to Si/Al ratio such as:
 - A- High silica: $\text{Si/Al} > 10$,
 - B- Intermediate silica: $1.5 < \text{Si/Al} \leq 10$ and
 - C- Low silica: $\text{Si/Al} \sim 1$.

There is a relation between the last two categories, because the zeolites which have Si/Al below 1.5 are hydrophilic as long as their framework carries a negative charge and the concentration of the cations extraframework or protonic extraframework is high (Busca, 2014, Hagen, 2006). In contrary, the zeolites are hydrophobic when they have Si/Al above 10 due to an increase in the covalent Si- O- Si bridges so, they act to take up the organic components from the mixture which consist from water and organic compounds.

2.2.9 Zeolites properties

There are several uses of zeolites including as adsorption materials or ion-exchange substances. Acidity and porosity are the most important properties for zeolites because the catalytic activity of zeolites depends on the amount of acidity, nevertheless, the porosity is effect on the shape selectivity.

2.2.9.1 Acidity of zeolites and aluminium content

Generally, zeolite has a strong acidity which it is an important feature because it is related to the ability of the zeolite to work as a catalyst in many industries (Guisnet and Gilson, 2002, Sandoval-Díaz et al., 2015, Hagen, 2006). The surface acidity is an essential property of zeolites that are used as catalysts. This activity generates strong acid sites on the surfaces of the zeolites (Weitkamp, 2000). Moreover, zeolites in the protonic form are used as acid catalysts because the protons work in the cavities to balance the cations (Busca, 2014, Hagen, 2006). In addition, the protonic zeolites are used in almost all hydrocarbon reactions such as Fluid Catalytic cracking (FCC), isomerisation and alkylation processes (Guisnet and Gilson, 2002, Busca, 2014). There are many important factors that must be understood when describing the acidity of zeolites, such as the nature of the acidic sites, density and strength of the acid centres, and sometimes the location of these acid sites (Weitkamp, 2000).

The structure of the zeolite includes both Brønsted and Lewis sites. Brønsted (protonic) acid sites can be defined as proton donor sites, while, Lewis (non-protonic) acid sites are defined as acceptors of a pair of electrons (Hattori, 2010, Sandoval-Díaz et al., 2015, Guisnet and Pinard, 2018). The acidic protons can be linked with the oxygen atoms which connect a silicon and an aluminium atom by covalent bonding as shown in Figure 2.8 (Guisnet and Gilson, 2002, Busca, 2014).

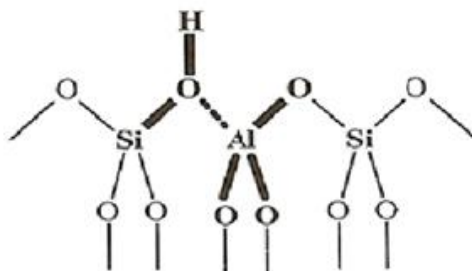


Figure 2.8. The hydroxyl bridge in the zeolite (van Bekkum et al., 2001).

Zeolites syntheses commonly have alkali metal ions to balance the charge of the framework (Hagen, 2006). There is no doubt that the zeolites are not working as a catalyst in this form and they can be changed to a protonic form to achieve the desired target. Although the alkali metal can be replaced directly by protons, another method is to replace the alkali metal with ammonium ions, which is considered to be the best approach. After that, the resulting ammonium ions are heated at between 500 and 600 °C to drive off ammonia and the proton will form, as explained in Figure 2.9 (Sandoval-Díaz et al., 2015, Hagen, 2006).

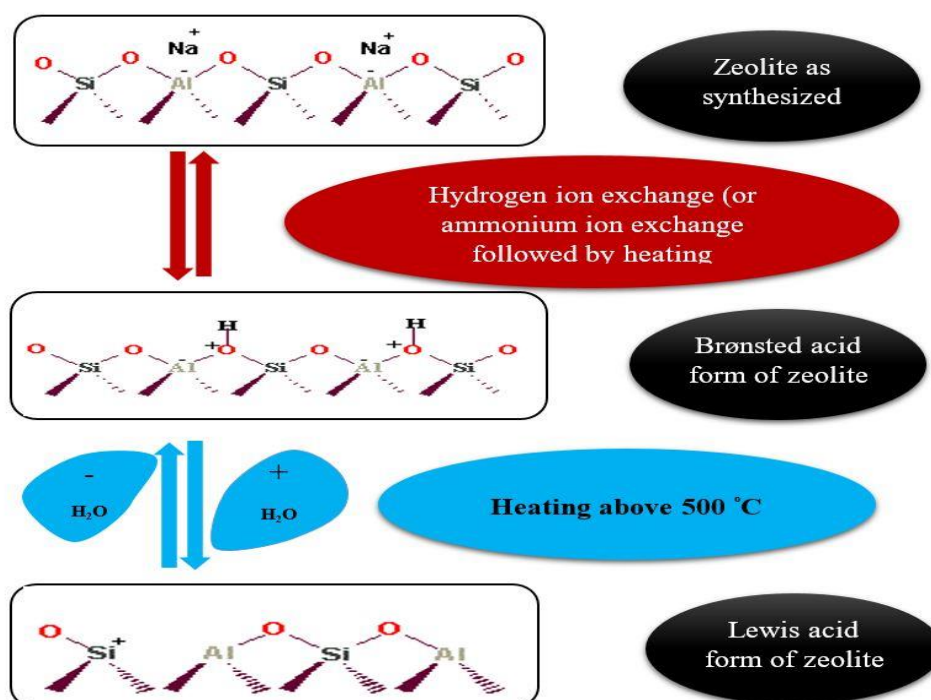


Figure 2.9. Formation of Brønsted and Lewis acid sites, adapted from (CIEC, 2015).

Brønsted acid sites are a better source of catalytic activity than Lewis acid sites (Weitkamp, 2000). Indeed, the effect of Lewis acid sites on catalytic activity is important because it promotes the strength of Brønsted sites (Wang et al., 2014, Figueiredo et al., 2008, Li et al., 2007). Brønsted acid site strength could be increased with increasing the Si/Al ratio, at the same time Lewis acid sites are not introduced (Wang et al., 2014). In contrast, the density of Brønsted acid sites decreases with increased Si/Al ratio; thereby the number of active centres will decrease. The strength of protonic sites is affected by the degree of substitution of sodium cations. The acid strength of protonic acid sites depends on the number of Al atoms (Hagen, 2006, Guisnet and Gilson, 2002). Moreover, the aluminium concentration becomes

necessary and affects the amount of Brønsted sites when the Al content is low and the zeolite is crystallised (Busca, 2014). There is a relationship between the density of protonic acid centres and the framework aluminium content (Weitkamp, 2000). Generally, FTIR, TPD and NMR are the best techniques to measure the density of Brønsted acid sites.

2.2.9.2 Shape selectivity

Shape selectivity is one of the crucial features in zeolites, and is related to the size and shape of the zeolite pore and cages at the location of the active sites (Figueiredo et al., 2008, Guisnet and Pinard, 2018). Many factors affect the size of the zeolite pores, such as number of tetrahedra and the kind of cation (Csicsery, 1984). There are several uses of shape selectivity, such as:

- A- The formation of coking can be decreased
- B- The selectivity of the required product increases
- C- Undesirable products such as impurities can be changed to small components or made into inoffensive materials

Generally, there are three types of selectivity:

- Reactant selectivity: this type can be explained when the mouth of pore allows reactants molecules that have a diameter lower than their aperture diameter to infiltrate inside the pore of the zeolite; thereby the reaction will happen at the active sites (Figure 2.10) (Busca, 2014, Figueiredo et al., 2008, Hagen, 2006).



Figure 2.10. Reactant selectivity (Bellussi and Millini, 2007).

Conversely, starting substance that has a size larger than the aperture diameter cannot enter the pore, thus, the interaction will not occur (Hagen, 2006).

- Product selectivity: this category shows that the product forms inside molecules, at the same time this product has the right size and shape to enable it to get out of the pore system (Figure 2.11) (Hagen, 2006). In contrast, if the size of the product is big, it cannot diffuse out of the pore (Figueiredo et al., 2008).



Figure 2.11. Product selectivity (Bellussi and Millini, 2007).

Several factors can affect the product selectivity, such as the size of the zeolite crystals, accumulation of some organic materials and/or cations in the structure of the zeolite and the mouth of the pores is closing (Hagen, 2006). There are several drawbacks from using this type of shape selectivity, especially when the molecule size is larger than the size of the pores aperture; in this situation, the product is still inside the pore and this leads to the generation of side products, the formation of coking and deactivation of the catalyst.

- Restricted transition state selectivity: the third kind of shape selectivity can avoid or prevent the formation of huge transition states and reaction intermediates in the zeolite cavities or channels because they require more space near the active sites than is available (Figure 2.12) (Guisnet and Gilson, 2002, Busca, 2014, Csicsery, 1984).

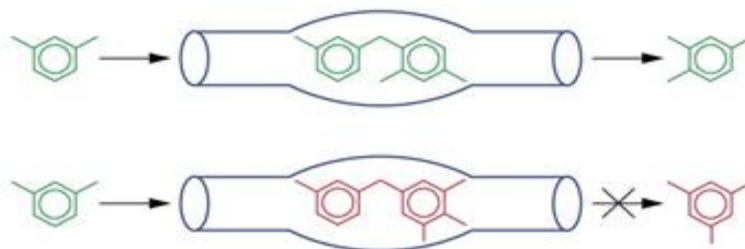


Figure 2.12. Restricted transition state selectivity (Bellussi and Millini, 2007).

Transition selectivity is similar to product selectivity so, it is difficult to distinguish between them, especially regarding the diffusion of the product when the size of the products molecules is bigger than the opening of pores, the product will be retained inside these pores and deactivation will happen (Hagen, 2006).

2.3 Zeolite modification

Many techniques are used to achieve the post-synthesis treatment of zeolites, including dealumination, desilication, ion exchange, silylation and pre-coking, which are considered as the main methods of modification (van Bekkum et al., 2001, Zheng et al., 2002).

2.3.1 Dealumination

Dealumination is the modification process that acts to remove aluminium from the framework of zeolite (Wei et al., 2015, Lutz, 2014, Figueiredo et al., 2008, Möller and Bein, 2013). Because of the complicated synthesis of Y-zeolite with a Si/Al ratio greater than 3, the dealumination modification is used (Zhang and Ostraat, 2016). In addition to producing a zeolite with Si/Al ratio above 3, this method produces a more stable and mesoporous structure.

The acidity and the thermal stability of zeolites are affected and regulated by the processes of dealumination (Pérez-Ramírez et al., 2009, Möller and Bein, 2013). Acid leaching is the widely used method for dealumination treatment (Wei et al., 2015, Silaghi et al., 2014). Barrer and Makki were the first to apply acid leaching to modify zeolites with hydrochloric acid at the beginning of 1960s (Weitkamp and Puppe, 1999, Silaghi et al., 2014). It works by immersing the zeolite in an inorganic acid, such as hydrochloric acid or acid nitric (Figueiredo et al., 2008, Lutz, 2014).

The number of acid sites is influenced by the Si/Al framework ratio, whereby the Si/Al ratio is increased through extraction of aluminium atoms from the framework (Silaghi et al., 2014, Wei et al., 2015, Zhang and Ostraat, 2016). The thermal and chemical stability of zeolite increases with an increasing Si/Al ratio when the concentration of aluminium is low.

The structure of the dealuminated zeolite has many atomic vacancies that result from the extraction of aluminium atoms. Silicon atoms act fill the vacancies caused by the removal of the aluminium ions from the zeolite structure, thereby forming a mesoporous structure as shown in Figure 2.13 (Zhang and Ostraat, 2016, Figueiredo et al., 2008).

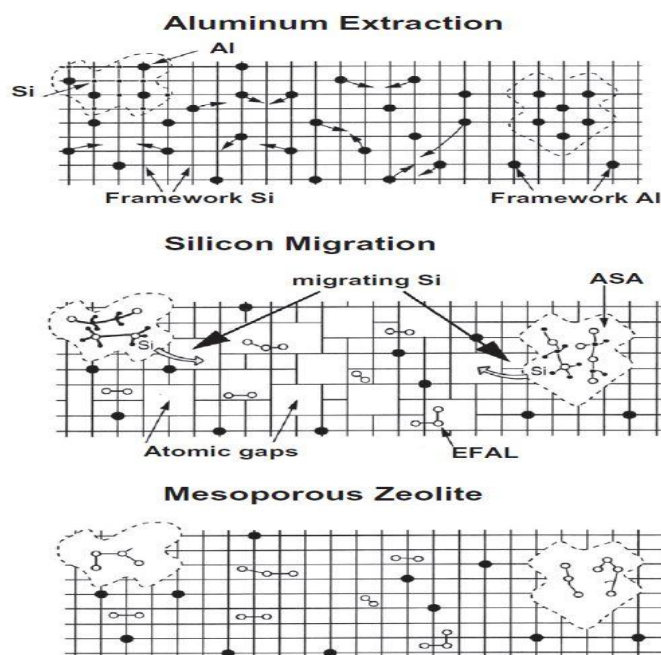


Figure 2.13. The generation of defect pores which are result from the acid leaching, adapted from (Figueiredo et al., 2008).

The important factors in the dealumination process are the concentration of acid and aluminium site stability because they have an effect on the generation of mesopores and the efficiency of the process (Figueiredo et al., 2008, Wei et al., 2015). For example, the structure of the Y zeolite is completely collapsed when the concentration of HCl is ~10 M, while it is preserved by using low concentrations of the same acid (Figueiredo et al., 2008). Furthermore, the Si/Al ratio of the starting zeolite must be taken into account because if it is less than 4.5, the structure will be demolished (Figueiredo et al., 2008, Weitkamp and Puppe, 1999). Moreover, the number of acid sites diminishes in the zeolite because of the extraction of Al atoms from the framework of the zeolite and, therefore, the acidity of the zeolites decreases after dealumination treatment (Wei et al., 2015, Horňáček et al., 2010a).

Horňáček *et al.* (2010a) discussed the impact of dealumination and the formation of mesopores on the alkylation of benzene with 1-hexadecene over zeolite Y. They found that the selectivity increases, most likely because of diminution of nonselective acid sites and formation of mesopores.

The selectivity for the phenyldodecane over the dealuminated Y zeolite was increased because of the formation of mesopores during the alkylation of benzene with 1-dodecene (Wang et al., 2001b).

2.3.2 Desilication

During the 1960s, Dean Arthur Young published the first patent focused on modification of a zeolite using alkaline media when pointed out that the performance of the zeolite increased by addition these materials (Young, 1967). Desilication (base leaching) can be defined as a process of extracting the silicon from the framework and the formation of mesopores by using base media, such as NaOH and Na₂CO₃ (Groen, 2007, Wei et al., 2015, Sadowska et al., 2013). Conceptually, a hierarchical micro-mesoporous zeolite is considered as an exemplary strategy because it acts to decrease the amount of coke deposited and increase the selectivity of the desired products (Li et al., 2018). In fact, NaOH is considered as an important medium that works to control the formation of mesopores because the removal of silicon by using NaOH is a simple and economical method.

Although the employing of microporous materials (i.e. zeolite) is attractive for hydrocarbon processes, they have many drawbacks, such as formation of side products which leads to coke formation thereby deactivating the zeolite and creating diffusion limitation problems (Christensen et al., 2003, Silaghi et al., 2014). One of the main drawbacks of zeolite is the low resistance to the formation and accumulation of coke precursors thereby rapidly deactivating this type of zeolite (Smirniotis and Ruckenstein, 1995, Siffert et al., 2000). Therefore, mesopores formation as a result of desilication treatment of the framework can be conducted to overcome these problems.

Mesoporous zeolite has many features, including high acidity and thermal stability, good mass transfer properties and high resistance to zeolite deactivation (Sadowska et al., 2013). Additionally, it works to improve the diffusion of the reactant and product by shortening the length of the diffusion path (Groen, 2007, Groen et al., 2005).

Generally, the amount of silicon in the zeolite framework is more than the amount of aluminium and this leads the creation of a network between micropores and mesopores by removing the silicon framework (Groen, 2007, Silaghi, 2014, Zhang

and Ostraat, 2016). Moreover, the role of the aluminium framework is important because it has an effect on the process of silicon framework extraction and the formation of intercrystalline mesopores (Groen et al., 2006, Wei et al., 2015). The optimal Si/Al ratio is about 25–50, as shown in Figure 2.14 (Verboekend and Pérez-Ramírez, 2011, Groen et al., 2006, Möller and Bein, 2013).

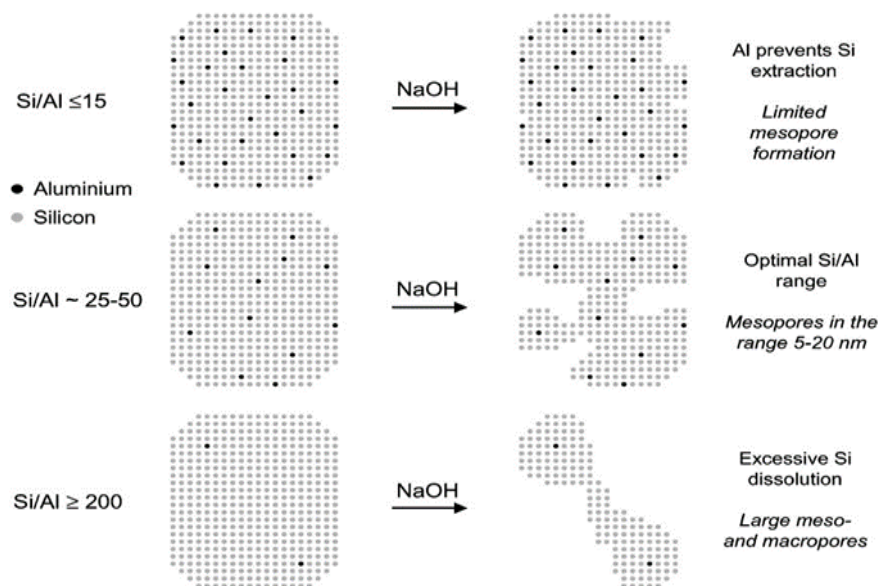


Figure 2.14. Schematic diagram shows the influence of Al content on the desilication of MFI zeolites in NaOH solution (Groen et al., 2006, Zheng et al., 2002).

When the Si/Al ratio is equal or below 15, the aluminium framework acts to prevent the formation of mesopores and the extraction of the silicon framework becomes low, while at Si/Al ratio is equal or above 200 there was excessive silicon extraction, which led to wide mesopores formation (Möller and Bein, 2013, Wei et al., 2015, Groen et al., 2006). Furthermore, the typical size of mesopores after the desilication process was about 10 nm (Wei et al., 2015, Silaghi, 2014).

Aslam *et al.* (2014) studied the role of desilication to improve the conversion and selectivity of the alkylation reaction of benzene with 1-dodecene over zeolite beta and mordenite. They got a good result, especially when the conversion and selectivity for the desired products increased for MOR and BEA, respectively. On the other hand, they obtained better diffusivity, which resulted from high stability as a consequence of the desilication.

Lin and co-worker investigated the effect of zeolite modification during linear alkylbenzene production through benzene alkylation with 1-dodecene in a FBR at pressure (101–2200 kPa) (Lin et al., 2013). They concluded the desilication modification of mordenite is more effective compared with other types of treatments because it acts to improve the stability of desilicated zeolite in addition to enhancing the selectivity of the desired product.

The catalytic stability was enhanced by desilication modification of ZSM-5 during the cracking of *n*-hexane as a result of the formation of mesopores which acts to make the coke diffusion easier (Mochizuki et al., 2012).

2.3.3 Silylation

Silylation is defined as a chemical modification which employs a bulky silylating reagent such as tetraethoxysilane [TEOS, $\text{Si}(\text{OC}_2\text{H}_5)_4$] which has a kinetic diameter of approximately 9.6-10.3 Å (O'Connor et al., 2007, Bauer et al., 2007b). This alkoxy silanes tries to react with hydroxyl groups that are located on the outer surface of the zeolite or at the pore mouth of the zeolite catalyst because it is difficult to penetrate inside the zeolite pores as shown in Figure 2.15. The deposition of TEOS on the zeolite catalyst is an irreversible reaction (Niwa et al., 1984).

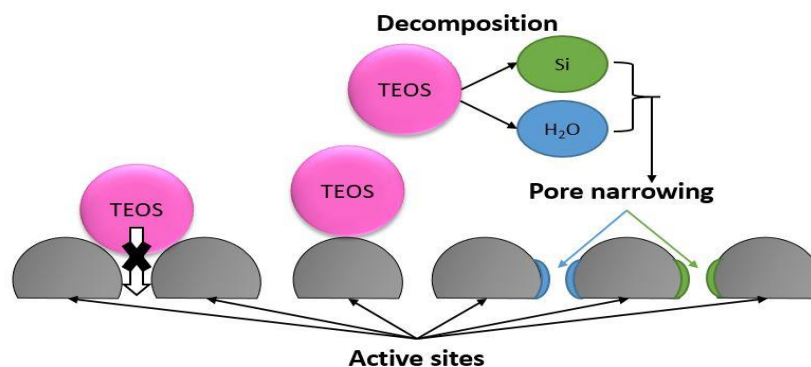
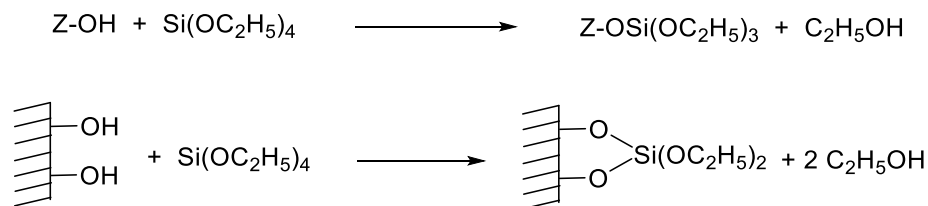
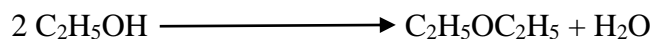


Figure 2.15. Silylation modification method.

A new zeolite catalyst is produced as a consequence of surface isolation (or vicinal isolation) by deposition of $\text{Si}(\text{OC}_2\text{H}_5)_4$ as shown in the equations below which represent the hydrolysis of TEOS:



The ethanol that is formed is converted on a zeolite catalyst into diethylether and water at temperature below 200 °C, as shown (Niwa et al., 1984):



Finally, silicon and carbonaceous materials are formed from the deposition of TEOS and during the calcination the carbonaceous materials are removed.

The objectives of silylation are improving the shape selectivity to desired products and enhancing the catalyst life time through deactivating the undesired selective sites (O'Connor et al., 2007, Bauer et al., 2004, Zheng et al., 2002). Therefore, the silylation acts to passivate undesired reactions which form on the outer surface layer and/or reduce the diffusivity of unwanted reactions. The first point happens by decreasing the concentration of strong acid sites (Brønsted sites) and covering most of the weak acid sites (Lewis sites). However, the second point occurs through either the production of some trace silicon species or water as a result of this organosilicate decomposition which leads to narrowing of the zeolite pores.

Chemical liquid deposition (CLD) is more appropriate for large-scale processes (Weber et al., 1998, Yue et al., 1996). Employing pure TEOS does not meet the requirements, especially when it reduces the external surface acidity by less than a quarter. Therefore, the use of a solvent is necessary because it impacts on the silane coverage and makes it more uniform (O'Connor et al., 2007, Weber et al., 1998). Hexane is the best solvent which can be used during silylation treatment because it helps to fully inactivate the acid sites on the exterior surface.

During the first cycle TEOS covers just the accessible sites which could prevent other molecules of TEOS reacting with more acid sites (O'Connor et al., 2007, Zheng et al., 2002, Weber et al., 2000, Niwa et al., 1984). To prevent this, the procedure is repeated several times to ensure distribution of TEOS on a large number of acid sites. Multicycles contributes to increased acid site accessibility owing to the calcination which acts to remove some of the larger ethoxyl groups on TEOS. This

activates the TEOS for another cycle as well as changing the colour of the sample from dark brown to light brown or from light brown to white. Moreover, the silylation reaction preferably occurs at temperatures below 200 °C to prevent the formation of any water drops as a result of TEOS decomposition.

Weber *et al.* (2000) employed three zeolite types (mordenite, beta and ZSM- 5) to study the effect of silylation modification through the chemical liquid deposition (CLD) procedure. They concluded that the zeolites which have high aluminium content (mordenite and beta) are influenced by pore narrowing and they were covered by TEOS more rapidly than zeolites that have siliceous content (ZSM- 5).

Shang and co-workers studied the effect of silylation modification of MCM- 22 zeolite during *n*-butene isomerisation (Shang *et al.*, 2008). They reported that the *iso*-butene selectivity was increased by controlled treatment as a result of decreasing the acid sites (not-responsible for the isomerisation reaction of *n*-butene) located on the external surface.

Niwa *et al.* (1984) indicated that the acidity of mordenite zeolite catalyst silylated by Tetramethoxysilane (TMOS) was not changed however, the pore apertures became narrower as a result of silicon alkoxide deposition. The same conclusions were reached by Kim *et al.* (1996) during the investigation of silylation modification effects on the toluene alkylation and xylene isomerisation over ZSM-5.

Hibino and co-workers revealed the increase of silane deposition acted to increase the product selectivity of *p*-xylene during the toluene methylation and disproportionation over ZSM-5 zeolite catalyst (Hibino *et al.*, 1991). In the same context, Krtil *et al.* (1997) also found the selectivity and yield of *p*-ethyltoluene were increased after the surface control modification during toluene ethylation over ZSM- 5 zeolite.

2.3.4 Modification trough pre-coked

Controlled pre-coking can be defined as a thermal modification method by using alkane, alkene or alcohol as a coke pre-cursor at high temperature before starting an experiment (Bauer *et al.*, 2001, Bauer *et al.*, 2007a, Bauer *et al.*, 2007b). The procedure of pre-coking is easy but studying features of coking, such as nature, position and formation steps, is complex (Bauer *et al.*, 2001). The understanding of

these features is important because they work to increase the lifetime of the catalysts and improve the selectivity (Bauer et al., 2007a, Chen et al., 2004, Al-Khattaf, 2007). Therefore, the main benefit from the external pre-coking is passivate the non-selective sites which are located on the outer surface of the zeolite whereas small molecules can be sneaked into the pores of zeolite, the latter leading to decreased zeolite activity (Bauer et al., 2001, Chen et al., 2004, Al-Khattaf, 2007).

The properties of coke overlayer rely on several factors such as catalyst structure, reaction conditions and nature of reactants (Fiedorow et al., 2004, Lisovskii and Aharoni, 1994). The amount of coke is one of the important criterions because any increase in this amount leads to deactivation of the catalyst, which means the treatment gives a reverse feedback (Gomez Sanz et al., 2016, Bauer et al., 2001). A reasonable amount of coke deposits on the pre-coked catalyst is usually between 0.1- 60 wt % (Haag et al., 1985, Haag and Olson, 1978b). Nevertheless, the molecular size of the carbonaceous component is a crucial part in the pre-coking treatment. The molecules which have a kinetic diameter bigger than the opening of the zeolite pores cannot penetrate the pores. Instead, they act to cover the external surface of the zeolite and the active centres that are responsible for side reactions. Thereby, it works to increase the selectivity of the desired product on account of the reduction in the unwanted products. It also works to reduce the diameter of channel apertures, which means the reaction occurs at the pore mouth of the catalyst. In fact, the coke that is deposited on the outer surface indicates there is no alteration appearing on the internal sites, as shown in Figure 2.16. (Olson and Haag, 1984).

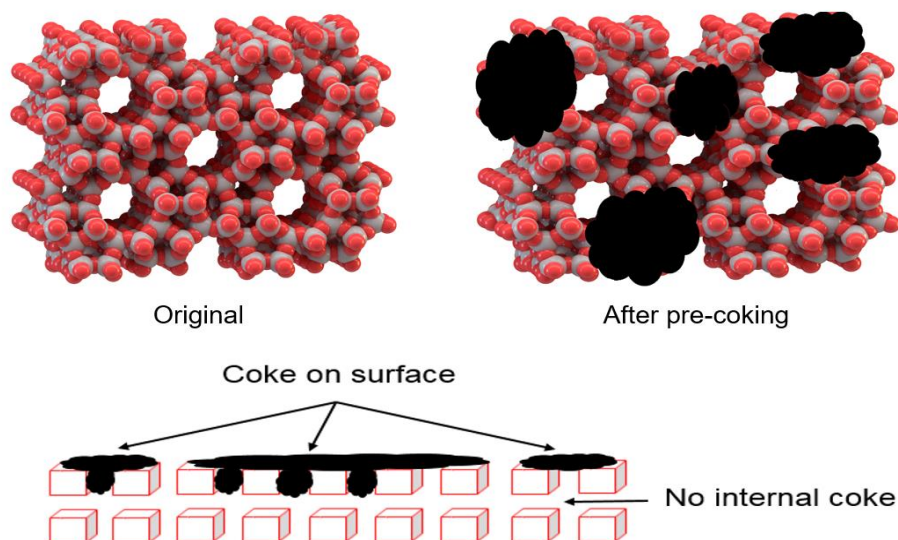


Figure 2.16. Model of coke formation on external surface of HY-zeolite, reproduced from (Tsai et al., 1999).

The type of coke plays a significant role in pre-coking, for example: non-polyaromatic coke can be removed easier than polyaromatic coke, which remains on the outer surface, and consequently, the activity becomes better whereas the selectivity of the desired product does not change (Al-Khattaf, 2007, Bauer et al., 2001).

Practically, aromatic feedstocks (in particular; toluene) are favoured as a coke source at elevated temperature (Bauer et al., 2001, Haag and Olson, 1978a). There are other feedstocks which could be employed as a coke pre-cursor in the pre-coking treatment, such as olefins, alcohols and paraffins. However, Craciun *et al.* (2007) disclosed that the deactivation becomes less significant when the conversion of 1-alkene increases more than 90%. This illustrates the olefin is the main reactant that is responsible for the deactivation of the zeolite, particularly when the selectivity of the alkylated product is increased with a decrease of olefin concentration, thereby the conversion of alkene is increased. In addition, McGregor and Gladden (2008) employed olefins as a coke pre-cursor to enhance the performance of the catalyst. And in a related context, McGregor and co-workers showed the hydrocarbonaceous laydown on the surface of the catalyst during the hydrogenation reaction has a beneficial effect on both activity and selectivity of this catalyst (McGregor et al., 2010a). Additionally, according to Gomez Sanz *et al.* (2016) the selectivity of styrene, which is an essential product in the dehydrogenation of ethylbenzene, is increased by

using aromatic molecules as a coke precursor in the pre-coking treatment compared with the fresh catalyst. Notwithstanding the above, the main disadvantage of using the small molecules is penetration of the feedstock pores which possibly leads to deactivation of some of the internal sites (Bauer et al., 2001). Cejka *et al.* (1996) studied the impact of pre-coking on the alkylation reaction of toluene with methanol by using HZSM-5 as the catalyst. They concluded that there was no change in the para-selectivity when the coke is located at the external surface while it can have a negative effect on the same product when the concentration is increased.

During the pre-coking modification, the number of acid sites decreased however, the acid strength did not change (Bauer et al., 2007b). Al-Khattaf (2007) reported the number of acid sites was influenced by the pre-coking treatment; however, there are still enough sites to enhance the reaction. Recently, Al-Khattaf et al. (2014) confirmed the previous conclusion by deducing that the total acidity reduces as a result of coke depositions relative to the coke amount.

On the other hand, alkylation and isomerisation reactions are improved by employing blocking compounds. As a matter of fact, it is rare to find that a reaction will not occur when using a fresh catalyst. If the reaction does not occur, it will do after a carbonaceous deposit is overlaid on the surface of the catalyst. For instance, Friedorow and his co-workers pointed out that despite the fresh alumina being inactive, active coke which produced from the precursor of carbon deposits on alumina to employed to enhance the products selectivity of alkyl substituted benzene reaction. Moreover, *p*-xylene alkylation was unreactive over the fresh FCC catalyst at 200 °C while it reacted on the catalyst pre-coked with isopropanol at 500 °C (Lee et al., 2004). These results are consistent with Tsai *et al.* (1999) who disclosed the selectivity of *p*-xylene was improved to 70 – 80 % after pre-coking treatment. This is owing to two reasons; narrowing the opening of the catalyst pores or/and poisoning the active sites on the external surface. On the other hand, Al-Khattaf *et al.* (2014) have recently employed HZSM-5 zeolite for ethylbenzene alkylation with ethanol. They concluded that the coke deposited on the HZSM-5 acts to increase the activity of this zeolite to desired products compared with the pure zeolite at temperatures of about 300- 350 °C.

Although there are many benefits from employing pre-coking treatment, there are several drawbacks which have appeared in the literature. Laforge *et al.*, studied the

m-xylene transformation reaction by employing MCM-22 pre-coked with *n*-heptane through a cracking reaction at a temperature of about 450 °C (Laforge et al., 2004). They revealed this paraffin did not quell the supercage sites; rather, it helped to fully deactivate this catalyst after one day of *m*-xylene transformation reaction at 350 °C. Cejka *et al.* (1996) found the effect of coke accumulated on HZSM-5 at temperature about 300-350 °C has a negative effect on the selectivity of *p*-xylene and secondary xylene isomerisation that occur on the outermost surface.

Pre-coked catalysts can be characterised to measure the amount, location and nature of coke by using various characterisation techniques, such as: thermogravimetric analysis (TGA), elemental analysis, Fourier transform infrared spectroscopy (FTIR), temperature programmed oxidation (TPO) and nitrogen sorption (Aslam et al., 2014).

2.4 Alkylation reaction

Linear alkyl-methylbenzene is the main biodegradable surfactant that is used to synthesise detergents; it is produced from alkylation of toluene with alkenes (Magnoux et al., 1997). Alkylation reaction of alkenes can be considered as a post-treatment method because it can be achieved using small amounts or no hydrogen and it acts to maintain the properties of octane number (Galadima and Muraza, 2015, Cadenas et al., 2014). Moreover, alkylation of aromatic components is a typical example of employing a heterogeneous solid catalyst which supports the environmental issues (Tsai et al., 1999). There are several applications of alkylation of aromatics with linear alkenes, such as petrochemical, chemical and refining industries (Cadenas et al., 2014). Conducting reaction in the liquid phase simplifies thermal control of the process and extends the lifetime of the zeolite catalyst (Hornáček et al., 2009a). Despite the fact that employing an acid catalyst like zeolite gives a high conversion, obtaining a high selectivity of the desired products is the main challenge (Craciun et al., 2007).

The alkylation reaction can occur by using homogeneous catalysts, such as hydrofluoric acid and sulfuric acid (de Almeida et al., 1994, Borutskii et al., 2007). Even though homogeneous catalysts have many advantages, like high activity and high selectivity for alkylation products, they have negative sides, such as causing pollution, industrial hazard, damage to equipment by corrosion and it is difficult to

separate the catalyst from the products (Wang et al., 2001a, de Almeida et al., 1994, Perego and Ingallina, 2002, Aslam et al., 2014). Finding alternative materials has become a key demand; therefore, heterogeneous catalysts appeared attractive, especially because they have acid properties, which is an interesting property in this type of interaction. Though zeolites have many positive features, such as high acidity and activity, their ability to accommodate large molecules like heptyltoluene, their safety, the fact that they can be reused multiple times and can be treated by several methods, there are several problems either because of the structure of zeolite (micropores) or reduction of heavy product diffusion by the formation of coke, which causes deactivation (Borutskii et al., 2007, Horňáček et al., 2010a, Cadenas et al., 2014, Lovás et al., 2014, Craciun et al., 2007).

The first plant for using zeolite Y in the production of alkylbenzene in the liquid phase came from Universal Oil Products (UOP) (Horňáček et al., 2009a, Horňáček et al., 2009b, UOP, 2007). In 1995, UOP announced about the first industrial process using zeolite as catalyst (Aslam et al., 2014, Kocal et al., 2001). Cowley *et al.* (2005) showed zeolite beta has a small pore structure as well as not having super-cages like Y zeolite; so, the favourable reaction will be the dimerisation of olefin instead of alkylation products because the size of the aromatic molecules is bigger than the alkene molecules. Therefore, Y zeolite exhibits higher activity for the alkylation reaction than the dimerisation and oligomerisation because it has an open pore system. On the other hand, production of all types of heptyltoluene isomers show there is non- shape selectivity as a result of using HY-zeolite (de Almeida et al., 1994). With the large pore size (i.e. Y zeolite), two factors are responsible for the zeolite activity: the acidity and ease of product desorption from the pores of the zeolite (Magnoux et al., 1997).

Monoalkylation and olefin isomerisation are the main products that result from the alkylation reaction of aromatics with alkenes over many types of zeolites (Da et al., 1999b, Craciun et al., 2007, Yadav and Doshi, 2002). Monoalkylated products are 2-, 3- and 4-alkylltoluene whereas, 2- and 3-olefin are obtained as a result of double bond shifts. 1-Heptene isomerisation is not the aim of this study but it occurs easily on a solid catalyst like zeolite (Cowley et al., 2005). Among all these products 2- heptene and 2-heptyltoluene are obtained in elevated yields however, 4- heptyltoluene is a bulk molecule and might be able to block the zeolite pores

(Craciun et al., 2007, Cao et al., 1999). Moreover, several by-products could be appearing and deactivating the zeolite, such as alkene oligomerisation and polyalkylation products. Heptene dimerisation and/or oligomerisation are the main side reactions during the alkylation reaction. The oligomeric products act to deactivate the zeolite through either blocking the active sites and pore openings or forming coke pre-cursors. In fact, all the monoheptyltoluene isomers are produced through the alkylation of toluene with 1-heptene by employing various types of zeolite (e.g. Y, mordenite and beta). Despite the fact that beta zeolite is known to have a stronger acid compared with Y zeolite, it shows a limited conversion with any Si/Al ratio probably because diffusion of products from this zeolite is difficult (Cao et al., 1999).

The shape selectivity is important to improve the selectivity of alkyltoluene products (Cowley et al., 2005). From the results of zeolite shape selectivity, the size of bi- and trialkyltoluene molecules seem bigger than the size of monoalkyltoluene. Therefore, the bi- and triheptyltoluene products are more slowly transported from the zeolite compared with monoheptyltoluene and this leads to monoheptyltoluene prevailing in the product. Additionally, the monoalkyltoluene finds it difficult to reenter the pores of the zeolite, if it is at all even possible. However, the presence of di and trialkylated products which have large molecules act to form heavy side products like toluene alkylated and olefin oligomerisations inside the pores of the zeolite (Magnoux et al., 1997). In spite of Y zeolite having a 3-dimensional cavity network and large apertures and cavities, it is non-shape selective (de Almeida et al., 1994, Cao et al., 1999).

1-Heptyltoluene is not detected in the literature and the present study because it is unstable; therefore, 2-heptyltoluene is the first stable product that can be detected (Craciun et al., 2007, de Almeida et al., 1994, Yadav and Doshi, 2002). 2-Heptyltoluene is the most biodegradable surfactant and has high solubility (Cao et al., 1999). In contrast, branched isomer forms of monoheptyltoluene have low biodegradability and are, therefore, unfavourable (Liu et al., 2009).

Furthermore, there are many factors that affect the distribution of alkylation products, such as the nature and type of zeolite catalyst, the Si/Al ratio, the density of the acid sites, the amount of zeolite and the operation conditions (Yadav and Doshi, 2002, Cowley et al., 2005). Furthermore, the lifetime of the zeolite during alkylation

reactions increases with an aromatic/alkene ratio is equal or above 5 and when the conversion of this alkene is increased (Craciun et al., 2007).

The role of temperature is important because of its effects on conversion, so finding an optimum temperature (critical) is important owing to the fact that the alkylation rate will increase accompanied with a decrease in oligomerisation selectivity (Cowley et al., 2005). Nevertheless, it is not an influential factor on the selectivity of alkylation products, because there is small variation in the alkylation rate of toluene and alkyltoluene. For example, in the alkylation reaction, if the temperature increases past the critical point, the conversion decreases owing to dealkylation (Wang et al., 2001a, Liang et al., 1996, Galadima and Muraza, 2015).

Furthermore, when the ratio of aromatics to alkenes is equal or above 5, this leads to decreased side products, thereby increasing the yield of the desired product and the thermal stability as well as decreasing the amount of coke trapped inside the pores (Galadima and Muraza, 2015, Cadenas et al., 2014, Lovás et al., 2014). Therefore, employing a high ratio of toluene to 1-heptene can promote the alkylation reaction path on the path way over of the isomerisation reaction; at the same time, the selectivity of 2-heptyltoluene will increase (Craciun et al., 2007). In contrast, double bond shift isomerisation is the main reaction when the concentration of toluene is low (Cadenas et al., 2014). Commonly, the mole ratio of aromatic: alkene is 6-8 in a commercial alkylation reaction (Cowley et al., 2005, Cadenas et al., 2014, Yadav and Doshi, 2002). Therefore, the choice of the specific ratio depends on a trade-off between the size of the reactor which gives the highest conversion and that which gives the greatest product selectivity.

TPD characterisation shows the interesting features of zeolite because it has strong acid sites that are responsible for the alkylation reaction (Wang et al., 2001a). Decreasing the Si/Al ratio leads to increases in activity because of a decrease of by- products. However, increasing the Si/Al ratio acts to increase the acid strength thereby increasing stability and decreasing the total acidity (decreased aluminium content) of the zeolite catalyst (Cao et al., 1999, Horňáček et al., 2009a).

Moreover, the conversion can be influenced by the water content, so the zeolite and reactants must be dehydrated before the alkylation reaction (Liang et al., 1996).

In addition, the reaction conversion reduces with increasing time on stream and refined use.

Several investigations have dealt with alkylation of aromatics with linear alkenes over zeolite, such as:

Da *et al.* (2001) employed two zeolites (HFAU and HBEA) in the alkylation of toluene with 1-heptene and 1-dodecene to produce linear alkylbenzene. Although the zeolite beta has small pore size, it is considered to be inactive, especially for the reaction of toluene with 1-dodecene, or slow active when using 1-heptene. This low activity is responsible for the slow desorption of products from the pores of zeolite and thereby the formation of coke. The amount of coke that is formed over HBEA is more than that formed over HFAU. In addition, the amount of coke formed over zeolite beta is similar (1-dodecene) or lower (1-heptene) than that formed by using faujasite. Monoheptyltoluene is the main product that is trapped in the beta zeolite, so the transalkylation reaction does not happen over this zeolite.

Magnoux *et al.* (1997) surveyed the production of long-chain linear alkylbenzene as well as the impact of acidity and structure of zeolite on the alkylation reaction of toluene with 1-heptene over two groups of zeolites. The first group is zeolite with large pores, such as HFAU, HMOR and HBEA and the second group has medium pores, like HMFI. They observed that the activity of the first group depends on the acidity and desorption of desired product from these pores. On the other hand, they found in the second group that the products are only formed in the pores because it is difficult to desorb these bulky molecules from the small pores of HMFI zeolite.

de Almeida *et al.* (1994) studied the production of linear alkylbenzene by the alkylation of benzene with 1-dodecene over three kinds of zeolites (HZSM-5, HZSM-12 and HY) and they showed the role of dealumination of zeolite HY. HZSM-5 and HZSM-12 zeolites in the observed low activity, whereas the activity of zeolite HY depends on the amount of aluminium, which means it depends on the Si/Al ratio. The selectivity of linear alkylbenzene reached 97–98% by using HY zeolite.

The effect of chain-length of olefins on the activity and selectivity of the alkylation reaction of benzene with 1-alkenes by using several kinds of zeolites was reported by (Hornáček *et al.*, 2009b, Hornáček *et al.*, 2010b). They found that when the chain-length increased, the conversion of 1-alkenes decreased. On the other hand,

the highest conversion was in the presence of zeolite Y and beta while the highest selectivity was achieved using zeolite mordenite. Additionally, when they used zeolite beta, they concluded that the activity and selectivity of this zeolite decreased when the Si/Al ratio increased because the amount of Al decreased or the amount of Si increased, and this led to decreased acidity. In the same context, Perego *et al.* (2013) reported that zeolite Y and beta are more active than ZSM-5, especially at low temperatures, in the alkylation reaction of benzene with olefins in the liquid phase.

Hornáček *et al.* (2009a) studied the influence of molar ratio between benzene and olefins, temperature, catalyst weight, pore size of zeolite and chain length of alkenes on the alkylation reaction of benzene with several types of olefins from C₆–C₁₈ over two sorts of zeolites, HY and HMOR. They found that the selectivity of HMOR ~59 % is more than that of HY ~21 %, whilst the conversion of HY ~100 % is higher than the conversion of mordenite ~95 %.

Yuan *et al.* (2002) pointed out that the activity and stability of Ultra-Stable Y (USY) zeolite for the alkylation of benzene with 1-dodecene by employing FBR at pressure ~3.0 MPa is affected by the reaction conditions and the temperature of the pre-treatment step which reduces the coke amount because they act to increase the strength of the acid sites and decrease both the number and density of the acid sites, as well as sometimes creating mesopores.

Cowley and co-workers investigated the influence of the zeolite structure for Y and Beta types through the toluene alkylation with 1-pentene in a FBR (Cowley *et al.*, 2005). They concluded the Y zeolite is more active than the Beta zeolite.

2.4.1 Mechanism of alkylation reaction

The reaction network of 1-heptane isomerisation and alkylation products is shown in Figure 2.17 (Magnoux et al., 1997).

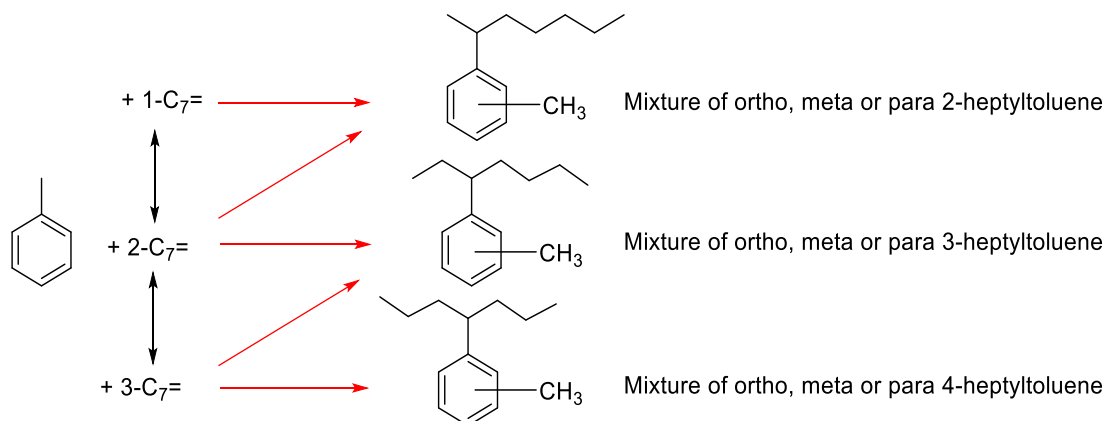


Figure 2.17. Production of monoheptyltoluene by alkylation of toluene with 1-heptene (Magnoux et al., 1997).

Alkylation is considered as irreversible reaction (Craciun et al., 2007, Magnoux et al., 1997). The mechanism of toluene alkylation with heptane shows that 2-heptyltoluene can be produced from alkylation of toluene with either 1-heptene or 2-heptene; 3-heptyltoluene can be produced by toluene alkylation with 2-heptene or 3-heptene; and 4-heptyltoluene can be produced from alkylation of toluene with 3-heptene only, as shown in Figure 3.3.

In this reaction, monoheptyltoluene is the main product from the alkylation of toluene with 1-heptene (Magnoux et al., 1997, Cowley et al., 2005, Craciun et al., 2007). It consists of a mixture of (ortho, meta and para) 2, 3 and 4-heptyltoluene. These three products are separated by GC; where 2 and 3 heptyltoluene appear in three peaks, the biggest two represent ortho and para isomers; however, 4 heptyltoluene appears in just one peak representing the ortho isomer. Biheptyltoluenes are formed as a result of alkylation of monoheptyltoluene, while triheptyltoluenes are produced by the alkylation of biheptyltoluene.

2.5 Coke and deactivation

Coke is defined as a complex mixture of carbonaceous compounds that consists of substances of a range of structures and origins (Guisnet and Pinard, 2018, Busca, 2014, Figueiredo et al., 2008). It is formed during the chemical reaction by the deposition of heavy by-products and it is the main reason for catalyst deactivation. The variation in the properties of the catalyst is called deactivation. Economically, the losses that come from catalyst deactivation are high, therefore studying the role of the coke structure, nature, composition and amount becomes important. Heavy by-products result from the organic compounds that interact with the heterogeneous catalyst; these products impact on the rate of deactivation (Argyle and Bartholomew, 2015, Guisnet and Magnoux, 2001, Mori et al., 1991). However, the term coke precursor represents the intermediate components that form during complicated reactions (Brillis and Manos, 2003). Several mechanical, chemical and physical changes happen to the catalyst during the reaction, either to increase or decrease the activity or selectivity; these alterations effect the stability of the catalyst (Wan et al., 2018, Guisnet and Ribeiro, 2011, Sie, 1980).

Obviously, the morphology and structure of pores, the acidity of zeolite, Si/Al ratio, operating conditions (time, temperature and concentration) and nature of reactant and location of the coke in/on the pores affect the deactivation (Zhou et al., 2017, Guisnet and Ribeiro, 2011, Brillis and Manos, 2003). The determination of coke composition is difficult because coke is a complicated compound and it is tricky to detach from the catalyst (Brillis and Manos, 2003, Guisnet and Magnoux, 2001).

Many ways act to reduce the formation of coke, thereby limiting deactivation, such as (Argyle and Bartholomew, 2015, Guisnet and Magnoux, 1997):

- 1- Choosing a special kind of zeolite which have three dimension (the cavities are large while the openings of pores are small).
- 2- Minimise the density and strength of the acid sites to select the desired product.
- 3- Change the operating conditions until finding the optimum conditions to avoid coke formation.

2.5.1 Effect of pore structure

The formation of coke is considered a shape selective reaction and Rollman and Walsh were discovered that (Chaouati et al., 2017, Argyle and Bartholomew, 2015, Guisnet and Magnoux, 1989). The pore structure of zeolite plays a main role in coke formation because it affects the rate of coke formation and thereby the deactivation (Zhou et al., 2017, Argyle and Bartholomew, 2015, Figueiredo et al., 2008). In general, most reactions occur in the cavities, cages and channel intersections of zeolite catalysts (Wan et al., 2018, Zhou et al., 2017). The coke is formed inside the pores of the zeolite more than on its external surface. Indeed, a high coking rate occurs when the cavities or channels in zeolite structure are large, so the zeolite has a big space to form the coke, or if the diffusion of coke is slow. The amount of coke is directly proportional to the zeolite deactivation i.e. when the coke content increases, the deactivation becomes faster (Guisnet and Magnoux, 1989). Therefore, choosing a suitable pore size is a crucial step. Selection of large pores helps to form the large molecule intermediates of the main products, however the small sizes act to prevent coke formation as a result of these intermediates becoming trapped inside the pores. In the case of zeolite Y, it contains large cages, thus the rate of coke formation is high or medium (Brillis and Manos, 2003, Figueiredo et al., 2008, Guisnet and Magnoux, 1989).

2.5.2 Role of mesopores

Interestingly, modification of protonic zeolites by dealumination, desilication and ion exchange act to limit some of the acid sites' properties, such as strength and density, which gives a high reaction rate as well as limiting or slowing the formation of coke (Zhou et al., 2017, Bleken et al., 2013, Guisnet and Ribeiro, 2011). The generated mesoporous structure acts to increase the longevity of zeolite catalysts (Kim et al., 2010). The mode of deactivation is changed after desilication treatment to acid sites coverage instead the pore blocking (Chaouati et al., 2017). However, Lee *et al.* (2017) detected the mesoporous could not decrease the coke amount but it acts to convert its location. Moreover, the mesoporous structure acts to increase the amount of coke because of the increase in both volume and external surface area of the zeolite catalyst which could then act as a reservoir for the coke (Wu et al., 2015).

Chaouati *et al.* (2017) reported that modification of the zeolite by desilication acts to remove some of Brønsted sites and forms extra framework aluminium (EFAl). This works to prevent the reactants accessing the protonic acid sites and/or increasing the strength of these acid sites and this acts to increase the rate of coke formation.

2.5.3 Effect of acid sites

Several factors control the deactivation process. These include; high acid site strength and density, the diffusion of intermediates and the rate of reaction (Brillis and Manos, 2003, Guisnet, 1990). Acidity is one of the most important factors that leads to deactivation of the zeolite *via* coke formation. In contrast, Wichterlová *et al.* (1999) showed that the selectivity increases and coke formation reduces with decreasing acid site density. The coke often prefers the strongest acid sites to form on and this leads to deactivation of these sites. A decrease of many factors in the acid sites, like number, activity and accessibility, lead to reduced activity of the catalyst and sometimes reduced selectivity for the main products. A Si/Al ratio below 3 is not preferred owing to high acid site concentrations which leads to the formation of more coke and a more rapid deactivation of the catalyst (Kim *et al.*, 2010).

2.5.4 Effect of operation conditions

2.5.4.1 Temperature

The temperature has a vital role on the nature of the coke (Wan *et al.*, 2018, Rojo-Gama *et al.*, 2017). The reaction rate increases with increasing reaction temperature, as shown by the Arrhenius equation, and this leads to the formation of more coke; in addition, it acts to increase the desorption rate of the coke pre-cursor (Brillis and Manos, 2003, Mori *et al.*, 1991, Guisnet and Magnoux, 1989). Coke which is formed at temperatures above 250 °C often has a C/H ratio below 0.8. The reactions that are affected by changing the temperature usually have the highest activation energy. Higher or stronger adsorption happens at low temperature in contrast with high temperatures that cause coke formation as a result of trapping the big molecules inside the pores.

2.5.4.2 Time-On-Stream (TOS)

In general, the deactivation is affected by the time-on-stream; usually the deactivation of fresh catalyst begins rapidly but becomes slower during the reaction

(Müller et al., 2015, Brillis and Manos, 2003, Hopkins et al., 1996). Brillis and Manos (2003) detected that the amount of coke increases at the lowest Weight Hourly Space Velocity (WHSV). Furthermore, during the first twenty minutes, approximately three-quarters of the coke is formed. The rate of coke formation decreases more sharply than the rate of reaction (Argyle and Bartholomew, 2015, Guisnet and Magnoux, 1989). Furthermore, Guisnet and Magnoux (2001) showed the coke composition depends mainly on the amount of the coke which is retained on the zeolite catalyst.

2.5.5 Coke and deactivation classification

There are two types of coke composition: catalytic and non-catalytic carbon (Figueiredo et al., 2008, Guisnet and Magnoux, 1989). The first kind occurs at temperatures below 300 °C when the surface of the heterogeneous catalyst reacts and the carbon can be determined from the nature of this surface. The second sort consists of tars and pyrolytic carbon, and is produced at temperatures above 500 °C.

Other classifications depend on the reaction temperature. There are two types of coke formation (Wan et al., 2018, Guisnet et al., 2009, Chen and Manos, 2004):

- 1- When the temperature is less than 200 °C, coke forming depends on the steps of condensation and rearrangement and the types of coke are non-polyaromatic, white and soft, and their properties depend on the reactant.
- 2- When the temperature is more than 350 °C, the kind of coke formed is polyaromatic, black and hard, and the formation of coke in the presence of acid zeolite depends on the hydrogen transfer step, condensation and rearrangement steps. This type of coke is analysed by XRD and Raman spectroscopy.

There are two types of coke: either soluble or non-soluble in methylene chloride. The first type works as an intermediate in the process of non-soluble coke formation (when the soluble coke is trapped inside the cavities or channels (Guisnet and Magnoux, 1989). Soluble coke occurs at low coke content and it is located on the outer surface of pores, whereas insoluble coke only forms at high coke content and it is often located inside the pores. Therefore, the internal coke has more effect on the zeolite deactivation compared with the external coke (Wan et al., 2018, Lee et al., 2017).

Additionally, depending on the operating conditions, the deactivation can be divided into two types: reversible and irreversible (Argyle and Bartholomew, 2015, Guisnet and Ribeiro, 2011, Sie, 1980). The first type happens when the active compounds pass through the catalyst and can be removed by oxidation, whereas in irreversible deactivation, the activity of the catalyst decreases so the catalyst needs to be treated by either rejuvenation or regeneration, like coke metals. Another classification is suggested by Menon (1990) as sensitive or insensitive coke. During the coke sensitive reaction, the coke acts to decay the activity of acid sites, whereas the coke which is formed in coke insensitive reactions also deposits on the active sites but it is not removed by any gasifying agent.

2.5.6 Coke characterisation

The nature of coke components is measured by FTIR, UV-vis and Raman. The advantages of these techniques are (Guisnet et al., 2009, Lange et al., 1988):

- 1- They are non-destructive so the sample can be used in other techniques.
- 2- They work to study the reaction and coke characterisation at the same time.
- 3- FTIR and Raman can be used to study the interaction between the active sites of the catalyst and the coke that forms on these sites.

Generally, FTIR spectroscopy is one of the most useful techniques as it gives important information pertaining to deactivation resulting from coke formation, such as (Guisnet and Ribeiro, 2011, Cerqueira et al., 2000):

- 1- The quantity of coke that deposits on/in the catalyst.
- 2- Coke components and their nature.
- 3- The impact of coke on the hydroxyl groups.

Elemental analysis gives information about the coke composition, such as the ratio of hydrogen to carbon (Guisnet et al., 2009, de Lucas et al., 1997). The hydrogen to carbon ratio is important in hydrocarbons transformation. Generally, the ratio of hydrogen to carbon decreases when the time-on-stream increases with increasing of the coke content (Guisnet and Magnoux, 1989). Furthermore, the type of hydrocarbon is necessary because it affects the rate of coke formation and the amount of coke deposited on/at the catalysts (Menon, 1990).

The amount of coke which formed on post-reaction catalyst is measured by thermogravimetric analyser (TGA) (Wu et al., 2015, Mekki-Berrada and Auroux, 2012). Temperature programmed oxidation (TPO) is employed as a thermo-analytical measurement to investigate the type of coke (Suwardiyanto et al., 2017).

2.5.7 Benefits of coke

Although coke formation is harmful, sometimes coke works as a partner in several main processes during the reaction or plays a useful role (Collett and McGregor, 2015, Guisnet and Pinard, 2018). Moreover, in many cases, coke works to increase the selectivity for the desired product. For instance, the selectivity increases to para isomers of alkylation by using zeolite HMF1 when coke is deposited inside or at the surface of the pores (Guisnet and Ribeiro, 2011). Keating and co-workers highlighted that the main advantage of coke in the production of para-xylene by using alkylation of toluene and methanol over zeolite ZSM-5 is that the selectivity increase from 24% to about 90% when the catalyst surface is coated by the carbonaceous polymers (Kaeding et al., 1981). In addition, Enchigoya and his co-workers contend that the catalyst activity increases with time on stream because the coke acts as active sites (Menon, 1990). In the 1970s, Somojai and his co-workers observed that a carbonaceous overlayer acted as an active region, especially in hydrocarbon reactions over metal solid catalysts. Moreover, in the Fischer–Tropsch synthesis, the carbon can be divided into two types: carbidic carbon, which is used as a reactive intermediate, or graphitic carbon, which acts to deactivate the catalyst.

2.5.8 Catalyst deactivation modes

The deactivation that results from coke formation can occur either by poisoning or blockage of the active sites of zeolite (the latter is the fastest and it is affected by the pore structure of zeolite) (Wan et al., 2018, Chaouati et al., 2017, Guisnet and Ribeiro, 2011, Hopkins et al., 1996). Acid site poisoning occurs as a result of irreversible adsorption of undesired coke on the active centres. However, pore blockage happens as a result of the diameters for both reactant molecules and zeolite pores being approximately the same. In general, pore blockage leads to more deactivation than active sites coverage (Argyle and Bartholomew, 2015, Guisnet et al., 2009).

There are three modes of deactivation (Guisnet and Magnoux, 1997, Guisnet and Magnoux, 1989):

- 1- Limiting or preventing the reactants from reaching the active sites.
- 2- Block the aperture of cavities or channels by filling with coke molecules.
- 3- The coke works to close the opening of the pores and then it prevents the reactants from accessing the active sites that are empty of coke.

The detention of coke molecules over the acid zeolite occurs because of either chemical factors, e.g., strong chemisorption (adsorption), or physical agents, such as decreased volatility (gas phase) or diminished solubility (liquid phase) (Guisnet and Ribeiro, 2011, Guisnet and Magnoux, 2001). Usually, in liquid phase reactions of organic materials using zeolite, deactivation occurs as a result of the strong chemisorption of the main product molecules in the micropores; therefore, the products will reside for a long time inside these pores, and thereby will change to coke (Guisnet and Ribeiro, 2011). Generally, deactivation can be divided into two types depending on the contact time; a long contact time leads to the rapid formation of coke as a result of aggregation of the coke pre-cursor and deactivation occurs as a consequence of pore mouth blockage (Argyle and Bartholomew, 2015). However, a short contact time forms the coke more slowly than the first case and the deactivation happens owing to coverage of the acid sites.

Mori et al. (1991) showed the mode of coke deposition over HY zeolite was acid site coverage and they failed to consider the pore blockage becoming the main reason for the deactivation because this zeolite has a three dimensional cages. Elsewhere, Guisnet and co-workers showed the deactivation of three dimensional zeolite (i.e. Y zeolite) is dependent on the coke content (Guisnet et al., 2009). At low content, site coverage is the main mechanism. This represents a transition phase because it gradually develops to the common case of pore blockage when the coke content is increased.

2.5.8.1 Acid site poisoning

Ordinarily, there are three models which contribute to limiting the poisoning of active sites: uniform poisoning, selective poisoning and pore mouth poisoning (Guisnet and Ribeiro, 2011, Hopkins et al., 1996, Melkote and Jensen, 1989, Butt and Peterson, 1988).

Firstly, the uniform site coverage occurs when coke acts to deactivate all the acid sites equally. It occurs when the poisoning reaction rate is smaller than the diffusion rate of the poison; therefore, the poison permeates deep in the zeolite pore and deactivates the active sites. Based on this model, the zeolite activity decreases linearly with the number of acid centres.

Secondly, selective poisoning happens when the zeolite catalyst has some acid sites which are more active compared with other sites and this leads to coke deactivating the acid sites unevenly. The acid strength of the zeolite catalyst is determined by measuring the Si/Al ratio, and it contributes to describing how the zeolite deactivates. During this model, the selectivity to the main product increases as a result of decreasing the undesired products, the last occurs as a consequence of the coke choosing either Brønsted or Lewis acid sites. The main assumption in this model is the catalytic activity reduces farther than the total number of acid centres, and this leads to alterations of the strength of the acid sites.

Finally, pore mouth poisoning occurs at the zeolite external surface near the pore mouth opening. This model is somewhat similar to the first ‘uniform poisoning’ type however, the difference is in the diffusion of the poison rate which is slower than the poisoning rate. As a result, for the high reaction rate, the acid sites near the outer surface are more active and contribute more to the reaction than the internal sites. The deactivation starts in a fluffy shell on the outer surface of the zeolite catalyst and then becomes larger to cover most of the exterior layer and includes the interior of the pores. In this case, the deactivation is faster, although a number of active centres are still available.

2.5.8.2 Pore blockage

Pore blockage occurs inside the zeolite pores when the coke accumulates and blocks the intersections of these catalysts and inhibits the reactants access to the active sites (Wiedemann et al., 2016, Guisnet and Pinard, 2018, Hopkins et al., 1996, Melkote and Jensen, 1989). Most of the coke is located near the pore mouth and a small amount covers the active centres. Deactivation in this way has more effect than site poisonings (Chaouati et al., 2017, Fiedorow et al., 2004, Lee et al., 2004). Indeed, there are three categories of pore blockage: pore mouth plugging, core plugging and bulk phase plugging (Chaouati et al., 2017, Guisnet and Ribeiro, 2011, Hopkins et al., 1996).

Pore mouth plugging assumes the catalytic activity reduces faster than the number of acid sites that are deactivated; additionally, through pore blocking, the diffusion rate is decreased.

Core plugging occurs when the coke penetrates inside the zeolite pores and blocks the deep intersections. In this case, the catalytic activity depends on the number of remaining active sites.

Bulk phase plugging covers both the two types described above with a greater formation of coke on the external surface of the catalyst. This inhibits the reactant molecule's access to the active sites.

2.5.8.3 Pore mouth catalysis

In some situations, the external surface plays an interesting role in guiding the selectivity towards a specific product (Wiedemann et al., 2016). For the sake of simplification, pore mouth catalysis expression represents the reaction location which is usually at the pore edge.

During oleic acid skeletal isomerisation over ferrierite zeolite catalyst, in spite of the rapid pore clogging, the selectivity still increases due to the phenomena of shape selectivity in the pore mouth (Wiedemann et al., 2016, Wiedemann et al., 2015, Wiedemann et al., 2014). In their interpretation, they relied on the pore mouth assumption because the blockage of external acid sites occurs through the use of large molecules. A decrease in the side reactions as well as the pores being filled by coke (pre-courser) support this hypothesis.

The hypothesis of pore mouth catalysis was the main explanation for the rise in isobutene selectivity during 1-butene isomerisation over ferrierite zeolite catalyst at long times on stream (Meunier et al., 2002, van Donk et al., 2001). They depended on the coke pre-courser which deposits in pore openings and acts to reduce the cracking reaction and thereby increase the isobutene selectivity. The filling of zeolite pores by undesorbing aliphatic carbonaceous components which are synchronous with increasing the 1-butene conversion indicates the role of pore mouth catalysis. However, increasing the time on stream leads to complete deactivation of these pore mouths as a result of polyromantic coke formation.

On the same context, Andy *et al.* (1998) explained pore mouth catalysis occurs as a result of zeolite pore filling by carbonaceous components which act as active sites near the pore mouth of the zeolite catalyst.

Mihindou-Koumba *et al.* (2008) highlighted the importance of active sites that are located at the pore mouths during methylcyclohexane transformation using H- EU- 1 zeolite catalysts. They showed that the cracking reaction occurred on the internal acid sites and this leads to blockage of these pores as a consequence of coke formation, therefore the isomerisation reaction occurs on the active sites located at the pore mouth. The high catalytic activity supports this hypothesis despite the fact that the micropores are filled by coke. To support that, they completed other experiments to show that pore mouth catalysis explains the main location of the isomerisation reaction by covering the external surface with 2,4-dimethylquinolin (collidine). Although the collidine could be close some of pore opening, it was enough to support the pore mouth catalysis phenomena.

In summary, the existing literature shows that coke deposits can play a positive role in enhancing the selectivity of the desired products during the transformation of hydrocarbons. In the present study, Chapter 5 illustrates the role of carbonaceous materials that are formed during toluene alkylation with 1-heptene over fresh, dealuminated and desilicated zeolite catalysts. The role of carbon deposits formed during the pre-coking treatment using the same reaction will be studied in Chapter 6.

Chapter 3

Characterisation techniques

3.1 Introduction

Several characterisation techniques are employed in this thesis to study the fresh zeolite and coke formed properties such as the acidity, pore size, morphology, Si/Al ratio and amount, structure and nature of coke. These techniques are:

3.2 X-ray diffraction

X-ray diffraction (XRD) is one of the most important techniques utilised to identify the phase of crystalline materials (Dutrow and Clark, 2016, Font-Bardia and Alcobé, 2012). It depends on the diffraction phenomena that occur following the collision between the X-ray diffraction such as electrons and neutrons with a solid sample (Figure 3.1) (Font-Bardia and Alcobé, 2012).

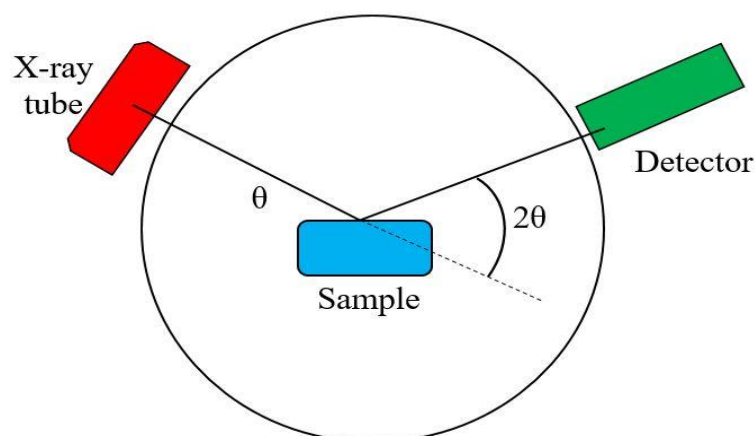


Figure 3.1. X-ray diffractometer parts adapted from (Connolly, 2007).

XRD can be used to investigate the properties of materials. In zeolite, applications include the study of the crystal structure and differentiating between amorphous and crystalline substances (Dutrow and Clark, 2016, Font-Bardia and Alcobé, 2012, Connolly, 2007).

Predominantly, XRD consists of three portions: a holder and goniometer, X-ray tubes and a detector (Font-Bardia and Alcobé, 2012, Connolly, 2007, Busca, 2014). Usually, the goniometer with the specimen stage is located in the centre. It is utilised to rotate the specimen in the path of the X-ray beam at an angle (θ). The X-ray

instrument consists of primary and secondary arms. The x-ray tube and the incident beam optics in its primary arm and the diffracted beam optics and a detector in its secondary arm. The detector is used to collect the reflected X-rays. It is mounted on the secondary arm and rotates at an angle (2θ) (Font-Bardia and Alcobé, 2012, Dutrow and Clark, 2016, Connolly, 2007).

The cathode ray tube generates the X-rays by heating the filament to produce electrons, these electrons are accelerated towards a target material (Cu, Mo, Ag, Fe and Cr) by applying a voltage (Dutrow and Clark, 2016, Font-Bardia and Alcobé, 2012). After that, the target material is bombarded with the electrons. In general, X-ray spectrum result when the energy of the electrons becomes able to displace inner shell electrons of the substance. Subsequently, X-ray beams emerge and collide with the sample. At the end, the detector records the intensity of diffracted X-rays and the results are displayed on the monitor.

Bragg's law is used to analyse the XRD data (Robson, 2001, Connolly, 2007):

$$n\lambda = 2d \sin\theta \quad \dots\dots (3.1)$$

where: n is an integer representing the diffraction peak order, λ is the wavelength of the X-ray, d is the distance between the two parallel planes in the atomic structure and θ shows the scattering angle.

Miller Indices are a group of three numbers or letters used to indicate the position of a face or internal plane of a crystal and determined on the basis of the reciprocal of the intercept of the face or plane on the crystallographic axes (Gerlach and Dotzel, 2008). Therefore, the (hkl) values have to be assigned to each of the reflections to determine the size and shape of the unit cell. When considering the general case of (hkl) planes, Equation 3.1 can be re-written as:

$$\lambda = 2d_{hkl} \sin \theta_{hkl} \quad \dots\dots (3.2)$$

Where, (d_{hkl}) incorporates higher orders of diffraction i.e. (n) greater than 1.

The peak position (2θ) can be calculated from Bragg's law (Equation 3.2) by using the following expression:

$$\theta_{hkl} = \arcsin \left(\lambda / 2d_{hkl} \right) \quad \dots\dots (3.3)$$

Zeolite-Y is a cubic unit cell. A simple manner is employed to drive the relationship between the (hkl) , d-values and the unit cell parameters a, b, c, α , β and α depending on the following crystal data for zeolite-Y: the dimensions: $a = b = c \approx 24.7 \text{ \AA}$, the angles: $\alpha = \beta = \gamma = 90^\circ$ and X-ray single crystal refinement, $R = 0.13$.

$$\text{Thus, } d_{hkl} = a_0 / \sqrt{N}$$

Where,

$$\sqrt{N} = \sqrt{h^2 + k^2 + l^2} \text{ and } a_0 \text{ is the dimension of a unit cell.}$$

The angular positions of the reflections contribute to the determination of the cubic symmetry of a unit cell. Treacy and Higgins (2007) determined the XRD-data for a standard faujasite (FAU) specimen, as shown in Table 3.1. This typical XRD-data contributes to the measurement of the purity of solid crystals by comparing the pattern of an X-ray diffractogram of the fresh zeolite sample with the modified sample.

Table 3.1. XRD-data for typical faujasite with Cu $K\alpha$ radiation; $\lambda = 1.5418 \text{ \AA}$, and $a_0 \approx 24.7 \text{ \AA}$ (Treacy and Higgins, 2007).

h	k	l	$2\theta^\circ$	d, \AA	I _{rel}	h	k	l	$2\theta^\circ$	d, \AA	I _{rel}
1	1	1	6.19	14.284	100	7	3	3	29.55 *	3.220	0.5
2	2	0	10.11 *	8.747	1.4	8	2	2	30.66 *	2.916	1.1
3	1	1	11.86 *	7.459	2.0	6	6	0	30.66	2.916	0.7
4	0	0	14.32	6.185	0.5	5	5	5	31.31 *	2.857	2.0
3	3	1	15.61 *	5.676	4.5	7	5	1	31.31	2.857	0.3
4	2	2	17.56	5.050	0.3	8	4	0	32.37 *	2.766	1.1
5	1	1	18.64 *	4.761	2.7	9	1	1	32.98	2.716	0.5
4	4	0	20.3 *	4.373	2.5	7	5	3	32.98	2.716	0.5
4	4	2	21.55	4.123	0.4	8	4	2	33.19	2.699	0.1
6	2	0	22.73	3.912	0.2	6	6	4	33.99 *	2.637	1.3
5	3	3	23.58 *	3.773	5.6	9	3	1	34.58	2.593	1.0
4	4	4	24.93	3.571	0.2	8	4	4	35.55	2.525	0.1
7	1	1	25.72	3.464	0.1	7	5	5	36.12	2.486	0.1
5	5	1	25.72	3.464	0.5	8	6	2	37.06	2.426	0.3
6	4	2	26.97 *	3.306	2.4	10	2	0	37.06	2.426	0.3
7	3	1	27.7	3.221	0.5	6	6	6	37.79 *	2.381	0.6
8	0	0	28.87	3.092	0.2	7	7	5	40.43	2.231	0.2

* These angles were selected carefully for the comparison of X-ray diffraction patterns of the reference sample with the modified specimen.

Figure 3.2 shows the fundamental features required to assess the peaks that result from XRD. The first of these is the intensity, which relies on the type and location of atoms in the unit cell (van Bekkum et al., 2001, Font-Bardia and Alcobé, 2012). It can be considered as the main property especially when determining the percentage of crystallinity (Ojha et al., 2004). A second feature is 2θ , the position of the peak. Each sample has a unique XRD diffraction pattern, therefore, to identify and classify the structure of unknown sample, these peaks must be compared with standard peaks (Al-zaidi, 2011). A further feature is the background line which uses to provide indication for the amorphous substances, it appears either the structure is crystalline or amorphous. The peak width is also necessary to consider, as it is related to the crystallite size.

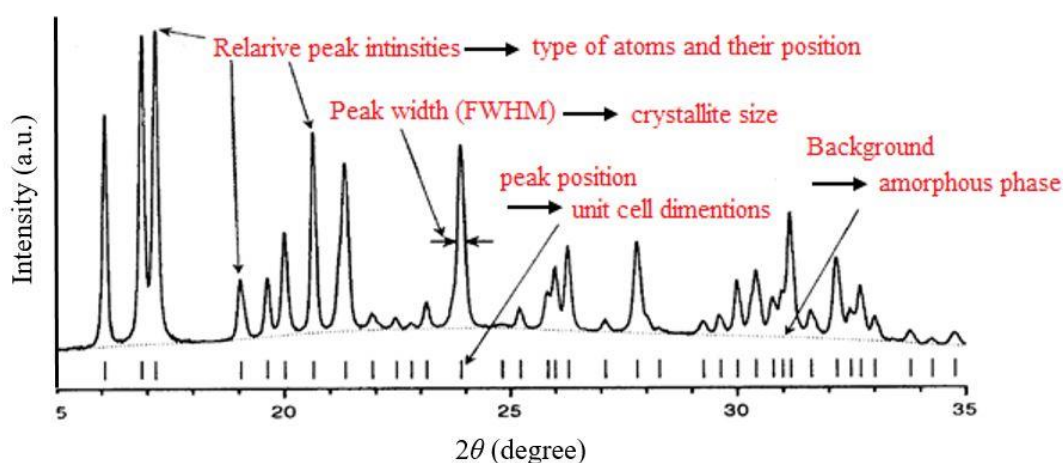


Figure 3.2. The essential features of the X-ray diffraction (van Bekkum et al., 2001).

In the present work, the XRD instrument used was a STOE STADI P CuK α 1, with condition as shown in Table 3.2. below:

Table 3.2. The operation conditions of X-ray diffraction.

Radiation wavelength	0.154 nm
Temperature	ambient temperature
2θ	2 - 100
Scan speed	10 ° min ⁻¹
Run time	28 min
Tension	40 kV
Current	35 A

3.3 Scanning electron microscope (SEM)

The scanning electron microscope (SEM) is a versatile device used to characterise the morphologic and crystalline structure as well as chemical composition of solid materials (Golding et al., 2016, Joy, 1997). Figure 3.3 shows the electron column, consisting of three chambers containing: an electron gun, an electron lens and a sample.

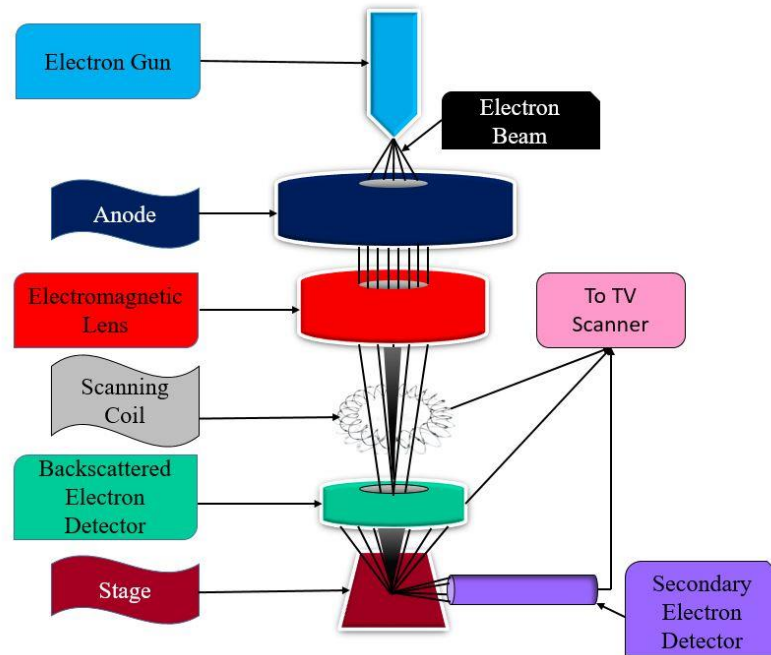


Figure 3.3. Schematic of a SEM adapted from (Bradbury et al., 2018).

Firstly, the electron gun produces electrons by heating up the tungsten loop and it works to accelerate these electrons by an anode plate to energy about 1-40 kV (Goldstein et al., 1992, Bogner et al., 2007). Secondly, the beam is made thinner and focused towards the sample by the use of a magnetic lens (electromagnets) (Goldstein et al., 1992, Zhou et al., 2006). Finally, the sample chamber is located at the base of the SEM, which consists of sample contained (Goldstein et al., 1992, Zhou et al., 2006).

The electron beam which comes from the electron lens hits the specimen; the reaction between these electrons and the surface of the sample generates many signals which form an image. Moreover, the scanning coils control the spot beam (Goldstein et al., 1992, Purdue-University, 2014). Backscattered and secondary electrons can

usually be collected *via* the detector and transferred to an image by cathode ray tube (CRT) or camera (Vernon-Parry, 2000, Bogner et al., 2007, Goldstein et al., 1992).

Furthermore, the sample has to be conductive in order to emit high secondary and backscattered electrons. Nonconductive specimens need to coat by precious metal such as platinum, silver or gold (Zhou et al., 2006). Zeolite is a nonconductive material (Al-zaidi, 2011).

In the present work, scanning electron microscopy (SEM, JEOL JSM-6010LA and AGAR SPUTTER COATER, B7340) were used to characterise and coat the zeolite respectively. Approximately 1 mg of zeolite was used for this characterisation, and gold was used with an argon atmosphere for coating.

3.4 Energy dispersive X-ray spectroscopy (EDX)

Energy dispersive X-ray (EDX) spectroscopy used for qualitative analysis by detecting the composition of a sample surface (Chang et al., 2014). In fact, the EDX system is an inseparable part of the SEM (EKB, 2015). It is noteworthy that every element has a specific structure compared with the other elements. The EDX is used for elemental analysis as it can provide information about the global Si/Al ratio of zeolite.

The EDX comprises of four units: a beam source, an X-ray detector, a pulse processor and an analyser (EKB, 2015, EESemi, 2004). In EDX, the beam of electrons first collides with the surface of the sample and number of reactions occur. Consequently, it is likely that an X-ray is generated. This X-ray is emitted from the specimen and hits the detector, creating a charge pulse. Thereafter, this charge is converted to a voltage pulse and finally, this voltage transforms to a digital signal.

The electrons bombard the specimen, leading to the removal of electrons from the orbit of the atoms. This creates a vacancy in the electron shell; this void will then be filled by the other electrons with a higher energy from the outer shell. The transfer of a high energy electron located at the external shell to the low energy will lead to the emission of part of energy in the X-formation as a result of the difference in energy.

3.5 X-ray fluorescence spectrometry

Zeolites are complex materials that are rich in silicon dioxide (SiO_2) and aluminium oxide (Al_2O_3) as shown previously in Section 2.2. (Pillay and Peisach, 1991). Therefore, the percentage of silicon to aluminium (Si/Al) ratio is important because it influences the performance and behaviour of a zeolite by determining the density, amount and strength of acid sites as well as the nature and stability of this zeolite (Pillay and Peisach, 1991, Corbin et al., 1987, Wirth and Barth, 2017). The using of non-destructive analytical techniques like XRF are useful to measure the Si/Al ratio.

X-ray fluorescence spectrometry (XRF) is one of the types of X-ray techniques that is used to identify the elements of zeolite catalyst (Keeley, 2000, Wirth and Barth, 2017). It works based on the principle of spectroscopy by measuring the energy or wavelength dispersion when a collision occurs between the sample and the primary X-ray (Guthrie, 2012, Wirth and Barth, 2017, Nummi, 2016). Although this method used at the beginning of last century, it has become one of an important elemental analysis in just the last forty years (Keeley, 2000, Guthrie, 2012).

XRF analyses the elements in the sample by studying the behaviour of atom which interacts with the X-ray beam. Therefore, the identification and/or quantification of elements for any sample depends on the amount of energy emitted from this specimen (Guthrie, 2012, Nummi, 2016).

The XRF consists of three parts: a source of X-rays, a specimen chamber and a detector system (Guthrie, 2012). The X-ray beam is generated from rhodium, tungsten, molybdenum or other elements depending on the aim of the analysis (Wirth and Barth, 2017, Guthrie, 2012, Busca, 2014). The process starts when this beam of X-rays illuminates the specimen, and the atom absorbs this X-ray energy *via* ionisation. The energy of the X-ray causes the ejection of the electrons from the lower energy, however these atoms are going to be unstable, so another electron from a higher energy replaces the dislodged electron as shown in Figure 3.4.

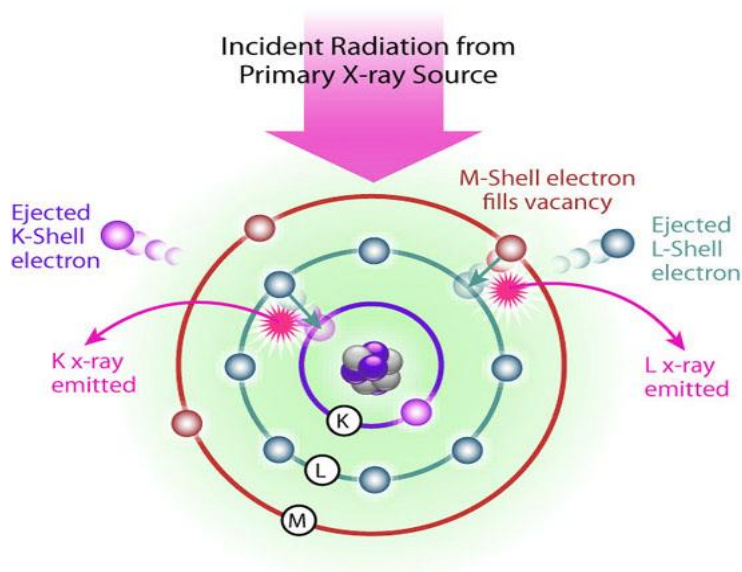


Figure 3.4. The interaction between the primary X-ray and an atom (Nummi, 2016).

Finally, the intensity of this emitted radiation beam is measured by several kinds of detectors such as gas flow proportional and scintillation depending on the type of spectrometer. The intensity is measured *via* the detector represents the abundance of element in the specimen.

In the present study, the XRF analyser was PANalytical Zetium. The zeolite powder was placed in a specific plastic cup which has a single foil sheet lining the bottom. More than 1 g of the sample was put in the cup and closed by a plastic cover. Then, the plastic cup was mounted inside a metal sample cup and put on the suitable sample trays then chose the Omnian37He application because it is appropriate for powder samples.

3.6 Temperature-programmed desorption (TPD)

The investigation of zeolite acid site properties is important in understanding the catalytic reaction on these acid catalysts (Gorte, 1999, Niwa and Katada, 1997, Wang and Manos, 2007a). TPD is a versatile technique employed for the analysis of the total acidity of the zeolite catalyst. It provides information about the density, strength and quantity of acid sites.

TPD of ammonia is the most widespread method employed to characterise the density of the acid sites because of the simplicity of the method however, the main

drawback is that the number of acid sites is overestimated (Niwa and Katada, 1997, Gorte, 1999, Craciun et al., 2012). Several factors contribute to make ammonia one of the most significant gases in TPD, such as; it has a small molecular size helping it to penetrate most of the zeolites micropores such as in Y zeolite. It has a high basicity which makes it able to titrate weak acid sites, although this type of acid site does not contribute to the zeolite activity. Despite all these features of ammonia, the TPD ammonia method is still cannot differentiate between Brønsted and Lewis acid sites and it usually overestimates the density of the acid sites (Gorte, 1999, Lónyi and Valyon, 2001).

From the amounts of gas desorbed at different temperatures, NH₃-TPD can measure the number and strength of acid sites in the zeolite catalyst (Wang, 2007, Figueiredo et al., 2008). The procedure of analysis begins by degassing, outgassing or pre-treatment to remove the physisorbed water, a stable mixture of inert gas and base flows through the specimen bed and interacts with the acid sites. Desorption starts by increasing the temperature linearly with time, accompanied with a continuous flow of inert gas through the specimen. When a critical temperature is reached, the activation energy is overcome by the thermal energy; this leads to the adsorbent molecules being liberated from the surface of the zeolite catalyst and being carried out with the flow of the continuous carrier gas. Nevertheless, a various heat levels are require to break these bonds and desorb the molecules from the zeolite surface, and from the difference in energy levels, the TCD detector plots peaks which represent the concentration versus temperature (Niwa and Katada, 1997, Figueiredo et al., 2008). The integration of these peaks provides information about the amount of the desorbed form and from a separate calibration, the response factor is calculated according to the relationship between the volume of ammonia and the TCD signal. By combining this factor with the area under the curve which was previously determined, the number and strength of the active sites are obtained. These peaks can be divided into two types (Niwa and Katada, 1997, Lónyi and Valyon, 2001, Li et al., 2018):

- i- A low temperature peak ~200 °C results from the amount of ammonia desorbed from the weak acid sites; this type often forms as a result of ammonia molecules physically bonded with the active sites.

- ii- A high temperature peak ~ 400 °C represents the connection between ammonia molecules desorbed from the protonic acid sites (strong acid sites). This kind is formed as a consequence of chemisorbed ammonia molecules.

Other studies showed three peaks instead of two which represented weak, medium and strong acid sites (Hajimirzaee et al., 2015, Triantafillidis et al., 2000, Cattanach et al., 1968).

In the present work, the acidity of fresh and modified zeolite catalysts was characterised by employing a Micromeritics Chemisorb 2720 (NH_3 -TPD) with a TCD detector and using helium as an inert gas. Approximately 50 mg of zeolite specimen was charged over a segment of quartz wool and put in a quartz U-tube reactor, that was then placed in a furnace. The sample was pre-treated at 300 °C for 1 h and at a rate of 10 °C min^{-1} under helium flowing at 25 ml min^{-1} to remove the moisture. Then, the temperature was reduced to 50 °C at a rate of 10 °C min^{-1} for 15 min. The temperature was increased to 110 °C at a rate of 10 °C min^{-1} with the same flowrate of the carrier gas and kept at this temperature. Adsorption of ammonia on the zeolite sample was carried out by 30 ml min^{-1} of 5 % ammonia/helium for 1 h. Subsequently, the sample was flushed with helium again at a flowrate of 25 ml min^{-1} for 1 h to ensure that all the physisorbed ammonia was taken out from the specimen. After that, the sample was heated to 600 °C at a rate of 10 °C min^{-1} and at the end the temperature was kept fixed for 10 min. The area under the peaks were calculated using the Origin 8.5.1 software and because of the overlap between the peaks for Y zeolite, peak deconvolution was used to determine these areas. The NH_3 -TPD calibration curve and the acidity are shown in Appendix A.

3.7 Nitrogen adsorption

Brunauer, Emmett and Teller (BET) surface area analysis assumes multilayer gas adsorption, and is an extension of Langmuir theory which proposes only monolayer adsorption (Bauer and Karge, 2007, Gregg and Sing, 1982, Bae et al., 2010). They are employed to study the properties of fresh and deactivated zeolite. BET theory is commonly employed in the characterisation of specific surface area and pore size distribution of solids and porous materials and involves applying adsorption data and using Equations 3.4:

$$\frac{P}{V_a(P^\circ - P)} = \frac{1}{V_m \cdot C} + \left[\frac{C-1}{V_m \cdot C} \right] \left(\frac{P}{P^\circ} \right) \quad \dots\dots (3.4)$$

Where,

P and P° are the equilibrium and the saturation pressure of the adsorbed gas at the temperature of adsorption,

V_a = Volume of gas adsorbed measured at the equilibrium pressure and temperature of adsorption,

V_m = Volume of the adsorbed gas in the monolayer ($\text{cm}^3 \text{g}^{-1}$),

C = BET constant, which is related to the energy of adsorption in the first adsorbed layer.

A linear mathematical form can be obtained by plotting $\left[\frac{P}{V_a(P - P^\circ)} \right]$ versus the relative pressure $\left[\frac{P}{P^\circ} \right]$ at a specific relative range between 0.05 to 0.25 (Bae et al., 2010).

$$\text{slope} = \left[\frac{C-1}{V_m \cdot C} \right] \text{ and } \text{Intercept} = \left[\frac{1}{V_m \cdot C} \right]$$

By solving the above equations algebraically, the values of both V_m and C can be obtained.

$$C = \left[\frac{\text{slope}}{\text{Intercept}} \right] + 1 \text{ and } V_m = \left[\frac{1}{\text{slope} + \text{Intercept}} \right]$$

The theoretical value of surface area (S_{BET}) for the sample in $\text{m}^2 \text{g}^{-1}$ can then be calculated from the following Equation 3.5:

$$S_{BET} = \left[\frac{V_m N_a A_m}{M_v} \right] \quad \dots\dots (3.5)$$

Where,

N_a = Avogadro number ($6.02 \times 10^{23} \text{ mol}^{-1}$)

A_m = Cross-sectional area of the adsorbate molecule ($16.2 \times 10^{-20} \text{ m}^2$), and

M_v = Molecular volume of the adsorbate molecules ($22414 \text{ ml mol}^{-1}$)

Therefore, the BET-surface area can finally be represented as:

$$S_{BET} = [V_m (4.35)]$$

Barrett, Joyner and Halenda (BJH) is the main method used to measure the pore size distribution depending on the nitrogen adsorption (Sing, 2001). Adsorption is defined as an enrichment process of a solid materials surface *via* gas or liquid molecules that adhere to the region near to the interface and this leads to the formation of an adsorbate film (Rouquerol et al., 1999). Adsorption phenomena are widely used for measuring the characteristics of surfaces and the distribution of pore sizes for powder solids and intracrystalline microporous catalysts like zeolite (Storck et al., 1998, Sing, 2001, Bae et al., 2010). On the contrary, desorption is defined as the process of one material being released from another, and occurs either through or from the surface (Nishi and Inagaki, 2016). Table 3.3 shows the definition of important terms which are used in the adsorption desorption phenomena:

Table 3.3. The main definitions of terms relating to porous solids, adapted from (Rouquerol et al., 1999, Kaneko, 1994).

Term	Definition
Porous Solid	Solid with cavities or channels which are deeper than wide
Open Pore	Cavity of channel with access to the surface
Pore Size	Pore width / minimum dimension
Pore Volume	Volume of pores determined by stated method
Porosity	Ratio of pore volume to apparent volume of particle or granule
Surface Area	Extent of total surface area as determined by given method under stated conditions
External Surface Area	Area of surface outside pores
Internal Surface Area	Area of pore wall
Micropore	Pore of internal width less than 2 nm
Mesopore	Pore of internal width between 2 and 50 nm
Macropore	Pore of internal width greater than 50 nm

Several gases and vapours are used in the porous characterisation, such as nitrogen, helium, argon and oxygen; however, nitrogen is the most widely used as an adsorptive for surface area characterisation (Mekki-Berrada and Auroux, 2012, Bauer and Karge, 2007, Sing, 2001). The size of nitrogen molecules is one of the interesting features which leads to its use in this measurement. It is suitably sized to penetrate into various pore sizes before and after the reaction when the coke is deposited as described in Section 2.5.

In 1985, IUPAC classified the adsorption-desorption isotherm into six types according to the texture of the porous solid, as shown in Figure 3.5 (Kaneko, 1994, Rouquerol et al., 1999, Figueiredo et al., 2008, Nishi and Inagaki, 2016):

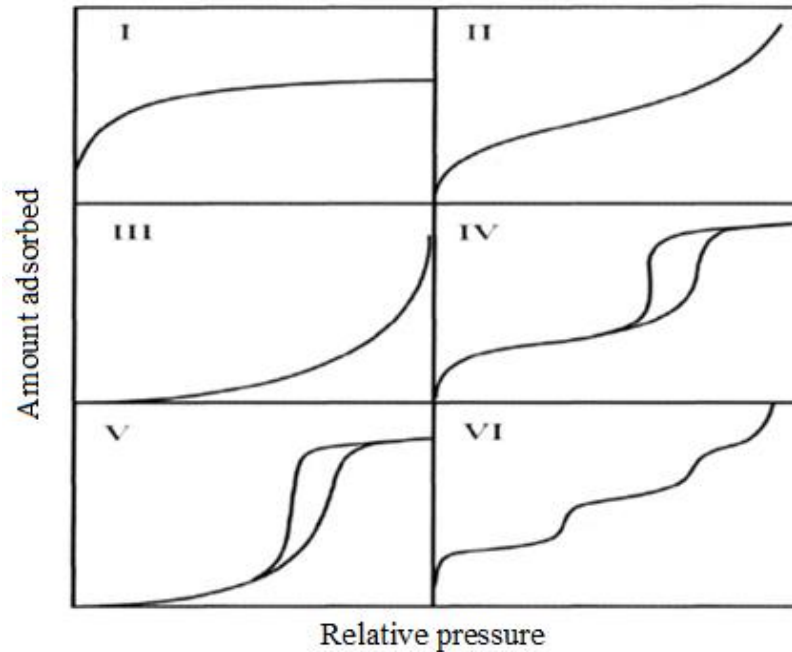


Figure 3.5. IUPAC classification of adsorption-desorption isotherm adapted from (Kaneko, 1994).

Type I: this type of adsorption isotherm indicates the presence of a microporous material (i.e. zeolite).

Type II: this kind indicates mono-multilayer adsorption, and indicates either nanopores or macropores adsorbents.

Type III: this type of isotherm is limited in a few systems. It emerges from either nonporous or microporous surfaces but the interactions of adsorbent-adsorbate molecules are weak.

Type IV: this type indicative of the presence of a mesoporous structure.

Type V: this type is rare and close to the type IV case. It arises from either meso or microporous surfaces however, the interactions between the adsorbent-adsorbate molecules are weak and this seems to look like the isotherm in type III.

Type VI: this type of isotherm is a stepwise isotherm and indicates the adsorption of non-porous molecules on a highly uniform surface.

BET analysis was employed to determine the surface area of the zeolite (Bae et al., 2010, Kaneko and Ishii, 1992). In the literature, use of this analysis is limited to porous materials that have a pore diameter equal to or bigger than 7 Å. In addition, it is convenient for analysing zeolites which have highly heterogenous surfaces. Therefore, this analysis is suitable for the HY zeolite catalyst because it does not contain ultra-micropores (Bae et al., 2010).

In the present work, a Micromeritics 3Flex instrument has been used to measure pore size, pore volume and surface area of fresh and spent zeolite, using the BET and BJH methods. 100 mg of zeolite, either as a powder or in a pellet form, is placed in a quartz tube. Then, the outgassing process is used to dry the zeolite at 200 °C for 4-12 h using a vacuum furnace to eliminate any moisture or any other contamination. After that, the tube weight is calculated to measure the weight of the sample after drying. The adsorbate used in this process was nitrogen gas, it is injected into the sample tube and it starts to adsorb on the surface of zeolite. Simultaneously, nitrogen is liquefied on the surface of the specimen at -196 °C, then the pressure is dropped until equilibrium is reached. Liquid nitrogen was used to obtain high specimen temperature stability through immersion of the quartz specimen tube during the analysis process. Additionally, adsorption analysis is used to study the desorption isotherm step. The software that is used in this measurement is 3Flex Version 3.02.

3.8 Thermogravimetric Analysis (TGA)

TGA is a beneficial technique used to determine the mass differences of a specimen over a certain time and a specific range of temperature (Mekki-Berrada and Auroux, 2012, Imelik and Vedrine, 1994, Chen and Manos, 2004). It employs to provide information about coke amount, type and composition.

TGA consists of several parts (see Figure 3.6): a furnace to generate the desired temperature, a crucible is used to hold the sample (Imelik and Vedrine, 1994, Mekki-Berrada and Auroux, 2012). An automatic balance with signal recording, it considers the most important part because the main target of TGA is the calculation of the mass variation with temperature. Finally, a control of the atmosphere acts to offer the best surrounding.

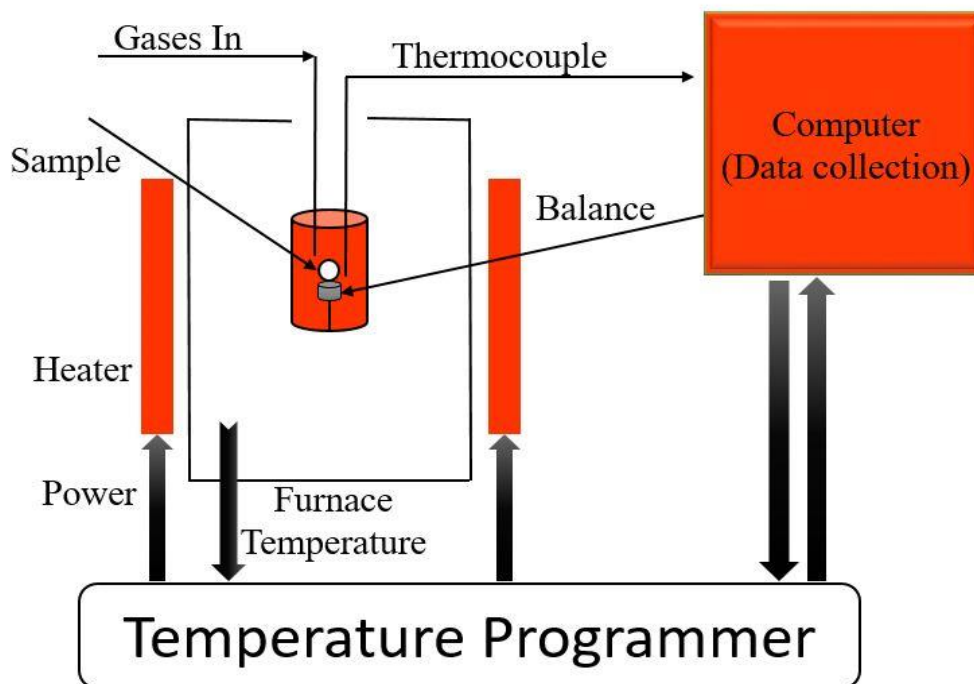


Figure 3.6. Schematic of TGA adapted from (Price, 2006).

In TGA, the empty ceramic pan is weighted then the sample is placed in it over the balance and the initial weight is recorded, then the specimen is heated using temperature programmed with either air or nitrogen as well as control of the atmosphere (Mekki-Berrada and Auroux, 2012). After that, the results can be recorded versus temperature and time.

Because the TGA system is capable of switching gases automatically. It can be used to measure the coke amount which has amassed over or inside the zeolite (Al-zaidi, 2011). In addition, derivative thermogravimetric analysis DTG is used to investigate the stability of the structure, where the curve of derivative weight loss gives the rate of weight loss.

In the present work, the amount of coke that formed during the alkylation reaction is measured by using a PerkinElmer TGA 4000 instrument. Approximately 15 mg of sample was heated from ambient temperature to 200 °C at a rate 10 °C min⁻¹ under flowing nitrogen at a flow rate of 20 ml min⁻¹. This temperature was maintained for one hour under flowing nitrogen at the same previous flow rate in order to remove volatile substances and adsorbed water (Wang and Manos, 2007b, Chen and Manos, 2004, Guisnet and Magnoux, 2001). After that, the gas was switched from nitrogen to

air and the temperature was raised to 400 °C, the difference in sample weight during this range of temperature explains the soft coke (Guisnet and Magnoux, 2001, Ahmed et al., 2011). This temperature was held for also one minute in order to reach a constant weight. Then, the temperature was increased to 800 °C and held for five minutes. The loss in specimen mass between 400 °C and 800 °C represents the mass of hard coke (Ahmed et al., 2011, Wang and Manos, 2007b). Then, the sample was cooled to ambient temperature at the same rate, 10 °C min⁻¹.

The mass percentage of total coke content was calculated as shown in Equation 3.6:

$$coke\% = \frac{W_{200} - W_{800}}{W_{800}} * 100 \quad \dots\dots (3.6)$$

W₂₀₀: weight of sample at 200 °C

W₈₀₀: weight of sample at 800 °C

3.9 Temperature programmed oxidation (TPO)

TPO is one of the widespread thermo-analytical measurements used to characterise coke deposits on heterogeneous catalysts such as zeolites (Suwardiyanto et al., 2017, Chen et al., 2013, Sánchez et al., 2009, Bayraktar and Kugler, 2002, Fung and Querini, 1992). It provides beneficial information regarding coke type, morphology, location, distribution, coke content, coke composition (hydrogen to carbon ratio, H/C) and information on the kinetics of coke formation; it is therefore considered as a quantitative and qualitative measurement (Querini and Fung, 1997, Bauer and Karge, 2007, Querini, 2004).

In general, several detection methods are used in TPO such as: thermal conductivity detector (TCD), flame ionisation detector (FID), mass spectrometer (MS), thermal gravimetric analysis (TGA), differential thermal analysis (DTA), differential scanning calorimetry (DSC) and Fourier transform infrared spectroscopy (FTIR) (Querini, 2004, Chen et al., 2013, Fung and Querini, 1992, Querini and Fung, 1997). In the present study, TCD was employed to determine the carbon dioxide amount.

According to Bauer and Karge (2007) zeolites in the H-form usually have two types of coke: hydrogen-rich carbonaceous (soft coke) which burned at temperature

about 327 °C and polyaromatic coke (hard coke) that burned at temperature around 427 °C.

A Micromeritics Chemisorb 2720 (TPO) device fitted with a TCD was used to characterise the zeolite post-alkylation reaction. About 50 mg of zeolite was used per cycle. The sample was put over piece of quartz wool and inside a quartz U-tube reactor, then placed in a furnace. After that, the specimen was purged *via* helium at a flowrate of 25 ml min⁻¹. Thereafter, the temperature of the furnace was increased from ambient temperature to 850 °C at a rate of 10 °C min⁻¹ and under 25 ml min⁻¹ flowrate of 5% oxygen/helium. The last temperature was held for approximately 30 min to ensure all the carbonaceous components were burned. Finally, the furnace was cooled down to ambient temperature again at a flowrate of 25 ml min⁻¹ of helium to remove any remaining oxygen.

3.10 Elemental analysis

Elemental analysis is one of an important characterisation technique used to provide information about the structure of carbonaceous deposits on zeolite through determination of the ratio of hydrogen and carbon (Bauer and Karge, 2007). The H/C ratio is generally determined by heating the samples which contain coke to 1000 °C in the presence of pure oxygen (Gomez Sanz et al., 2016). At this high temperature, nitrogen converts to either nitrogen gas or nitrogen oxides; carbon to carbon dioxide; hydrogen to water and sulphur to oxides of sulphur (Thompson, 2008, Braun and Pantano, 2014). In addition, a micro-analytical standard such as 2,5-Bis(5-tert-butyl-benzoxazol-2-yl) thiophene (BBOT) is a high purity component used in the calibration to quantify the hydrogen and carbon elements (Thompson, 2008).

Firstly, the powdered specimen is weighed in a silver crucible then placed in the auto-sampler, as shown in Figure 3.7.

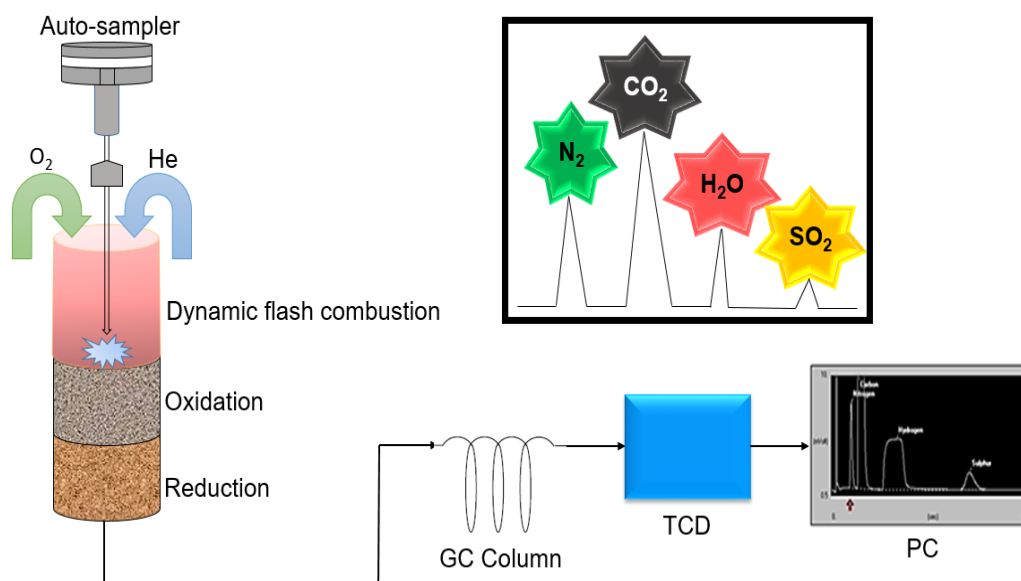


Figure 3.7. Principle of the CHNS elemental analysis adapted from (Thompson, 2008).

When the sample drops through the reactor, the oxygen will burn it in an exothermic reaction. The gas mixture that is produced from the reaction (N_2 , CO_2 , H_2O and SO_2) will flow through a chromatographic column which separates the gases and then sends them to the TCD detector.

Bauer and Karge, (2007) classified the coke into two types depending on the H/C ratio:

- 1- Coke type I; hydrogen-rich coke; soft coke; white coke or amorphous coke with H/C ratio more than 1, this coke is formed at temperatures less than 250°C .
- 2- Coke type II; hydrogen-deficient coke; hard coke; black coke or graphitic coke with H/C ratio less than 0.8, usually formed at temperatures higher than 250°C .

Qualitative analysis of coke in different samples after the alkylation of toluene with 1- heptene was achieved using a Flash 2000, Organic Elemental analysis. About 3 mg of specimen was used to determine the H/C ratio using pure oxygen at 900°C . The combustion products were analysed using a GC column, and then detected by the TCD. The carrier gas employed was He at a flow rate of 130 mL min^{-1} . The data were collected as elemental weight percentage using Eager Xperience software version 1.1.

3.11 Fourier-transform infrared spectroscopy (FTIR)

FTIR is one of the main techniques employed to identify the chemical compounds (aliphatic, olefinic and aromatic) of coke deposits on the catalyst during the hydrocarbon reactions (Bauer and Karge, 2007, Querini, 2004). There are many advantages to using FTIR; such as: the sample is not destroyed after analysis and it provides appropriate information to study the mechanism of reaction and coke formation (Ibáñez et al., 2016, Bauer and Karge, 2007).

FTIR works according to the radiation interference difference between two beams that have various pathlengths (Stuart, 2004). It consists of beam sources, an interferometer, a specimen, a detector, an amplifier, a digital converter and a computer. The radiation originates from the source and passes through an interferometer to the specimen, and then reaches a detector. The signal is amplified and converted to digital data to be read by the computer.

Coke is the main cause of zeolite deactivation *via* deposition of carbonaceous materials during the hydrocarbon reaction. Knowledge of the coke nature is significant because of its effect on the catalyst activity; for example, it can be easily removed if the coke is soft, whereas it becomes difficult to remove if it turns into graphitic coke which will then probably leads to deactivation of the catalyst (de-Silva et al., 2010).

The technique of potassium bromide powder (KBr) pellet is used for non-absorbent substances to dilute these samples to extract information about the nature of the coke (Dent, 2018, Chen et al., 2014). The main reason for choosing the KBr method is that it does not have bands in the middle of the FTIR spectrum region.

Coke deposits on zeolites are classified depending on spectra regions (Table 3.4) (Ibáñez et al., 2016, Bauer and Karge, 2007, Querini, 2004):

Table 3.4. FTIR bands which formed as a result of coke deposits, adapted from (Ibáñez et al., 2016, Bauer and Karge, 2007, Querini, 2004).

Band (Cm ⁻¹)	Assignment
1390-1360, 1490-1420	CH stretching modes of paraffinic species
1524-1513	Double bonds aromatics
1595-1583	Double bonds aromatics/polyromantic
1390, 1630-1625	Olefinic species
3000-2800	CH stretching modes of aliphatic species
2935-2915, 2865-2845	= CH ₂ symmetrical/asymmetric stretching
2970-2950, 2880-2860	-CH ₃ symmetrical/asymmetric stretching
2960	Saturated CH / polyolefin +aromatic
2990-2970	Saturated CH / stretching CH / olefinic species
3200-3000	CH stretching modes of aromatics
3700-3500	Structural hydroxyl groups species
3800-3700	Silanol group Si-OH groups

Usually, the aliphatic oligomeric type is considered the most widespread species that is formed during the alkylation reaction and their bands are between 2750 to 3040 cm⁻¹ (Querini, 2004).

In the present study, FTIR spectroscopy was employed to quantitatively evaluate the nature of hydrocarbonaceous deposits through the toluene alkylation with 1-heptene over HY zeolite. The transmission FTIR spectroscopy in the range of 400- 4000 cm⁻¹ was recorded on a Shimadzu IRAffinity-1S using the KBr technique. In order to obtain the main information about the nature of any carbonaceous species formed on the zeolite, approximately 1 mg of sample was pressed into a pellet with 150 mg of potassium bromide, FTIR Grade Powder (KBr). The pressure was equivalent to 9 ton/cm² and the size of the disk was 13 mm in diameter. Then, the specimen was dried at 120 °C for 1 h to remove the physisorbed water. A pure KBr pellet was used as a background in the measurement. All % transmission measurements were obtained at ambient temperature with a resolution of 4 cm⁻¹ and 16 scans with a DLATGS detector.

Chapter 4

*Materials, experimental
work and methodology*

4.1 Introduction

The production of linear heptyl-methylbenzene can be achieved through liquid phase alkylation reactions. In this work, HY, H-Beta and H-mordenite zeolites have been used to study the impact of the zeolite framework structure and influence of modification (dealumination, desilication, silylation and pre-coking) on this reaction at different times.

This chapter focuses on the materials that have been employed in this work, the post-synthesis modifications and the reactor set-up. In addition, the analytical methods of the liquid phase, gas chromatography/ flame ionisation detector (GC/FID) and gas chromatography/mass spectrometry (GC/MS), are described.

4.2 Materials

4.2.1 Gases and liquids

The main gases that serve the experimental rig were: nitrogen to purge the system and accelerate the reaction, helium used as a carrier gas in both the GC-MS and GC-FID and air to activate the zeolite catalyst and to produce a flame in the GC- FID.

Toluene (99.5 %), tetraethyl orthosilicate (TEOS, ≥ 99 %), sodium hydroxide (≥ 97.0 %), hexane (≥ 97.0 %), ethanol (≥ 99.8 %) and hydrochloric acid (37 %) were supplied from Sigma-Aldrich. 1-Heptene (98 %) and ammonium nitrate (99+ %) were obtain from Acros Organics.

4.2.2 Catalysts

Three types of zeolites from Alfa Aesar have been used in this work: HY zeolite (HY5.1) ($\text{SiO}_2/\text{Al}_2\text{O}_3=5.1:1$, surface area = $730 \text{ m}^2 \text{ g}^{-1}$), (HY30) ($\text{SiO}_2/\text{Al}_2\text{O}_3=30:1$, surface area = $780 \text{ m}^2 \text{ g}^{-1}$), H-Beta zeolite ($\text{SiO}_2/\text{Al}_2\text{O}_3=360:1$, surface area = $620 \text{ m}^2 \text{ g}^{-1}$) and NH_4 -mordenite zeolite ($\text{SiO}_2/\text{Al}_2\text{O}_3=20:1$, surface area = $500 \text{ m}^2 \text{ g}^{-1}$). Mordenite zeolite was converted from the ammonium to hydrogen form through calcination at $500 \text{ }^\circ\text{C}$ for 4 h with static air.

4.3 Experimental set-up and operating procedures

4.3.1 Batch reactor (BR)

The experimental work was carried out using a 50 ml borosilicate glass flask linked with reflux and placed inside an oil bath. A stirred heater was employed to control the temperature and speed of the magnetic stirring; the magnetic stirrer was used to mix the materials inside the reactor, as shown in Figure 4.1.

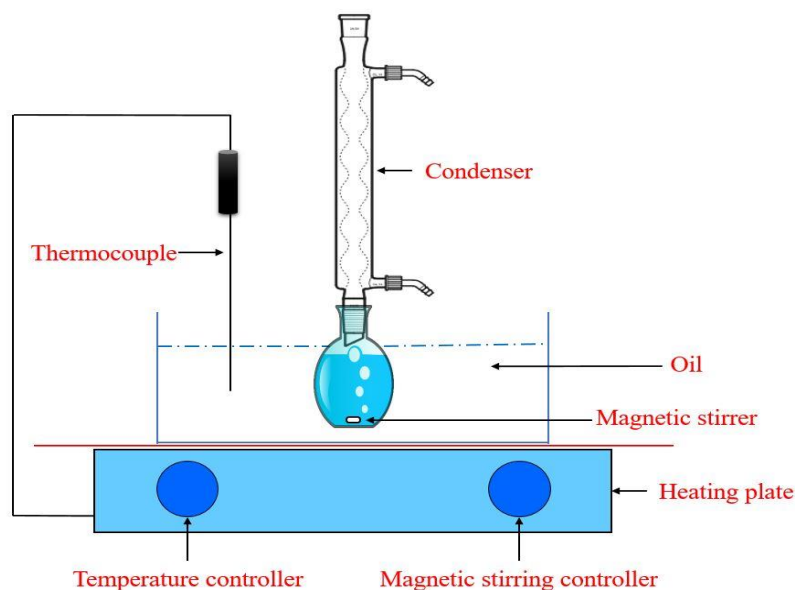


Figure 4.1. Scheme of the batch reactor.

The alkylation reaction was conducted at a temperature of 90 °C, atmospheric pressure and a stirrer speed of 200 rpm. Three types of zeolites have been used in this work: HY zeolite, H-Beta zeolite and H-mordenite zeolite. The mixture of reactants consists of toluene/1-heptene with a molar ratio of 3. The total volume was 10 ml (7 ml toluene and 3 ml 1-heptene) over 0.25 g of zeolite (activated at 150 °C for 2 h) in each experiment. Different reaction times were used; 20, 120 and 360 minutes, and the time was started simultaneously with stirring when the temperature reached 90 °C. When the reaction reached the end time, the reaction was quenched by placing the reactor in iced water. Then, the sample was separated from the zeolite catalyst by employing filter paper under vacuum in order to analysis the liquid products. The zeolite catalyst was collected and washed using 15 ml of *n*-pentane for ~30 min to expel any adsorbed substance from the zeolite pores, after which it was then dried at 120 °C overnight.

4.3.2 Fixed bed reactor (FBR)

The alkylation of toluene with 1-heptene was carried out in a fixed bed reactor (FBR) at 90 °C, atmospheric pressure, for 240 min TOS, T: H ratio is 8: 1, WHSV of 17 h⁻¹, 30 ml min⁻¹ of N₂ flowrate using 0.5 g of HY5.1 and HY30, or modified HY, as shown in Figure 4.2.

The zeolite is supplied as a powder. In order to do a typical experiment, the hydraulic piston is employed to press the powder into tablets under 5 tonnes of pressure. Then, the tablets are crushed and sieved to form pellets with particle sizes between 0.3-0.6 mm. The zeolite sample was put in a specially designed mesh basket between two layers of quartz wool in the middle of the reactor at the heating zone.

A carbolite furnace with a 15 ml diameter and a length of 150 mm was used as a heating source with a 40 mm heating zone which is located at the centre of the furnace. The temperature controller is employed to control the reaction temperature through particular program acts to take control on the furnace.

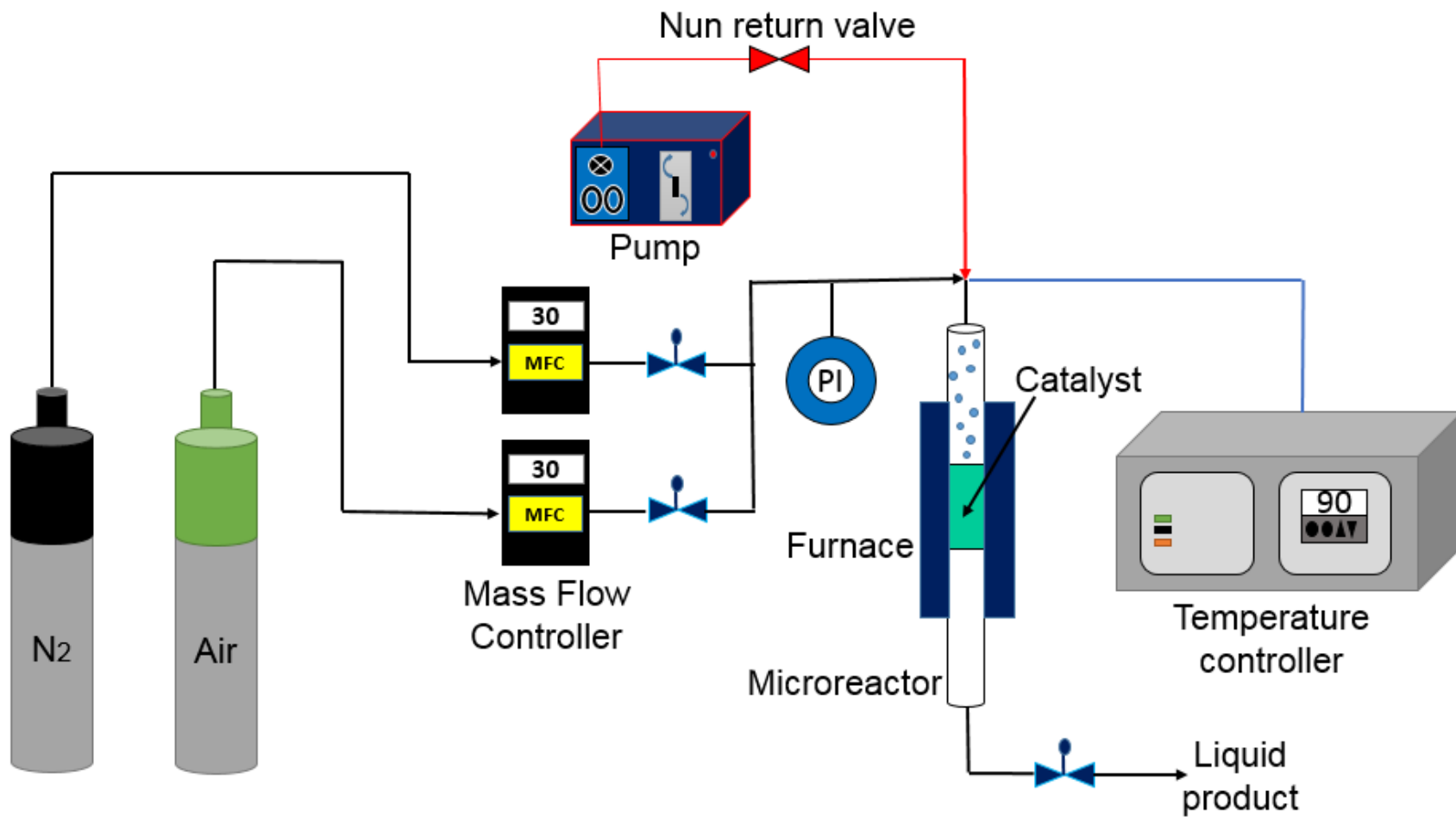


Figure 4.2. Scheme of the fixed bed reactor.

The reactor is made from stainless steel, with a 9 mm internal diameter and a 230 mm length. 4 g of inert glass bed (3 mm) were placed upstream of the zeolite bed to avoid back-mixing and distribute the liquid evenly on the zeolite packing. Mass flow controllers (MFCs) were employed to monitor both the flow of air and nitrogen gas from the cylinders. The type of MFCs used in this work were digital AALBORG, model GFC17, with a flow range of 0-200 ml min⁻¹ and they can avoid the back pressure issues. They were calibrated before the experiments to check the actual flow rate of both gases and the results of this work are shown in Figure 4.3. When the reactor is inside the furnace, checking for gas and liquid leakages takes place by employing soapy foam at each joint in the reactor system.

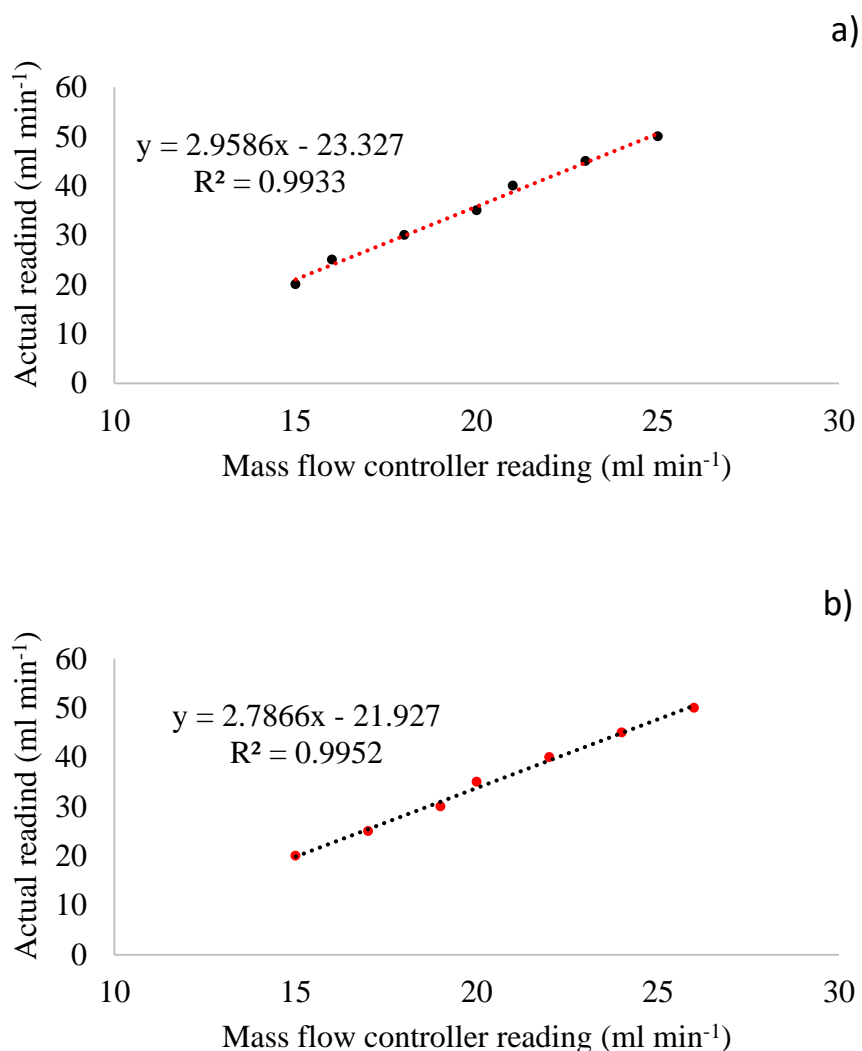


Figure 4.3. The calibration of mass flow controller using a) nitrogen and b) air.

0.5 g of crushed zeolite pellets (15 mm height) was employed in each experiment. It was activated at 300 °C under 30 ml min⁻¹ of air flow for 2 h to eliminate physisorbed water. It was then cooled to the reaction temperature 90 °C and the air flow was switched off. The sample was then flushed with nitrogen at the same flow rate 30 ml min⁻¹. Liquid-phase reactants (toluene to 1-heptene ratio was 8:1) were introduced to the FBR *via* a peristaltic pump (Thermo Scientific FH10) at a flowrate of 10 ml h⁻¹, weight hourly space velocity (WHSV) 17 h⁻¹ and a residence time ~0.06 h. Approximately 4.5 ml of products were collected after every 30 minutes on stream to identify the alkylation products using a Shimadzu Gas Chromatography Mass Spectrometer (GCMS-QP2010 SE). It is then quantitatively analysed *via* a Thermo Scientific Gas Chromatography flame ionisation detector (TRACE 1310).

At the end of the reaction, the reactant pump is shut off; however, the helium flowrate is continued for a further 2 hours to purge the system. The reactor is cooled down by switching off the furnace. After that, the helium flow is turned off and the coked zeolite is collected for characterisation.

90 °C is the chosen reaction temperature because both the reactants and products were in a liquid phase at this temperature; the boiling point of the reactants is 105 °C and the products is ~266 °C. In addition, the gaseous effluent from the reactor is separated by condensing the heavy products in a small condenser at a temperature of approximately -15 °C. It is then collected in gas sampling bag and analysed off-line using both the GC-MS and GC-FID. The chromatogram of these gases showed no gas-phase products were formed in significant quantities during this reaction.

A blank test experiment was completed at the same reaction conditions to prove there is no alkylation or isomerisation products, as well as showing the reactor tubes work as inert materials.

4.3.3 Water removing

The presence of physisorbed water in zeolite catalysts has a negative effect on the alkylation reaction (Weitkamp and Puppe, 1999). Therefore, the removal of water before and/or throughout the reaction is considered an important step to increase the stability of the zeolite catalyst. There are three sources for this type of water moisture; 1) the atmosphere, 2) impure carrier gases, and 3) liquid reactant with low purity below

100 %. To reduce the effect that water molecules had on the alkylation reaction, many steps were taken:

- 1- Activating the zeolite at a temperature ~ 300 °C under 30 ml min^{-1} of air flow to ensure that all the physisorbed water was removed and when the zeolite was then cooled, it was decreased to a temperature approaching the reaction temperature to avoid the return of any water molecules.
- 2- The zeolite sample was placed between two layers of quartz wool to decrease contact with the atmosphere and the reactor was closed carefully to prevent air entering the reactor.
- 3- The gases pass through molecular sieve drying traps before entering the reactor.
- 4- The inlet lines of the reactants and carrier gas were heated to the same temperature as the reaction temperature to remove any water.
- 5- To investigate the effect of water from impure reactants and/or carrier gases on the alkylation reaction, the model reaction was repeated using various bottles of reactant which had different ages to study the effect of reactant contamination which results from usage of the reactant over a long time. The reproducibility error of this reaction using the FBR, at 90 °C, a TOS of 240 min and 0.5 g of HY5.1 zeolite catalyst, a N_2 flowrate of 30 ml min^{-1} , a WHSV of 17 h^{-1} and a toluene to 1-heptene ratio of 8 was ± 2 % for 1-heptene conversion whereas it was ± 2 % for the selectivity of 2-heptyltoluene and it was ± 3 % for coke selectivity.

4.4 Gas Chromatography

Gas chromatography is a widely used physical technique which is used in the identification of the components in a mixture (Karasek and Clement, 1988). Martin and Synge have proposed in the 1940s the use of a technique which depends on gas-liquid division chromatography for analysis. Between the 1940s-1950s, Martin and his co-workers developed gas chromatography and they published the article which depicted the first GC (Martin and Synge, 1941).

The aim of using the GC-column is to separate the components from the mixture dependent on the variation in the retention times (Chromacademy, 2015). The retention time is used to define the unknown compounds and it represents the time required for the specimen to pass through the fractionation column. The components are separated depending on the level of affinity between the sample and the stationary phase, therefore, the components which have lowest levels of affinity are eluted at the beginning and so on until the high levels of affinity are eluted from the column toward the detector. Any eluted compound reaching the end of the column moves directly to the detector which identifies this compound. In general, the results from the GC- column are shown as a collection of peaks which indicate the components injected into the GC. Furthermore, retention time is the factor which specifies the location of the peaks, and from the area under the peak, the concentration of compounds is calculated.

The GC instrument process is divided into three parts: the injection port, the column and the detector as shown in Figure 4.4 (Chromacademy, 2015).

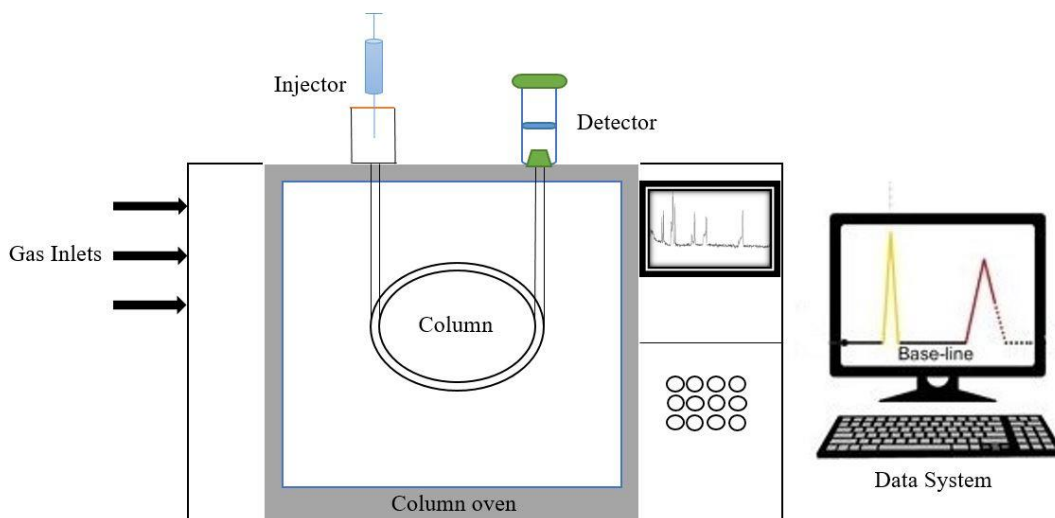


Figure 4.4. Schematic diagram of a Gas Chromatography (GC) instrument reproduced from (Chromacademy, 2015).

The sample is first fed to the column through an injection port (at the top of the column), it enters the column with the carrier gas at a high temperature to ensure that all the components of specimen is evaporated (Linde, 2015).

The second part is the column. In this section the sample is distributed between two phases: a mobile phase and a stationary phase (Karasek and Clement, 1988, Chromacademy, 2015). In the mobile phase, the inert gas such as helium, hydrogen or nitrogen is often used as a carrier gas and it must be regulated. The stationary phase is usually a thin layer covering all the interval column surface and it is preferably inert.

The third part is the detector. In this part the sample identifying depends on a physical-chemical property and the results are obtained by the PC which receives signals from the amplified detector (Chromacademy, 2015, Linde, 2015). There are several types of detectors, the choice of which depends on the aim of the analysis required. The detector types include: mass spectrometer (MS), flame ionisation (FID), thermal conductivity (TCD), electron capture (ECD), nitrogen phosphorous (NPD) and flame photometric (FPD).

In the present study, two detections have been used with the GC which are MS and FID.

MS is an analytical detector which is used to give information (qualitative and quantitative) about the molecular weight and atoms of a sample (Ashcroft, 2015, Linde, 2015). This detector works according to the mass (m) to charge (z) ratio of gas phase ions, where m represents particle mass (Da) and z is the number of electrostatic charges (e), so, the term m/z can be calculated by Da/e . It consists of three main sections: an ionisation chamber, an analyser and a detector (Chromacademy, 2015, Karasek and Clement, 1988, De Hoffmann and Stroobant, 2007, Downard, 2004). Ionisation can be defined as a process which either adds electrons to, or removes electrons from, molecules in order to produce ions because the control on ions is easier than the original molecules. The mass analyser is used to separate and extract the ions resulting from ionisation, depending on the ratio between mass to charge m/z . Finally, the ions which leave the mass analyser will enter the detector. The detector is an important part of the MS because it is able to generate a signal from the incident ions.

FID is a wide separate analytical technique that is commonly employed for the hydrocarbon materials in gas chromatography which detects the carbon amount of specimen (JoVE, 2018, AirProducts, 2018). It works according to combustion principle therefore any compounds that non-combustible will not detect by this detector. The stream that exterior of the column is burned in a flame of hydrogen and

air. Consequently, carbon ions are generated. After that, these ions are collected to form an electrical signal that is subsequently measured.

4.4.1 GC-MS analysis

A Shimadzu Gas Chromatography Mass Spectrometer (GCMS-QP2010 SE) was used in the analysis. Lab Solution software with NIST MS version 2.0 is employed to analysis the results; its library has a number of mass spectra references for several compounds. This GC-MS has many futures such as: low sampling error, low noise and high sensitivity. 72.9 ml min⁻¹ of helium gas with a split ratio = 50:1 (supplied from Helium cylinder) at 147.8 kPa was used to carry the alkylation products which they are resulting from reactor and they injection to the GC by Shimadzu auto injector (AOC-20i) at 250 °C in order to vaporise all components before it will enter to the column. The column which is used in this work is a DB-1MS column 59.4 m length, 0.25 mm I.D., 0.25 µm film thickness, a maximum temperature of 360 °C and a linear velocity of 30 cm s⁻¹. The temperature program of the column is demonstrated in Table 4.1.

Table 4.1. Properties of chromatographic method as used for the analysis of the samples.

Temperature rate (°C/min)	Final temperature (°C)	Time (min)
-	40	0
10	100	1
10	200	1
10	250	0

The analytical process takes approximately 23 minutes. With a cut time of 7 minutes to shown only the alkylation products and avoid a detector saturation by 1- heptene and toluene. However, in the case of unreacted 1-hepten, the sample was mixed with ethanol to make it as a diluted solution to avoid the detector saturation, and the cut time in this case was taken 4 minutes.

4.4.2 GC-FID analysis

A Thermo Scientific Gas spectroscopymeter with flame ionisation detector (TRACE 1310) was employed for quantitative analysis with a DB-5HT column (30 m length, 0.32 mm I.D. and 0.1 μm film thickness and a maximum temperature of 400 $^{\circ}\text{C}$). 0.5 ml of the product was withdrawn and mixed with 0.05 ml of *n*-hexane which is employed as an internal standard.

The main benefit of using the internal standard is that it acts to overcome the error of injection volume that results from manual injection. An exemplary internal standard should have many features such as; high purity, easily obtainable, it is not one of the reactants or products and it does not overlap the retention time for both reactants and products in the GC chromatography. In the context of the present work, *n*-hexane was chosen as the internal standard as it fulfils all the conditions detailed above.

Liquid products were analysed using 50 ml min^{-1} of helium gas (99.996 % purity) provided from a cylinder at 147.8 kPa and split with a split ratio of 50:1 at an injector temperature of 200 $^{\circ}\text{C}$. The FID was operated at a H_2/air ratio of 1:10 which is considered sufficient to form a flame capable of ionising the hydrocarbon compositions.

Table 4.2 shows the temperature program of the column. Approximately 26.5 minutes was the time taken to analysis the alkylation products. In practice, each sample was injected three times to check for the accuracy of GC.

Table 4.2. Properties of the chromatographic method employed for the analysis of the samples.

Temperature rate ($^{\circ}\text{C}/\text{min}$)	Temperature ($^{\circ}\text{C}$)	Hold time (min)
-	40	0
10	100	0
3	130	5
20	240	0

4.5 Zeolite modification

4.5.1 Dealumination technique using hydrochloric acid aqueous solution

Acid leaching is one of the best techniques used to remove the aluminium atoms from the framework of zeolite (Wei et al., 2015). This modification involves using pure or dilute acid. Usually, zeolite-Y catalyst, which has strong acid sites that are deactivated rapidly, requires dealumination treatment to increase the Si/Al ratio as a result of alteration of the Al content (Al-Zaidi et al., 2012). The influence of such treatments on the catalytic performance of HY zeolite in alkylation reactions has been investigated to enhance the selectivity and increase the zeolite lifetime. Additional information is shown in Section 2.3.1.

The hydrochloric acid which was used in the experimental work was at a concentration of 37 wt%, this concentration was chosen to provide molarities ranging from about 0.001 to 0.5 M HCl. The molarity of this acid solution were calculated and are illustrated in Appendix B.

For HY zeolites, 1 g was dispersed in 20 ml of aqueous solution 0.25 M by employing 100 ml flask linked with a reflux condenser then heating the mixture to 60 °C for 2 h. After the desired time, the flask was put in iced water. The solution was then separated using a rotary centrifuge (Heraeus Multifuge 3 S R) and washed with distilled water several times until the liquid over the sediment zeolite reached to about 7. Finally, the water was removed and the solid was dried at 100 °C overnight.

4.5.2 Desilication technique by using sodium hydroxide aqueous solution

Base leaching is used to modify the zeolite by removing the silicon atoms from the zeolite framework, more details of which are provided in Section 2.3.2. The alkaline treatment was applied using sodium hydroxide (NaOH) in the range 0.025- 10 M. The molarity of this base solution were calculated and presented in Appendix C.

Similar to the process of acid leaching, the base leaching was conducted by dispersing 3 g of HY5.1 and HY30 zeolite in an aqueous solution of 0.5 g NaOH with 250 ml water (0.05 M), were put in a flask linked with reflux. The mixture was heated

to 85 °C for 1 h. After the desired time, the flask was put in iced water to stop the reaction. The solution was then separated using the same rotary centrifuge and washed with distilled water several times until the pH dropped to 7. The solid was then dried at 100 °C overnight. The solid which resulted from this process was in Na-form so it was exchanged in a flask combined with reflux using ammonium nitrate (99+ %) at 0.5 M and 80 °C for 2 h. The reaction was then stopped using iced water, and the solution subsequently separated using the same rotary centrifuge and washed five times with water. The wet solid was put in the oven overnight at 110 °C. The zeolite that were produced were transformed to the H-form by calcination at 500 °C for 4 h.

4.5.3 Silylation technique by employing tetraethoxysilane

This modification was done using 4 g of zeolite suspended in 100 ml of *n*-hexane at ambient temperature (see Section 2.3.3). The purity of *n*-hexane ($\geq 97\%$) plays a vital role during this treatment because increasing the amount of water leads to an increase in the degree of polymerisation of TEOS with itself, as shown previously by Ng and McCormick (1996) and Jang *et al.* (2001). 0.6 ml of tetraethyl orthosilicate (TEOS) was added; this amount of TEOS was added according to a loading of 4% silicon dioxide (SiO₂) (Zheng *et al.*, 2002, Gründling *et al.*, 1996). The 1 hour silylation was achieved under reflux with a speed stirrer ~1000 rpm. Then, the evaporator was used to remove the *n*-hexane and the zeolite was calcinated at 500 °C for two hours. The exothermic peak of the TEOS decomposition appeared at 650 °C which means that the calcination at 500 °C was not effective using this silylation agent (Shehab, 2018). Silylation was performed by repeating all the steps above three times.

4.5.4 Pre-coking technique by employing the individual reactant species toluene and 1-heptene

Pre-coking was conducted by adsorbing 1-heptene and toluene as coke precursors (more information is available in Section 2.3.4). 0.5 g of zeolite was put in the FBR and activated at 300 °C with 30 ml min⁻¹ of air for 2 h, after which the system was cooled down to room temperature. Toluene was introduced at a flowrate of 10 ml h⁻¹ at 90 °C for 2 h; however, 1-heptene was inserted at the same flowrate but at 80 °C and for 1 h. In all cases an inert nitrogen flow at 30 ml min⁻¹ was used to purge and accelerate the reaction. The variation in the pre-coking reaction conditions,

especially the reaction temperature, is ascribable to the deference in the volatility of these reactants.

4.6 Calculations

4.6.1 Volumetric flowrate

The actual flowrate was measured using the bubble meter. After the gas passes through the MFC, it was connected with a small vessel which contains a liquid mixture of soap and water. The volumetric flowrate can be calculated according to the Equation 4.1.

$$\text{Volumetric flowrate of feed (ml min}^{-1}\text{)} = \frac{\text{Volume displaced (ml)}}{\text{Time (min)}} \quad \dots (4.1)$$

4.6.2 1-Heptene calibration according to GC-FID

The standard sample for calibration was prepared with diluted 1-heptene (98 %) in ethanol (≥ 99.8 %) with a specific amount of *n*-hexane (≥ 97 %) as an internal standard, as shown below in Table 4.3:

Table 4.3. 1-Heptene calibration standard.

No.	Percentage (%)	Ethanol (μl)	1-Heptene (μl)	<i>n</i> -Hexane (μl)	Concentration (g cm^{-3})
1	20 %	1000	200	100	0.1162
2	10 %	1000	100	100	0.0634
3	6.7 %	1000	66	100	0.0436
4	2 %	1000	20	100	0.0137
5	1 %	1000	10	100	0.0069

These steps were repeated two times and the average taken with relative standard error ± 0.03 % as shown in Figure 4.5.

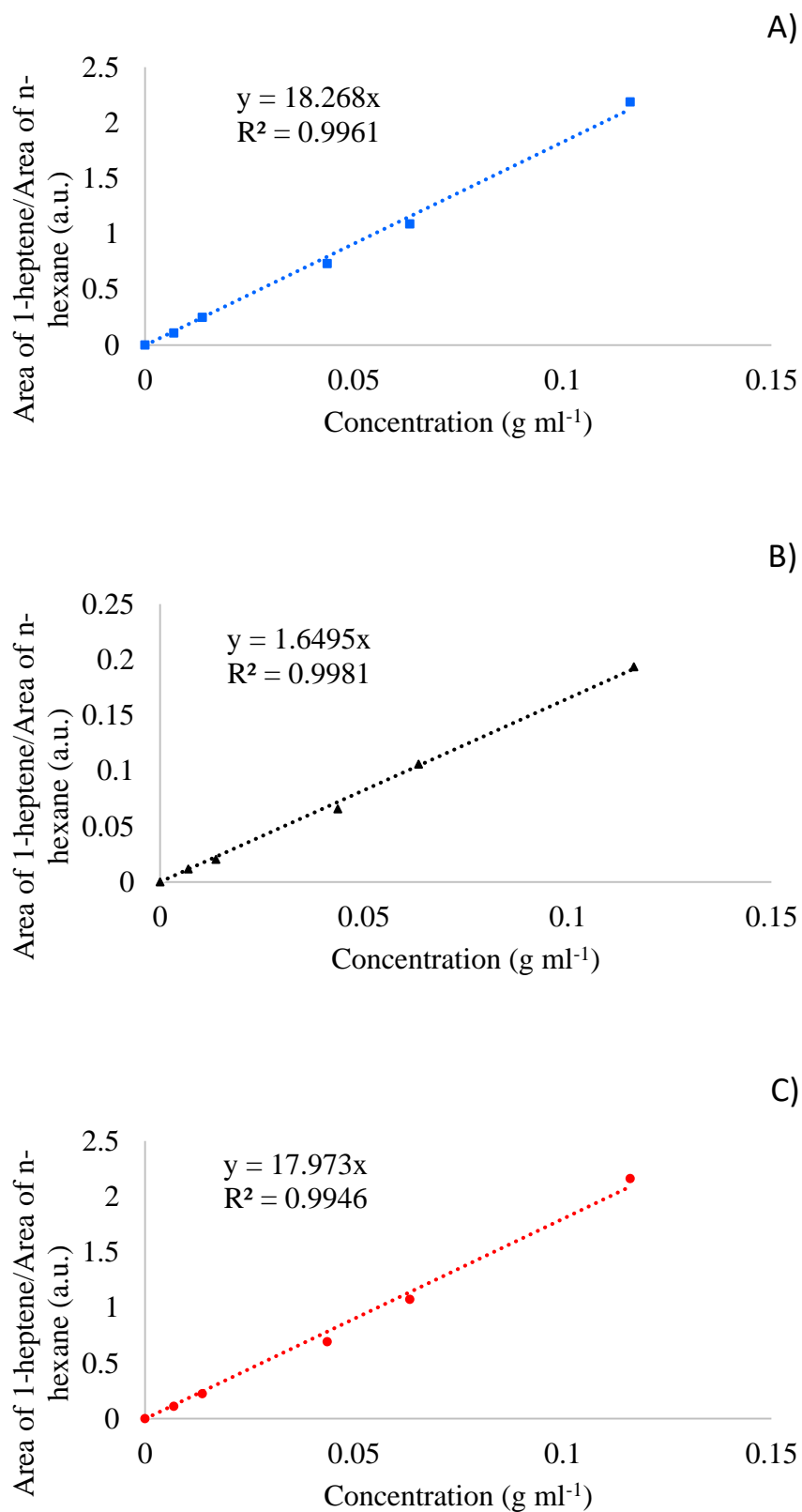


Figure 4.5. Calibration curve of 1-heptene using GC-FID; A) Run 1; B) Run 2 and C) Average

4.6.3 Weight hourly space velocity (WHSV)

WHSV represents the feed weight per catalyst weight per hour, as shown in Equation 4. 2 (Zhou et al., 2015).

$$\text{WHSV} = \frac{\text{Feed mass flowrate (g h}^{-1}\text{)}}{\text{Catalyst mass (g)}} \quad \dots (4. 2)$$

4.6.4 Conversion

The conversion of the limiting reactant (1-heptene) was determined by dividing the number of moles consumed by the initial number of moles of the limiting reactant, as shown in Equation 4. 3.

$$\% \text{ Conversion} = 100 \times \left[\frac{\text{no. of moles of 1-heptene consumed}}{\text{no. of moles of 1-heptene introduced}} \right] \quad \dots (4. 3)$$

From the GC-FID, the areas of unreacted and all products were obtained. However, the number of moles of the limiting reactant at the inlet to the reactor was determined by taking the reactant before the reaction and mixed with the internal standard then injected in the GC-FID. All these areas were measured according to a specific amount of internal standard.

From the calibration in Section 4.5.2., the moles of initial reactants and un- reactants were determined. After that, the area of one mole of initial 1-heptene was calculated according to the carbon number of 1-heptene equal to 7.

As illustrated previously, the injection procedure was completed three times and the average value was used in the calculation.

4.6.5 Selectivity

Selectivity to all products was calculated according to Equation 4. 4, which takes into account coke as one of the products.

$$\% \text{ Selectivity} = 100 \times \left[\frac{\text{no. of moles of monoheptyltoluene}}{\text{no. of moles of 1-heptene consumed}} \right] \quad \dots (4. 4)$$

The presence of 1-heptene and toluene were readily identified; however, monoheptyltoluene products (three peaks of 2-heptyltoluene and 3-heptyltoluene and one peak of 4-heptyltoluene) are observed, which correspond to ortho, meta and para isomers as shown in Figure 4.6. All these products (2, 3 and 4-heptyltoluene) were

difficult to identify due to these products not being commercially obtainable as reference components. Therefore, the carbon number method was used to calculate the moles of all products.

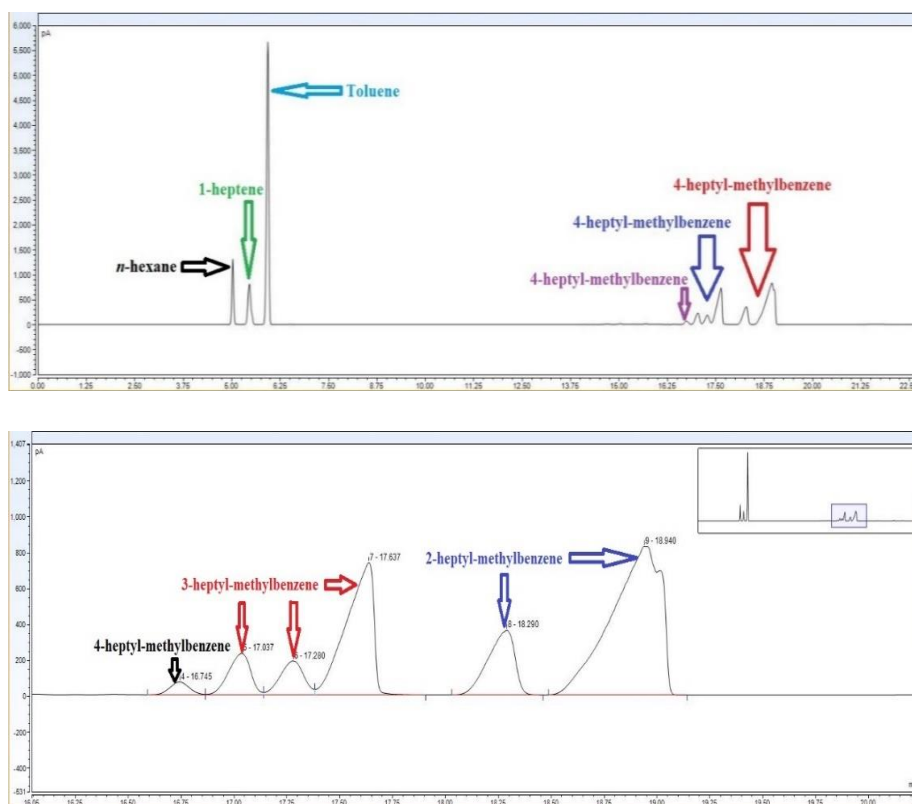


Figure 4.6. GC/FID Chromatogram for reaction products of toluene alkylation with 1-heptene at 90 °C, atmospheric pressure, 0.25 g HY5.1 zeolite, reaction time of 360 min, T: H ratio is 3: 1 and using BR.

From the calibration in Section 4.5.2., the moles of initial reactants and un- reactants were determined. After that, the area of one mole of initial 1-heptene was calculated according to the carbon number of 1-heptene equal to 7.

Moles of products were calculated depended on dividing the (area of any product / area of internal standard) per area of one mole of 1-heptene inlet, then divided this result on carbon number of monoheptyltoluene which is equal 14.

Finally, the selectivity of coke was determined according to equation 4. 5.

$$\% \text{ Selectivity} = 100 - \sum \text{selectivity of all other products} \quad \dots (4. 5)$$

4.6.4 Experimental error

The experimental error was measured via repetition of chosen experiment three times at various times according to Equation (4. 6):

$$E = \frac{\sigma}{\mu} \times 100 \quad \dots (4. 6)$$

Where E is the error, σ is the standard deviation and μ is the average of the three calculations.

$$\sigma = \sqrt{\frac{1}{N} \sum_{i=1}^N (x_i - \mu)^2} \quad \dots (4. 7)$$

Where N is the number of experiments (three experiments) and x_i is the value of each experiment ($i= 1, 2$ and 3).

$$\mu = \frac{1}{N} \sum_{i=1}^N x_i \quad \dots (4. 8)$$

Chapter 5

*Role of coke deposits
during the toluene
alkylation with 1-
heptene over fresh and
modified zeolites*

5.1 Introduction

The primary reason for choosing aromatic hydrocarbons (e.g. toluene) for use in the alkylation reaction is the prediction of the decrease in price of toluene in the coming years (Smirniotis and Ruckenstein, 1995, Tsai et al., 1999). Toluene is favoured over benzene because it is more reactive and less toxic. Alkylation is considered environmentally friendly because it relies on zeolite-based catalysts which makes the alkylation reaction cleaner and less polluting than the homogenous catalysts. Experimentally, either a batch reactor or a flow reactor is preferred for investigations of zeolite deactivation and coke formation because they are easier to use than other reactors (Mori et al., 1991).

The main reason for choosing temperature ~ 90 °C for the alkylation reaction is ascribed to a thermodynamic study which showed that this reaction is exothermic meaning low temperatures favour thermodynamic equilibrium (Tsai et al., 2003, Corma et al., 2000). The low toluene to 1-heptene ratio was chosen to give the highest conversion of 1-heptene (the limiting reactant) using a small reactor size therefore, in the present study the toluene to 1-heptene ratio was 3:1 because it shows in detail the main two reactions (double bond shift and alkylation of toluene). However, the FBR which is used for commercial alkylation works with a 6-8 toluene to 1-heptene ratio (Cowley et al., 2005). The purpose of employing various Si/Al ratios for zeolite, is to investigate the role of zeolite acid properties in the toluene alkylation reaction (Craciun et al., 2007). Hajimirzaee *et al.* (2015) showed the distribution of acid sites can be altered by changing the Si/Al ratio of the zeolite catalyst which also leads to alterations of the total acidity.

The dealumination and desilication treatments of zeolite by acid leaching and base leaching have been previously investigated (Silaghi et al., 2014). However, the influence of these dealuminated zeolites on the catalytic performance during the toluene alkylation with 1-heptene has been rarely reported (Magnoux et al., 1997).

The dealumination process is one of the most important methods to form mesopores, which simplify the desorption of alkylation products because they act to increase the stability and activity of the zeolite (Da et al., 1999a, Magnoux et al., 1997, Yuan et al., 2002, Hornáček et al., 2010a). The formation of mesopores increases the likelihood of the diffusion of heavy products located inside the zeolite pores, and

thereby increases the reaction rate (Hornáček et al., 2010a). Moreover, the selectivity towards the main product increases by using dealuminated zeolite because the alkylation activity increases by increasing the acid strength with increases to the Si/Al ratio (de Almeida et al., 1994, Craciun et al., 2007). Additional details are described in Section 2.3.1.

The desilication treatment acts to improve zeolite stability which increases the diffusivity of both coke pre-cursors and dimer side products (Chaouati et al., 2017, Lin et al., 2013, Lee et al., 2017). Additionally, it contributes to the formation of a mesoporous structure which works to decrease the deactivation because this structure makes the products and by-products diffuse faster. Extra information can be found in Section 2.3.2.

Therefore, studying the effect of thermal modifications such as dealumination and desilication treatments *via* acid and base solutions respectively. Through these treatments; two hypotheses were taken into account:

- A- Dealumination acts to reduce the coke deposits either by decreasing the aluminum content thereby decreasing the acidity of the zeolite catalyst or through the formation of mesopores;
- B- Desilication involves the formation of a mesoporous structure which leads to improved diffusion properties and enhanced selectivity of the desired products and decreased coke formation that results from trapped bulky molecules.

A few authors have investigated the role of coke deposits during the toluene alkylation with olefin over different types of zeolite catalysts.

Da *et al.* (1999a) studied the alkylation of toluene with 1-dodecene using a FBR over HFAU catalyst (Si/Al ratio was 25) with a toluene to 1-dodecene ratio of 3:1. They observed that monododecyltoluene was the main product, however, coke was formed as a result of bidodecyltoluene and tridodecyltoluene accumulating in small amounts. However, they are bulkier than the pore opening, so they cannot desorb from the zeolite pores (Da et al., 1999a, Guisnet, 2002).

The alkylation reaction of toluene with 1-heptene using HFAU was studied by (Da et al., 1999b). They reported that monoheptyltoluene is the desired product; it forms quickly and selectively. Usually, a small amount of biheptyltoluene appears,

especially when the conversion becomes more than 50%. Coke is formed by monoheptyltoluene, biheptyltoluene and triheptyltoluene. The number of coke molecules increase with the time-on-stream because the amount of monoheptyltoluene increases and biheptyltoluene decreases. The same conclusion was made by Cowley and co-workers (Cowley et al., 2005).

Although toluene alkylation with 1-heptene over HY zeolite in a batch reactor and fixed bed reactor (FBR) has been investigated previously, there are few works interested with the formation and deactivation of coke and through this reaction. Generally, the side reactions (dimerisation, oligomerisation and di-alkylation) are the main carbonaceous compounds that are formed during the alkylation reaction over zeolite catalyst and they lead to catalyst deactivation. However, Guisnet (2002) suggested that these carbonaceous deposits could play a positive role when they act to enhance the reaction *via* working as active or beneficial centres. Therefore, the main target of this work is exploiting the role of carbon deposition in enhancing the toluene alkylation with 1-heptene as well as studying the effect of these carbonaceous material properties on the catalytic performance. The coke deposits that are formed during the alkylation reaction will be characterised *via* several types of thermal and spectroscopy characterisation techniques. However, there are a few steps which need to be completed before the coke can be studied, such as: investigating the toluene alkylation with 1-heptene by employing batch reactor and FBR by using several zeolites and operation conditions to choose the appropriate zeolite structure for this reaction;

The present work was divided into two sections:

The first section is concerned with the toluene alkylation reaction with 1-heptene over three types of fresh zeolite catalyst (HY5.1, H-Beta and H-mordenite) at various reaction times (20, 120 and 360 min). The toluene to 1-heptene ratio was 3 and the role of coke during toluene alkylation with 1-heptene at the reaction temperature was 90 °C. BR was employed, as described in Sections 5.4.1.1. After that, two types of fresh (HY5.1 and HY30) zeolites, which were chosen as the most appropriate zeolite catalysts from the BR, were used in the FBR run at 90 °C and with a toluene to 1-heptene ratio of 8:1. 30 ml min⁻¹ of nitrogen was used as an inert gas, and the TOS was 240 min, as shown in Section 5.4.1.2.

In addition, the temperature between 80 and 90 °C was examined, as explained in Section 5.4.1.2.1. The influence of TOS was studied and is presented in Section 5.4.1.2.2. Then, the effect of catalyst weight has been investigated for 0.5, 0.75 and 1 g of HY5.1 zeolite, as shown in Section 5.4.1.2.3. Then, investigating the influence of Si/Al ratio by employing different ratios of SiO₂/Al₂O₃ of HY zeolite (HY5.1 and HY30) on the catalytic performance was investigated, as explain in Section 5.4.1.2.4. Identifying the structure most affective at the toluene alkylation with 1-heptene among the fresh and modified zeolites (dealumination which is presented in Section 5.5.1., desilication as shown in Section 5.5.2.).

There are many advantages to characterising the coke deposits formed during the alkylation reaction, such as: it helps in choosing the most appropriate structure that gives the lowest coke amount and acts to decrease the deactivation rate thereby increasing the longevity of the zeolite. Therefore, the second section is concerned with the properties of coke deposits (nature, composition, structure and type) that are formed during this reaction and its effect on the catalytic performance. In this section, the zeolites were chosen at 120 min reaction time and at 90 °C for all samples using the BR. In the FBR, the temperature was 90 °C, the pressure was atmospheric and the TOS was 240 min. Several characterisation techniques were used to study the properties of the coke that was formed during the alkylation reaction.

5.2 Materials and methods

The four types of zeolite catalyst employed in the toluene alkylation with 1- heptene are HY5.1, HY30, H-mordenite and H-Beta (all the physical properties were described in Section 4.2). Moreover, two modifications (dealumination and desilication treatments) were made to all these zeolites, as described early in Section 4.5.

Properties of the fresh and modified zeolite samples were studied using several types of characterisation technique, such as: X-ray diffraction (XRD); scanning electron microscope (SEM); energy dispersive X-ray spectroscopy (EDX); X-ray fluorescence spectrometry (XRF); nitrogen adsorption-desorption and temperature-programmed desorption (TPD). All these instruments were described previously with methods in Chapter 3.

The methods developed for both GC-MS and GC-FID were detailed in Section 4.4. The reaction was performed using a BR or FBR, as previously described in Section 4.3. The catalytic activities (conversion of 1-heptene and selectivity of monoheptyltoluene, heptene isomers and coke) were illustrated in Section 4.6.

Finally, spent zeolite samples were collected and characterised off-line by employing different techniques (thermal and spectroscopy) to determine the amount, nature and type of coke deposits on the zeolite during the alkylation reaction. These techniques comprised: nitrogen sorption; thermogravimetric Analysis (TGA); elemental analysis; temperature programmed oxidation (TPO) and Fourier-transform infrared spectroscopy (FTIR). Information about these techniques is detailed in Chapter 3.

5.3 Results and Discussion

5.3.1 Zeolite catalyst characterisation

5.3.1.1 XRD

The XRD pattern of dealuminated HY5.1 (0.25M) is typical of HY zeolite, however all the higher concentrations of acid solution above 0.25M HCl resulted in collapse of the zeolite structure, as shown in Figure 5.1. This result is in agreement with that obtained by (Yan et al., 2003).

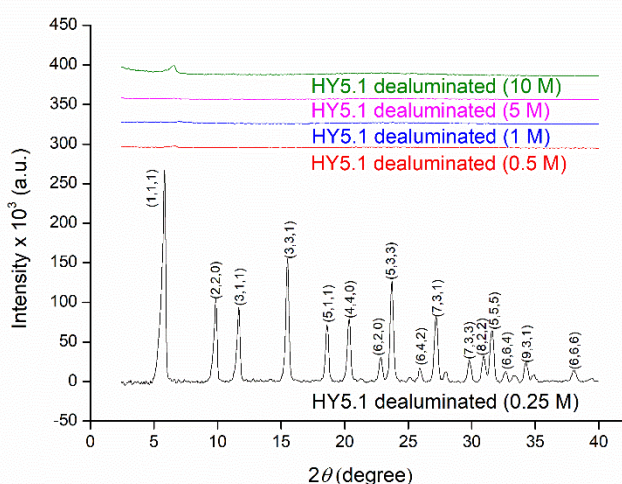


Figure 5.1. The XRD patterns of HY5.1 dealuminated with different molarities of acid solution.

The intensity of dealuminated and desilicated HY5.1 and HY30 decreases compared with the fresh zeolites which indicates that the crystallinity was reduced during these modifications (Figure 5.2). Similar findings were obtained by Al-Zaidi *et al.* (2012), Möller and Bein (2013). Although there is a difference in the XRD diffractions for the post-treated zeolites, the structure of desilicated HY5.1, dealuminated HY30 and desilicated HY30 remains intact which indicates the durability of the zeolite. However, the structure of the dealuminated HY5.1 seems to be partially collapsed.

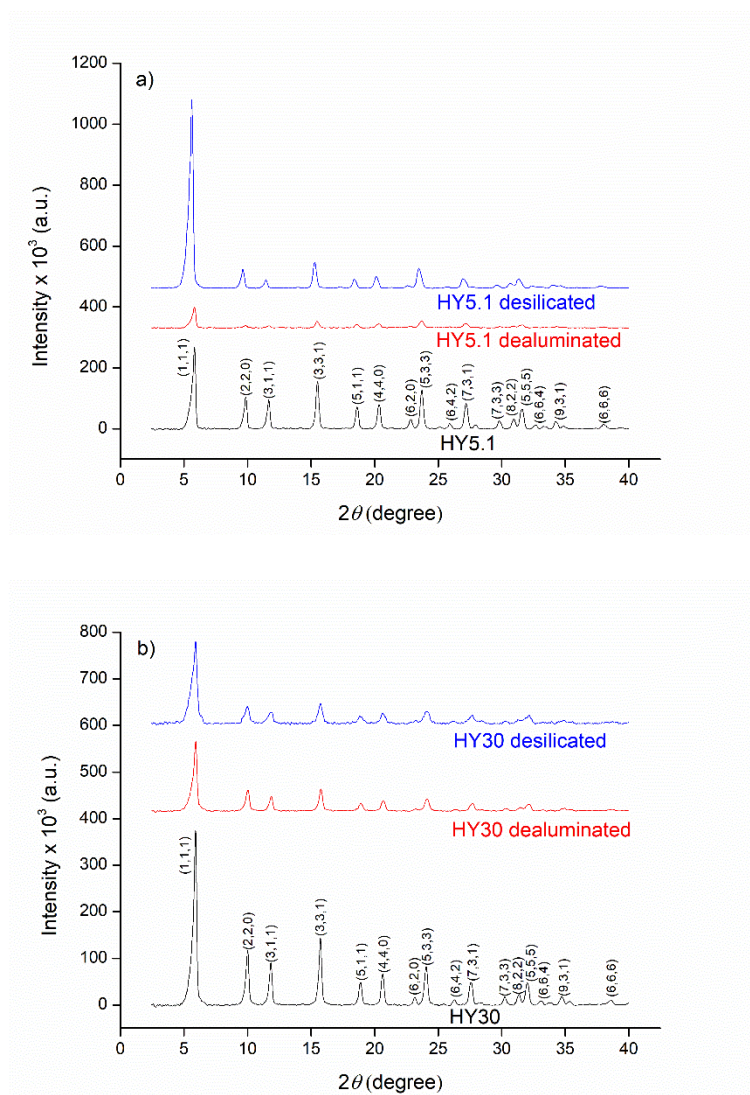


Figure 5.2. The XRD patterns of fresh and modified a) HY5.1; b) HY30 zeolite catalysts.

Indeed, the intensity of desilicated HY5.1 in the 2θ range of 4-6° seems stronger than that of the fresh sample at the same range, possibly because the recrystallisation of this specific disrupted region through the base leaching treatment. The same matter was reported in another work but using beta alkali-treatment (Zhang et al., 2017).

5.3.1.2 SEM

SEM images of HY30, dealuminated HY30 and desilicated HY30 zeolite catalysts show the alterations in the morphology of the zeolite samples after the modifications (Figure 5.3, Figure 5.4 and Figure 5.5). In general, the particles of all these three samples were uniform. As is clear, the SEM images of the dealuminated and desilicated samples illustrate there was no appreciable change in the morphology and size of the zeolite particles (Figure 5.4 and Figure 5.5). In addition, the zeolite crystals after modification were obviously segregated, have bulk sizes and sharp edges. This conclusion is in agreement with the results that were obtained by XRD in Section 5.3.1.1.

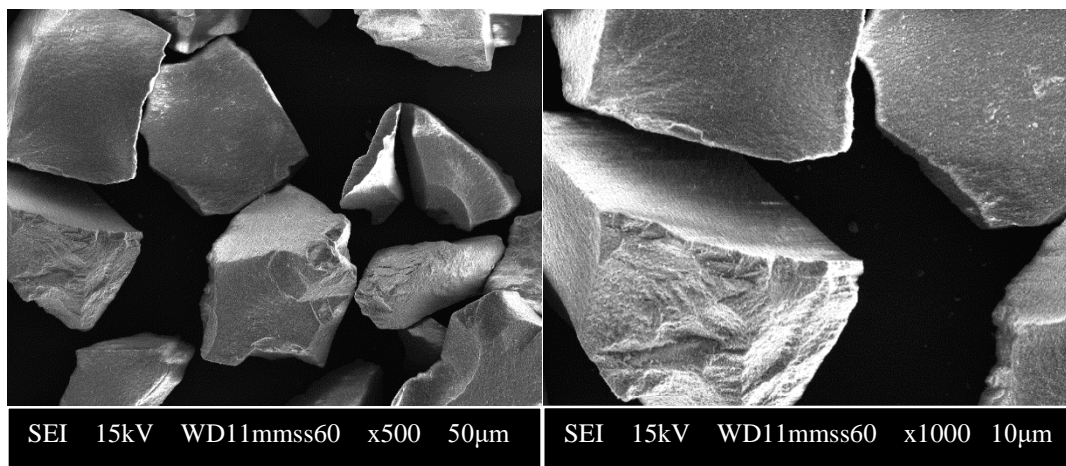


Figure 5.3. The SEM image of fresh HY30.

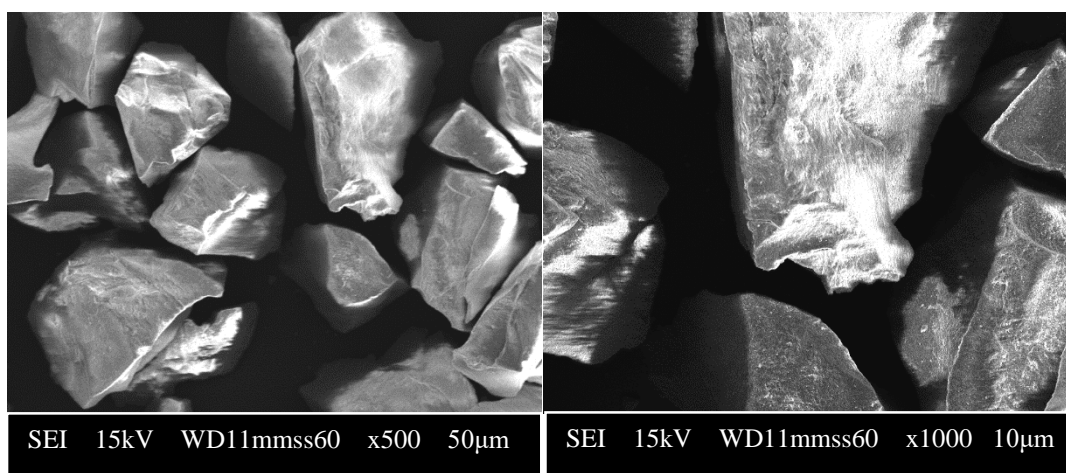


Figure 5.4. The SEM image of HY30 dealuminated zeolite in 0.025 M of HCl solution.

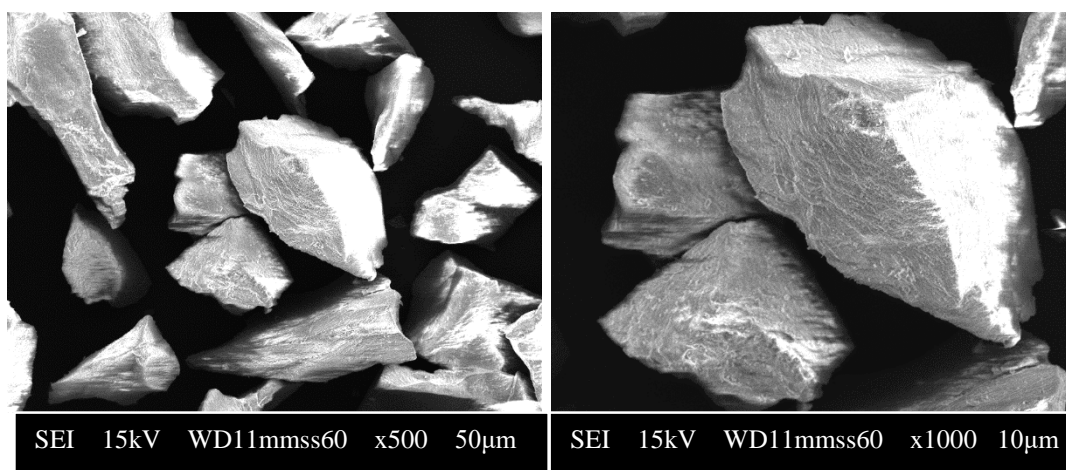


Figure 5.5. The SEM image of HY30 desilicated zeolite in 0.05 M of NaOH solution.

5.3.1.3 XRF and EDX results

The Si/Al ratio of fresh and modified HY5.1 and HY30 were determined using XRF and EDX (see Table 5.1). For the EDX, two scans have been completed; in each image, 4 locations have been randomly chosen in order to find the average value. There are only slight differences between the results of these techniques. In both cases, the Si/Al ratio was increased after the dealumination treatment, and decreased for the desilicated samples, except for the desilicated HY5.1. This zeolite did not change after the desilication treatment which could be a result of the low concentration of sodium hydroxide ~0.05 M that was employed during this modification, as described in Section 4.5.2.

Table 5.1. The results of Si/Al mole ratio using XRF and EDX for fresh and modified zeolite catalysts.

Zeolite	Si/Al (XRF)	Si/Al (EDX)
HY5.1	3.3	3 ± 0.07
HY5.1 dealumination	4.5	3.8 ± 0.14
HY5.1 desilication	3.3	2.9 ± 0
HY30	15.1	16.3 ± 0.35
HY30 dealuminated	26.6	28.6 ± 0.14
HY30 desilication	13.6	15 ± 0.71

5.3.1.4 Nitrogen adsorption-desorption results

Firstly, calibration for nitrogen sorption was been done to check the error percentage for this equipment and to check the accuracy of calculations compared with the results that were provided by Alfa Aesar company. It can be seen that the BET surface areas are 713.7 and 714.1 m² g⁻¹ with ± 0.06 % error for the two calibrations and ± 2.2 % error percentage compared with that provided from the company, which was 730 m² g⁻¹.

When the relative pressure is (0-0.45), the HY samples had similar nitrogen uptakes (Figure 5.6); this means all these samples have approximately the same microporosity as shown in Section 3.6. However, at relative pressure above 0.45, the hysteresis loops appeared which indicates the existence of mesopores.

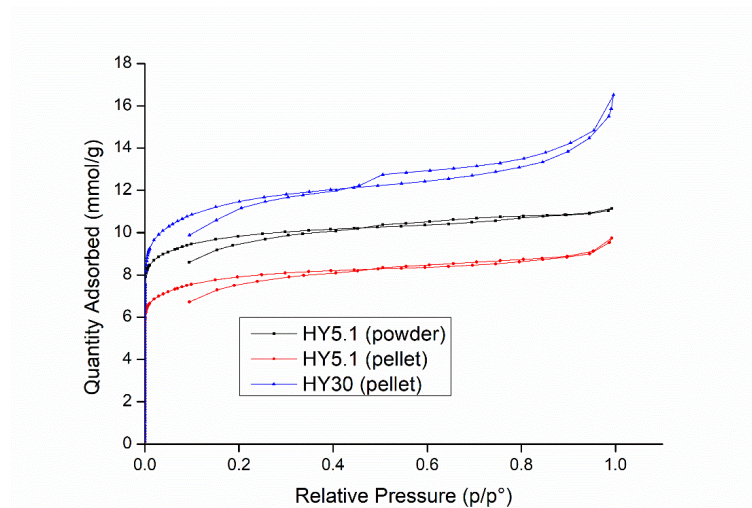


Figure 5.6. Nitrogen sorption isotherms of fresh HY5.1 (powder), HY5.1 (pellet) and HY30 (pellet) zeolite catalysts.

Nitrogen adsorption-desorption isotherms of HY5.1 and its modified samples showed typically type I curve of hysteresis loop which indicates the presence of micropores as shown in Section 3.6. The hysteresis loop of HY30 and its modified samples was typically type IV which refers to the existence of micro and mesopores.

Table 5.2 shows the textural parameters of fresh and modified zeolite samples. The BET method was employed to measure the specific surface area; the t -plot method was used in the determination of the micropore volume; the BJH method was used to determine the mesopore size; and the Horvath-Kowazoe method was employed to determine the micropore size distribution.

Figure 5.7 shows the isotherms of fresh HY30, dealuminated HY30 and desilicated HY30 zeolite samples, it seems there was a slight change in the hysteresis loops of the desilicated samples compared with the fresh zeolite; this alteration could be ascribed to the creation of mesopores as the pore size distribution and mesopore volume was slightly increased. The decrease in both micropore area and volume of the dealuminated HY30 zeolite can be traced back to some of these micropores shrinking as a result of Al-O bond removal. These results are similar to those obtained by Al-Zaidi *et al.* (2012), Hornáček *et al.* (2010a).

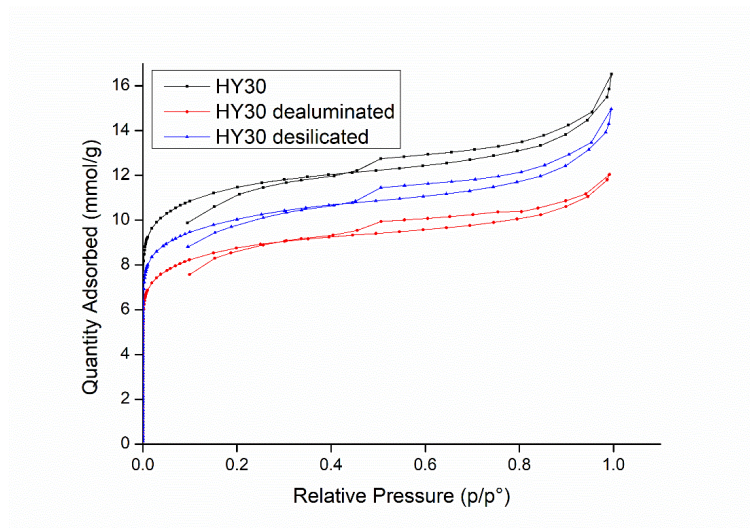


Figure 5.7. Nitrogen sorption isotherms of fresh HY30, dealuminated HY30 and desilicated HY30 zeolite catalysts.

Additionally, the external area was slightly increased post alkali-treatment of the HY30 probably because of the formation of mesopores which have a larger pore volume and pore size than the micropores, as indicated in Table 5.2. A similar result was given by Groen *et al.* (2005).

Table 5.2. The results of surface area of parent and modified zeolite catalysts.

Zeolite	S_{BET} ($\text{m}^2 \text{g}^{-1}$)	S_{mic} ($\text{m}^2 \text{g}^{-1}$)	S_{ext} ($\text{m}^2 \text{g}^{-1}$)	V_{tot} ($\text{cm}^3 \text{g}^{-1}$)	V_{mic} ($\text{cm}^3 \text{g}^{-1}$)	V_{meso} ($\text{cm}^3 \text{g}^{-1}$)	$d_{\text{p meso}}$ (Å) BJH	$d_{\text{p mic}}$ (Å) Horvath-Kowazoe
HY5.1 (powder)	713.7	694.3	19.5	0.387	0.349	0.038	38.6	7.07
HY5.1 (pellet)	577.1	548.6	28.5	0.339	0.269	0.070	50.59	6.96
HY30 (pellet)	844.9	760.4	84.6	0.556	0.369	0.187	58.45	7.53
HY30 dealuminated (pellet)	650.8	588.7	62.1	0.418	0.287	0.131	53.32	7.64
HY30 desilicated (pellet)	848.9	757.8	91.1	0.505	0.313	0.192	60.46	7.71

5.3.1.5 TPD

Figure 5.8 shows the NH₃-TPD profile of fresh HY5.1 and HY30 zeolite catalysts. Clearly, the fresh HY5.1 had a higher acid amount compared with the fresh HY30. Similar results were obtained by Craciun *et al.* (2007).

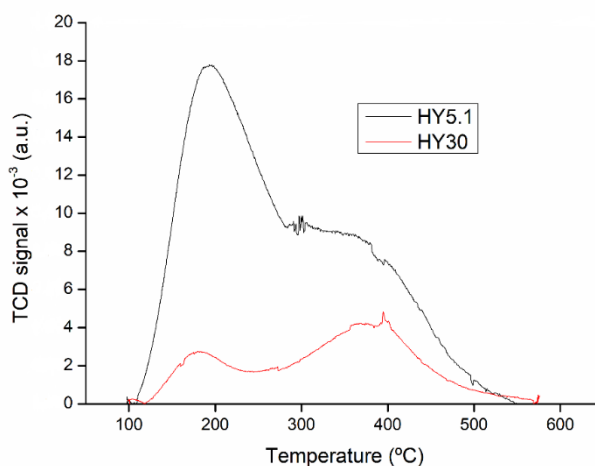
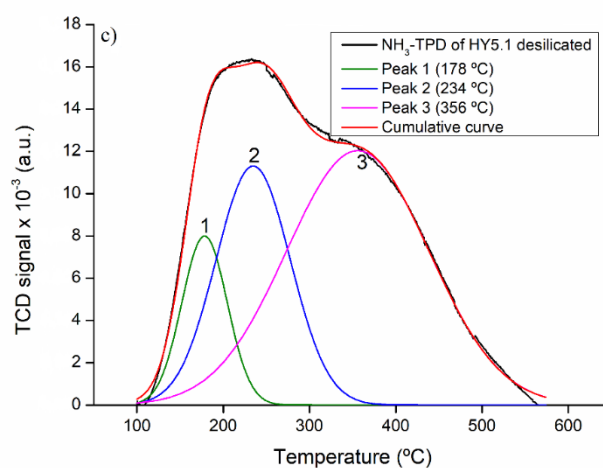
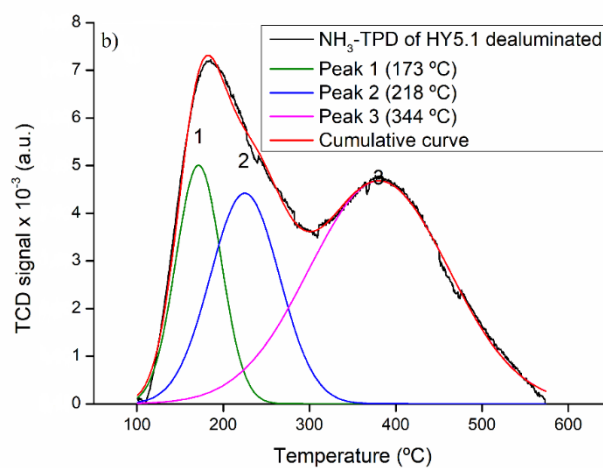
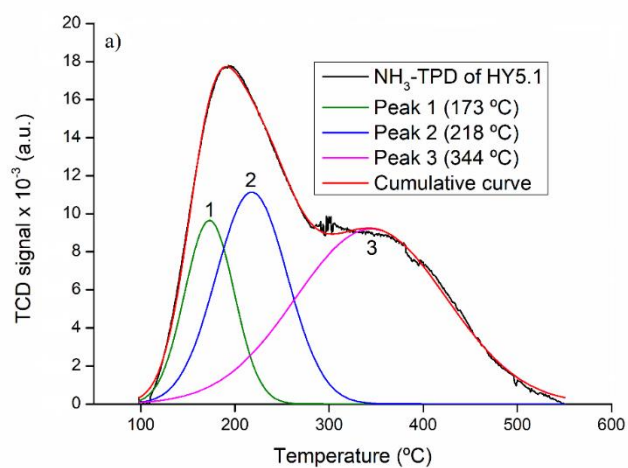


Figure 5.8. NH₃-TPD profile of fresh HY5.1 and HY30 zeolite catalysts.

Generally, the peaks of HY5.1, HY30 and their modified zeolite samples overlapped however, they cannot be separated readily (Figure 5.8). Therefore, the TPD profiles have been mathematically deconvoluted to three Gaussian peaks by employing Origin software (OriginPro 8.5.1) as shown in Figure 5.9. The selection of initial band position was corresponding to the previous studies for TPD analysis of fresh and modified zeolite catalyst (Triantafillidis *et al.*, 2000, Hajimirzaee *et al.*, 2015).



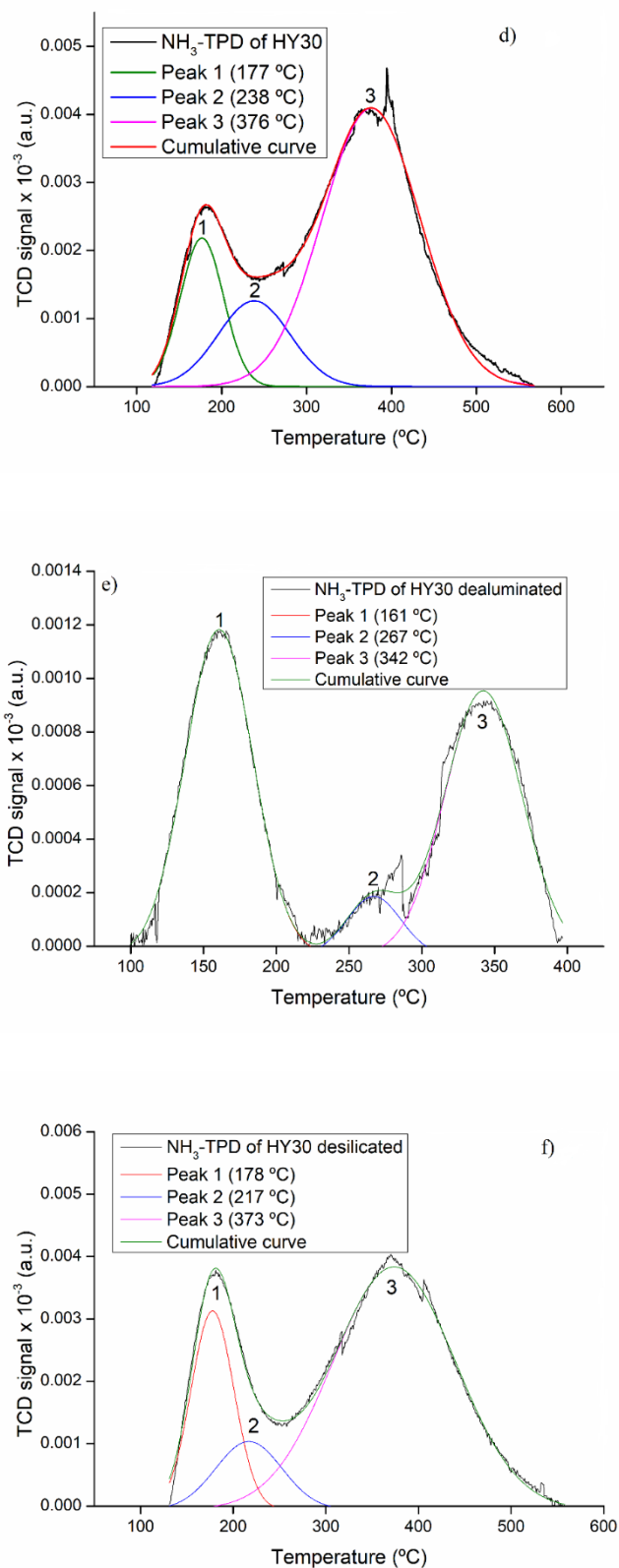


Figure 5.9. Experimental and deconvoluted NH_3 -TPD curves of a) fresh HY5.1, b) HY5.1 dealuminated, c) HY5.1 desilicated, d) fresh HY30, e) HY30 dealuminated and f) HY30 desilicated zeolite samples (refer to Table 5.3).

Table 5.3 indicates the NH₃-TPD results of HY5.1 and HY30 and their post-treated specimens. All these samples have three peaks corresponding to weak, medium and strong acid sites. The first peak appeared between 160 and 180 °C and represents the weak acid sites. The second peak corresponds to the medium acid sites and appeared between 215 and 270 °C. The third peak is above 350 °C and represents the strong acid sites. These results are in agreement with those that were obtained by Triantafillidis *et al.* (2000).

The total acid amount was reduced after the HCl treatment for both HY5.1 and HY30 as shown in Table 5.3. This could be a result of the reduction in aluminium content which could indicate that the dealumination modification took place. This result is in agreement with the work of Wang *et al.* (2001b).

In contrast, Table 5.3 shows the amount of acid was increased for both HY5.1 ~23% and HY30 ~5% after the base treatment (employing NaOH solution), probably because this modification influenced the zeolite structure *via* the formation of mesopores. The ammonia molecules are smaller than the mesopores and hence their accessibility is increased after the treatment. The same results were obtained by Zhang and Ostraat (2016), Zhang *et al.* (2017), Groen *et al.* (2005), Zhou *et al.* (2017).

Table 5.3. Fresh and modified acid properties of HY5.1 and HY30 zeolite catalysts.

Zeolite	Weak acid sites (mmol g⁻¹)	Medium acid sites (mmol g⁻¹)	Strong acid sites (mmol g⁻¹)	Total acid amount (mmol g⁻¹)	decrease of acid site concentration after modification (%)
HY5.1	0.25 (173 °C)	0.42 (218 °C)	0.73 (344 °C)	1.4	-
HY5.1 dealuminated	0.13 (171 °C)	0.18 (225 °C)	0.39 (380 °C)	0.7	50 %
HY5.1 desilicated	0.23 (178 °C)	0.52 (234 °C)	1.07 (356 °C)	1.82	+23.1 %
HY30	0.06 (177 °C)	0.06 (238 °C)	0.25 (376 °C)	0.36	-
HY30 dealuminated	0.031 (161 °C)	0.004 (267 °C)	0.031 (342 °C)	0.066	81.7 %
HY30 desilicated	0.07 (178 °C)	0.04 (217 °C)	0.27 (373 °C)	0.38	+5.3 %

5.4 Catalytic activity measurements

Toluene alkylation with 1-heptene was carried out using two reactor types; BR and FBR. In the BR, the reaction was conducted over HY5.1, H-mordenite and H-Beta to investigate the influence of zeolite structure on this reaction. In addition, two HY zeolites with a Si/Al ratio of 5.1 and 30 were chosen to investigate the influence of zeolite acid properties on toluene alkylation with 1-heptene. In the FBR, the reactions were carried out over two zeolites; HY5.1 and HY30 on the basis of results from the BR studies.

Several reaction conditions influence the alkylation reaction, such as: reaction temperature; pressure; toluene/1-heptene mole ratio; time-on-stream (TOS); weight hourly space velocity (WHSV); amount of zeolite; and inert gas flowrate. The typical operating conditions of this reaction were chosen according to Da *et al.* (1999b), (2001). They were carried out in the BR at 90 °C for 20, 120 and 360 min reaction times, using 0.25 g of zeolite, and with a toluene to 1-heptene ratio of 3:1.

In the FBR, the reaction was carried out at a reaction temperature chosen according to Section 5.4.1.2.1, atmospheric pressure, the WHSV was constant at 17 h⁻¹. The TOS was chosen as a result of the study in Section 5.4.1.2.2, the weight of the zeolite catalyst was selected as a result of the investigation in Section 5.4.1.2.3 and a constant flowrate of N₂ of 30 ml min⁻¹ was used.

For both reactors, the liquid products were identified by employing the GC-MS as described previously in Section 4.4.1. The products were divided into three groups: alkylation products (2-, 3- and 4-heptyltoluene), isomerisation products (2- and 3-heptene) and coke (which represents the side products) as shown in Section 2.4.1. Neither dimerisation nor oligomerisation products were detected. The analysis of the gas phase showed there were no components that appeared in the gas chromatogram during this reaction as mentioned in Section 4.3.2. Catalytic activity measurements were described in Section 4.6.

The reproducibility of the alkylation reaction using the BR was determined by repeating a model reaction three times on different days, per each experiment. The operating conditions were a temperature of 90 °C, a reaction time of 120 min, 0.25 g of HY5.1 zeolite catalyst, and a toluene to 1-heptene ratio of 3. The reproducibility

error for conversion of 1-heptene was ± 4 % while it was ± 3 % for the 2-heptyltoluene selectivity and ± 4 % for coke selectivity. The operating conditions for the same reaction but using the FBR were a temperature of 90 °C, a TOS of 240 min, 0.5 g of HY5.1 zeolite catalyst, a N₂ flowrate of 30 ml min⁻¹, a WHSV of 17 h⁻¹ and a toluene to 1-heptene ratio of 8. The reproducibility error was ± 1 % for 1-heptene conversion whereas it was ± 1 % for the selectivity of 2-heptyltoluene and it was ± 2 % for coke selectivity. In general, these error percentages are considered acceptable because they are less than 5 % in all cases.

5.4.1 Impact of zeolite structure and coke formation on the activity and selectivity

5.4.1.1 Batch reactor

The effect of zeolite pore structure on 1-heptene conversion has been studied over three zeolites which have different acidities, pore sizes and Si/Al ratios. The distribution of the heptyltoluene isomer robustly relies on many factors, such as: reaction temperature, kind and nature of catalyst, toluene to 1-heptene ratio and reactor type (Magnoux et al., 1997, Yadav and Siddiqui, 2009). The main reason for choosing HY5.1, HY30, H-mordenite and H-Beta is because of their catalytic properties which are considered excellent compared with other types (Horňáček et al., 2013). A mole ratio of toluene to 1-heptene of 3:1 at the reaction temperature 90 °C (Da et al., 2001, Cadenas et al., 2014). Furthermore, the main reason for choosing a low catalyst ~0.25 g to reactant ratio is predominantly so that the initial selectivity can be observed, even though the conversion is low (Nel and de Klerk, 2007).

In fact, the coke which is formed during the alkylation reaction predominately is postulated to be a liquid coke which could act to close the zeolite pores or poison most of the active centres (Horňáček et al., 2010a, Cowley et al., 2005). It is noteworthy that the expression ‘liquid coke’ refers to the combination of dimers or oligomers of olefin and polyalkylated aromatics.

Results of toluene alkylation with 1-heptene over HY5.1, H-mordenite and H- Beta zeolite catalysts are presented in Figure 5.10, Figure 5.11 and Figure 5.12.

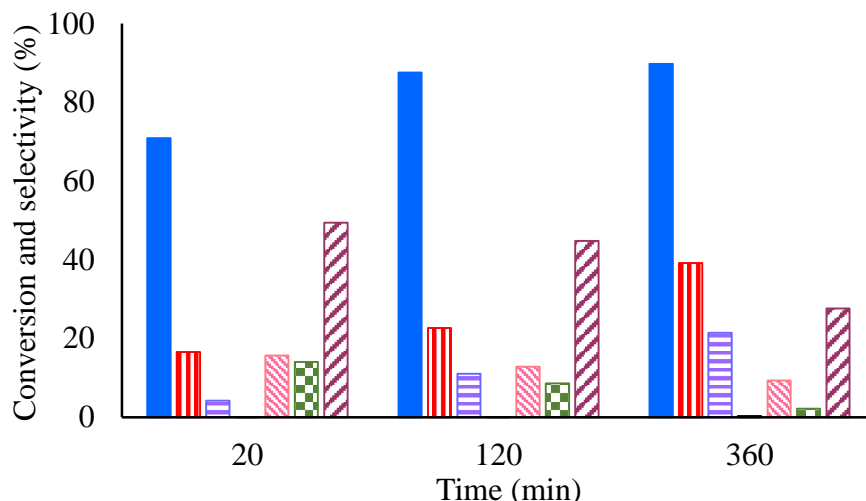


Figure 5.10. Conversion of 1-heptene (■), selectivity of 2-heptyltoluene (■), selectivity of 3-heptyltoluene (■), selectivity of 4-heptyltoluene (■), selectivity of 2-heptene (■), selectivity of 3-heptene (■) and selectivity of coke (■) during toluene alkylation with 1-heptene at 90 °C, atmospheric pressure, 0.25 g HY5.1 zeolite, reaction time of 20, 120 and 360 min, T: H ratio is 3: 1 and using BR.

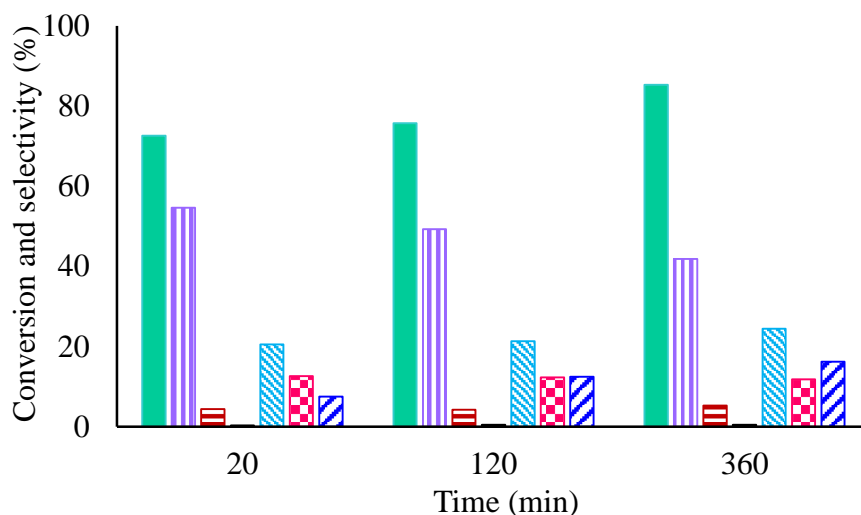


Figure 5.11. Conversion of 1-heptene (■), selectivity of 2-heptyltoluene (■), selectivity of 3-heptyltoluene (■), selectivity of 4-heptyltoluene (■), selectivity of 2-heptene (■), selectivity of 3-heptene (■) and selectivity of coke (■) during toluene alkylation with 1-heptene at 90 °C, atmospheric pressure, 0.25 g H-mordenite zeolite, reaction time of 20, 120 and 360 min, T: H ratio is 3: 1 and using BR.

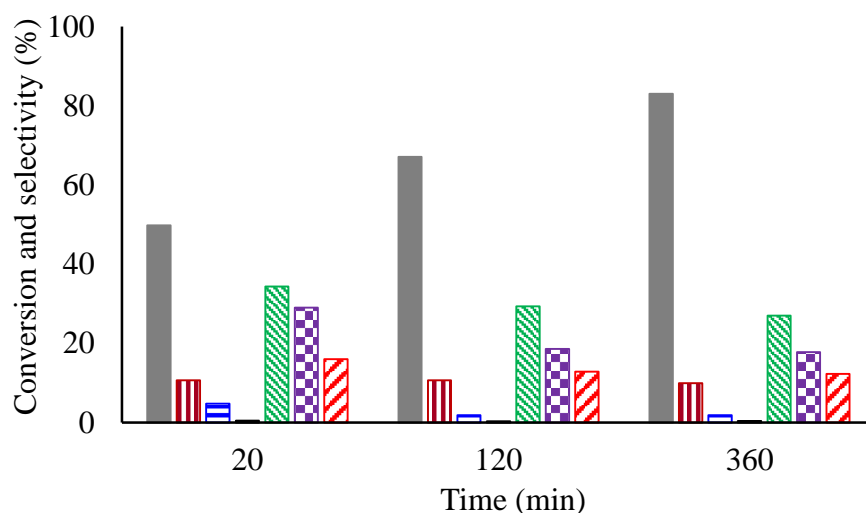


Figure 5.12. Conversion of 1-heptene (■), selectivity of 2-heptyltoluene (■), selectivity of 3-heptyltoluene (■), selectivity of 4-heptyltoluene (■), selectivity of 2-heptene (■), selectivity of 3-heptene (■) and selectivity of coke (■) during toluene alkylation with 1-heptene at 90 °C, atmospheric pressure, 0.25 g H-Beta zeolite, reaction time of 20, 120 and 360 min, T: H ratio is 3: 1 and using BR.

It can be seen that, the conversion of 1-heptene increased with increasing reaction time. It increased from ~71 % at 20 min up to ~90 % at 360 min over HY5.1 zeolite catalyst (Figure 5.10). Moreover, at times greater than 120 min, the conversion was only slightly increased from ~88 % at 120 min to ~90 % at 360 min; this could be because HY5.1 was deactivated after a reaction time of 120 min (this will be discussed further in Section 5.6.2.). Figure 5.11 shows that the conversion of 1-heptene using H-mordenite increased from ~73 % at 20 min up to ~85 % at 360 min. Over the H-Beta zeolite, the 1-heptene conversion increased gradually with increasing reaction time from ~50 % at 20 min up to ~83 % at 360 min (Figure 5.12). In summary, the conversion of 1-heptene over HY5.1 was higher than the other types such as H-mordenite and H-Beta as illustrated at 120 min when the conversion of 1-heptene over HY5.1 was ~88 %, while it was ~76 % and ~67 % over H-mordenite and H-Beta, respectively. This means that HY5.1 is more active than H-mordenite and H-Beta because it has a total acidity ~1.4 mmol g⁻¹, as explained in Table 5.3, and the Si/Al mole ratio of HY5.1 is much lower than the other two zeolite catalysts, as shown in Table 5.1. The alkylation of toluene over HY5.1 zeolite was favoured more than that over the H-Beta zeolite, and this seems clear when the conversion of 1-heptene over HY5.1 zeolite was approximately ~25 % higher than that over H-Beta at 120 min. This may be because H-Beta has a smaller pore size than HY5.1 so its channels did not

provide adequate space to form bulky molecules inside these pores, so the reaction took place on the outer surface of the zeolite. Shehab (2018) measured the pore size of the H- Beta which was used in this study; it was $\sim 21 \text{ \AA}$ which is smaller than that obtained for the HY5.1 $\sim 39 \text{ \AA}$, (Table 5.2). This difference in the pore size could be acting to limit the desorption of bulky alkylation products thereby decrease the selectivity of 2- heptyltoluene and another probable effect could be the low activity of the H-Beta compared with HY5.1.

All the previous data indicate that there is another parameter which must be considered along with the total acidity to determine the zeolite activity. The coke selectivity of HY5.1 was initially high and represented $\sim 50 \%$ of the total selectivity, possibly because this zeolite has high acidity (as described previously in Section 5.3.1.5) which acts to promote the coke formation. However, this coke does not appear to deactivate the acid sites that are responsible for the alkylation reaction, as shown by the increasing 1-heptene conversion with rising reaction time. From that, it can be concluded that coke could play a beneficial role in the alkylation reaction.

The coke selectivity of H-mordenite has contrasting behaviour to HY5.1. Here, the coke selectivity increases from $\sim 8 \%$ at 20 min to $\sim 16 \%$ at 360 min. This is probably due to the fact that H-mordenite has lower acidity than HY5.1 when it has higher Si/Al mole ratio (it is 20 for H-mordenite whereas it is 5.1 for HY5.1), as illustrated in Table 5.1. On the other hand, the selectivity of coke when using H-Beta has similar behaviour of the HY5.1 in that the selectivity decreased with increasing 1- heptene conversion. It was $\sim 16 \%$ during the first 20 min, possible because its pore size is smaller than that of HY5.1 (as shown above) and this leads to bulky molecules becoming trapped as a result of diffusion limitation. Moreover, the carbonaceous deposits during this reaction over H-Beta were much more toxic than those over HY5.1, but they also had a positive role in the isomerisation reaction, as shown in Figure 5.12.

Generally, in all experiments and with different experimental conditions, the selectivity of 2- and 3- heptyltoluene are the main alkylation products whereas, the selectivity of 4-heptyltoluene is $\sim 1 \%$ compared with the other monoheptyltoluene products. The 2-heptyltoluene selectivity $\sim 40 \%$ increased with rising conversion $\sim 90 \%$ and reaction time 360 min over HY5.1, probably because the structure of this

zeolite has open pore systems. This result is in agreement with the results obtained by Cao *et al.* (1999). 2- Heptyltoluene selectivity seems higher when using H-mordenite zeolite compared with the other types such as HY and H-Beta. Figure 5.11 shows the selectivity of 2- heptyltoluene reached ~55 % using H-mordenite at 20 min and decreased to ~41% in 360 min. Similar results were obtained by Magnoux *et al.* (1997) when they showed the monoheptyltoluene fraction is more preferred over H-mordenite than with other zeolite catalysts. The comparison between HY5.1 and H-mordenite at the same conversion ~87 % displays; the selectivity of 2-heptyltoluene over HY5.1 was ~23 % at 120 min but is approximately twice as high when using the H-mordenite at the 360 min mark. This variation in the selectivity ascribed to the difference in the porous structure, channels or cavities system of these zeolite catalysts. The logical interpretation for the high 2-heptyltoluene selectivity could be demonstrated by the shape selectivity of H-mordenite, where the steric constraints influence on the production of 3- and 4-heptyltoluene thereby increasing the 2-heptyltoluene production. However, the selectivity of 2-heptyltoluene was constant at ~10 % during all the three reaction times over H-Beta and it was less than that obtained for both HY5.1 and H-mordenite. This could be because the coke formed over H-Beta acted to deactivate most of the acid sites that are responsible for the alkylation reaction meaning the reaction had constant selectivity perhaps because the reaction occurred at the pore mouth region.

1-heptene isomerisation was not an objective of this study. Between the heptene isomers, 2-heptene and 3-heptene represented the main products formed when using H-Beta zeolite (Figure 5.12), probably due to its low acidity which makes it unsuitable for alkylation reactions but means it supports isomerisation reactions.

5.4.1.2 Fixed bed reactor

Monoheptyltoluene selectivity increases when using a toluene to 1- heptene ratio above 5:1, and simultaneously the double bond isomerisation decreases (Cadenas *et al.*, 2014, Liang *et al.*, 1996). Therefore, 8:1 is used instead of 3:1 in the fixed bed reactor.

From the BR study, it can be seen that the HY5.1 is the favourite zeolite for production of the alkylation products while, the H-mordinite showed high selectivity to the desired products ~50 % at 120 min. However, the main drawback of

H-mordenite compared with HY zeolite is the size of the pores; H-mordenite has narrower pores than those of HY zeolite and this makes it have a low activity compared with HY zeolite (Hornáček et al., 2013). Therefore, HY5.1 was chosen for the next steps of this investigation when using the FBR to study the role of coke that is formed during the alkylation reaction and to enhance the selectivity of desired products.

5.4.1.2.1 Influence of reaction temperature

The influence of reaction temperature on toluene alkylation with 1-heptene was illustrated using HY5.1 zeolite and two temperatures; 80 and 90 °C. The TOS, WHSV and nitrogen flowrate were maintained at 240 min, 17 h⁻¹ and 30 ml min⁻¹, respectively. It can be remarked from Figure 5.13 that the catalyst activity rises along with increasing reaction temperature. The conversion of 1-heptene increased from ~74 % to ~89 % at 150 min TOS by increasing the temperature from 80 to 90 °C. At temperature 80 °C, the zeolite deactivates more quickly than that at temperature 90 °C, as shown in Figure 5.13. Presumably because the carbonaceous materials which formed at low temperatures act to cover most of the acid sites, meaning only a few sites are available for alkylation reaction at this temperature.

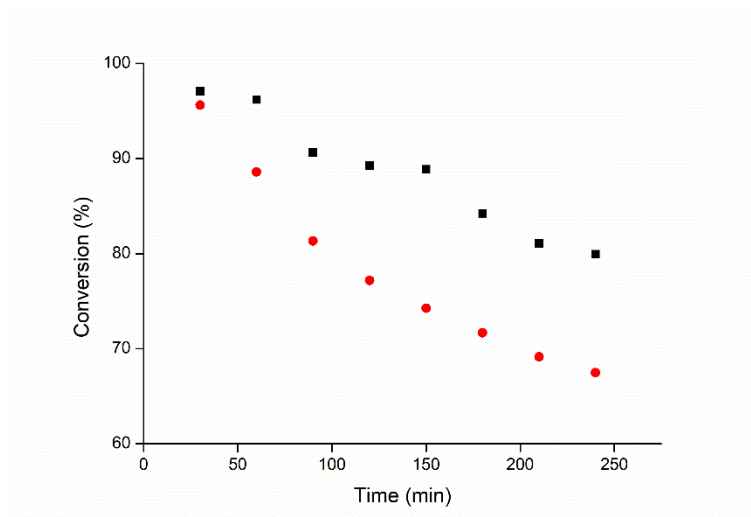


Figure 5.13. Effect of reaction temperature on 1-heptene conversion during toluene alkylation with 1-heptene at 80 °C (●) and 90 °C (■), atmospheric pressure, 0.5 g HY5.1 zeolite, TOS of 240 min, T: H ratio is 8: 1, WHSV of 17 h⁻¹, 30 ml min⁻¹ of N₂ flowrate and using FBR.

When the reaction temperature increased, the selectivity of 2-heptyltoluene increased from ~22 % to ~25 % and when the conversion of 1-heptene was ~88 %, the selectivity of 3-heptyltoluene increased from ~12 % to ~17 % (Figure 5.14). This is probably because the diffusion of bulkier monoheptyltoluene at high temperatures becomes easier than that at low temperatures or the shifting of 1-alkene to its isomers becomes quicker to reach an equilibrium state.

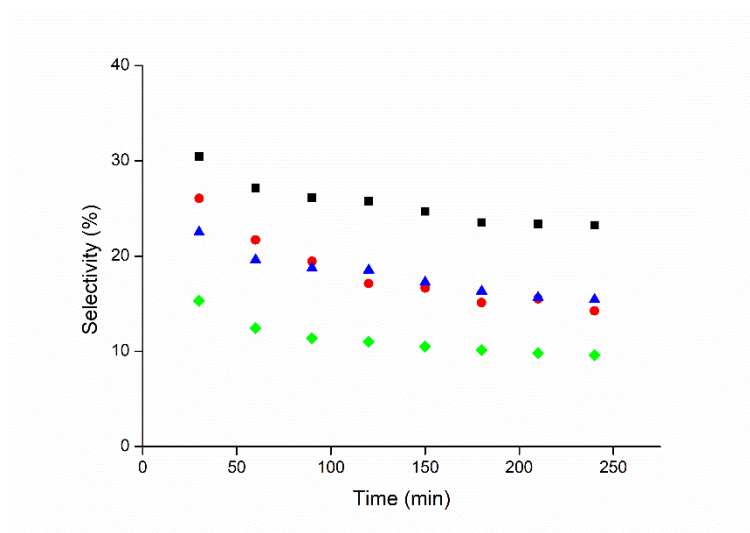


Figure 5.14. Effect of reaction temperature on selectivity of 2-heptyltoluene at 80 °C (●) and 90 °C (■) and 3-heptyltoluene at 80 °C (◆) and 90 °C (▲) during toluene alkylation with 1-heptene at atmospheric pressure, 0.5 g HY5.1 zeolite, TOS of 240 min, T: H ratio is 8: 1, WHSV of 17 h⁻¹, 30 ml min⁻¹ of N₂ flowrate and using FBR.

Figure 5.15 displays the coke selectivity as a function of TOS at two different reaction temperatures; 80 and 90 °C. It can be seen that the selectivity of coke decreased with increases to the reaction temperature from ~48 % to ~43 %. This could be owing to the formation of undesired reactions (1-heptene dimerisation and diheptyltoluene) reducing at 90 °C. This result is in agreement with that obtained by Cowley *et al.* (2005) when they reported that the production of side products increased at temperature below 200 °C during their investigation of toluene alkylation with 1- pentene.

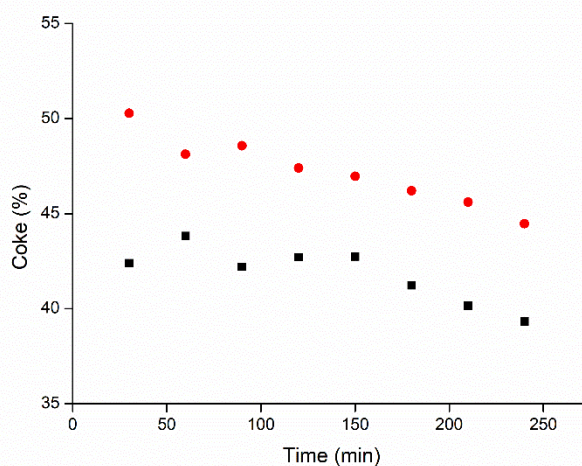


Figure 5.15. Effect of reaction temperature on selectivity of coke during toluene alkylation with 1-heptene at 80 °C (●) and 90 °C (■), atmospheric pressure, 0.5 g HY5.1 zeolite, TOS of 240 min, T: H ratio is 8: 1, WHSV of 17 h⁻¹, 30 ml min⁻¹ of N₂ flowrate and using FBR.

5.4.1.2.2 Effect of TOS

Figure 5.16 explains the effect of TOS of 1-heptene conversion and selectivity of 2-heptyltoluene, 2-heptene and coke at 90 °C, atmospheric pressure, WHSV of 17 h⁻¹, 0.5 g zeolite and 30 ml min⁻¹ N₂ flowrate. It is clear that the activity of the HY5.1 zeolite catalyst reduces with TOS from ~97 % at 30 min to ~74 % at 720 min. The conversion decreases rapidly during the first 210 min then it reduces slower than the first period, possibly owing to the coke which was formed rapidly in the first minutes because this fresh zeolite catalyst has a total acidity ~1.4 mmol g⁻¹ (as shown in Section 5.3.1.5) which contributes to the quick formation of carbonaceous materials. On the other hand, no appreciable changes were observed in 2-heptyltoluene selectivity, especially after 60 min TOS (when it reduced from ~32 % (30 min) to ~26 % (60 min)). Similar results were obtained by Chua *et al.* (2010) when they reported the activity of MFI zeolite during alkylation of benzene with ethane reduced with TOS rapidly in the first 48 h then the activity of the catalyst remained stable for the remaining time while there was no significant change in the selectivity.

The selectivity of 2-heptene and coke increased with TOS. The selectivity of coke was different in two periods. In the first period, between 60 and 330 min, the coke selectivity was stable at ~40 % however, in the second period, between 330- 720 min, it increased to ~50 %. This in turn indicated that the coke was formed

during the first minutes of the reaction and that it was still accumulated during the reaction as a result of side product formation. Moreover, the deposition of these carbonaceous deposits presumably acts to improve the relative stability of the zeolite catalyst after a short TOS. In contrast, the selectivity of 2-heptene also increased from ~4 to ~25 % which means that the isomerisation reaction could be occurring on the external surface or at the pore mouth of the zeolite catalyst after the carbonaceous compounds are formed. Guisnet (2002) reported that the coke deposits can interact with the protonic sites of the zeolite to form new active sites which can contribute to the enhancement of the isomerisation reaction.

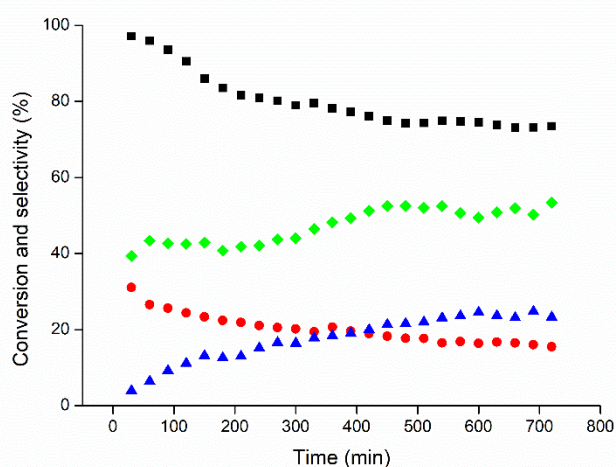


Figure 5.16. Influence of TOS on 1-heptene conversion (■), 2-heptyltoluene selectivity (●), 2-heptene selectivity (▲) and coke selectivity (◆) during toluene alkylation with 1-heptene at 90 °C, atmospheric pressure, 0.5 g HY5.1 zeolite, TOS of 720 min, T: H ratio is 8: 1, WHSV of 17 h⁻¹, 30 ml min⁻¹ of N₂ flowrate and using FBR.

5.4.2.2.3 Impact of zeolite amount

Figure 5.17 shows the effect of catalyst loading on toluene alkylation conversion over the HY5.1 zeolite catalyst. This was investigated at 90 °C, atmospheric pressure, WHSV of 17 h⁻¹, 240 min TOS, toluene to 1-heptene ratio of 8 and 30 ml min⁻¹ of nitrogen flowrate. It can be seen that 1 g showed approximately constant conversion at ~99 % whereas, 0.75 g shows a slight reduction of 1-heptene conversion to ~95 % at 240 min TOS. As described in Section 4.3.2., the zeolite catalysts were loaded vertically in the reactor. Therefore, these results mean the reaction happened on the uppermost layers of the zeolite bed and the last layers were

still unaffected. 0.5 g showed a different behaviour; the conversion of 1-heptene significantly reduced with TOS which means a decay in zeolite activity during the reaction and the influence of carbonaceous materials becomes more clear.

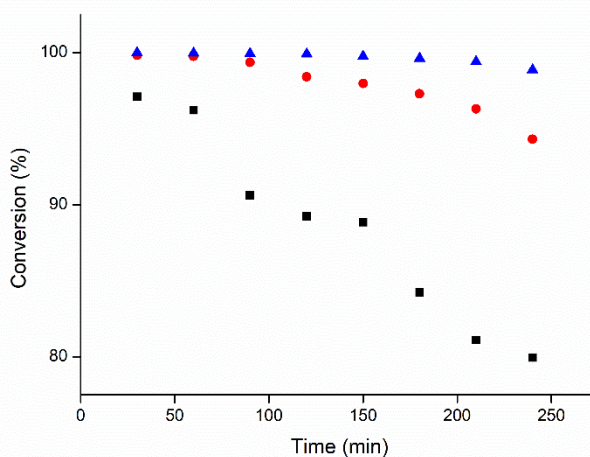


Figure 5.17. Effect of zeolite catalyst loading on 1-heptene conversion during toluene alkylation with 1-heptene at 90 °C, atmospheric pressure, 0.5 (■), 0.75 (●) and 1 (▲) g HY5.1 zeolite, TOS of 240 min, T: H ratio is 8: 1, WHSV of 17 h⁻¹, 30 ml min⁻¹ of N₂ flowrate and using FBR.

According to the results above, 90 °C was chosen as the optimum reaction temperature for the next steps of this investigation. Moreover, 240 min was selected as an optimum time for this study due to the fact that toluene alkylation with 1-heptene over HY5.1 zeolite became stable at this time. Additionally, because the main target of this study is investigating the role of coke deposits through the alkylation reaction, 0.5 g was selected as the catalyst loading for the next steps of this study.

5.4.1.2.4 Influence of Si/Al mole ratio of HY zeolite

The influence of the Si/Al ratio on the alkylation of toluene with 1-heptene was investigated over two different HY zeolite catalysts using the FBR (Figure 5.18). Indeed, the activity and stability of HY30 were higher than HY5.1. Although the HY5.1 showed higher acidity ~1.4 mmol g⁻¹ than HY30 ~0.36 mmol g⁻¹, as described in Section 5.3.1.5, the conversion of 1-heptene was ~99 % when using HY30 at 150 min TOS while it decreased to ~89 % for HY5.1 at the same time. Perhaps this is because of the increased average acid strength associated with increasing the Si/Al mole ratio of the HY30 zeolite. Similar behaviour is observed early in benzene

alkylation with 1-octene over three Y zeolite catalysts with different Si/Al ratios of 5.8, 13 and 30, they reported the highest conversion was obtained with a Si/Al ratio of 30 (Craciun et al., 2007).

The conversion drastically reduced after the first 60 min of reaction, perhaps because the coke formation leads to deactivation of the HY5.1 zeolite. However, the conversion of HY30 is still high ~98 % at long TOS, which means either the zeolite is active or the reaction rate is high.

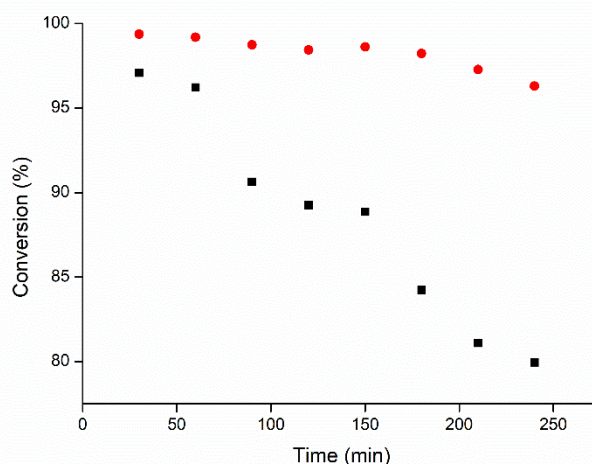


Figure 5.18. Effect of TOS on 1-heptene conversion during toluene alkylation with 1-heptene at 90 °C, atmospheric pressure, 0.5 g HY5.1 (■) and HY30 (●) zeolite, TOS of 240 min, T: H ratio is 8: 1, WHSV of 17 h⁻¹, 30 ml min⁻¹ of N₂ flowrate and using FBR.

On the other hand, the selectivity of 2-heptyltoluene and 3-heptyltoluene using HY30 were strikingly higher than that of HY5.1 (Figure 5.19). The selectivity of 2- heptyltoluene was ~27 % for HY5.1 whereas, it was ~30 % for the HY30 at the same conversion of ~96 %. This indicates that the selectivity of 2-heptyltoluene was affected significantly by the acid strength of the zeolite catalyst. Additionally, from the results in Section 5.3.1.4, HY30 possesses higher BET 884.9 m² g⁻¹, pore volume and pore size distribution than HY5.1 and its hysteresis loop indicated the presence of micro and mesopores instead of just the micropores in the HY5.1. The same results were obtained by de Almeida and co-worker de Almeida *et al.* (1994) during benzene alkylation with 1-dodecene over HY zeolite with Si/Al ratios in the range of 2.7 to 26.4.

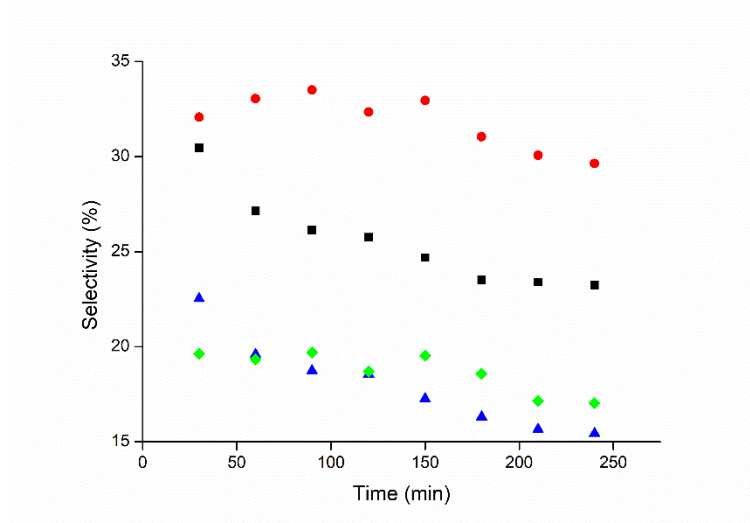


Figure 5.19. Influence of TOS on 2-heptyltoluene selectivity using HY5.1 (■) and HY30 (●) zeolite and 3-heptyltoluene selectivity using HY5.1 (▲) and HY30 (◆) zeolite during toluene alkylation with 1-heptene at 90 °C, atmospheric pressure, 0.5 g, TOS of 240 min, T: H ratio is 8: 1, WHSV of 17 h⁻¹, 30 ml min⁻¹ of N₂ flowrate and using FBR.

Though there is a significant enhancement in 2-heptyltoluene selectivity for HY30 compared with HY5.1 (Figure 5.19), the coke selectivity shows that HY30 ~47 % has slightly more coke than HY5.1 ~44 % (Figure 5.20). This could be because it has a mesoporous structure which acts to retain more coke than micropores and this coke led to increases in the relative stability and acted to enhance the selectivity of monoheptyltoluene.

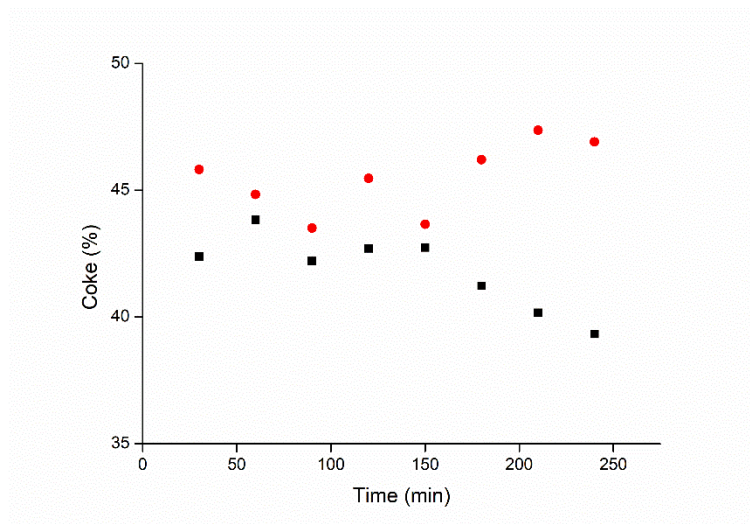


Figure 5.20. Effect of TOS on selectivity of coke during toluene alkylation with 1-heptene at 90 °C, atmospheric pressure, 0.5 g HY5.1 (■) and HY30 (●) zeolite, TOS of 240 min, T: H ratio is 8: 1, WHSV of 17 h⁻¹, 30 ml min⁻¹ of N₂ flowrate and using FBR.

5.5 Zeolite modifications

5.5.1 Dealumination modification

Figure 5.21 illustrates the catalytic performance of fresh and dealuminated HY5.1 in toluene alkylation with 1-heptene at 90 °C and at a reaction time of 120 min using the BR. The activity of the modified sample was reduced more than 50% compared with the unmodified sample. This is presumably because the total acidity of dealuminated HY5.1 is ~50 % less than the fresh HY5.1, as described in Section 5.3.1.5. The results of XRF and EDX support that, and showed an increase in the Si/Al ratio. Furthermore, the selectivity of 2-heptyltoluene also decreased after dealumination of HY5.1 from ~23 % to ~13 %, perhaps because the coke that was formed acted as a diffusion hindrance to the reactants and products and the increase of the coke selectivity proved this hypothesis.

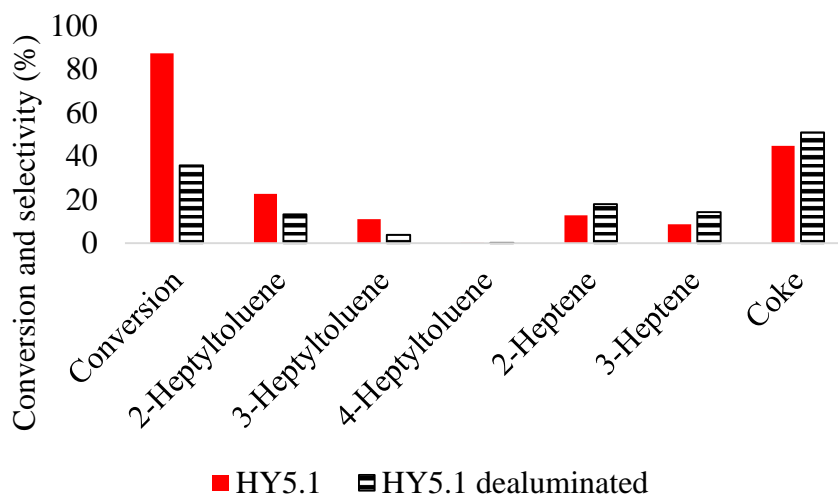


Figure 5.21. Conversion of 1-heptene and selectivity to various reaction products during toluene alkylation with 1-heptene at 90 °C, atmospheric pressure, 0.25 g HY5.1 and HY5.1 dealuminated zeolite, reaction time of 120 min, T: H ratio is 3: 1 and using BR.

Figure 5.22 explains the catalytic activities of HY5.1 and dealuminated HY5.1 in alkylation of toluene with 1-heptene at 90 °C, 240 min TOS, WHSV of 17 h⁻¹, 0.5 g of zeolite and 30 ml min⁻¹ nitrogen flowrate using a FBR. The activity of the dealuminated sample was reduced compared with the fresh sample from ~89 % to ~18 % at 150 min TOS, possibly because the acidity of the dealuminated sample decreased compared with the unmodified sample, as shown in Section 5.3.1.5. Although both the EDX and XRF data in Section 5.3.1.3 indicated the dealumination modification was done correctly, XRD results in Section 5.3.1.1 showed the structure of the dealuminated sample was partially collapsed and the crystallinity percentage reached the lowest values as a result of decreasing the XRD intensities.

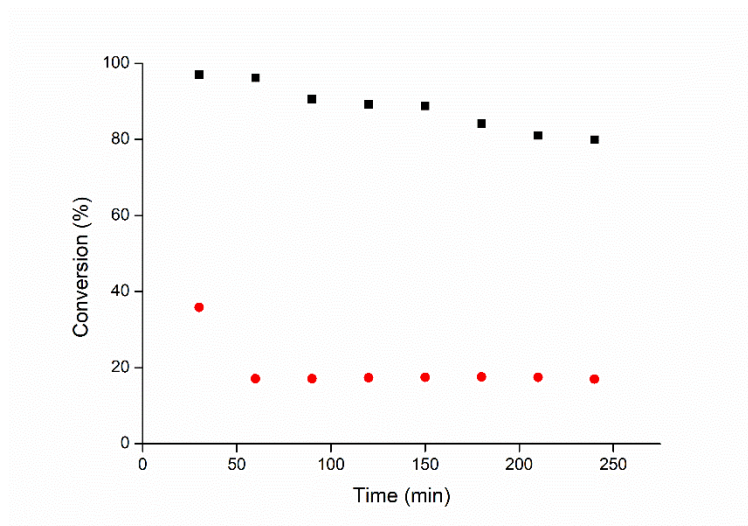


Figure 5.22. Influence of TOS on 1-heptene conversion during toluene alkylation with 1-heptene at 90 °C, atmospheric pressure, 0.5 g HY5.1 (■) and HY5.1 dealuminated (●) zeolite, TOS of 240 min, T: H ratio is 8: 1, WHSV of 17 h⁻¹, 30 ml min⁻¹ of N₂ flowrate and using FBR.

The selectivity of 2-heptyltoluene decreases and reaches its lowest values ~ less than 1 % after just 60 min TOS (Figure 5.23). From the results of the TGA in Section 5.3.4.2, the amount of coke that formed during this reaction over the dealuminated sample was lower than that of the unmodified sample by more than 50%. This means the coke pre-cursor that formed during this interaction acted to block the pores thereby preventing the reactant to reach the internal acid sites. Alternatively, the coke acted to block the active sites that are responsible for the alkylation reaction and leave the sites that are responsible for the side reaction therefore, the coke selectivity significantly increased to ~99 %, as shown in Figure 5.24.

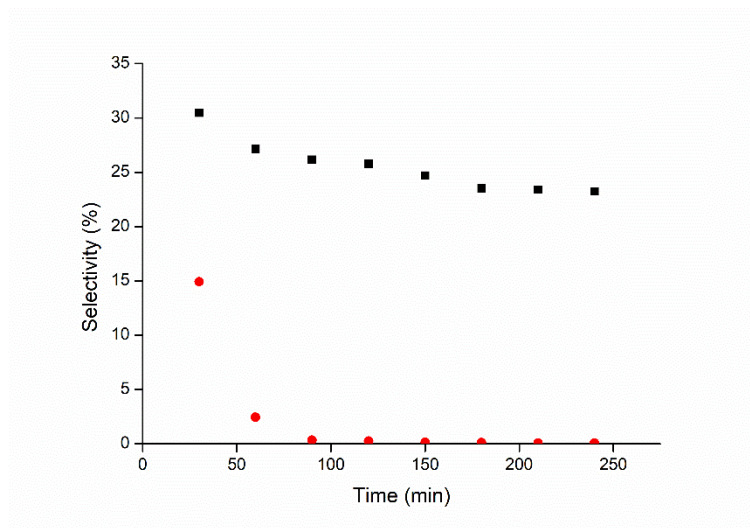


Figure 5.23. Influence of TOS on selectivity of 2-heptyltoluene during toluene alkylation with 1-heptene at 90 °C, atmospheric pressure, 0.5 g HY5.1 (■) and HY5.1 dealuminated (●) zeolite, TOS of 240 min, T: H ratio is 8: 1, WHSV of 17 h⁻¹, 30 ml min⁻¹ of N₂ flowrate and using FBR.

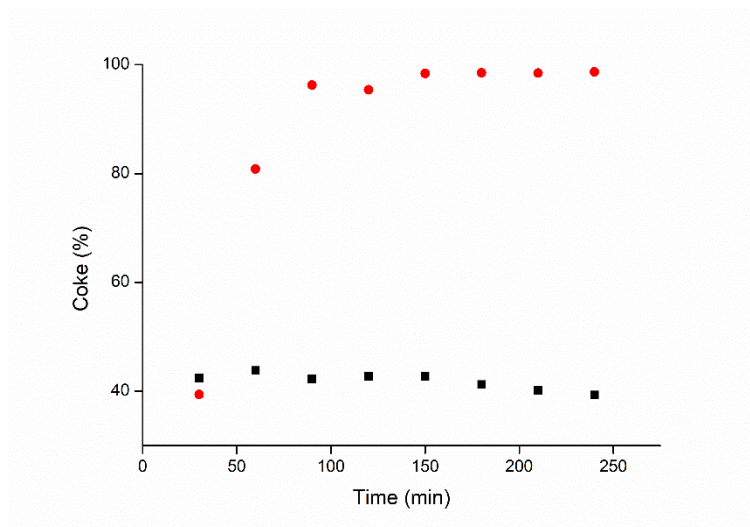


Figure 5.24. Influence of TOS on selectivity of coke during toluene alkylation with 1-heptene at 90 °C, atmospheric pressure, 0.5 g HY5.1 (■) and HY5.1 dealuminated (●) zeolite, TOS of 240 min, T: H ratio is 8: 1, WHSV of 17 h⁻¹, 30 ml min⁻¹ of N₂ flowrate and using FBR.

Figure 5.25 shows the conversion of 1-heptene using HY30 and dealuminated HY30 in the alkylation of toluene at 90 °C, 240 min TOS, WHSV of 17 h⁻¹, 0.5 g of zeolite and 30 ml min⁻¹ nitrogen flowrate using a FBR. The activity of the modified sample decreased somewhat compared with the fresh sample perhaps because the acidity of the modified sample dramatically decreased, as described in Section 5.3.1.5.

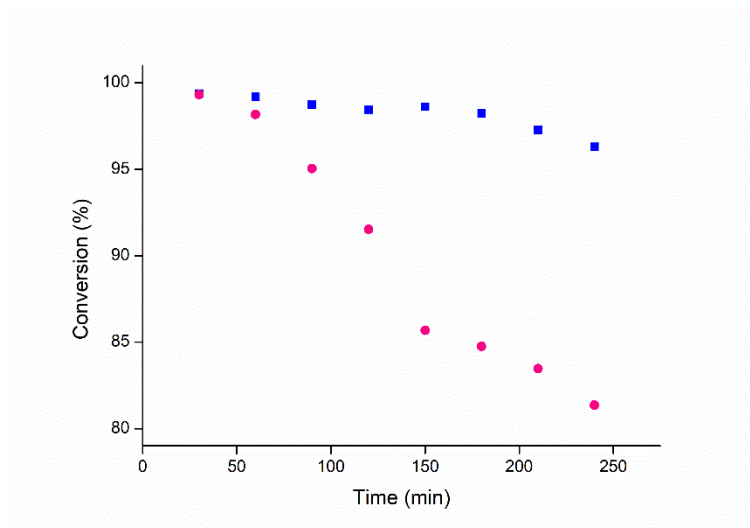


Figure 5.25. Influence of TOS on 1-heptene conversion during toluene alkylation with 1-heptene at 90 °C, atmospheric pressure, 0.5 g HY30 (■) and HY30 dealuminated (●) zeolite, TOS of 240 min, T: H ratio is 8: 1, WHSV of 17 h⁻¹, 30 ml min⁻¹ of N₂ flowrate and using FBR.

Indeed, there was a slight increase in the 2-heptyltoluene selectivity of the dealuminated sample. The selectivity was ~36 % for the modified sample while it was ~31 % for the fresh sample at a constant conversion of ~98 % (Figure 5.26). This is probably owing to the increase in the micropore size of the modified sample compared with the unmodified one, as shown in Section 5.3.1.4 or the coke that accumulated during the first minutes of the reaction acts to enhance the selectivity of the desired product (2-heptyltoluene).

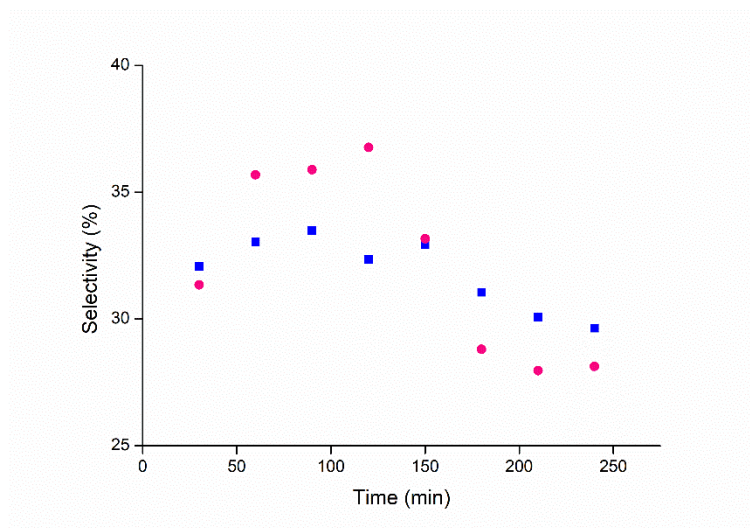


Figure 5.26. Influence of TOS on selectivity of 2-heptyltoluene during toluene alkylation with 1-heptene at 90 °C, atmospheric pressure, 0.5 g HY30 (■) and HY30 dealuminated (●) zeolite, TOS of 240 min, T: H ratio is 8: 1, WHSV of 17 h⁻¹, 30 ml min⁻¹ of N₂ flowrate and using FBR.

Finally, the coke selectivity was decreased (Figure 5.27) and TGA results of dealuminated HY30 also show that the coke percentage decreased a little amount ~11 wt. % compared with the decrease in coke percentage from the same reaction over the fresh HY30 ~11.8 wt. % (as shown in Section 5.6.2) likely because the Si/Al ratio increases as a result of reducing the Al content which confirms the previous result, as depicted in Section 5.3.1.3. This leads to reductions in the aluminium content thereby decreasing the acidity and the coke selectivity from ~46 % for the fresh HY30 to ~42 % for the dealuminated sample.

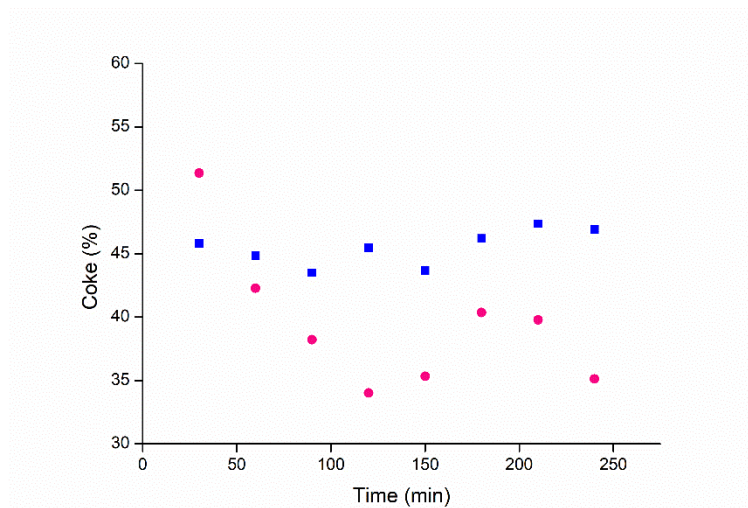


Figure 5.27. Influence of TOS on selectivity of coke during toluene alkylation with 1-heptene at 90 °C, atmospheric pressure, 0.5 g HY30 (■) and HY30 dealuminated (●) zeolite, TOS of 240 min, T: H ratio is 8: 1, WHSV of 17 h⁻¹, 30 ml min⁻¹ of N₂ flowrate and using FBR.

As a consequence of the above, the catalytic performance was improved for dealuminated HY30 which means the dealumination modification is considered as an effective and useful treatment particularly when it acts to improve the selectivity and stability of zeolite catalysts.

5.5.2 Desilication modification

Figure 5.28 showed the catalytic activity of fresh and desilicated HY5.1 zeolite samples in toluene alkylation with 1-heptene at 90 °C, 120 min reaction time using a BR. It can be seen that the activity of desilicated HY5.1 decreased after modification. The conversion decreased after the desilicated treatment from ~88 % to ~74 % for the HY5.1 zeolite sample. This diminishment is ascribed to increases in the acidity of ~23 % compared with the fresh sample which increases the speed of coke formation. This has been shown by TGA results in Figure 5.36, Section 5.3.4.2. However, there was a fluctuating behaviour for the selectivity of 2- and 3-heptyltoluene when the selectivity of the first product decreased from ~23 % to ~19 % while it slightly increased for the second product from ~11 % to ~12 %. This fluctuation was probably a result of either pore blocking or active site deactivation meaning the reaction occurs at the pore mouth or on the remaining acid sites.

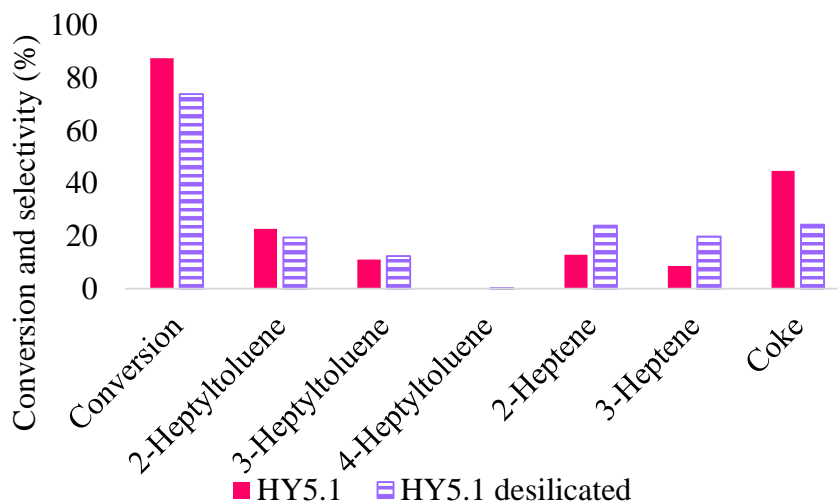


Figure 5.28. Conversion of 1-heptene and selectivity to various reaction products during toluene alkylation with 1-heptene at 90 °C, atmospheric pressure, 0.25 g HY5.1 and HY5.1 desilicated zeolite, reaction time of 120 min, T: H ratio is 3: 1 and using BR.

Figure 5.29 explains the activity of HY5.1 and desilicated HY5.1 in alkylation of toluene with 1-heptene at 90 °C, 240 min TOS, WHSV of 17 h⁻¹, 0.5 g of zeolite and 30 ml min⁻¹ nitrogen flowrate using a FBR. Obviously, there is a significant reduction in activity of the desilicated sample compared with the fresh one, probably because the coke forms rapidly which acts to reduce the activity directly. Moreover, this decrease is likely owing to the fact that the desilication treatment did not reach its target. This is supported by the fact that the XRF results show there is no difference in the Si/Al ratio for the fresh and desilicated sample, as described previously in Section 5.3.1.3. As demonstrated in Section 2.3.2., a Si/Al ratio below 15 is considered the main reason for preventing the desilication treatment reaching its target and forming a mesoporous structure (Möller and Bein, 2013, Wei et al., 2015, Groen et al., 2006).

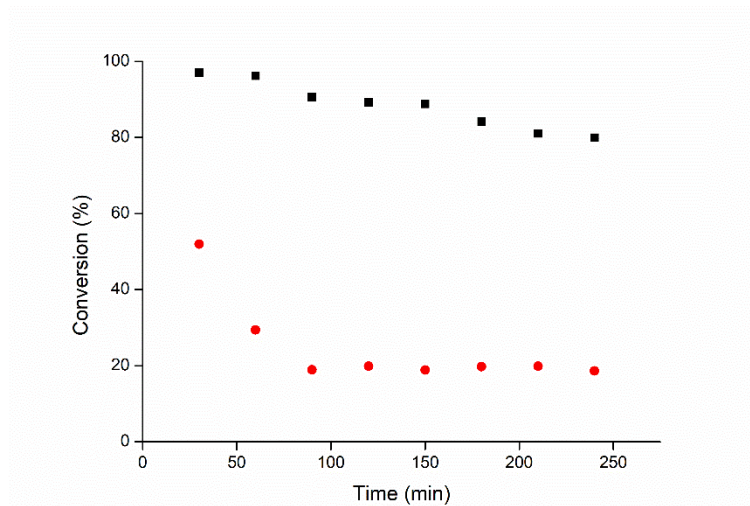


Figure 5.29. Influence of TOS on 1-heptene conversion during toluene alkylation with 1-heptene at 90 °C, atmospheric pressure, 0.5 g HY5.1 (■) and HY5.1 desilicated (●) zeolite, TOS of 240 min, T: H ratio is 8: 1, WHSV of 17 h⁻¹, 30 ml min⁻¹ of N₂ flowrate and using FBR.

Figure 5.30 illustrates the selectivity of 2-heptyltoluene decreasing with increasing TOS until it approaches zero after 150 min, probably because the acidity was increased ~23 % compared with the unmodified sample. This makes the coke form rapidly and perhaps the coke then encapsulates the catalyst, therefore there are no products. Figure 5.31 confirms this suggestion as the accumulated coke reaches ~90 % after 150 min.

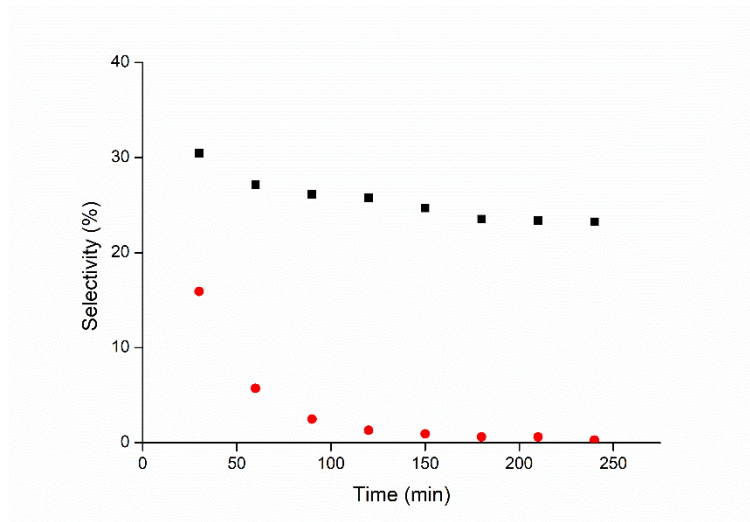


Figure 5.30. Influence of TOS on selectivity of 2-heptyltoluene during toluene alkylation with 1-heptene at 90 °C, atmospheric pressure, 0.5 g HY5.1 (■) and HY5.1 desilicated (●) zeolite, TOS of 240 min, T: H ratio is 8: 1, WHSV of 17 h⁻¹, 30 ml min⁻¹ of N₂ flowrate and using FBR.

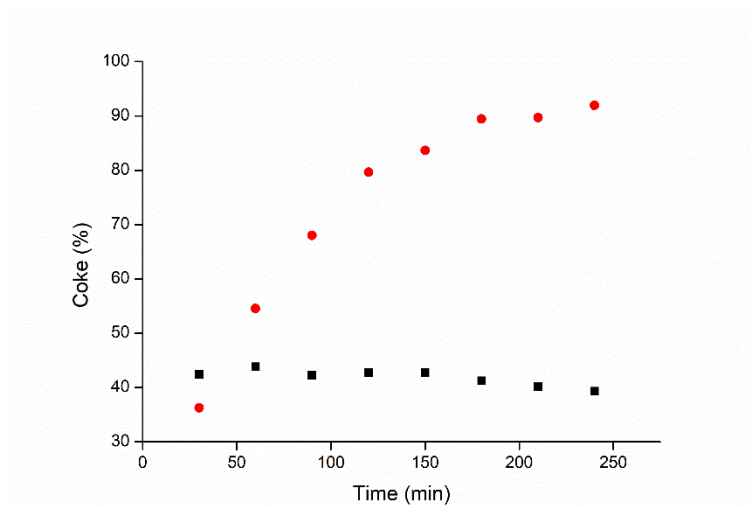


Figure 5.31. Influence of TOS on selectivity of coke during toluene alkylation with 1-heptene at 90 °C, atmospheric pressure, 0.5 g HY5.1 (■) and HY5.1 desilicated (●) zeolite, TOS of 240 min, T: H ratio is 8: 1, WHSV of 17 h⁻¹, 30 ml min⁻¹ of N₂ flowrate and using FBR.

The activity of HY30 increases after the desilication treatment; the conversion increases from ~88 % for the fresh HY30 to ~99 % for the desilicated sample of the same zeolite, as shown in Figure 5.32. This raise in 1-heptene conversion can be ascribed to increases in the acidity of more than 5 %, as described in Section 5.3.1.5. This slight increase in activity contributes to the acid site distribution meaning the coke selectivity was slightly decreased after this modification from ~44.5 % to ~43 %. In addition, the selectivity of 2- and 3-heptyltoluene also increases from ~25 % to ~31 % for the 2-heptyltoluene and from ~17 % to ~26 % for the 3-heptyltoluene as a result of decreasing coke selectivity. These increases are perhaps due to the improvement in the pore size distribution and volume of mesopores, as depicted in Section 5.3.1.4.

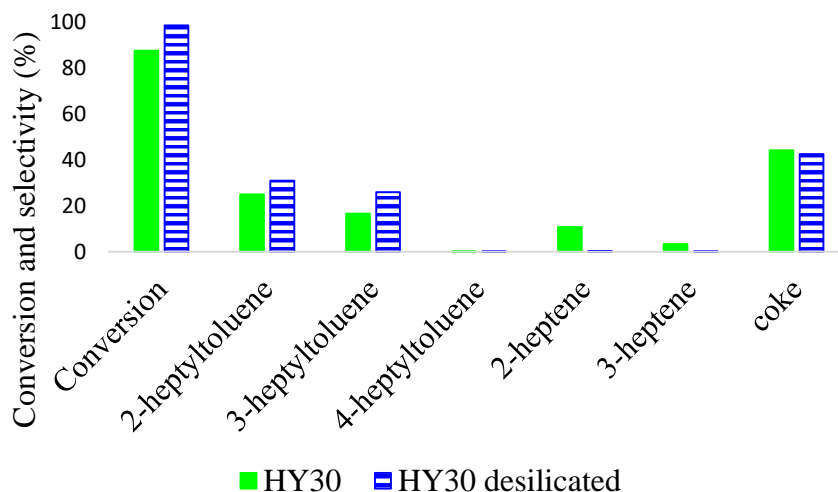


Figure 5.32. Conversion of 1-heptene and selectivity to various reaction products during toluene alkylation with 1-heptene at 90 °C, atmospheric pressure, 0.25 g HY30 and HY30 desilicated zeolite, reaction time of 120 min, T: H ratio is 3: 1 and using BR.

Figure 5.33 shows the activity of the fresh and desilicated HY30 in toluene alkylation with 1-heptene at 90 °C, 240 min TOS, WHSV of 17 h⁻¹, 0.5 g of zeolite and 30 ml min⁻¹ nitrogen flowrate using a FBR. It can be seen that the conversion of desilicated HY30 has approximately the same activity which means the alteration in acidity has only a slight influence on the catalytic activity. Nevertheless, the stability of desilicated HY30 throughout this reaction can contribute to enhancing the diffusivity of bulky molecules and coke pre-cursors.

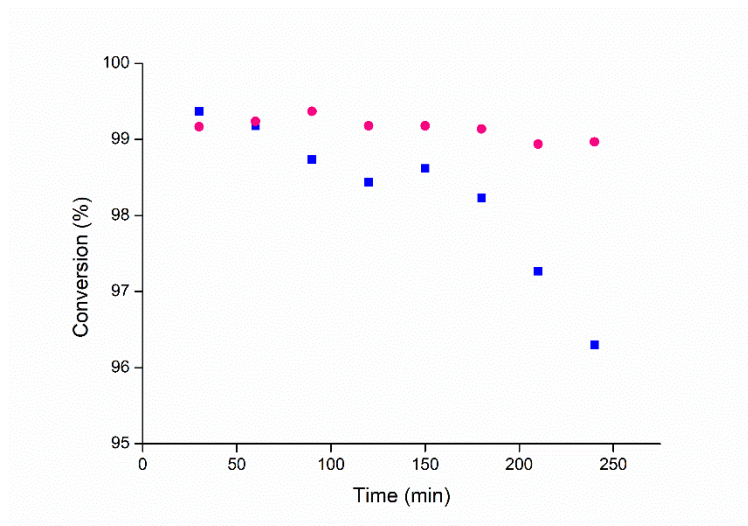


Figure 5.33. Influence of TOS on 1-heptene conversion during toluene alkylation with 1-heptene at 90 °C, atmospheric pressure, 0.5 g HY30 (■) and HY30 desilicated (●) zeolite, TOS of 240 min, T: H ratio is 8: 1, WHSV of 17 h⁻¹, 30 ml min⁻¹ of N₂ flowrate and using FBR.

The selectivity of 2-heptyltoluene increased from ~33 % to ~39 % after desilication modification at a constant conversion of ~99 % (Figure 5.34). This could be because of the slight enhancement of surface area, pore volume and pore size for both mesopores and micropores, as described previously in Section 5.3.1.4. The mesopores acted to collect additional amounts of coke and this coke has a positive role, especially when it acts to enhance the selectivity of 2-heptyltoluene.

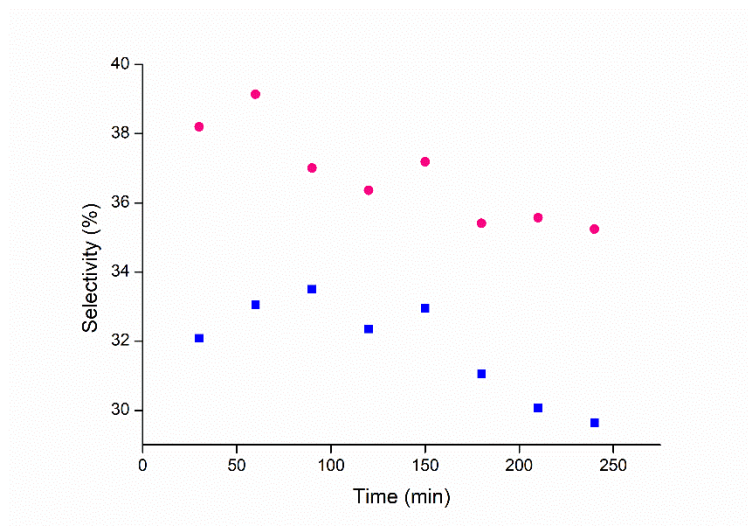


Figure 5.34. Influence of TOS on selectivity of 2-heptyltoluene during toluene alkylation with 1-heptene at 90 °C, atmospheric pressure, 0.5 g HY30 (■) and HY30 desilicated (●) zeolite, TOS of 240 min, T: H ratio is 8: 1, WHSV of 17 h⁻¹, 30 ml min⁻¹ of N₂ flowrate and using FBR.

Figure 5.35 shows the selectivity of coke is reduced after the desilication treatment from ~45 % to ~31 % at a constant conversion of ~99 %. This can be ascribed to an improvement of the diffusion properties as a result of mesoporous structure which acts to make the desorption of bulky molecules easier, thereby decreasing the coke deposits.

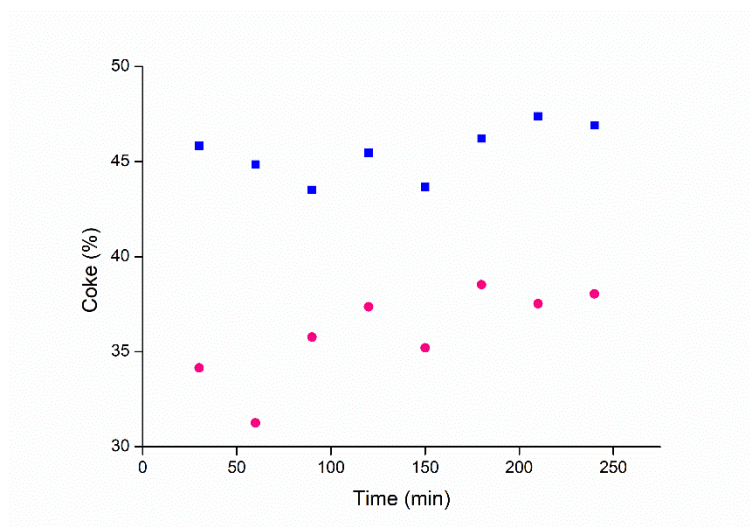


Figure 5.35. Influence of TOS on selectivity of coke during toluene alkylation with 1-heptene at 90 °C, atmospheric pressure, 0.5 g HY30 (■) and HY30 desilicated (●) zeolite, TOS of 240 min, T: H ratio is 8: 1, WHSV of 17 h⁻¹, 30 ml min⁻¹ of N₂ flowrate and using FBR.

5.6 Coke characterisations

The TGA, TPO, elemental analysis, nitrogen adsorption/desorption and FTIR are employed to characterise the deactivated zeolite catalyst.

5.6.1 Nitrogen sorption results of post-reaction samples

For the fresh HY5.1, HY30 and their modified zeolite catalysts, the conversion was reduced and the amount of coke was determined for these partially deactivated zeolites by employing the BET surface area, micropore area and pore volume analysis. They all decreased, as shown in Table 5.4. These variations in micropore and mesopore areas showed that the coke forms and deposits in the micropores excessively more than in the mesopore.

Table 5.4. The results of surface area of fresh and spent zeolite catalysts.

Zeolite	S_{BET} ($\text{m}^2 \text{g}^{-1}$)	S_{mic} ($\text{m}^2 \text{g}^{-1}$)	S_{ext} ($\text{m}^2 \text{g}^{-1}$)	V_{tot} ($\text{cm}^3 \text{g}^{-1}$)	V_{mic} ($\text{cm}^3 \text{g}^{-1}$)	V_{meso} ($\text{cm}^3 \text{g}^{-1}$)	$d_{\text{p meso}}$ (Å) BJH	$d_{\text{p mic}}$ (Å) Horvath-Kowazoe
HY5.1 (powder)	713.7	694.3	19.5	0.387	0.349	0.038	38.6	7.07
HY5.1 post-reaction BR	596	568.6	27.4	0.329	0.279	0.05	39.42	6.9
HY5.1 (pellet)	577.1	548.6	28.5	0.339	0.269	0.07	50.59	6.96
HY5.1 post-reaction FBR	97.3	79.8	17.6	0.088	0.035	0.053	54.19	15.7
HY30 (pellet)	844.9	760.4	84.6	0.556	0.369	0.187	58.45	7.53
HY30 post-reaction FBR	697.1	613.7	83.4	0.461	0.282	0.179	60.06	7.56
HY30 dealuminated (pellet)	650.8	588.7	62.1	0.418	0.287	0.131	53.32	7.59
HY30 dealuminated post-reaction FBR	248.1	197.9	50.2	0.213	0.1	0.113	59.41	8.58
HY30 desilicated (pellet)	848.9	757.8	91.1	0.505	0.313	0.192	60.46	7.71
HY30 desilicated post- reaction FBR	496.7	430.4	66.5	0.36	0.211	0.149	60.98	7.74

The BET surface area of all samples decreased after reaction perhaps because of the decreasing micropore area which happened as a result of the deposition of coke in these micropores. The reduction in both BET surface area and micropore area did not influence the lifetime of the zeolite catalyst (conversion still high after 240 min), Section 5.4. that means there are other factors can be contributed with the pore structure on the zeolite deactivation.

Table 5.4 showed when the mesopore size increased of fresh HY30, as shown Section 5.6.2, the coke amount increasing could be owing to these mesopores act as reservoir for the coke deposition.

5.6.2 TGA

The weight percentages of coke accumulated on several types of fresh and modified zeolite catalyst during the alkylation of toluene with 1-heptene were calculated using the TGA. According to the combustion temperature of the coke deposits, the coke was classified into two types; soft coke between 200 to 400 °C and hard coke between 400 to 800 °C (Guisnet and Magnoux, 2001, Ahmed et al., 2011, Wang and Manos, 2007b). The drop in the weight of the specimen at 200 °C was attributed to physisorbed water and some hydrocarbons which have low volatility whereas the loss of weight at temperatures above 200 °C was ascribed to burning of the coke deposits arising through the reaction.

Figure 5.36 shows the change in the mass of HY5.1 and its modified (dealuminated and desilicated) zeolite samples in a BR as a function of the oxidation temperature. It shows that the amount of coke increases quickly ~9 % for HY5.1 during the early minutes 20 min of the alkylation reaction but thereafter increases more slowly ~11 % and ~11.5 % for HY5.1 at 120 and 360 min respectively. Similar results were obtained by Da *et al.* (1999b), Cao *et al.* (1999). Moreover, Figure 5.37 displays the same behaviour as the amount of coke was increased from 10 wt. % at 240 min TOS to 11.9 wt. % at 720 min TOS. These results support those obtained during the previous study on the influence of reaction time on the catalytic activity, as shown in Section 5.4.1.2.2.

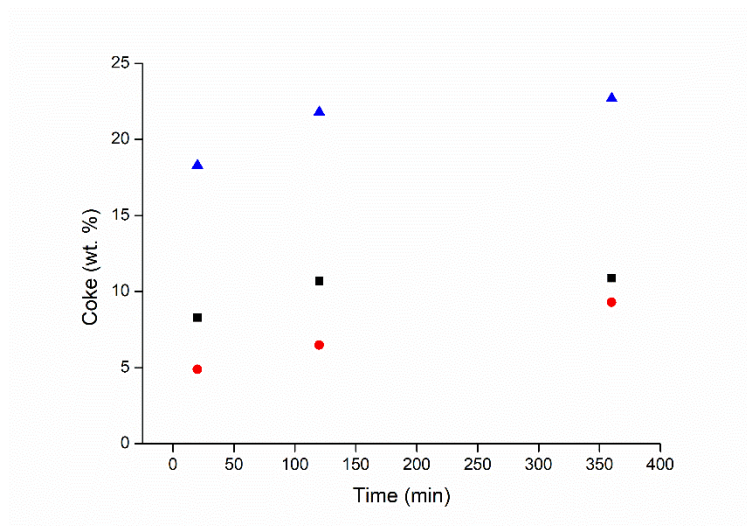


Figure 5.36. TGA showing the coke % of fresh HY5.1 (■); dealuminated HY5.1 (●) and desilicated HY5.1 (▲) during toluene alkylation with 1-heptene at 90 °C, atmospheric pressure, 0.25 g zeolite, reaction time of 120 min, T: H ratio is 3: 1 and using BR.

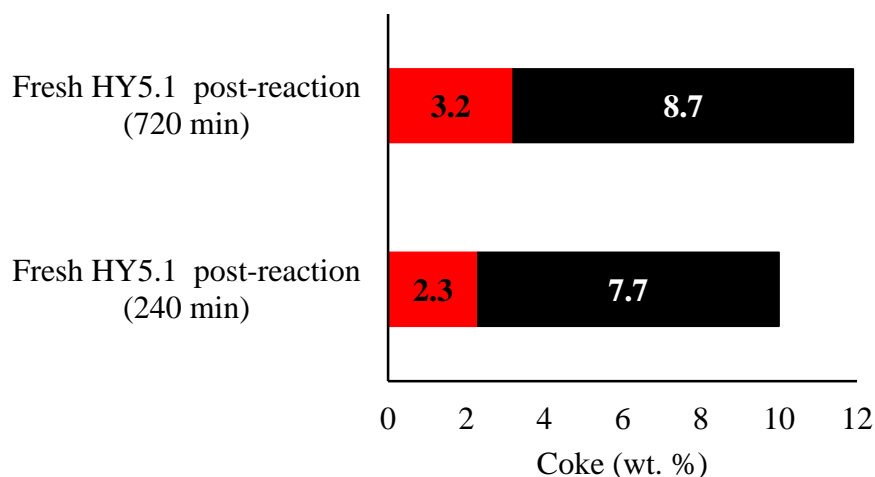


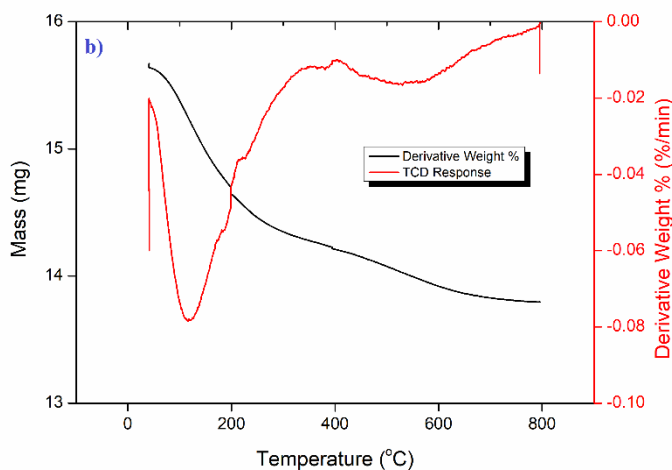
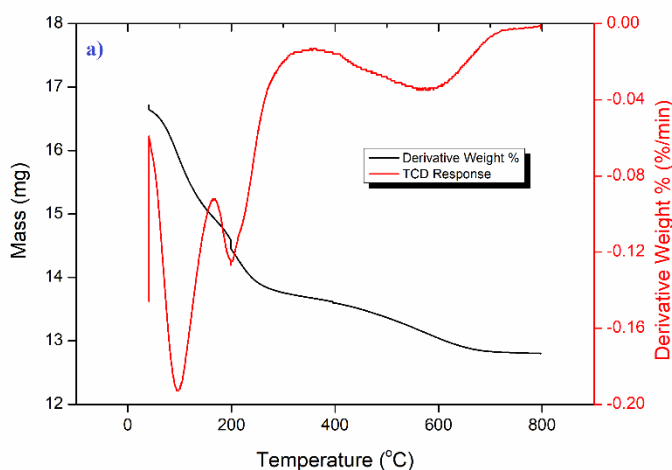
Figure 5.37. Soft coke (■) and hard coke (■) % of fresh HY5.1 post-reaction at different TOS 240 and 720 min during toluene alkylation with 1-heptene at 90 °C, atmospheric pressure, 0.5 g zeolite, TOS of 240 min, T: H ratio is 8: 1, WHSV of 17 h⁻¹, 30 ml min⁻¹ of N₂ flowrate and using FBR.

Figure 5.38 and Table 5.5 illustrate the effect of HY5.1 and HY30 modifications on the amount of coke formed. It can be remarked that the amount of coke increased after the desilication treatment for both HY zeolites (Table 5.5 and Figure 5.36), perhaps because the total acidity was increased. This result is in agreement with the work of Mochizuki and co-worker in which they reported the amount of coke deposited on the parent HZSM-5 is less than that deposited on the

desilicated zeolite. In contrast, the amount of coke formed decreased after the dealumination modification of both zeolites, probably because the total acidity was decreased as a result of reducing the aluminium content (Mochizuki et al., 2012). These results confirm those that were shown in Section 5.3.1.5.

The most acceptable explanation of the large amount of coke formed during the toluene alkylation with 1-heptene is that the reaction temperature 90 °C leads to the formation of non-volatile oligomers that become trapped inside the zeolite pores and thereby increase the coke content (Li and Brown, 1999, Wan et al., 2018, Rojo-Gama et al., 2017).

To ensure the amount of coke was accurately determined, each sample was analysed more than once and the standard error was used to evaluate the accuracy of these results, as shown in all Tables below that relate to TGA results.



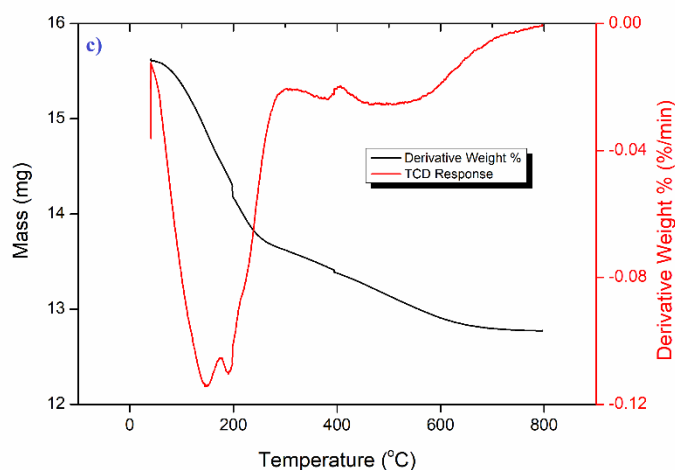


Figure 5.38. TGA and dTG profiles for a) HY5.1, b) HY5.1 dealuminated and c) HY5.1 desilicated during toluene alkylation with 1-heptene at 90 °C, atmospheric pressure, 0.5 g zeolite, TOS of 240 min, T: H ratio is 8: 1, WHSV of 17 h⁻¹, 30 ml min⁻¹ of N₂ flowrate and using FBR.

Table 5.5. The coke % after dealumination and desilication treatments of HY5.1 and HY30 zeolite catalysts during toluene alkylation with 1-heptene at 90 °C, atmospheric pressure, 0.5 g zeolite, TOS of 240 min, T: H ratio is 8: 1, WHSV of 17 h⁻¹, 30 ml min⁻¹ of N₂ flowrate and using FBR.

Zeolite	Soft coke wt. % (200-400 °C)	Hard coke wt. % (400-800 °C)	Total coke wt. % (200-800 °C)
Fresh HY5.1 post-reaction (240 min)	2.3 ± 0.35	7.7 ± 0.28	10 ± 0.64
HY5.1 dealuminated post-reaction (240 min)	1.4 ± 0.14	3.2 ± 0.07	4.6 ± 0.21
HY5.1 desilicated post-reaction (240 min)	2.6 ± 0.07	9 ± 0.07	11.6 ± 0.14
Fresh HY30 post-reaction (240 min)	1.8 ± 0.14	10 ± 0.07	11.8 ± 0.21
HY30 dealuminated post-reaction (240 min)	2 ± 0.14	9 ± 0.07	11 ± 0.21
HY30 desilicated post-reaction (240 min)	1.9 ± 0.14	11.1 ± 0.71	13 ± 0.85

Although the Si/Al ratio of HY30 is higher than HY5.1 (according to XRF results, it is 15.1 for HY30 and 3.3 for HY5.1), the amount of coke deposited on the HY30 zeolite is more than on the HY5.1 (Table 5.1), probably owing to the surface

area of HY30 $844.9 \text{ m}^2 \text{ g}^{-1}$ compared with HY5.1 $577.1 \text{ m}^2 \text{ g}^{-1}$, as shown in Section 5.3.1.4. This result is in agreement with those obtained by Radwan *et al.* (2000).

5.6.3 Elemental analysis

The percentage of carbon, hydrogen and H/C mass ratio present on the fresh HY5.1 and HY30 and their modified zeolite samples was determined by CHNS elemental analysis, as shown in Table 5.6.

Table 5.6. The H/C mass ratio obtained by the elemental analysis after dealumination and desilication treatments of HY5.1 and HY30 zeolite catalysts during toluene alkylation with 1-heptene at $90 \text{ }^\circ\text{C}$, atmospheric pressure, 0.5 g zeolite, TOS of 240 min, T: H ratio is 8: 1, WHSV of 17 h^{-1} , 30 ml min^{-1} of N_2 flowrate and using FBR.

Zeolite	%H (wt. %)	%C (wt. %)	H/C mass ratio
HY5.1 (BR)	2.3 ± 0	6.8 ± 0.14	0.34 ± 0
HY5.1 dealuminated (BR)	1.5 ± 0	1.6 ± 0.14	1.0 ± 0.07
HY5.1 desilicated (BR)	2.8 ± 0	8.5 ± 0.49	0.33 ± 0.07
HY5.1 (FBR)	2.5 ± 0.07	10.7 ± 0.21	0.23 ± 0
HY30 (FBR)	7.0 ± 0.07	36.9 ± 0.85	0.19 ± 0
HY30 dealuminated (FBR)	6.2 ± 0.49	22.4 ± 1.06	0.28 ± 0.01
HY30 desilicated (FBR)	7.5 ± 0.71	31.6 ± 0.28	0.24 ± 0.01

Generally, at temperatures below $327 \text{ }^\circ\text{C}$, the amount of coke deposited is higher than that at temperatures above $427 \text{ }^\circ\text{C}$ because the coke pre-cursors in the zeolite catalyst are more easily retained at this low temperature (Cerqueira *et al.*, 2000). Table 5.6 illustrates the carbonaceous deposits during the toluene alkylation with 1-heptene of most samples are hydrogen-deficient coke, except HY5.1 dealuminated in a BR which is hydrogen-rich coke, as demonstrated previously in Section 3.10. The coke structure for the used samples from the BR are less aromaticity or amorphous while those using the FBR are highly-ordered or polyatomic coke (Bauer and Karge, 2007, Fan and Watkinson, 2006). These results confirm those which were obtained using the TGA, as shown in Section 5.3.4.2.

The fresh samples of coke have a hard structure, however, after the dealumination treatment the structure tends to become softer or less ordered, probably because the acidity decreases after this treatment, as explained in Section 5.6.2.

5.6.4 TPO

Several thermal characterisation techniques have been employed during this study to investigate the coke residues, such as TGA and elemental analysis which provided much information about the type and structure of these carbonations compounds. However, while there is no information about the coke behaviour as a result of thermal treatment or on the coke reactivity with the active sites of catalyst. Therefore, TPO is widely used to determine this information (Querini and Fung, 1997).

Figure 5.39 shows the TPO profile of the HY5.1 and HY30 zeolite samples after toluene alkylation with 1-heptene. It can be seen both these used samples have three peaks as a result of variations in the carbon nature. The maximum temperature of the first one is located at ~ 100 °C which is attributed to physisorbed water; the second one is located at ~ 200 °C and represents the hydrogen-rich carbonaceous deposits; and the last peak appeared at higher than 500 °C and is ascribed to the existence of structurally ordered or graphitic-like carbon (Bauer and Karge, 2007, Altin and Eser, 2001).

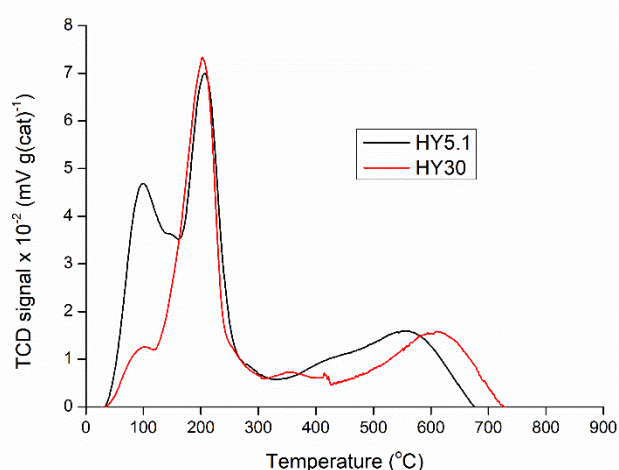


Figure 5.39. TPO profiles of the HY5.1 and HY30 post-reaction during toluene alkylation with 1-heptene at 90 °C, atmospheric pressure, 0.5 g zeolite, TOS of 240 min, T: H ratio is 8: 1, WHSV of 17 h⁻¹, 30 ml min⁻¹ of N₂ flowrate and using FBR.

Bayraktar and Kugler (2002) showed that the area under each peak represents the amount of coke formed on the catalyst. Moreover, each individual peak indicates unique carbon structural orders and has a different reactivity with the acid sites (Alonso-Morales et al., 2013). The profiles of TPO spectra have many peaks which often overlap, meaning it is not easy to resolve them. Therefore, the deconvolution becomes necessary to isolate and recognise the individual peaks and divide them up into different types depending on the structure and nature of these carbon species.

Origin software (OriginPro 8.5.1) has been employed for TPO curve deconvolution; it deconvoluted this profile to six Gaussian peaks. An initial temperature value was chosen based on literature concerning TPO characterisation (Bayraktar and Kugler, 2002, Petkovic and Ginosar, 2004, Suwardiyanto et al., 2017, Chen et al., 2013).

The TPO analysis of spent HY5.1 was replicated twice. The deconvolution showed the error % of the peak area of each individual peak to be $\pm 3\%$, whereas the centre location of each peak is shifted $\pm 6\%$.

Figure 5.40 and Figure 5.41 explain the TPO profile deconvolution for HY5.1 and HY30 post-reaction, respectively. The cumulative curve is remarkably consistent with the TPO curve which shows the deconvolution is acceptable and valid.

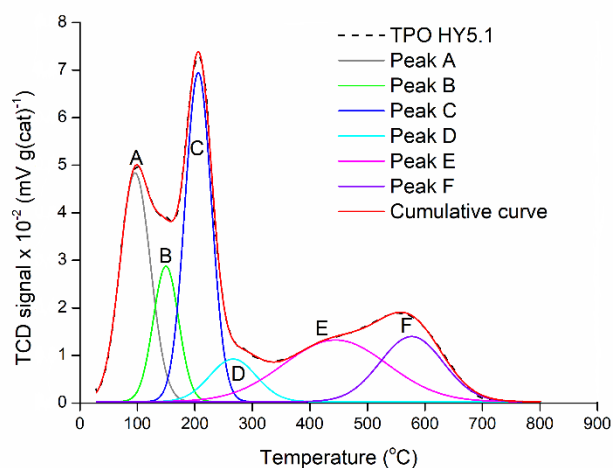


Figure 5.40. Peak deconvolution of TPO spectrum for spent HY5.1 during toluene alkylation with 1-heptene at 90 °C, atmospheric pressure, 0.5 g zeolite, TOS of 240 min, T: H ratio is 8: 1, WHSV of 17 h⁻¹, 30 ml min⁻¹ of N₂ flowrate and using FBR.

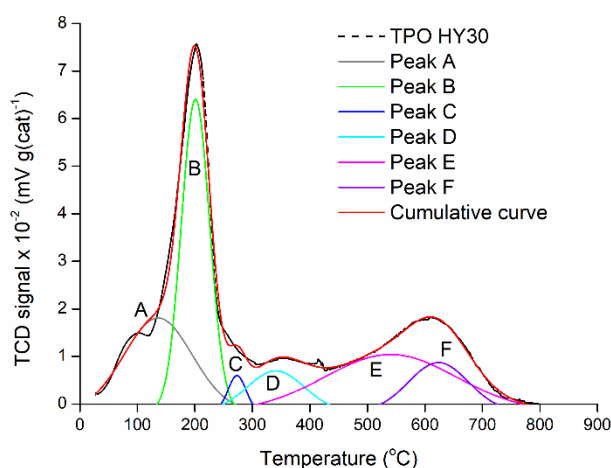


Figure 5.41. Peak deconvolution of TPO spectrum for spent HY30 during toluene alkylation with 1-heptene at 90 °C, atmospheric pressure, 0.5 g zeolite, TOS of 240 min, T: H ratio is 8: 1, WHSV of 17 h⁻¹, 30 ml min⁻¹ of N₂ flowrate and using FBR.

Table 5.7 summarises the results of the maximum temperature and peak areas. The summation of C-F peaks of HY5.1 is ~9.7 and B-F peaks of HY30 is ~10.1. These results are in agreement with those obtained by TGA, as described earlier in Section 5.6.2.

Table 5.7. The fit peak areas and maximum temperature deconvoluted peaks for spent HY5.1 and HY30 during toluene alkylation with 1-heptene at 90 °C, atmospheric pressure, 0.5 g zeolite, TOS of 240 min, T: H ratio is 8: 1, WHSV of 17 h⁻¹, 30 ml min⁻¹ of N₂ flowrate and using FBR.

Zeolite	Fit peak area (Temperature °C)						Total
	A	B	C	D	E	F	
HY5.1	3.2 (96)	1.6 (150)	4 (206)	0.9 (266)	2.9 (445)	1.9 (577)	14.5
HY30	2.9 (136)	4 (201)	0.3 (273)	1.1 (341)	3.4 (540)	1.3 (623)	13

It can be remarked that the sixth peak of HY30 was observed at ~623 °C while it appeared at ~577 °C for the HY5.1. This shift in the oxidation temperature denotes an alteration in the structural nature of the carbonaceous deposits which become more polyaromatic and strongly bound to the acid sites of the zeolite catalyst (Zachariou et al., 2019). These results confirm those obtained from elemental analysis in Section 5.6.3.

The TPO profiles of the HY30, dealuminated HY30 and desilicated HY30 post-reaction through the alkylation reaction are shown in Figure 5.42. The deconvoluted peaks of these profiles are shown in Figure 5.43 and Figure 5.44.

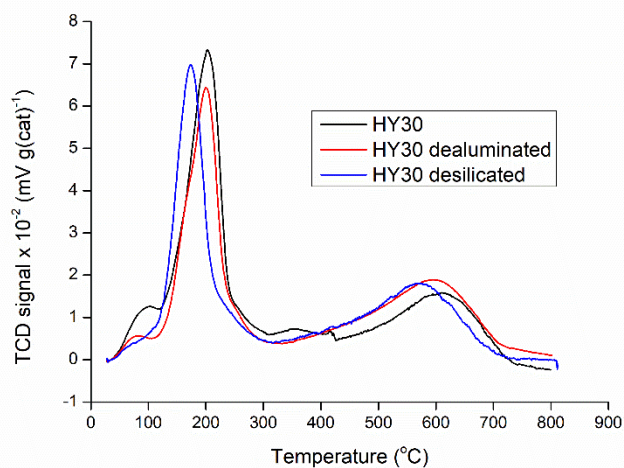


Figure 5.42. TPO profiles of the spent HY30 and its modified zeolite samples during toluene alkylation with 1-heptene at 90 °C, atmospheric pressure, 0.25 g zeolite, TOS of 240 min, T: H ratio is 8: 1, WHSV of 17 h⁻¹, 30 ml min⁻¹ of N₂ flowrate and using FBR.

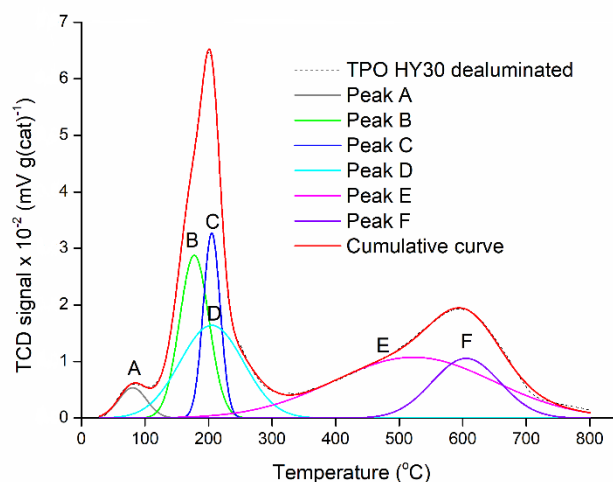


Figure 5.43. Peak deconvolution of TPO spectrum for spent HY30 dealuminated during toluene alkylation with 1-heptene at 90 °C, atmospheric pressure, 0.5 g zeolite, TOS of 240 min, T: H ratio is 8: 1, WHSV of 17 h⁻¹, 30 ml min⁻¹ of N₂ flowrate and using FBR.

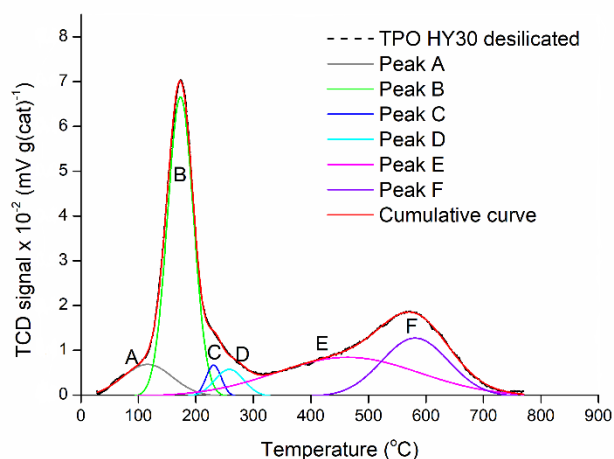


Figure 5.44. Peak deconvolution of TPO spectrum for spent HY30 desilicated during toluene alkylation with 1-heptene at 90 °C, atmospheric pressure, 0.5 g zeolite, TOS of 240 min, T: H ratio is 8: 1, WHSV of 17 h⁻¹, 30 ml min⁻¹ of N₂ flowrate and using FBR.

The maximum temperature and area of each individual peak are given in Table 5.8. The combination of B-F peaks is ~10.1, ~9.8 and ~9 for HY30, dealuminated HY30 and desilicated HY30, respectively. The results of fresh HY30 and its dealuminated form agree with the results obtained using TGA, as shown in Section 5.6.2. However, in contrast with the TGA results, the desilicated HY30 showed a decrease in the sum of the peak areas and a small shift in the maximum temperature ~570 °C compared with the fresh HY30 zeolite ~610 °C. This could indicate that there is a change in the coke structure as a result of the formation of a mesoporous structure, as shown previously in Section 5.3.1.4. These results are supported by the selectivity results of 2-heptyltoluene when it was shown to slightly increase in comparison with the fresh HY30 zeolite catalyst from ~33 % to ~39 %, as described in Section 5.5.2.

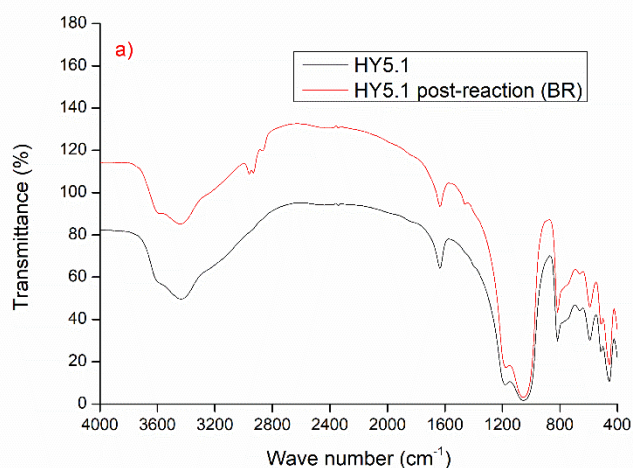
Last but not least, this table is completely compatible with the TGA and elemental analysis results in the division of coke to hard and soft where it shows the hard coke represents the largest percentage.

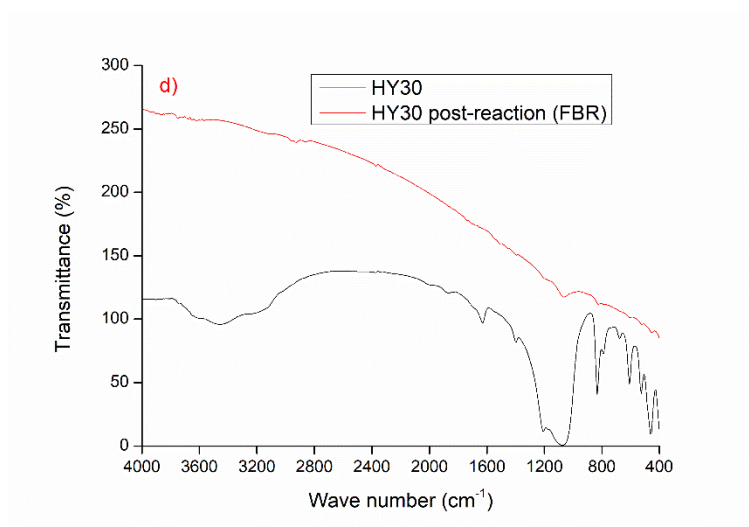
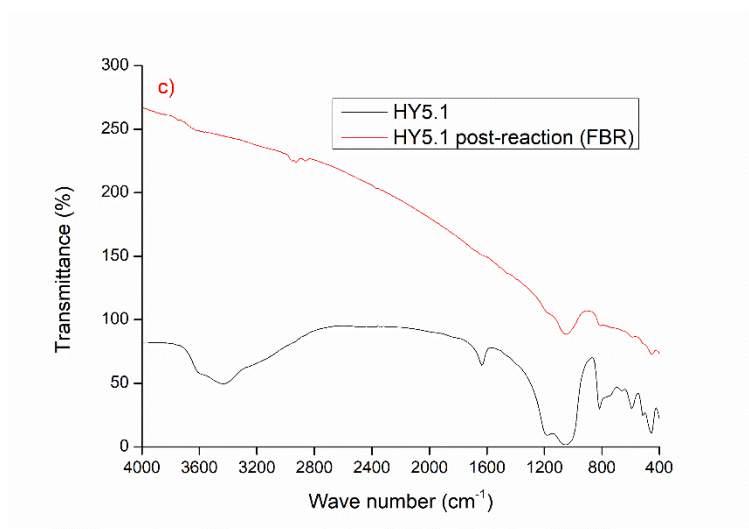
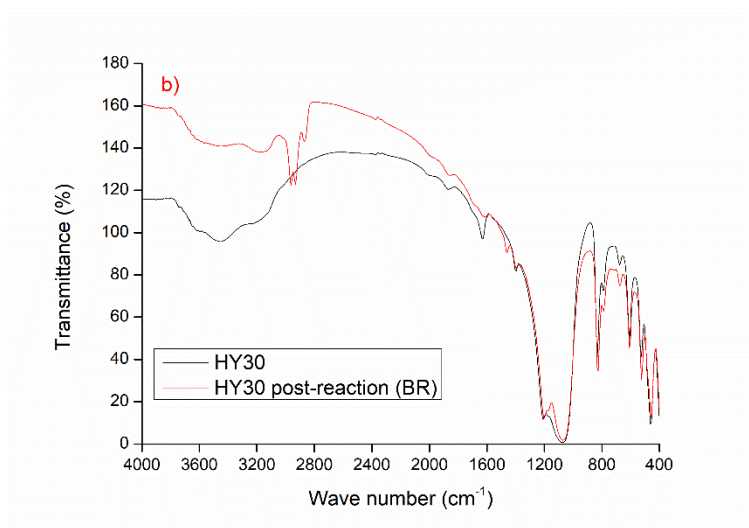
Table 5.8. The fit peak areas and maximum temperature deconvoluted peaks for spent HY30, HY30 dealuminated and HY30 desilicated during toluene alkylation with 1-heptene at 90 °C, atmospheric pressure, 0.5 g zeolite, TOS of 240 min, T: H ratio is 8: 1, WHSV of 17 h⁻¹, 30 ml min⁻¹ of N₂ flowrate and using FBR.

Zeolite	Fit peak area (Temperature °C)						Total
	A	B	C	D	E	F	
HY30	2.9 (136)	4 (201)	0.3 (273)	1.1 (341)	3.4 (540)	1.3 (623)	13
HY30 dealuminated	0.3 (80)	1.7 (178)	1.1 (205)	2.1 (205)	3.4 (522)	1.4 (605)	10
HY30 desilicated	0.8 (116)	3.8 (173)	0.2 (230)	0.4 (258)	2.7 (464)	1.9 (581)	9.8

5.6.5 FTIR

Figure 5.45 shows the FTIR spectra of fresh, modified and post-treated HY5.1 and HY30 zeolite samples. The -CH stretching region of hydrocarbon products appeared between 2800 - 3000 cm⁻¹ and represents the aliphatic species model of -CH stretching (Bauer and Karge, 2007, Querini, 2004, Ibáñez et al., 2016). It is noteworthy that, all graphs in Figure 5.45 (a-g) showed three peaks of -CH stretching bands spanning from 2862 to 2970 cm⁻¹. The peak at 2931- 2925 cm⁻¹ represents ν_{as} CH₂ aliphatic species while, the peaks at 2962-2955 and 2870-2862 cm⁻¹ represent ν_{as} CH₃ aliphatic species. Similar results were shown in an earlier study by Petkovic and Ginosar (2004).





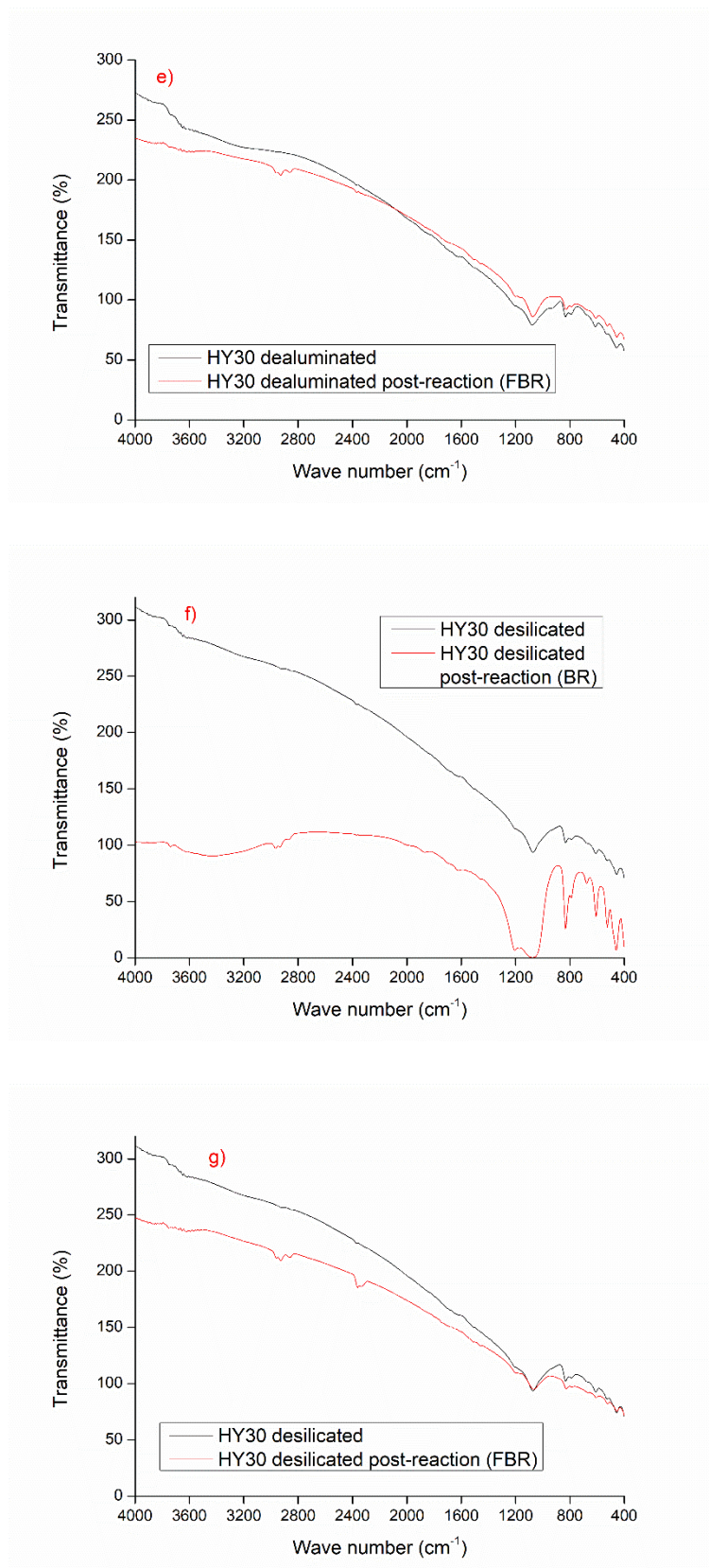
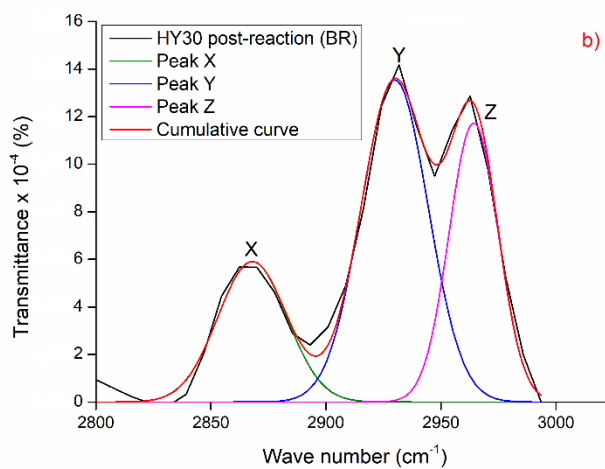
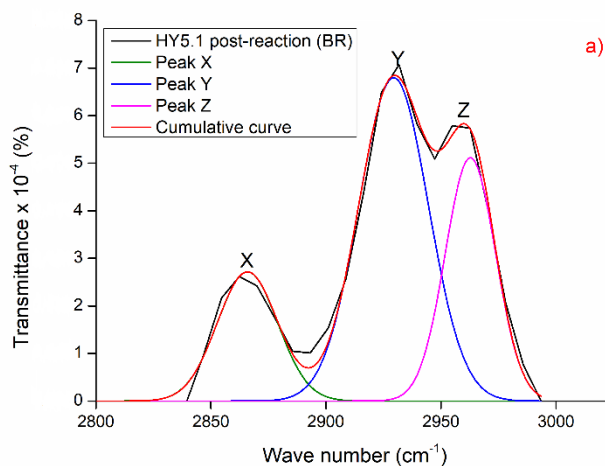
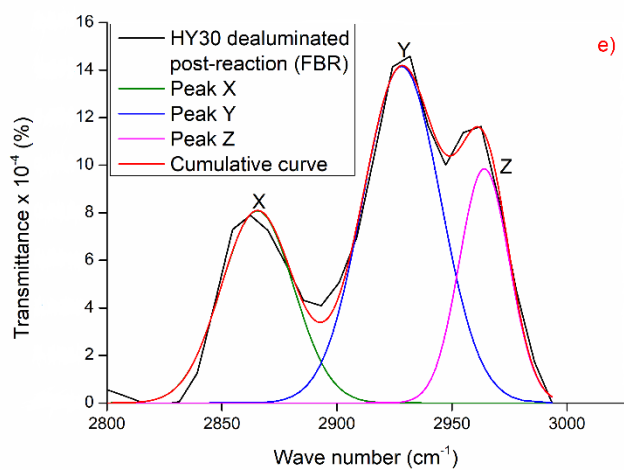
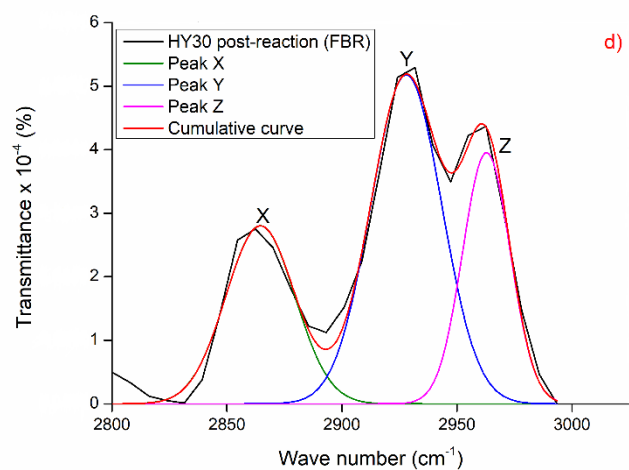
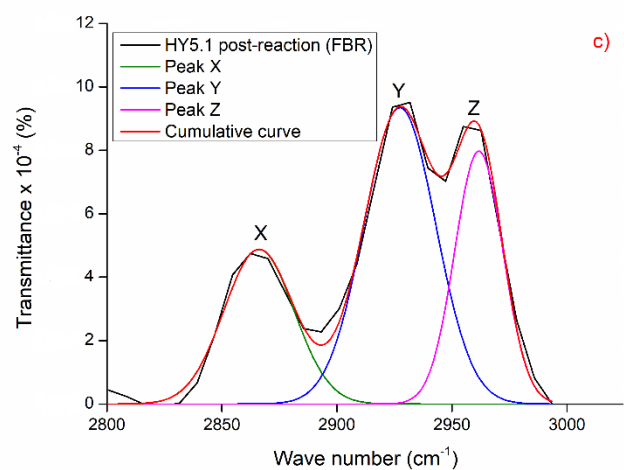


Figure 5.45. The FTIR spectra in the $\nu(\text{CH})$ region for fresh and post-reaction zeolite catalysts of a) HY5.1 (powder); b) HY30 (powder); c) HY5.1 (pellet); d) HY30 (pellet); e) HY30 dealuminated (pellet); f) HY30 desilicated (powder) and g) HY30 desilicated (pellet).

FTIR spectrum of spent zeolite catalyst has been deconvoluted into three Gaussian peaks using Origin software (OriginPro 8.5.1) (Epelde et al., 2014). The deconvolution is shown in Figure 5.46 at the region between 2800-3000 cm^{-1} for all the post-reaction zeolite samples that are shown above.





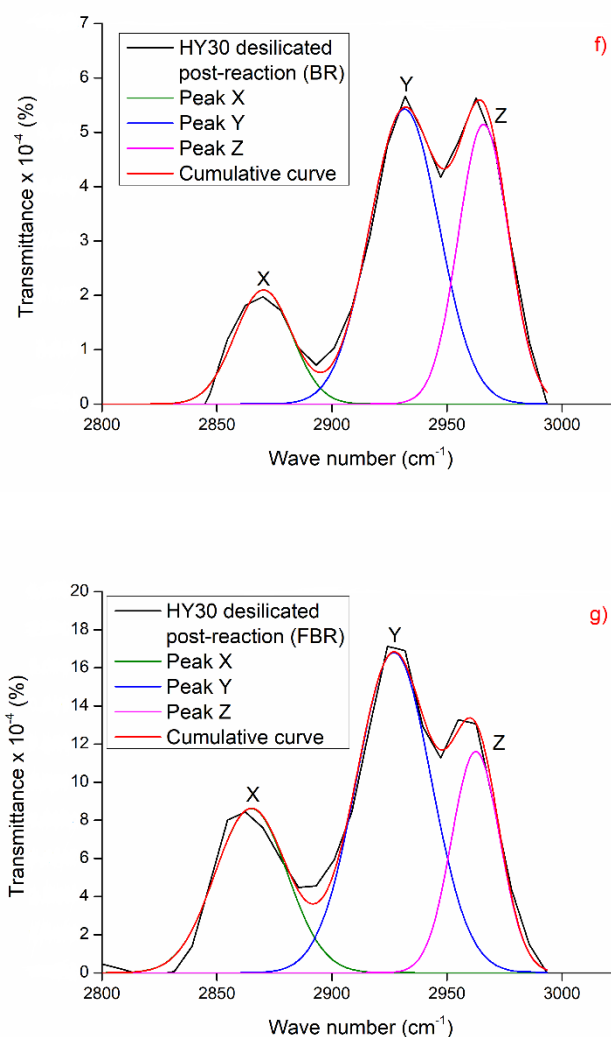


Figure 5.46. Peak deconvolution of FTIR spectra in the $\nu(\text{CH})$ region for fresh and spent zeolite catalysts of a) HY5.1 (powder); b) HY30 (powder); c) HY5.1 (pellet); d) HY30 (pellet); e) HY30 dealuminated (pellet); f) HY30 desilicated (powder) and g) HY30 desilicated (pellet).

Table 5.9 summarises the results of the peak areas at the three different bands. The band of $\nu_{\text{as}} \text{CH}_2$ aliphatic species $\sim 2930 \text{ cm}^{-1}$ was the highest, while $\nu_{\text{as}} \text{CH}_3$ aliphatic species $\sim 2870 \text{ cm}^{-1}$ was the lowest and represents approximately one third of the highest peak height. This means the aliphatic chains of the coke pre-cursor were naphthenic or longer (Castaño et al., 2011).

Table 5.9. The fit peak areas of deconvoluted peaks of FTIR spectra in the $\nu(\text{CH})$ region for fresh and used of a) HY5.1 (powder); b) HY30 (powder); c) HY5.1 (pellet); d) HY30 (pellet); e) HY30 dealuminated (pellet); f) HY30 desilicated (powder) and g) HY30 desilicated (pellet).

Zeolite	Fit peak area		
	$\sim 2870 \text{ cm}^{-1}$	$\sim 2930 \text{ cm}^{-1}$	$\sim 2962 \text{ cm}^{-1}$
HY5.1 (BR)	0.009	0.026	0.014
HY30 (BR)	0.023	0.049	0.031
HY5.1 (FBR)	0.002	0.004	0.002
HY30 (FBR)	0.001	0.002	0.001
HY30 dealuminated (FBR)	0.003	0.006	0.003
HY30 desilicated (BR)	0.007	0.021	0.014
HY30 desilicated (FBR)	0.003	0.007	0.003

Generally, all the samples that were obtained by BR have higher intensities than those using FBR which referring the nature of coke pre-cursor in the zeolite was broadly unsaturated.

5.7 Conclusions

Toluene alkylation with 1-heptene has been performed to investigate the variation in the amount, nature and type of pre-cursor deposited and to study the role of these carbonaceous deposits on the catalytic performance. Two reactors have been employed for this reaction; BR and FBR. A BR was used to perform reactions over four types of zeolite; HY5.1, HY30, H-mordenite and H-Beta. The reactions were completed at 90 °C and atmospheric pressure using 0.25 g of zeolite catalyst. The toluene to 1-heptene mole ratio was 3 and reaction times of 20, 120 and 360 min were used. The reactions in the FBR were completed over HY5.1 and HY30, identified from the preliminary work in the BR as the optimum structures for the alkylation reaction. The operation conditions which were employed in the FBR were slightly different to those used in the BR. The reaction temperature was still the same at 90 °C (highest activity and stability), atmospheric pressure and a TOS of 240 min were used (at this time the conversion and selectivity reached high stability). A nitrogen flowrate of 30 ml min⁻¹, 0.5 g of zeolite catalyst (the role of coke was clear), a WHSV of 17 h⁻¹ and a toluene to 1-heptene mole ratio of 8 were used. Two modifications were

employed in both reactors to study the effect of these treatments on the coke properties as well as the role of the carbonaceous deposits on the catalytic activities. HY30 and its modified samples can be considered as the optimum structures for the alkylation of toluene with 1-heptene in both reactors. However, the other structures, such as HY5.1 and H-Beta, showed improvements in some aspects and they can be used as corroborating evidence.

The carbonaceous deposits acted to increase the zeolite stability when the reduction of 1-heptene conversion became slower than that on the fresh catalyst. This compliments the hypothesis that these carbonaceous deposits can play a positive role in enhancing the selectivity of 2- and 3-heptyltoluene.

The role of the zeolite modification on the coke formation becomes clear owing to the various types of characterisation techniques. TGA showed the amount of coke was decreased after dealumination treatment which coincides with a decrease in 1-heptene conversion. In contrast, the amount of coke was increased after the desilication modification, as was the selectivity of the 2- and 3-heptyltoluene as a result of mesoporous formation; this indicates the positive effect that coke deposits can have on the selectivity of the desired products. On the other hand, the TGA classified the nature of coke as two types; hard and soft. In general, the coke deposits on the fresh and desilicated zeolites was hard however, it became softer on the dealuminated zeolite catalysts. This was clear in the results of elemental analysis where the H/C ratio was increased after the dealumination treatment which indicated changes in the coke nature from hard to either soft or less aromaticity.

TPO measurements exhibited the alterations in the coke structure and oxidation temperature. The TPO profiles showed there are two main species of carbon that have different structural natures and oxidation temperatures. The first type appeared at temperatures of ~200 °C and represents the hydrogen-rich carbon and the second peak appeared at temperatures of ~500 °C or more and represented graphitic-like or structurally ordered carbon. The desilicated zeolite displayed showed no change in the coke nature but it was altered to become softer as a result of the formation of mesopores.

Chapter 6

*Tailored carbon
deposition of several
zeolites for toluene
alkylation with 1-
heptene*

6.1 Introduction

The petrochemical industry relies on heterogeneous catalysts to improve the activity of its processes and selectivity to key products (van Bekkum et al., 2001). Although these solid catalysts are applied in several processes, a significant limitation is the formation of heavy by-products, such as coke. In the last fifty years, several investigations have focused on the role of carbonaceous deposits on zeolites when using hydrocarbon materials because they have a vital effect on the activity and selectivity of this zeolite catalyst (Gomez Sanz et al., 2016, de-Silva et al., 2010, Collett and McGregor, 2015). Predominantly, these studies observed two main reasons for the effect on the zeolite performance; either blocking of the zeolite pores or poisoning of the active centres (Fiedorow et al., 2004, Lee et al., 2004). However, in addition to coke deposits having a negative impact, recent studies have shown that the different structures of the coke can play different roles, ranging from deactivation through to enhancement of both catalyst activity and selectivity (McGregor et al., 2010b, Collett and McGregor, 2015). Broadly, most of these investigations act to promote the selectivity of the desired product *via* pre-treatment surface modifications which clog the non-selective acid centres through one of the following methods; silylation which uses organ-silicate materials (Cejka et al., 1996) and pre-coking, which employs the adsorption agents of hydrocarbons (McGregor et al., 2010a).

Pre-coking and silylation treatments are typical examples of surface modifications; they act to passivate the non-selective acid centres on the outer surface of the zeolite. The external surface of the zeolite catalyst is completely accessible to the reactant molecules and is more exposed for the deactivation by coke precursors (Tsai et al., 1999, Cejka et al., 1996). Therefore, several studies have focused on this section and the surface modifications are just one of these investigations. In addition, these treatments have another positive feature; by narrowing the pore apertures they limit the diffusion properties which could be involved in increasing the selectivity of the desired products.

Pre-coking is an effective method used to modify the catalyst surface through the deposition of hydrocarbonaceous material (Bauer et al., 2001, Bauer et al., 2007b). Through studying the coke formation, an understanding of the main precursor molecules of the reactants participating in the tailored coke deposition on the zeolite

catalyst can be developed. Moreover, enhancing the catalyst selectivity as a result of pre-coking. Further details are described in Section 2.3.4.

Coke formation is rapid on the zeolite catalyst when the reactant is olefin because it immediately transforms through either oligomerisation or alkylation reactions (Brillis and Manos, 2003, Guisnet and Magnoux, 1989, Holmes et al., 1997, van Donk et al., 2001). However, the coke pre-cursor which is formed from toluene is polyaromatic and it deposits on both the internal and external surfaces of zeolite catalysts (Argyle and Bartholomew, 2015, Uguina et al., 1993).

Silylation is widely used as a type of surface modification which employs bulky organosilicate materials (Zheng et al., 2002). This treatment acts to enhance the selectivity of the desired products and reduce the production of side products through either narrowing the pore openings or covering the external acid sites which are responsible for these unwanted products. This contributes to an increase in the lifetime of the zeolite. Although several investigations in the literature have been concerned with the silylation modification and have tried to use the catalyst silylated in many reactions, there are a few studies which have employed this catalyst in the alkylation reaction.

The aim of the present study is to employ reactant pre-coking and silylation treatment to understand deactivation and potentially contribute to process enhancement of the alkylation of toluene with 1-heptene for the selective production of heptyltoluene over zeolite catalysts.

Through pre-coking with individual reactant species, it is possible to determine the differing influences that coke derived from these pre-cursors has on the reaction. This allows determination of which reactant is responsible for the zeolite deactivation and hence gives a greater insight into catalyst operation. The use of pre-coking to enhance catalyst selectivity is well-established in petrochemical processing. Based on the above, a set of zeolite catalysts were pre-coked by adsorbing the reactants of the alkylation reaction (toluene and 1-heptene).

Silylation treatment was completed using tetraethoxysilane [TEOS] to cover the acid sites on the external surface and narrow the pore openings, thereby reducing the diffusion of undesired products. Both these steps contribute to enhancement of the

selectivity of the desired alkylated products. More information can be found in Chapter 2, Section 2.3.3.

Subsequently, the fresh, silylated and pre-coked zeolite catalysts were employed to evaluate the role of silylation and pre-coking treatment compared with the fresh zeolite on the toluene alkylation reaction. Various characterisation techniques have been employed to study the fresh and post-reaction catalysts to provide information on; the main pre-cursors that are responsible for the deactivation; the structure of coke that results from the depositions of these pre-cursors, and; the role of silicon deposits on the outer surfaces of the zeolite catalysts.

This chapter consists of three sections: first is concerned with the, preparation of zeolite modifications such as: silylation, as mentioned in Section 6.2.2., and pre-coking, which is presented in Section 6.2.3. The second is concerned with studying the toluene alkylation with 1-heptene using either a batch reactor (BR) or a fixed bed reactor (FBR). The BR was operated at a reaction temperature of 90 °C, for a reaction time of 120 min, with 0.25 g of zeolite and a toluene to 1-heptene ratio of 3. The FBR was operated at a reaction temperature of 90 °C and atmospheric pressure. 30 ml min⁻¹ nitrogen flowrate was used as an inert gas and a TOS of 240 min was used. The reactions were performed over the fresh, silylated and pre-coked zeolite, as shown in Section 6.3. The third section characterises the coke formed over the post reaction HY5.1 and HY30 zeolite using the fresh and modified zeolites by employing several different techniques such as TPO, TGA, elemental analysis, FTIR and nitrogen adsorption, as explain in Section 6.3.3.

6.2 Experimental

6.2.1 Catalysts

Four types of zeolite HY5.1, HY30, H-mordenite and H-Beta were modified by silylation then employed during the toluene alkylation with 1-heptene using a BR and a FBR. Two of these catalysts, HY5.1 and HY30, were pre-coked with 1-heptene as an olefinic pre-cursor and toluene as an aromatic pre-cursor then used in the alkylation of toluene with 1-heptene in a FBR.

6.2.2 Silylation modification

The four zeolite catalysts were prepared by suspending each sample in a mixture of *n*-hexane and TEOS which is as a silylation agent, as described previously in Section 4.5.3. The samples were then used in the alkylation of toluene with 1-heptene to investigate the effect of a silicon layer on the external surface and pore mouth of the zeolites to improve the catalytic performance.

6.2.3 Pre-coking procedure

Pre-coking was conducted by adsorbing 1-heptene and toluene as coke pre-cursors in a FBR using the same conditions as were described in Section 4.3.2, and the same off-line GC-FID connected with DB-5 capillary column. The product of the toluene pre-coking treatment was analysed by GC-FID and it showed just one peak for toluene; this indicates that no reaction occurred during this process. In contrast, the product of the 1-heptene pre-coking treatment was also analysed by GC-FID and showed three peaks. These represent 1-, 2- and 3-heptene which means that the isomerisation reactions have occurred during this process.

6.2.4 Catalytic activity measurements

The same experimental procedure that was employed in Chapter 5 and demonstrated earlier in Section 4.3, is used to study the catalytic activity of fresh, silylated and pre-coked zeolite catalysts using both the BR and FBR.

GC-MS and GC-FID have been employed to analyse the liquid products as shown in Section 4.4. The catalytic performance calculations were also previously explained in Section 4.6.

6.3 Results and discussion

6.3.1 Characterisation techniques

Several characterisation techniques were employed to study the effect of silylation and pre-coking treatments and the structure of coke that formed during the alkylation reaction, such as; energy dispersive X-ray (EDX); X-ray fluorescence (XRF); temperature-programmed desorption (TPD); nitrogen adsorption-desorption; thermogravimetric Analysis (TGA); elemental analysis; temperature programmed oxidation (TPO) and Fourier-transform infrared spectroscopy (FTIR). Detailed information about these techniques was shown in Chapter 3.

6.3.1.1 XRF and EDX results

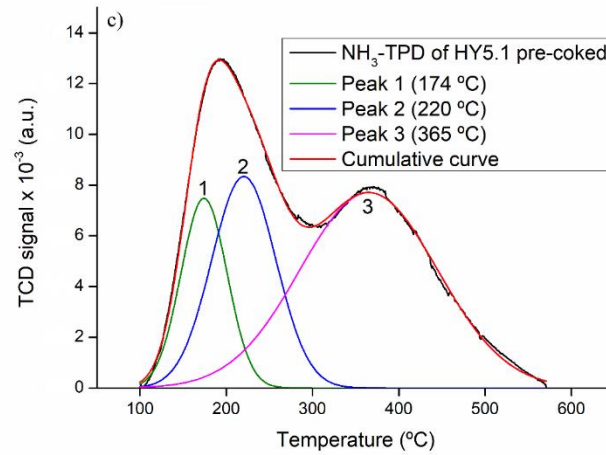
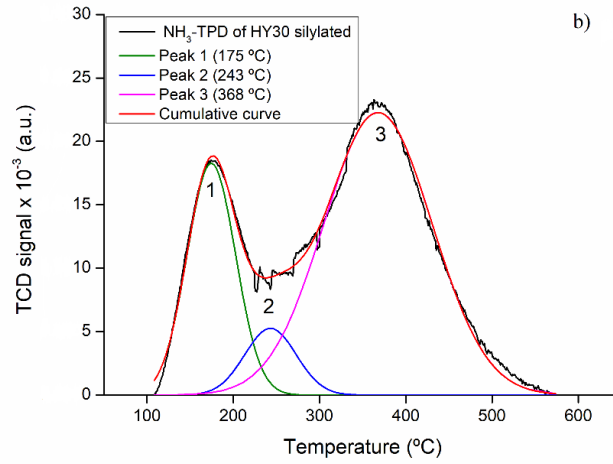
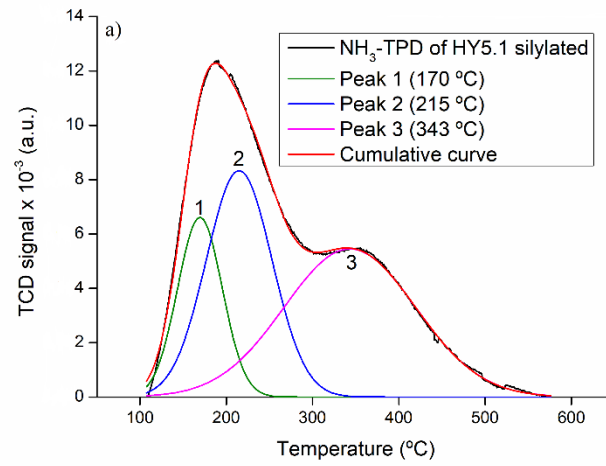
Table 6.1 shows the bulk Si/Al ratio of fresh and silylated HY5.1 and HY30. In general, there is a slight increase in the Si/Al ratio of all silylated samples compared to the unmodified samples which indicates that the silylation modification has occurred correctly. A similar result was reported by Weber *et al.* (2000), who showed that the Si/Al ratio slightly increases as a result of silicon deposition.

Table 6.1. The results of Si/Al mole ratio using XRF and EDX for fresh and silylated zeolite catalysts.

Zeolite	Si/Al (XRF)	Si/Al (EDX)
HY5.1	3.3	3 ± 0.07
HY5.1 silylation	3.4	3.2 ± 0
HY30	15.1	16.3 ± 0.35
HY30 silylated	16.3	21.8 ± 0

6.3.1.2 TPD results

The NH₃-TPD profiles have been deconvoluted to three Gaussian peaks using an Origin software (OriginPro 8.5.1), as shown in Figure 6.1 and as described earlier in Section 5.3.1.5, except HY30 pre-coked with toluene which has just two peaks, the first peak appeared at ~180 °C and represents the weak acid sites, while, the second peak appeared above 350 °C and represents the strong acid sites. These results are identical to those found by Li *et al.* (2018). The position of the initial bond was chosen according to previous studies which used TPD analysis of fresh and modified zeolite catalyst (Triantafillidis *et al.*, 2000, Hajimirzaee *et al.*, 2015).



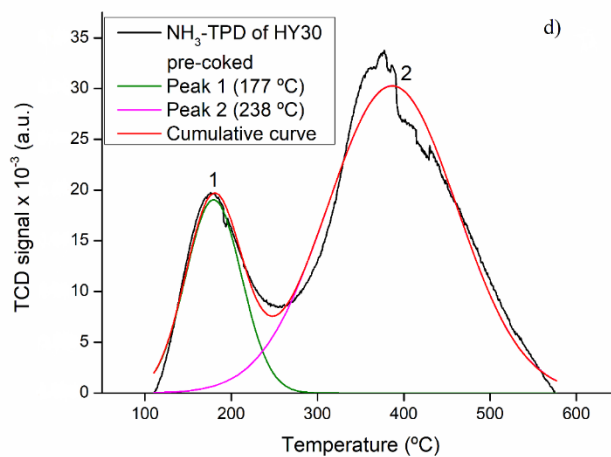


Figure 6.1. Experimental and deconvoluted NH_3 -TPD curves of A) silylated HY5.1, B) silylated HY30, C) HY5.1 pre-coked with toluene, and D) HY30 pre-coked with toluene samples (refer to Table 6.2).

Three-cycles of silylation of the HY zeolite acted to reduce the amount of acid sites by 34.2 % for HY5.1 and 36.8 % for HY30, as shown in Table 6.2. These results are similar to those obtained by Zheng *et al.* (2002), Al-Khattaf (2007).

Table 6.2. Fresh and modified acid properties of HY5.1 and HY30 zeolite catalysts.

Zeolite	Weak acid sites (mmol g⁻¹)	Medium acid sites (mmol g⁻¹)	Strong acid sites (mmol g⁻¹)	Total acid amount (mmol g⁻¹)	decrease of acid site concentration after modification (%)
HY5.1	0.25 (173 °C)	0.42 (218 °C)	0.73 (344 °C)	1.4	-
HY5.1 silylated	0.18 (170 °C)	0.33 (215 °C)	0.43 (343 °C)	0.94	33 %
HY5.1 pre-coked with toluene	0.21 (174 °C)	0.33 (220 °C)	0.65 (365 °C)	1.19	15 %
HY30	0.06 (177 °C)	0.06 (238 °C)	0.25 (376 °C)	0.36	-
HY30 silylated	0.06 (175 °C)	0.02 (243 °C)	1.5 (368 °C)	0.23	36 %
HY30 pre-coked with toluene	0.06 (180 °C)	-	0.24 (386 °C)	0.3	17 %

The desorption peaks for the silylated and pre-coked samples appeared at the same temperature locations. Moreover, the strength of these samples were not changed, however there was variation in the number of acid sites. Similar results were given by Bauer *et al.* (2007b), Kim *et al.* (1996). The unchanging acid strength supports the alkylation reaction due to the acidity and pore structure which represent important features in determining the catalytic activity of the zeolite during this reaction.

Figure 6.2 and Figure 6.3 display both areas of the high and low temperature peaks were decreased and the desorption temperature (T_{max}) location was shifted somewhat for the silylated and pre-coked samples compared with the fresh sample. Shang *et al.* (2008) concluded the same as these results.

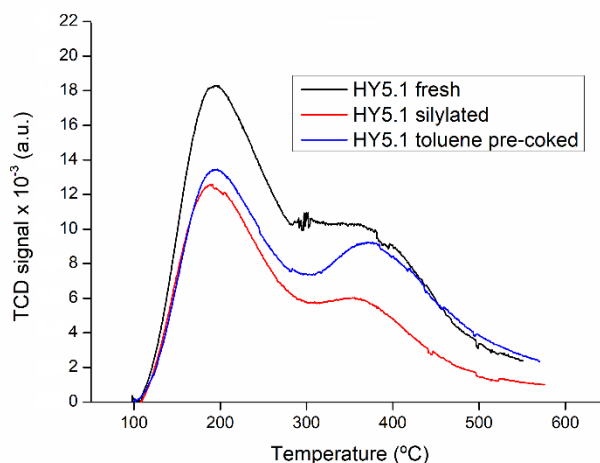


Figure 6.2. NH₃-TPD profile of fresh, silylated and toluene pre-coked HY5.1 zeolite catalyst.

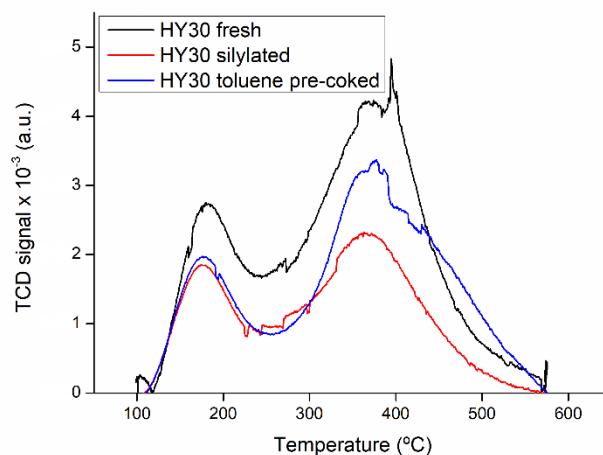


Figure 6.3. NH_3 -TPD profile of fresh, silylated and toluene pre-coked HY30 zeolite catalyst.

6.3.1.3 Nitrogen sorption results

Figure 6.4 shows the isotherms of fresh and silylated HY5.1 and HY30. It can be seen, that both the fresh and silylated zeolite samples have the same hysteresis loop type; the parent and silylated HY5.1 show type I however, the HY30 and its silylated form show type VI. The BET surface area and the total pore volume of all silylated and pre-coked HY5.1 zeolite samples were slightly reduced (Table 6.3); however, the decrease was striking in the HY30 zeolite samples.

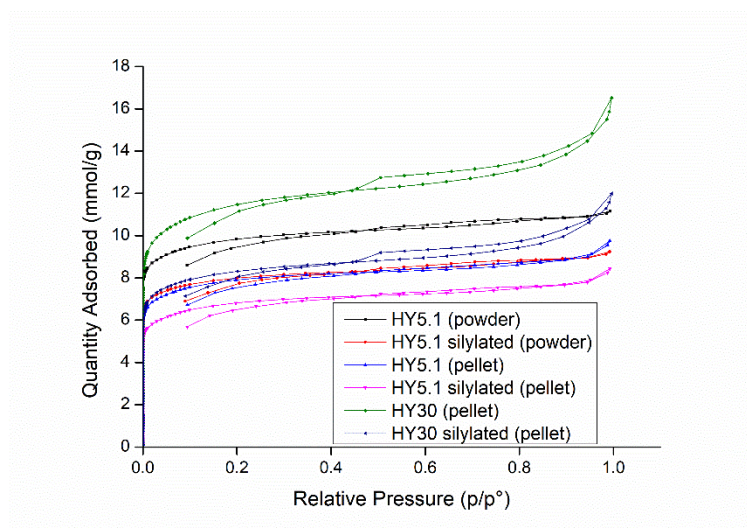


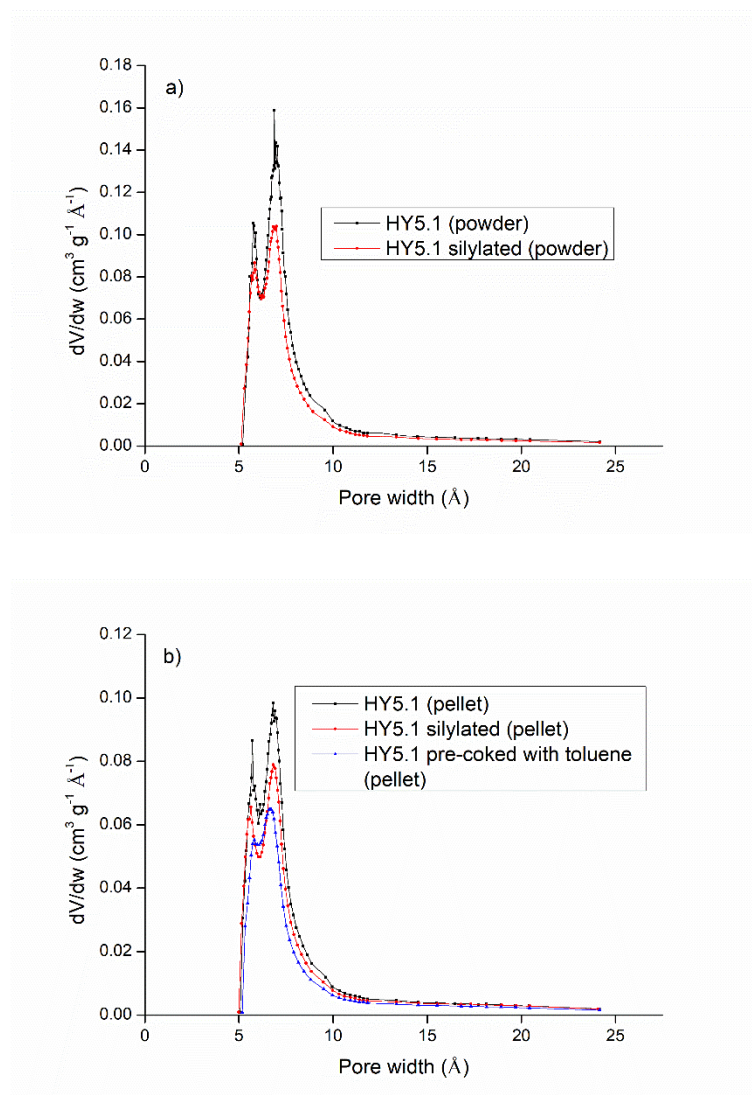
Figure 6.4. Nitrogen sorption isotherms of fresh and silylated HY5.1 (powder), HY5.1 (pellet) and HY30 (pellet) zeolite catalysts.

Table 6.3. The results of surface area of parent and modified zeolite catalysts.

Zeolite	S_{BET} ($\text{m}^2 \text{g}^{-1}$)	S_{mic} ($\text{m}^2 \text{g}^{-1}$)	S_{ext} ($\text{m}^2 \text{g}^{-1}$)	V_{tot} ($\text{cm}^3 \text{g}^{-1}$)	V_{mic} ($\text{cm}^3 \text{g}^{-1}$)	V_{meso} ($\text{cm}^3 \text{g}^{-1}$)	$d_{\text{p meso}}$ (Å) BJH	$d_{\text{p mic}}$ (Å) Horvath-Kowazoe
HY5.1 (powder)	713.7	694.3	19.5	0.387	0.349	0.038	38.6	7.07
HY5.1 silylated (powder)	611.1	593.3	17.8	0.321	0.275	0.046	41.96	6.94
HY5.1 (pellet)	577.1	548.6	28.5	0.339	0.269	0.07	50.59	6.96
HY5.1 silylated (pellet)	503.1	477.7	25.4	0.293	0.233	0.06	53.61	6.94
HY30 (pellet)	844.9	760.4	84.6	0.556	0.369	0.187	58.45	7.53
HY30 silylated (pellet)	610.3	551.4	58.8	0.405	0.268	0.137	64.63	7.48
HY5.1 pre-coked with toluene (pellet)	408.5	382.4	26.1	0.25	0.186	0.064	53.7	6.88
HY30 pre-coked with toluene (pellet)	377	316.5	60.5	0.283	0.151	0.132	58.78	7.45

Because the HY5.1 and HY30 zeolites have high surface areas (see Table 6.3), they needed an additional amount of TEOS; a multicycle was necessary to achieve this.

Table 6.3 shows the size distributions of the mesopores (which were calculated according to the BJH method) increased after silylation and pre-coking treatment. On the other hand, the size distributions of the micropores (Figure 6.5) were calculated according to the Horvath-Kawazoe method for the silylated and pre-coked samples. It showed that the pore sizes of the silylated samples were slightly smaller than the fresh zeolite samples, meaning the TEOS molecules cannot penetrate into the pores of HY zeolite. However, for the pre-coked samples, it was also smaller than the parent zeolites but it was somewhat smaller than that of silylated samples probably due to some of the toluene molecules penetrating inside these pores.



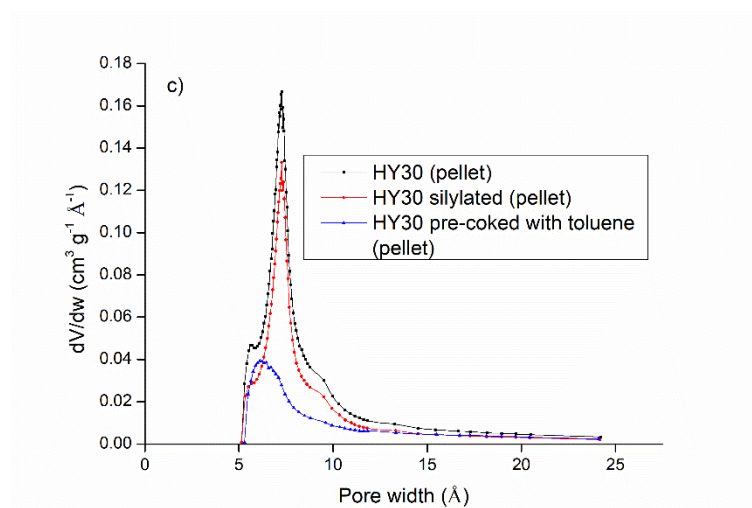


Figure 6.5. Differences of pore size distribution using Horvath-Kawazoe method for a) HY5.1 powder; b) HY5.1 pellet and c) HY30 pellet zeolite catalysts before and after silylation and pre-coking modifications.

6.3.1.4 TGA results for zeolite pre-coked

TGA data shows that deposits of coke were ~6 wt. % and ~5 wt. % for toluene pre-coked HY5.1 and HY30, respectively (Table 6.4). It is clear that hard coke represents twice the amount of soft coke. The type of coke pre-cursor that is formed on the outer surface is important because the alkylaromatic coke was effectively removed whereas, the polyaromatic coke remains on the external surface of the zeolite and this contributes to the enhancement of the selectivity of the desired products (Bauer et al., 2001).

The TGA data of 1-heptene pre-coked HY5.1 at two different TOS of 15 and 60 min is shown in Table 6.4. It can be seen that there is approximately the same amount of coke formed during this modification, regardless of the TOS. This means that the olefin pre-cursor acts to deactivate the zeolite from the first moments of the reaction. These results support those that were obtained during the study of the effect of 1-heptene pre-coking on the catalytic activity during the alkylation reaction.

Table 6.4. The coke % after pre-coking *via* toluene and 1-heptene over 0.5 g of HY5.1 and HY30 zeolites at 90 °C (toluene) and 80 °C (1-heptene) for 2 and 1 h, respectively.

Zeolite	Soft coke wt. % (200-400 °C)	Hard coke wt. % (400-800 °C)	Total coke wt. % (200-800 °C)
Toluene pre-coked HY5.1 (120 min)	2±0.07	3.9±0.14	5.9±0.21
Toluene pre-coked HY30 (120 min)	1.5±0	3.2±0	4.7±0
1-heptene pre-coked HY5.1 (60 min)	2.2 ± 0.14	8.1 ± 0.14	10.3 ± 0
1-heptene pre-coked HY5.1 (15 min)	2.1 ± 0.14	8.3 ± 0	10.4 ± 0.14

6.3.1.5 Elemental analysis for zeolite pre-coked

The percentage of carbon, hydrogen and the mass ratio between them present on the fresh HY5.1, HY30 and their pre-coked samples was determined by employing the elemental analysis. The results are shown in Table 6.5:

Table 6.5. The H/C mass ratio obtained by the elemental analysis after toluene and 1- heptene pre-coking treatments over 0.5 g of HY5.1 zeolite at 90 °C (toluene) and 80 °C (1-heptene) for 2 and 1 h, respectively.

Zeolite	%H (wt. %)	%C (wt. %)	H/C mass ratio
Toluene pre-coked HY5.1 (120 min)	2.1 ± 0.35	3.1 ± 0.49	0.67 ± 0.02
Toluene pre-coked HY30 (120 min)	1.9 ± 0.21	7.9 ± 0.57	0.24 ± 0.01
1-heptene pre- coked HY5.1 (60 min)	1.7 ± 0.14	11 ± 0.49	0.16 ± 0.01
1-heptene pre- coked HY5.1 (15 min)	2.2 ± 0.07	11.9 ± 0.14	0.17 ± 0

This table shows that both zeolites pre-coked with aromatic molecules have less carbon content (3.1 and 7.9 for HY5.1 and HY30, respectively) compared with those pre-coked with olefin samples of the same zeolites (11 and 11.9 wt. %). In addition, Table 6.5 shows that coke derived from 1-heptene is more polyaromatic (H/C = 0.16) than that derived from the aromatic precursor (H/C = 0.67) which is amorphous or less polyaromatic. On the other hand, the structure of the pre-coked coke sample

which has a higher Si/Al ratio (HY30) is less altered after the modification than that which has a low Si/Al ratio (HY5.1) (see section 6.3.1.1), probably because the HY30 is more stable.

6.3.1.6 TPO results of pre-coked zeolite

Figure 6.6 illustrates the TPO measurements of HY5.1 pre-coked with toluene and 1-heptene. It is clear that there are three main peaks. The first one appears at ~ 100 °C and represents the water content. The second peak is at ~ 200 °C and indicates hydrogen-rich carbonaceous deposits. The last one appears at ~ 500 °C and represents the structurally ordered deposits (Suwardiyanto et al., 2017).

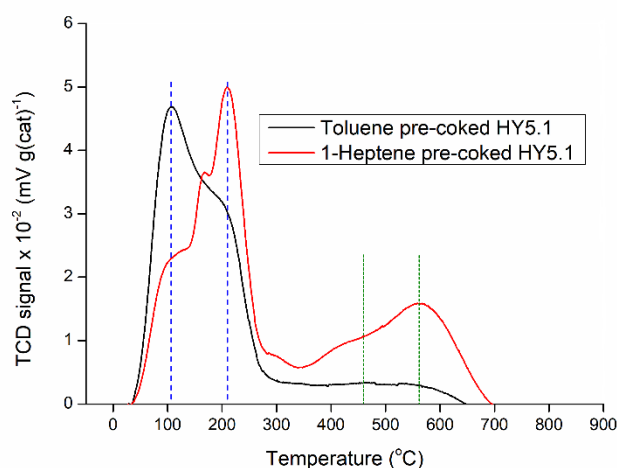


Figure 6.6. TPO profiles after toluene and 1-heptene pre-coking treatments over 0.5 gm of HY5.1 zeolite at 90 °C (toluene) and 80 °C (1-heptene) for 2 and 1 h, respectively.

The oxidation temperatures were shifted to either higher or lower values which indicates a change in the coke structure (Bauer and Karge, 2007). The oxidation temperature of the 1-heptene pre-coked samples is higher ~ 550 °C, which indicates a more ordered structure. Whereas the temperature of the HY5.1 pre-coked with toluene is lower ~ 470 °C which indicates a more disordered structure. These results confirm those which were obtained by the TGA and elemental analysis.

Figure 6.7 explains the TPO profile of HY30 pre-coked with toluene. It is noted that there are also three peaks, however, they appear at various oxidation temperatures. The first peak is at ~ 100 °C and indicates physisorbed water, whereas, the second and third peaks appear at ~ 350 and ~ 620 °C and represent amorphous carbon and structurally order coke, respectively (Choudhary et al., 1997).

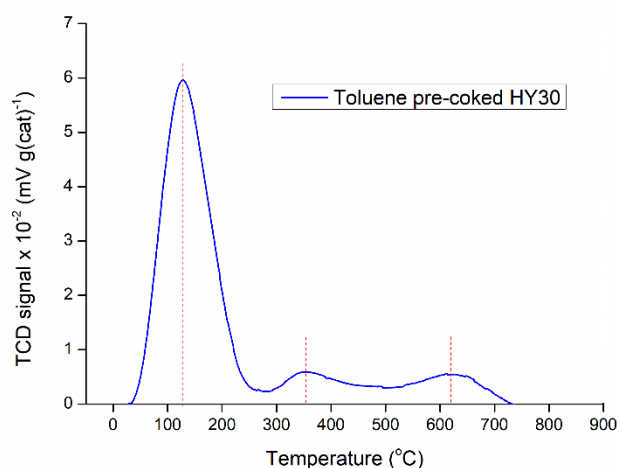
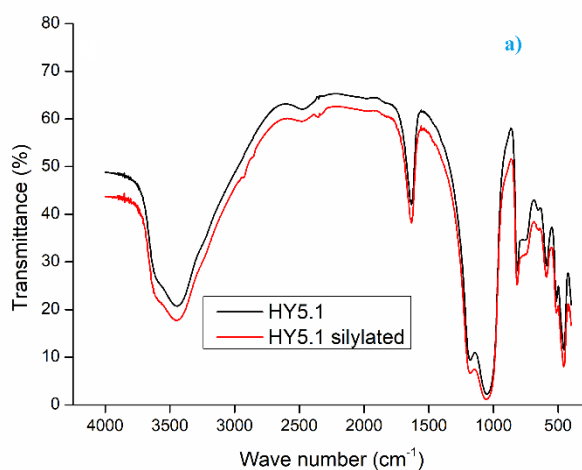


Figure 6.7. TPO profiles after toluene pre-coking treatments over 0.5 gm of HY30 zeolite at 90 °C for 2 h.

6.3.1.7 FTIR results

Figure 6.8 shows the FTIR spectra of fresh and silylated HY30 zeolite samples. The FTIR bands of 2960-2800 cm⁻¹ reveal a new branch of CH stretching absorption as a result of Si(OCH₃)₄ deposition. Similar results were obtained by Zhang et al. (2006). The peaks at 890-870 cm⁻¹ are a result of Si-C bonding. This result is in agreement with that obtained in earlier studies by Shewale et al. (2008) and Bhagat and Rao (2006).



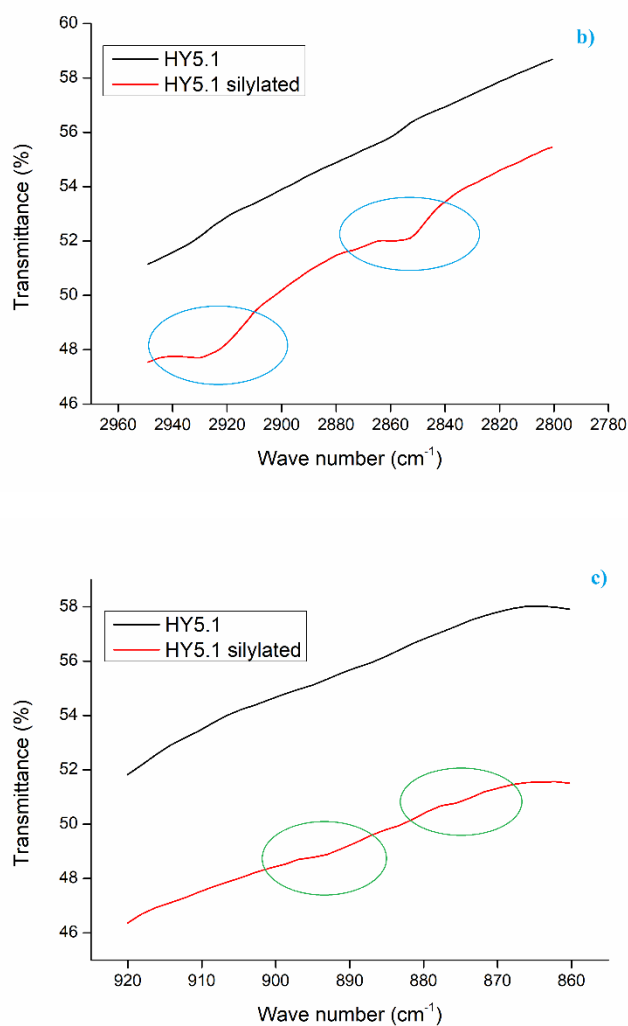


Figure 6.8. The FTIR spectra in the $\nu(\text{CH})$ region for fresh and silylated HY5.1 zeolite catalysts at a) 4000-400 cm^{-1} ; b) 2950-2800 cm^{-1} and c) 920-860 cm^{-1} .

FTIR spectra of fresh and silylated zeolite catalysts have been deconvoluted into three Gaussian peaks using Origin software (OriginPro 8.5.1) according to Niwa et al. (1984). The deconvolution is shown in Figure 6.9 at the region between 4000-2600 cm^{-1} for both fresh and modified zeolite samples that are shown above.

The deposition of $\text{Si}(\text{OCH}_3)_4$ had little effect on the hydroxyl bridging groups $\sim 3610 \text{ cm}^{-1}$ in the HY5.1 silylated zeolite as shown in Figure 6.9 The band of hydroxyl bridging groups $\sim 3610 \text{ cm}^{-1}$ was decreased after the silylation modification. The same result was obtained by Jiang et al. (2009).

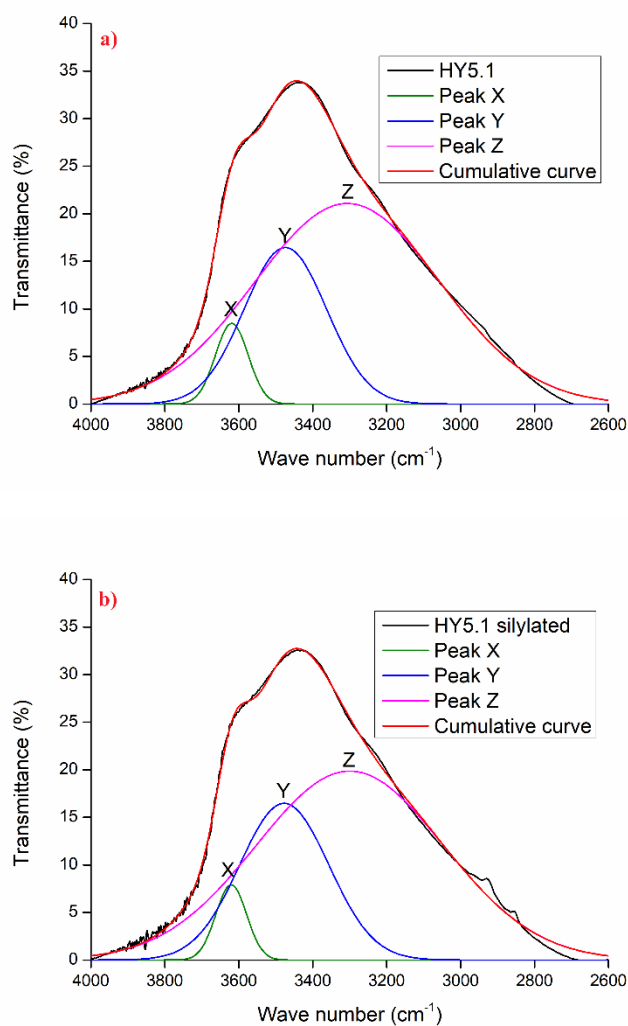


Figure 6.9. Peak deconvolution of FTIR spectra in the $\nu(\text{CH})$ region for zeolite catalysts of a) HY5.1 and b) HY5.1 silylated.

6.3.2 Catalytic activity measurements

6.3.2.1 Silylation treatment

Alkylation of toluene with 1-heptene was performed over HY5.1 and HY30 silylated using a BR (as described in Section 4.3.1) and a FBR (as shown in Section 4.3.2). The same operation conditions that were used in Chapter 5 are employed during the present work. For the BR; 90 °C, atmospheric pressure, a reaction time of 120 min, a toluene to 1-heptene ratio of 3 and 0.25 g of zeolite, while the FBR worked at: 90 °C, atmospheric pressure, 240 min TOS, toluene to 1-heptene ratio of 8, 0.5 g of zeolite and a 30 ml min⁻¹ flowrate of nitrogen. The steps taken for silylation treatment were illustrated previously in Section 4.5.3.

Through silylation treatment; two hypotheses were taken into account:

- A) Silylation acts to passivate some of the external acid sites to decrease the production of undesired products, such as olefin dimerisation and oligomerisation;
- B) Silylation acts to narrow the pore size either through the presence of water which is formed as a result of TEOS decomposition or by the penetration of some silicon molecules into the cavities of the HY zeolite.

Conducting the silylation modification at the present operating conditions (temperature, type of solvent, number of cycles and the amount of TEOS) helped with the success of this treatment. When using the non-polar *n*-hexane, the hexane covered the external surface of the HY zeolite, and $\text{Si}(\text{OC}_2\text{H}_5)_4$ was able to adsorb and decompose on the acid sites of the external surface. However, the polar water molecules were adsorbed preferentially onto the acid sites on the external surface and cover the surface, meaning the $\text{Si}(\text{OC}_2\text{H}_5)_4$ had to compete with water molecules for space to adsorb onto the acid sites (Weber et al., 1998). Therefore, the presence of non-polar molecules (*n*-hexane) allowed the decomposition of $\text{Si}(\text{OC}_2\text{H}_5)_4$. Moreover, the choice of a low temperature (ambient temperature) inhibited the formation of water *via* ethanol dehydration, which catalyses the deposition reaction. Multi deposition cycles were necessary to confirm the occurrence of silylation because a single deposition cycle in a liquid phase system did not allow for the removal of the TEOS decomposition species, such as ethanol. The molar ratio of TEOS to *n*-hexane was maintained at 1:250 and the weight ratio of TEOS to HY zeolite was ~12 %. The sponge like pores coating was difficult to obtain because the weight ratio of TEOS to HY zeolite was much less than 90% (Xia et al., 2017). Moreover, the low amount of TEOS prevented or reduced the physisorption of the material onto the zeolite catalyst especially at low temperatures, which may be polymerised the TEOS during calcination. These results are similar to those obtained by Weber *et al.* (2000). In addition, all the previous characterisation techniques such as TPD, FTIR and nitrogen adsorption indicate that silylation treatment is successful after three cycles.

Figure 6.10 shows a comparison between the fresh and silylated HY5.1 using a BR at a reaction time of 120 min. It explains that the HY5.1 silylated zeolite has approximately the same activity as the fresh sample, at ~88 %. In addition,

Figure 6.11 and Figure 6.12 illustrate the conversion of 1-heptene achieved by employing the fresh and silylated HY5.1 and HY30 and using the FBR. Despite the fact that the acidity decreased after the silylation modification, the conversion of 1-heptene for both HY5.1 and HY30 zeolites seem approximately constant or only slightly changed. This could be because the bulky silylating reagent acts to cover the external acid sites which are not responsible for this reaction (non-selective acid sites), while, the remaining acid sites that are located on the internal surface and at the pore mouth tried to recompense this shortfall value in acidity.

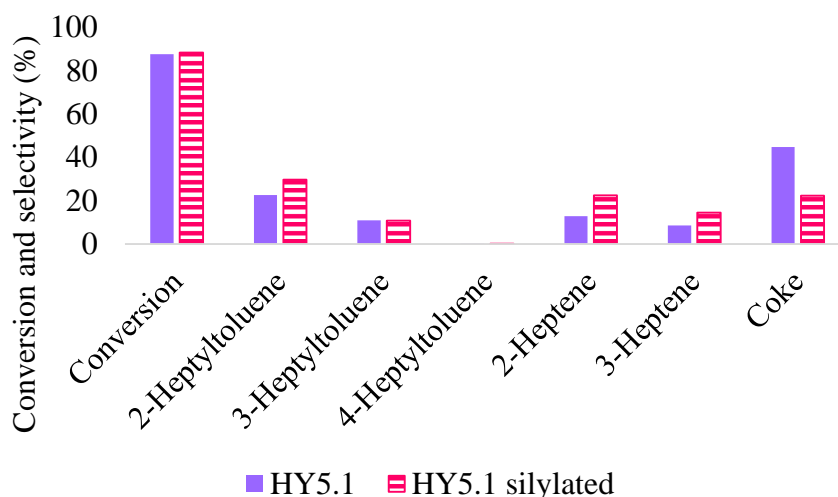


Figure 6.10. Conversion of 1-heptene and selectivity to various reaction products during toluene alkylation with 1-heptene at 90 °C, atmospheric pressure, 0.25 g HY5.1 and silylated HY5.1 zeolite, reaction time of 120 min, T: H ratio is 3: 1 and using BR.

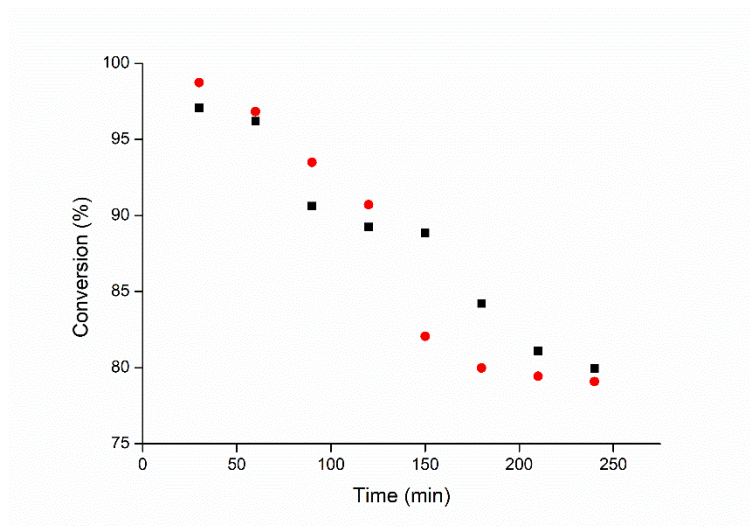


Figure 6.11. Influence of TOS on 1-heptene conversion during toluene alkylation with 1-heptene at 90 °C, atmospheric pressure, 0.5 g HY5.1 (■) and silylated HY5.1 (●) zeolite, TOS of 240 min, T: H ratio is 8: 1, WHSV of 17 h⁻¹, 30 ml min⁻¹ of N₂ flowrate and using FBR.

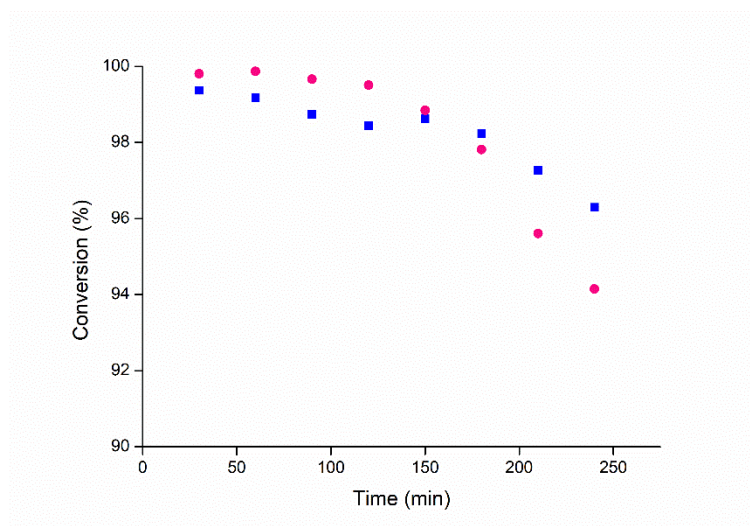


Figure 6.12. Influence of TOS on 1-heptene conversion during toluene alkylation with 1-heptene at 90 °C, atmospheric pressure, 0.5 g HY30 (■) and silylated HY30 (●) zeolite, TOS of 240 min, T: H ratio is 8: 1, WHSV of 17 h⁻¹, 30 ml min⁻¹ of N₂ flowrate and using FBR.

Figure 6.10 shows the selectivity of 2-heptyltoluene increased from ~23 % to ~30 % for the fresh HY5.1 and its silylated form. Comparing the 2-heptyltoluene selectivity of fresh and silylated HY5.1 and HY30 zeolites using the FBR achieves approximately the same level of conversion, ~97 % and ~98 %, respectively. Figure 6.13 and Figure 6.14 show the selectivity was ~27 % for HY5.1 while it became ~34 % after the silylation treatment, whereas, for the fresh HY30, it was ~31 % and increased

to ~35 % for silylated HY30. This increase in the 2-heptyltoluene selectivity could perhaps because the size distribution of mesopores was increased for the three samples after silylation treatment, as depicted in Section 6.3.1.3.

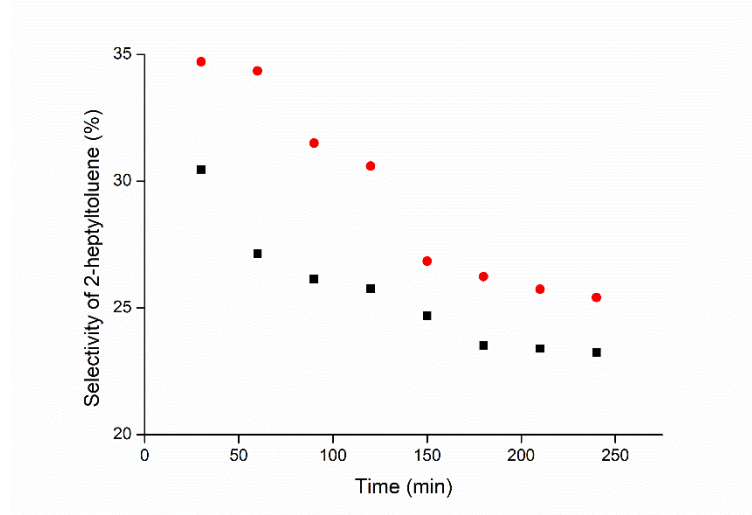


Figure 6.13. Influence of TOS on selectivity of 2-heptyltoluene during toluene alkylation with 1-heptene at 90 °C, atmospheric pressure, 0.5 g HY5.1 (■) and silylated HY5.1 (●) zeolite, TOS of 240 min, T: H ratio is 8: 1, WHSV of 17 h⁻¹, 30 ml min⁻¹ of N₂ flowrate and using FBR.

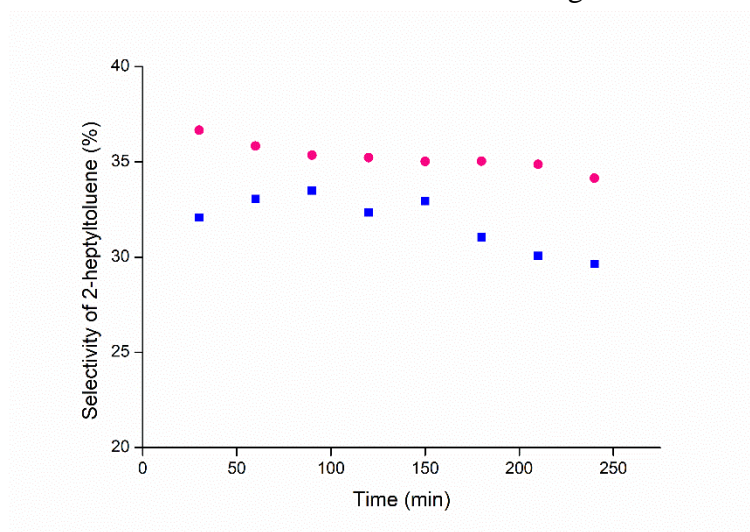


Figure 6.14. Influence of TOS on selectivity of 2-heptyltoluene during toluene alkylation with 1-heptene at 90 °C, atmospheric pressure, 0.5 g HY30 (■) and silylated HY30 (●) zeolite, TOS of 240 min, T: H ratio is 8: 1, WHSV of 17 h⁻¹, 30 ml min⁻¹ of N₂ flowrate and using FBR.

Figure 6.15 and Figure 6.16 show the selectivity of coke for the fresh and silylated HY5.1 and HY30, respectively. Obviously, the coke selectivity decreased after the silylation treatment for both the two samples compared with the fresh

samples. As shown above, the comparison was performed at the same level of 1-heptene conversion. The selectivity of coke was ~44 % for the fresh HY5.1 and it reduced to ~32 % after silylation treatment, whereas, it was ~46 % for the parent HY30 and it decreased to ~41 % after the modification. The main reason for this reduction in the selectivity of coke may be ascribed to either the decrease in the acidity as a result of bulky TEOS deposition which leads to a reduction in the number of side reactions (as shown in Section 6.3.1.2) or as a result of decreasing the surface area, pore volume and micropore size which effects the desorption of undesired products from the pores or cavities of the zeolite catalysts, as explained in Section 6.3.1.3.

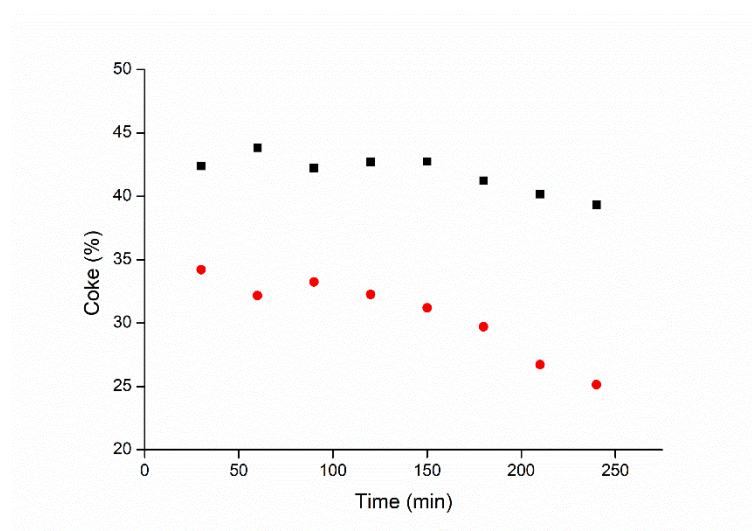


Figure 6.15. Influence of TOS on selectivity of coke during toluene alkylation with 1-heptene at 90 °C, atmospheric pressure, 0.5 g HY5.1 (■) and silylated HY5.1 (●) zeolite, TOS of 240 min, T: H ratio is 8: 1, WHSV of 17 h⁻¹, 30 ml min⁻¹ of N₂ flowrate and using FBR.

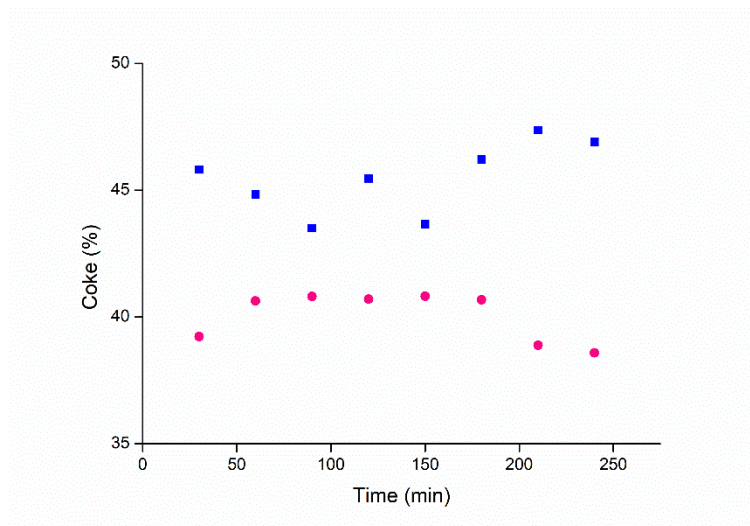


Figure 6.16. Influence of TOS on selectivity of coke during toluene alkylation with 1-heptene at 90 °C, atmospheric pressure, 0.5 g HY30 (■) and silylated HY30 (●) zeolite, TOS of 240 min, T: H ratio is 8: 1, WHSV of 17 h⁻¹, 30 ml min⁻¹ of N₂ flowrate and using FBR.

6.3.2.2 Pre-coking modification

Toluene alkylation with 1-heptene was performed over the HY5.1 and HY30 pre-coked with toluene and 1-heptene as a coke pre-cursor using the FBR (which is described previously in Section 4.3.2). The operation conditions of the alkylation reaction which have been used in this work are the same conditions which were used in Chapter 5; 90 °C, atmospheric pressure, 240 min TOS, toluene to 1-heptene ratio of 8, 0.5 g of zeolite and a nitrogen flowrate of 30 ml min⁻¹.

Through pre-coking with individual reactant species, two hypotheses were taken into account:

- i) The coke pre-cursor deposits play a positive role when they are either closed or non-selective acid sites that are located on the external surface or act as active sites at the pore mouth thereby enhancing the selectivity to heptyltoluene;
- ii) 1-heptene is the main source of zeolite deactivation.

As elucidated in Section 5.4.1.2, the alkylation of toluene with 1-heptene over fresh HY5.1 and HY30 at the operation conditions which given above explained that the HY30 was more stable and gave a higher 1-heptene conversion and 2- heptyltoluene selectivity compared with HY5.1. The coke selectivity was achieved

during the first moments of the reaction and did not change significantly with increasing the TOS. Several factors contributed to the rapid formation of the coke, such as; high acidity that acts to provide a suitable environment for the coke to accumulate and/or diffusional limitation which occurs as a result of forming some bulky molecules inside or at the pore openings thereby acting to block these pores.

Figure 6.17 and Figure 6.18 show the conversion of 1-heptene as a function of TOS for the fresh HY5.1 and HY30 catalyst and the catalysts pre-coked with either toluene or 1-heptene, respectively.

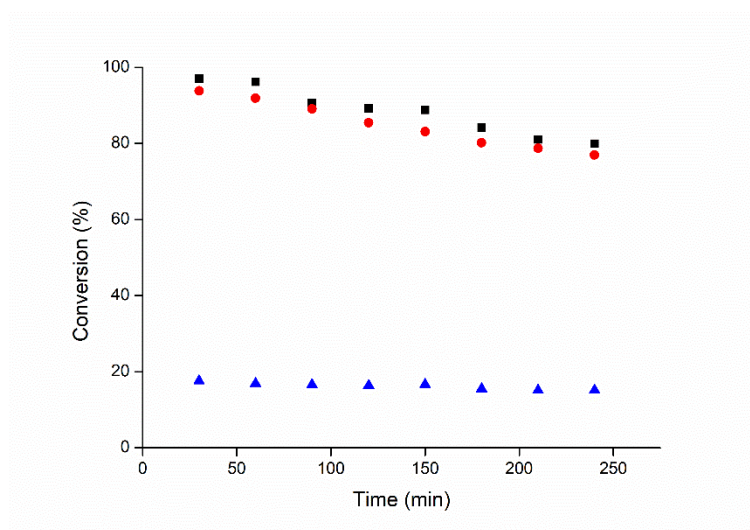


Figure 6.17. Effect of TOS on 1-heptene conversion during toluene alkylation with 1-heptene at 90 °C, atmospheric pressure, 0.5 g fresh HY5.1 (■), HY5.1 pre-coked with toluene (●) and HY5.1 pre-coked with 1-heptene (▲), TOS of 240 min, T: H ratio is 8: 1, WHSV of 17 h⁻¹, 30 ml min⁻¹ of N₂ flowrate and using FBR.

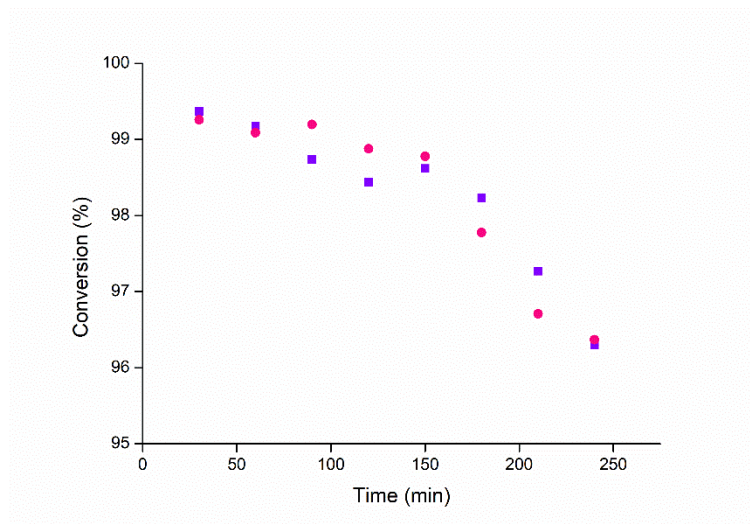


Figure 6.18. Influence of TOS on 1-heptene conversion during toluene alkylation with 1-heptene at 90 °C, atmospheric pressure, 0.5 g fresh HY30 (■) and HY30 pre-coked with toluene (●), TOS of 240 min, T: H ratio is 8: 1, WHSV of 17 h⁻¹, 30 ml min⁻¹ of N₂ flowrate and using FBR.

HY5.1 pre-coked with 1-heptene was prepared as illustrated earlier in Section 4.5.4. Two TOSs were employed during this pre-treatment; 15 min and 1 h. Surprisingly, both pre-coked zeolites have almost the same amount of coke and H/C ratio, as described in Section 6.3.1. The conversion of HY5.1 pre-coked with 1-heptene was ~18 % after the first 30 min TOS and decreased slightly with increasing the TOS until it reached ~15 % after 240 min TOS (Figure 6.17). The alkene pre-coked catalyst has approximately the same coke content ~10.4 % as the fresh catalyst after 240 min of reaction ~10 % (as shown in Section 6.3.1.4 and Section 6.4.2), however, while the fresh catalyst is still active at that time no appreciable conversion is achieved over the pre-coked catalyst. Conclusively, this percentage ~10.4 % of coke led to the deactivation of the zeolite catalyst instead of its modification. In a follow-up study, elemental analysis showed that the coke deposited during 1-heptene pre-coked HY5.1 has a H/C ratio of ~0.17 which indicates that this coke has a polyaromatic structure, as shown in Section 6.3.1.5. The TPO profile illustrates that the coke obtained by 1-heptene pre-coking is structurally ordered or has a graphitic-like carbon structure and that it is strongly bounded with the acid sites, which is similar to that obtained by the fresh post-reaction HY5.1 as depicted earlier in Section 5.6.4.

In contrast, pre-coking with toluene shows radically different behaviour. It is clear that the conversion of modified samples follows the same behavior as the fresh samples, as shown in Figure 6.17 and Figure 6.18. For the pre-coked HY5.1, the conversion slightly decreased compared with the fresh HY5.1, possibly because the acidity was reduced because the coke pre-cursor acted to block the apertures of the zeolite and/or deactivate some of the acid sites during the pre-coking modification, as shown in Section 6.3.1.2. Although the acidity of HY30 pre-coked with toluene decreased ~16 % compared with the fresh sample, the conversion of 1-heptene was still constant which could be because toluene molecules acted to cover some of the acid sites. However, the remaining acid sites are enough to enhance the zeolite activity.

Figure 6.19 and Figure 6.20 show the selectivity of 2-heptyltoluene as a function of TOS over the fresh and pre-coked HY5.1 and HY30, respectively. Selectivity of 3-heptyltoluene is explained in Figure 6.21 and Figure 6.22 for the parent and pre-coked HY5.1 and HY30, respectively.

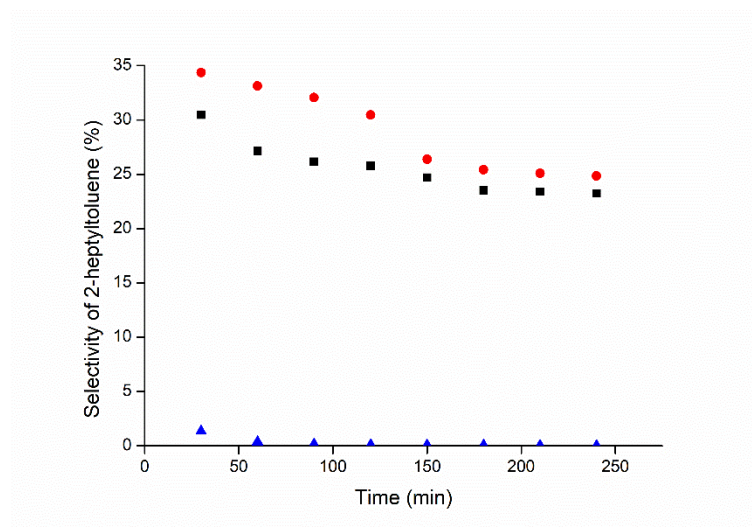


Figure 6.19. Effect of TOS on selectivity of 2-heptyltoluene during toluene alkylation with 1-heptene at 90 °C, atmospheric pressure, 0.5 g fresh HY5.1 (■), HY5.1 pre-coked with toluene (●) and HY5.1 pre-coked with 1-heptene (▲), TOS of 240 min, T: H ratio is 8: 1, WHSV of 17 h⁻¹, 30 ml min⁻¹ of N₂ flowrate and using FBR.

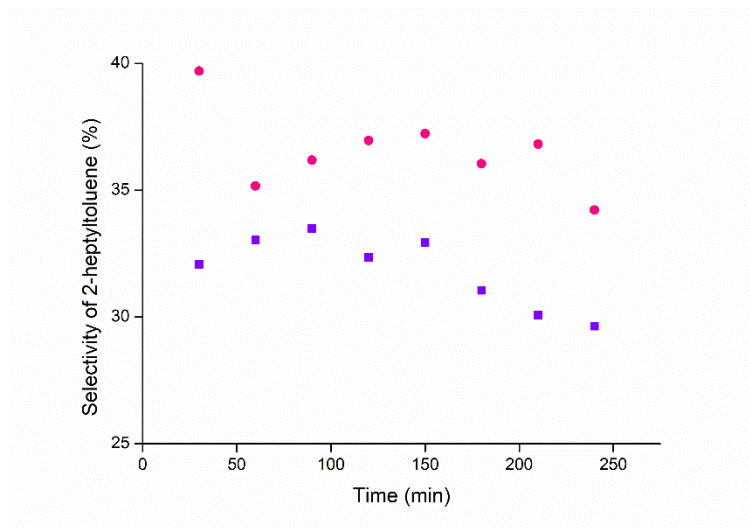


Figure 6.20. Influence of TOS on selectivity of 2-heptyltoluene during toluene alkylation with 1-heptene at 90 °C, atmospheric pressure, 0.5 g fresh HY30 (■) and HY30 pre-coked with toluene (●), TOS of 240 min, T: H ratio is 8: 1, WHSV of 17 h⁻¹, 30 ml min⁻¹ of N₂ flowrate and using FBR.

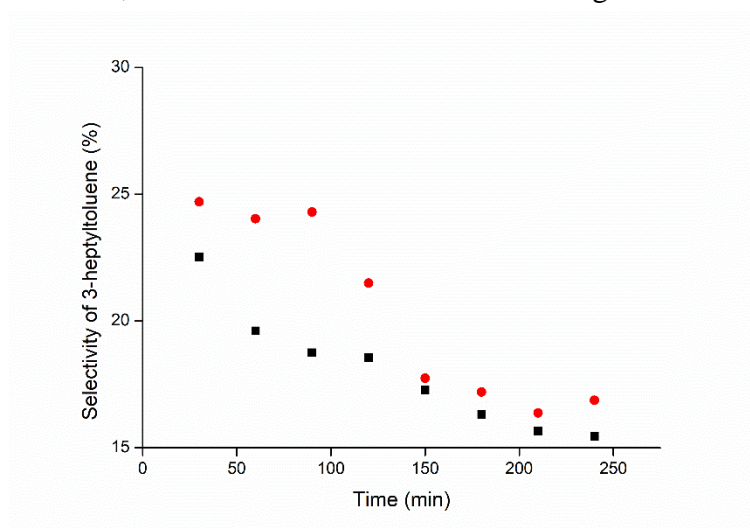


Figure 6.21. Effect of TOS on selectivity of 3-heptyltoluene during toluene alkylation with 1-heptene at 90 °C, atmospheric pressure, 0.5 g fresh HY5.1 (■) and HY5.1 pre-coked with toluene (●), TOS of 240 min, T: H ratio is 8: 1, WHSV of 17 h⁻¹, 30 ml min⁻¹ of N₂ flowrate and using FBR.

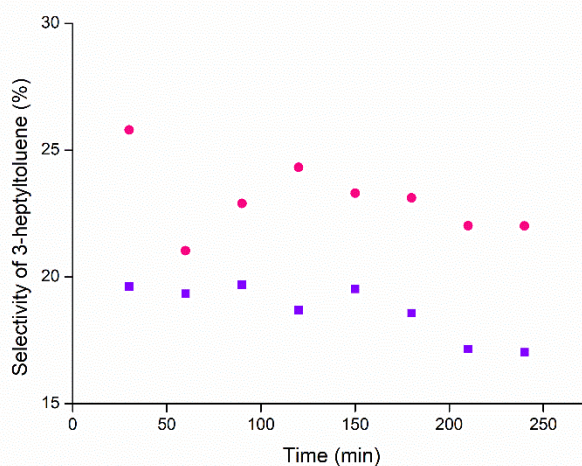


Figure 6.22. Influence of TOS on selectivity of 3-heptyltoluene during toluene alkylation with 1-heptene at 90 °C, atmospheric pressure, 0.5 g fresh HY30 (■) and HY30 pre-coked with toluene (●), TOS of 240 min, T: H ratio is 8: 1, WHSV of 17 h⁻¹, 30 ml min⁻¹ of N₂ flowrate and using FBR.

Figure 6.19 shows that the HY5.1 pre-coked with 1-heptene was not selective towards 2-heptyltoluene, probably owing to the fact that the coke pre-cursors act to block the pore openings and deactivate the acid sites during this modification.

The selectivity of 2-heptyltoluene was compared at the two different conversion levels of 1-heptene. At ~91 % conversion, the selectivity of the fresh HY5.1 was ~26 % however, it increased to ~33 % after toluene pre-coking treatment. At ~99 % conversion of 1-heptene, the 2-heptyltoluene selectivity of the fresh HY30 was ~33 % and ~39 % after toluene pre-coking modification. 3-heptyltoluene selectivity was compared at the same conversion as shown above ~99 %. The selectivity of the parent HY5.1 was ~19 % whilst it increased to ~24 % for the pre-coked sample. The selectivity of 3-heptyltoluene of the unmodified HY30 was ~19 % whereas, it increased to ~23 % after the pre-coking treatment with toluene. This is possibly because the pore size distribution, measured by BJH method, was slightly increased for the both samples, as described earlier in Section 6.3.1.3. Similar results were obtained by Bauer et al. (2007b) when they showed that pre-coked zeolite showed a slight increase in pore size distribution. Alternatively, perhaps the carbonaceous deposits during this treatment act either to deactivate non-selective acid sites or create new active sites when they interact with the protonic sites that are situated at the mouth opening of zeolite pores.

TGA data showed that toluene pre-coking deposits significant ~6 wt. % and ~5 wt. % coke on the HY5.1 and HY30 catalyst, respectively. However, as Figure 6.17 and Figure 6.18 show, this coke has no appreciable effect on the conversion of 1-heptene but does result in a slight enhancement in selectivity to the desired product, as shown in Figure 6.19, Figure 6.20, Figure 6.21 and Figure 6.22. Moreover, the results of elemental analysis showed the H/C ratio of HY5.1 and HY30 pre-coked with toluene were 0.67 and 0.24, respectively, as described in Section 6.3.1.5. These results indicate that the coke pre-cursors are polyaromatic however, HY5.1 showed low aromaticity. The TPO results were in agreement with both the results from the TGA and elemental analysis. It showed the structure of coke that formed on the HY5.1 was of the disordered carbonaceous form however, it was structurally ordered for HY30, as depicted in Section 6.3.1.6.

Coke selectivity is shown in Figure 6.23 and Figure 6.24 for unmodified and pre-coked HY5.1 and HY30, respectively. In Figure 6.23, the coke selectivity of HY5.1 pre-coked with 1-heptene is approximately constant at ~99 % for the duration of the reaction; it confirms the conclusion that was obtained for the selectivity of 2-heptyltoluene when it was shown that the pores were blocked by a coke pre-cursor and/or the acid sites were deactivated.

Generally, the coke selectivity of pre-coked samples with toluene is lower than that of fresh zeolite samples for both HY5.1 and HY30 (Figure 6.23 and Figure 6.24). The coke selectivity of HY5.1 pre-coked with toluene is lower than that of HY30 pre-coked with toluene. At a TOS of 180 min, the selectivity of coke for HY5.1 and HY30 pre-coked with toluene is ~38 % and ~46 %, respectively. This could be because the coke pre-cursors acted to cover most of the acid sites that are responsible for the side reactions thereby decreasing the coke accumulation.

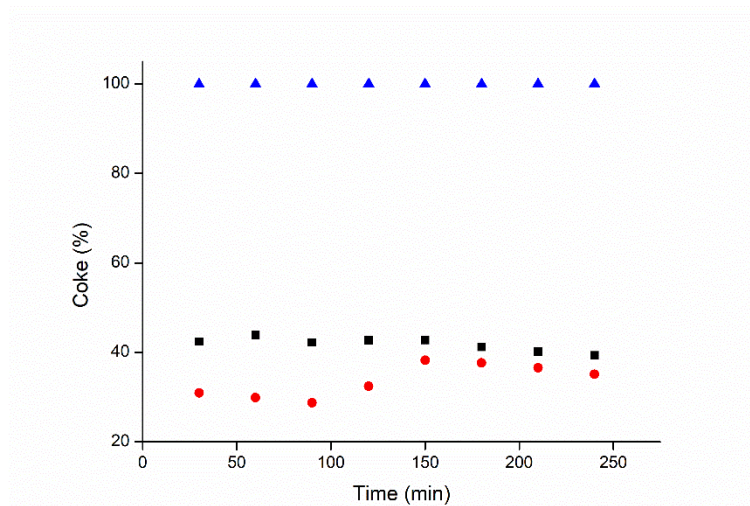


Figure 6.23. Effect of TOS on selectivity of coke during toluene alkylation with 1- heptene at 90 °C, atmospheric pressure, 0.5 g fresh HY5.1 (■), HY5.1 pre-coked with toluene (●) and HY5.1 pre-coked with 1-heptene (▲), TOS of 240 min, T: H ratio is 8: 1, WHSV of 17 h⁻¹, 30 ml min⁻¹ of N₂ flowrate and using FBR.

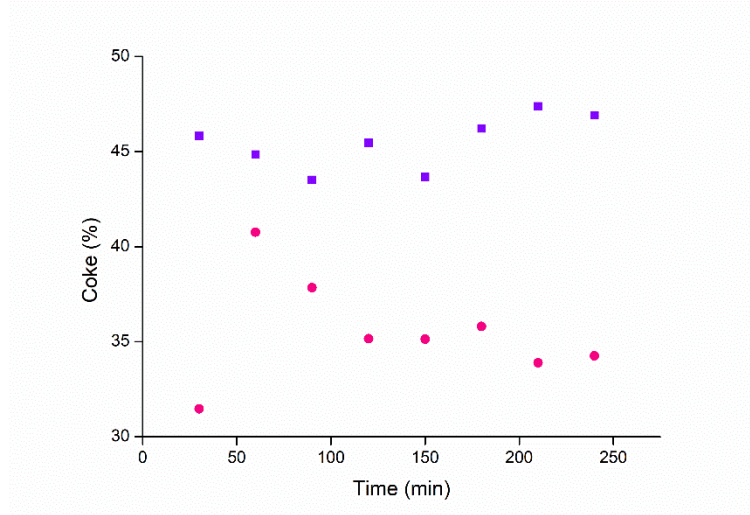


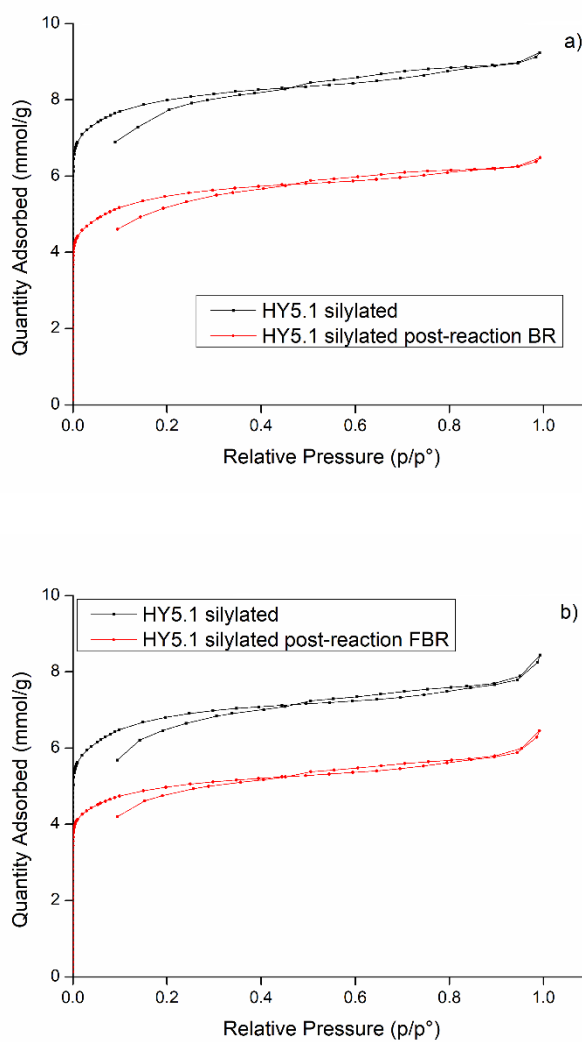
Figure 6.24. Influence of TOS on selectivity of coke during toluene alkylation with 1-heptene at 90 °C, atmospheric pressure, 0.5 g fresh HY30 (■) and HY30 pre-coked with toluene (●), TOS of 240 min, T: H ratio is 8: 1, WHSV of 17 h⁻¹, 30 ml min⁻¹ of N₂ flowrate and using FBR.

Based on the results above, it can be concluded, that the zeolites that have low Si/Al mole ratio (HY5.1) are more appropriate for the pre-coking treatment because they showed enhanced selectivity of the desired products and lower coke selectivity compared with those which have high a Si/Al mole ratio (HY30) (see section 6.3.1.1). In contrast, zeolites which have a high Si/Al mole ratio (HY30) showed higher conversion and higher stability than the zeolites which have low Si/Al mole ratio (HY5.1), as illustrated in Figure 6.17 and Figure 6.18.

6.4 Coke characterisation

6.4.1 Nitrogen adsorption-desorption results of post-reaction samples

Figure 6.25 displays the isotherm of silylated HY5.1, silylated HY30 and their post-reaction zeolite specimens using a BR and a FBR. All the spent silylated samples still have the same typical type of hysteresis loop; type I for silylated HY5.1 samples and type IV for the silylated HY30 sample. Table 6.6 shows there is a significant decrease in the total pore volume of the spent HY5.1 sample using the FBR compared with the fresh sample. However, there is only a slight reduction after the silylation treatment which means the TEOS molecules did not penetrate or act to close the pores of the zeolite catalyst.



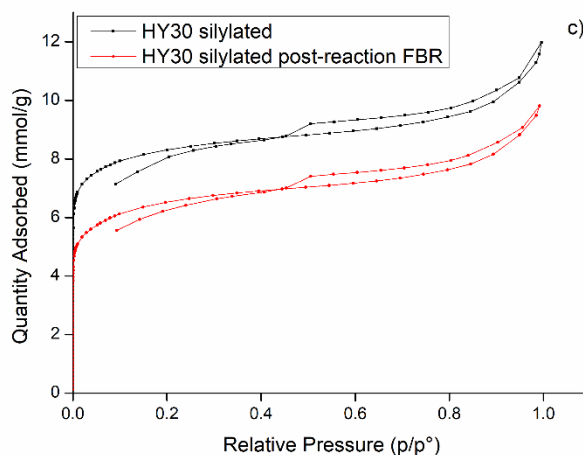


Figure 6.25. Nitrogen sorption isotherms of a) silylated and silylated spent HY5.1 using BR, b) silylated and silylated spent HY5.1 using FBR and c) silylated and silylated spent HY30 using FBR.

Figure 6.26 displays the isotherm of HY5.1 pre-coked with toluene and its spent zeolite samples. There is convergent behaviour for both the fresh and post-reaction samples. It can be seen in Table 6.6 that the BET surface area of HY5.1 pre-coked with toluene is not affected by the reaction and this indicates a reduced effect of the pore blocking owing to the toluene pre-coking modification. Furthermore, the surface area after reaction dropped about 83 % compared with the fresh zeolite; however, it is just 3 % after this modification.

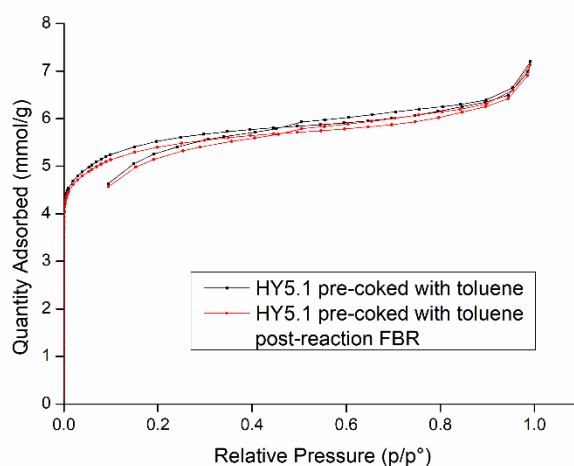


Figure 6.26. Nitrogen sorption isotherms of toluene pre-coked and toluene pre-coked spent HY5.1.

Table 6.6. The results of surface area of parent and modified zeolite catalysts.

Zeolite	S_{BET} ($\text{m}^2 \text{g}^{-1}$)	S_{mic} ($\text{m}^2 \text{g}^{-1}$)	S_{ext} ($\text{m}^2 \text{g}^{-1}$)	V_{tot} ($\text{cm}^3 \text{g}^{-1}$)	V_{mic} ($\text{cm}^3 \text{g}^{-1}$)	V_{meso} ($\text{cm}^3 \text{g}^{-1}$)	$d_{\text{p meso}}$ (Å) BJH	$d_{\text{p mic}}$ (Å) Horvath-Kowazoe
HY5.1 silylated (powder)	611.1	593.3	17.8	0.321	0.275	0.046	41.96	6.94
HY5.1 silylated post-reaction BR	406.8	388.1	18.6	0.225	0.191	0.034	37.97	6.97
HY5.1 silylated (pellet)	503.1	477.7	25.4	0.293	0.233	0.06	53.61	6.94
HY5.1 silylated post-reaction FBR	367.2	342.7	24.4	0.224	0.168	0.056	52.82	6.85
HY30 silylated (pellet)	610.3	551.4	58.8	0.405	0.268	0.137	64.63	7.48
HY30 silylated post-reaction FBR	486.4	428.8	57.6	0.341	0.207	0.134	63.32	7.42
HY5.1 pre-coked with toluene (pellet)	408.5	382.4	26.1	0.25	0.186	0.064	53.7	6.88
HY5.1 pre-coked with toluene post-reaction FBR	397.7	369.8	27.9	0.248	0.18	0.068	56.8	6.85
HY30 pre-coked with toluene (pellet)	377	316.5	60.5	0.283	0.151	0.132	58.78	7.45
HY30 pre-coked with toluene post-reaction FBR	112.4	71.6	40.8	0.127	0.028	0.099	65.24	15.21

Table 6.6 shows that the surface area and pore volume of the silylated samples are reduced compared with the unmodified samples, probably because some of zeolite pores were blocked during this modification.

The situation is different in HY30 pre-coked with toluene when compared with its post-reaction sample, as shown below in Figure 6.27. The hysteresis loop of HY30 pre-coked with toluene sample is typically type IV, relating to the existence of micro and mesopores. However, the hysteresis loop typically becomes a type I curve for the post-reaction, relating to the presence of micropores only.

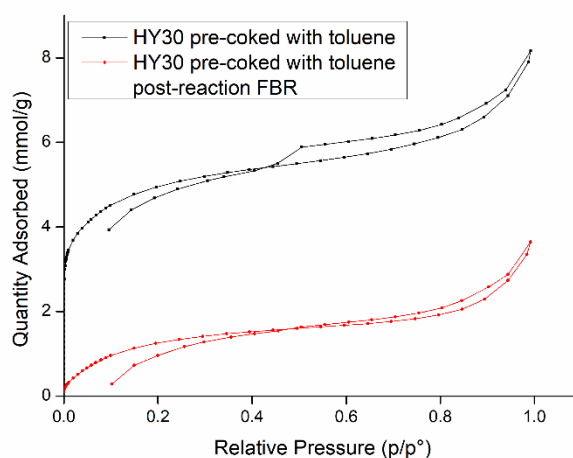


Figure 6.27. Nitrogen sorption isotherms of toluene pre-coked and toluene pre-coked spent HY30.

6.4.2 TGA results for the spent samples

Table 6.7, Figure 6.28 and Table 6.8 show the amount of coke formed over the silylated zeolites was decreased compared with unmodified zeolite catalysts. This could be because the TEOS acts to reduce the surface area, as shown in Section 6.4.1, and this acts to reduce the amount of coke.

Table 6.7. The coke % of fresh and silylated post-reaction HY5.1 zeolite catalysts during toluene alkylation with 1-heptene at 90 °C, atmospheric pressure, 0.25 g zeolite, reaction time of 120 min, T: H ratio is 3: 1 and using BR.

Zeolite	Reaction time (min)	Soft Coke%	Hard coke%	Total Coke%
Fresh HY5.1 post-reaction	120	2.2 ± 0.07	8.5 ± 0.14	10.7 ± 0.07
HY5.1 silylated post-reaction	120	2.2 ± 0.14	6.1 ± 0	8.3 ± 0.14

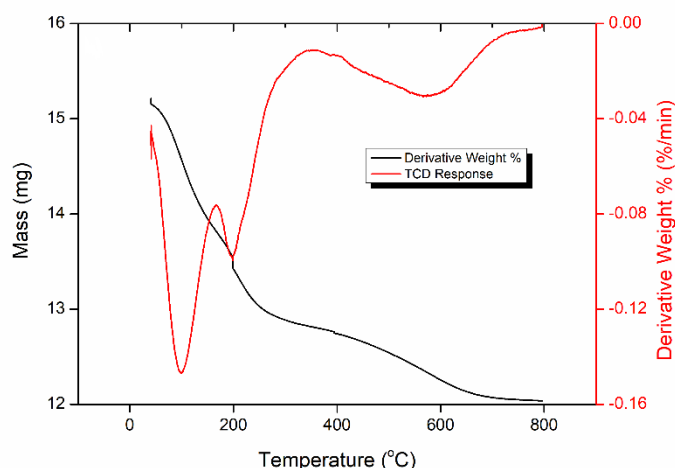


Figure 6.28. TGA and dTG profiles for HY5.1 silylated during toluene alkylation with 1-heptene at 90 °C, atmospheric pressure, 0.5 g zeolite, TOS of 240 min, T: H ratio is 8: 1, WHSV of 17 h⁻¹, 30 ml min⁻¹ of N₂ flowrate and using FBR.

Table 6.8. The percentage of coke content of fresh and silylated post-reaction HY5.1 and HY30 zeolite catalysts during toluene alkylation with 1-heptene at 90 °C, atmospheric pressure, 0.5 g zeolite, TOS of 240 min, T: H ratio is 8: 1, WHSV of 17 h⁻¹, 30 ml min⁻¹ of N₂ flowrate and using FBR.

Zeolite	Soft coke wt. % (200-400 °C)	Hard coke wt. % (400-800 °C)	Total coke wt. % (200-800 °C)
Fresh HY5.1 post-reaction (240 min)	2.3 ± 0.35	7.7 ± 0.28	10 ± 0.64
HY5.1 Silylated post-reaction (240 min)	3.3 ± 0.14	4.1 ± 0.07	7.4 ± 0.07
Fresh HY30 post-reaction (240 min)	1.8 ± 0.14	10 ± 0.07	11.8 ± 0.21
HY30 Silylated post-reaction (240 min)	2.1 ± 0.07	8 ± 0.21	10 ± 0.28

In general, both the above tables demonstrate that the hard coke is the main carbonaceous deposit formed during the alkylation reaction over all types of fresh zeolite. However, these amounts decrease after the silylation treatment and this is considered one of the main reasons which leads to the enhanced performance of the catalyst, as elucidated in Section 6.3.2.1.

Figure 6.29 and Table 6.9 details the coke content on the pre- and post-reaction of the fresh HY5.1, toluene pre-coked HY5.1, 1-heptene pre-coked HY5.1, HY30 and toluene pre-coked HY30. The net coke accumulated during the alkylation reaction over toluene pre-coked HY5.1 and HY30 decreased by ~50 % compared with that formed on the fresh zeolite during the same reaction and same conditions.

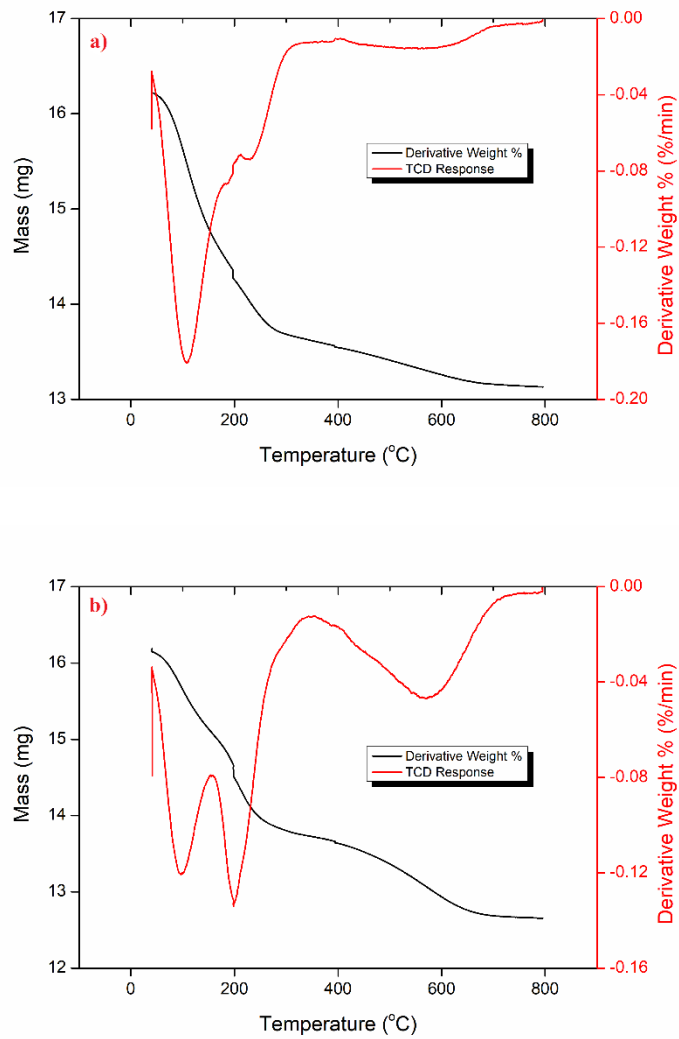


Figure 6.29. TGA and dTG profiles for a) HY5.1 toluene pre-coked at 90 °C and b) post-reaction HY5.1 toluene pre-coked during toluene alkylation with 1-heptene at 90 °C, atmospheric pressure, 0.5 g zeolite, TOS of 240 min, T: H ratio is 8: 1, WHSV of 17 h⁻¹, 30 ml min⁻¹ of N₂ flowrate and using FBR.

Table 6.9. TGA showing the coke % after pre-coking *via* toluene and 1-heptene over 0.5 gm of HY5.1 and HY30 zeolites at 90 °C (toluene) and 80 °C (1-heptene) for 2 and 1 h respectively.

Zeolite	Initial coke formed wt. % (200-800 °C)	Total coke formed wt. % (200-800 °C)	Net coke formed wt. % (200-800 °C)
Fresh HY5.1 post-reaction (240 min)	-	10 ± 0.64	10
Toluene pre-coked HY5.1 (120 min for pre-coking) post reaction (240 min)	5.9 ± 0.21	10.5 ± 0.56	4.6
1-heptene pre-coked HY (60 min for pre-coking) post-reaction (240 min)	11.3 ± 0	11.9 ± 0	0.6
Fresh HY30 post-reaction (240 min)	-	11.8 ± 0.21	11.8
Toluene pre-coked HY30 (120 min for pre-coking) post reaction (240 min)	4.7 ± 0	11.3 ± 0.07	6.6

Pre-coking with 1-heptene however, shows radically different behavior. The alkene pre-coked catalyst has slightly more coke content than the fresh catalyst after 240 min of reaction however, while the fresh catalyst is still active at that time no appreciable conversion is achieved over the pre-coked catalyst; it is not selective towards 2-heptyltoluene, as illustrated in 6.3.2.2.

6.4.3 Elemental analysis results for post-reaction samples

Figure 6.30 shows the percentage of the H/C mass ratio of the carbon deposits over the post reaction HY5.1, HY30 and their silylated forms using a BR and a FBR. They were determined *via* CHNS elemental analysis.

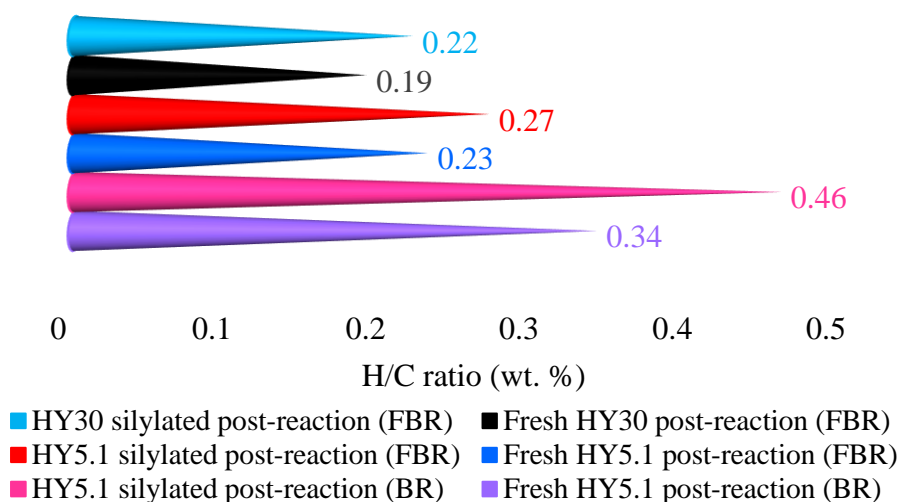


Figure 6.30. The H/C mass ratio obtained by the elemental analysis after silylation treatment of HY5.1 and HY30 zeolite catalysts during toluene alkylation with 1-heptene using BR and FBR.

It shows the H/C ratio of all silylated samples are higher than that of the fresh samples which means the structure of the coke after modification tends to be less hydrogen-deficient. These results confirm the results showing an increase in selectivity after silylation treatment from ~27 % to ~34 % for HY5.1 and from ~31 % to ~35 % for HY30, as shown in Section 6.3.2.1, and those from the TGA, as described in Section 6.4.2.

6.4.4 TPO results for the spent samples

Figure 6.31 shows the TPO profiles of spent HY5.1 and its silylated form, while Figure 6.32 displays the HY30 and silylated HY30 post-reaction during the alkylation of toluene with 1-heptene. These figures indicate a change in either the amount of coke, as shown in Figure 6.31, or a shift in the pyrolysis temperature to form a low ordered structure, as explained in Figure 6.32. These results confirm those in Section 6.3.2.1, where it was shown that an improvement in the desired product selectivity was achieved after the silylation modification from ~27 % to ~34 % for HY5.1 and from ~31 % to ~35 % for HY30. Moreover, they are in agreement with the results that were obtained by TGA, as explained in Section 6.4.2, and elemental analysis, as demonstrated in Section 6.4.3.

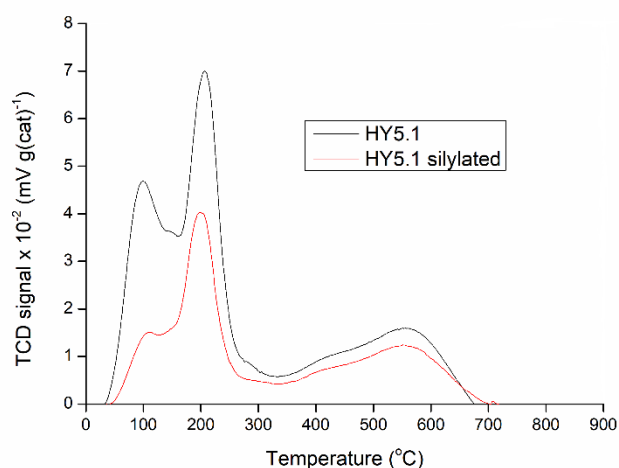


Figure 6.31. TPO profiles of the spent HY5.1 and its silylated during toluene alkylation with 1-heptene at 90 °C, atmospheric pressure, 0.5 g zeolite, TOS of 240 min, T: H ratio is 8: 1, WHSV of 17 h⁻¹, 30 ml min⁻¹ of N₂ flowrate and using FBR.

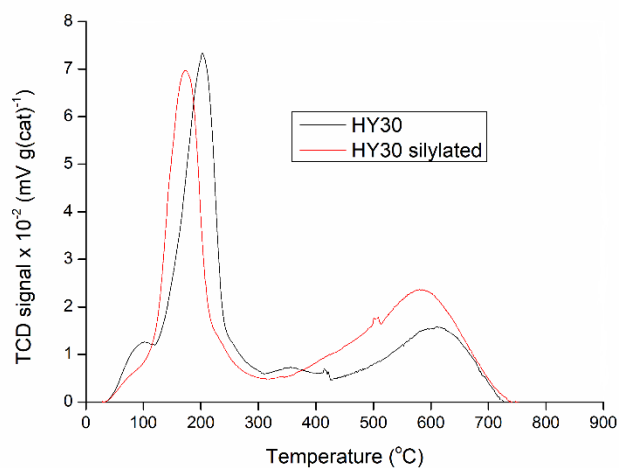


Figure 6.32. TPO profiles of the spent HY30 and its silylated during toluene alkylation with 1-heptene at 90 °C, atmospheric pressure, 0.5 g zeolite, TOS of 240 min, T: H ratio is 8: 1, WHSV of 17 h⁻¹, 30 ml min⁻¹ of N₂ flowrate and using FBR.

Figure 6.33 illustrates the reactivity profiles of HY5.1, toluene pre-coked and toluene pre-coked post-reaction. They have approximately the same pyrolysis temperature however, the amount of coke is different which means coke derived from the aromatic agent is much less than that form on the fresh HY5.1 zeolite and this could be played a positive role through the toluene alkylation with 1-heptene. This result supports those obtained in Section 6.3.2.2.

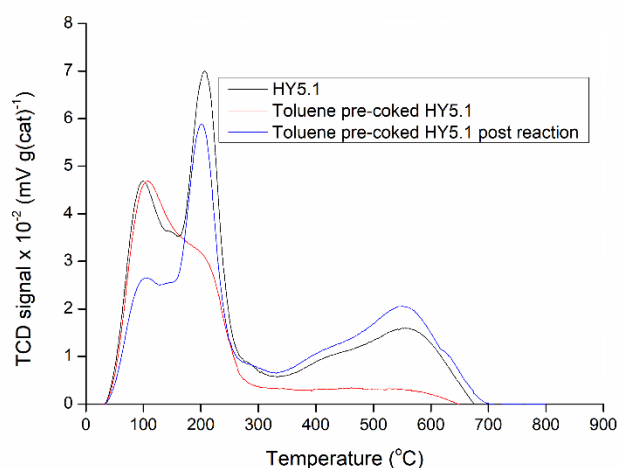


Figure 6.33. TPO profiles of the spent HY5.1, toluene pre-coked HY5.1 and toluene pre-coked HY5.1 post reaction during toluene alkylation with 1-heptene at 90 °C, atmospheric pressure, 0.5 g zeolite, TOS of 240 min, T: H ratio is 8: 1, WHSV of 17 h⁻¹, 30 ml min⁻¹ of N₂ flowrate and using FBR.

As demonstrated previously in Section 5.6.4, the overlap problem in the TPO peaks requires the use of an appropriate software to overcome this issue (Alonso-Morales et al., 2013). Therefore, the TPO profile of HY5.1 and its pre-coked zeolite samples were deconvoluted into six Gaussian peaks by employing Origin software (OriginPro 8.5.1), as displayed below.

Figure 6.34, Figure 6.35 and Figure 6.36 show the deconvolution of TPO profiles for HY5.1 post-reaction, toluene pre-coked HY5.1 and toluene pre-coked HY5.1 post-reaction. It can be remarked that the cumulative curve palpably conforms with the TPO curve which means that the deconvolution is acceptable.

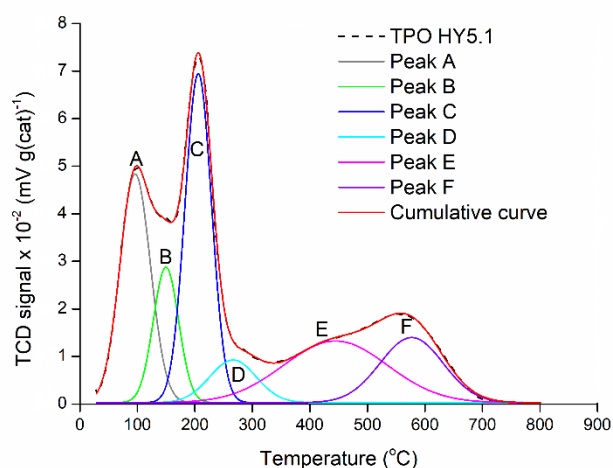


Figure 6.34. Peak deconvolution of TPO spectrum for spent HY5.1 during toluene alkylation with 1-heptene at 90 °C, atmospheric pressure, 0.5 g zeolite, TOS of 240 min, T: H ratio is 8: 1, WHSV of 17 h⁻¹, 30 ml min⁻¹ of N₂ flowrate and using FBR.

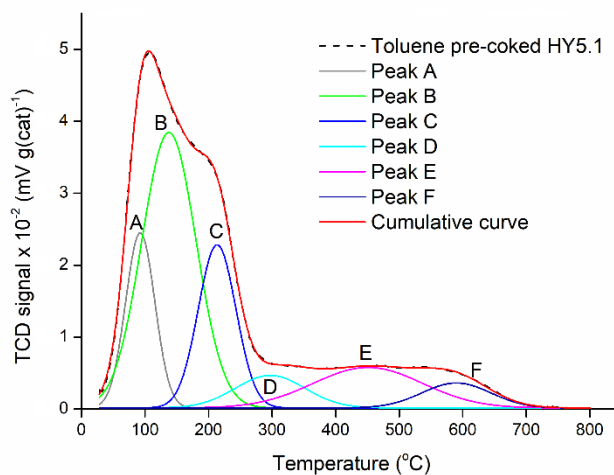


Figure 6.35. Peak deconvolution of TPO spectrum for toluene pre-coked of HY5.1 at 90 °C, atmospheric pressure, 0.5 g zeolite, TOS of 120 min, WHSV of 17 h⁻¹, 30 ml min⁻¹ of N₂ flowrate and using FBR.

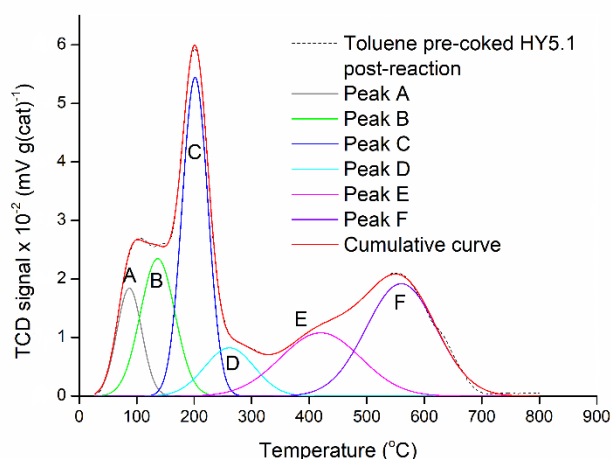


Figure 6.36. Peak deconvolution of TPO spectrum for spent toluene pre-coked of HY5.1 during toluene alkylation with 1-heptene at 90 °C, atmospheric pressure, 0.5 g zeolite, TOS of 240 min, T: H ratio is 8: 1, WHSV of 17 h⁻¹, 30 ml min⁻¹ of N₂ flowrate and using FBR.

Table 6.10 summarises the results of the fitted peak areas and maximum temperatures. It can be seen that the summation of C-F peaks is ~9.7, ~4 and ~9.4 for HY5.1, toluene pre-coked HY5.1 and toluene pre-coked HY5.1 post-reaction, respectively. These results are in agreement with those obtained by TGA, as described earlier in Section 6.4.2. In addition, the difference in the pyrolysis temperature between the spent sample of the toluene pre-coked HY5.1 compared with the spent sample of the fresh HY5.1 indicates a slight enhancement in the 2-heptytoluene selectivity after the pre-coking treatment from ~26 % to ~33 %. This difference in temperature also indicates that the coke derived from the aromatic reactant does not induce deactivation and may enhance selectivity.

Table 6.10. The fit peak areas and maximum temperature deconvoluted peaks for spent HY5.1, toluene pre-coked HY5.1 and toluene pre-coked HY5.1 post-reaction during toluene alkylation with 1-heptene at 90 °C, atmospheric pressure, 0.5 g zeolite, TOS of 240 min, T: H ratio is 8: 1, WHSV of 17 h⁻¹, 30 ml min⁻¹ of N₂ flowrate and using FBR.

Zeolite	Fit peak area (Maximum temperature °C)						Total
	A	B	C	D	E	F	
HY5.1	3.2 (96)	1.6 (150)	4 (206)	0.9 (266)	2.9 (445)	1.9 (577)	14.5
Toluene pre-coking HY5.1	1.4 (92)	4.1 (138)	1.7 (213)	0.6 (297)	1.2 (451)	0.5 (590)	9.5
Toluene pre-coking HY5.1 post-reaction	1 (87)	1.8 (136)	3.4 (201)	1 (261)	2.1 (420)	2.9 (560)	12.2

On the other hand, combining the TPO profile with derivative thermogravimetric (dTG) curve of spent HY5.1, toluene pre-coked HY5.1 and toluene pre-coked HY5.1 post-reaction (Figure 6.37, Figure 6.38 and Figure 6.39) illustrates that there is a good degree of agreement between these curves and this can be considered as a measure of the accuracy of both these characterisation techniques.

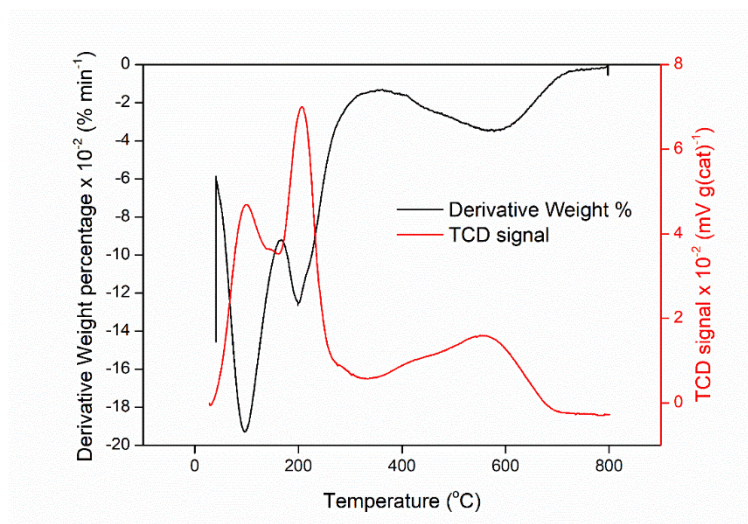


Figure 6.37. TPO and dTG profiles for HY5.1 post-reaction during toluene alkylation with 1-heptene at 90 °C, atmospheric pressure, 0.5 g zeolite, TOS of 240 min, T: H ratio is 8: 1, WHSV of 17 h⁻¹, 30 ml min⁻¹ of N₂ flowrate and using FBR.

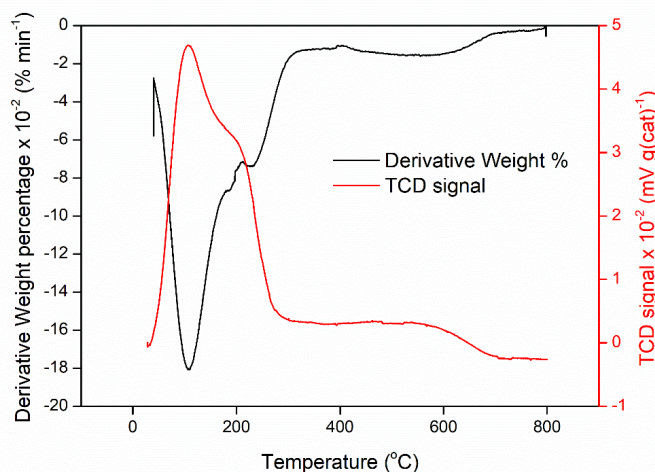


Figure 6.38. TPO and dTG profiles for toluene pre-coked HY5.1 during toluene alkylation with 1-heptene at 90 °C, atmospheric pressure, 0.5 g zeolite, TOS of 240 min, T: H ratio is 8: 1, WHSV of 17 h⁻¹, 30 ml min⁻¹ of N₂ flowrate and using FBR.

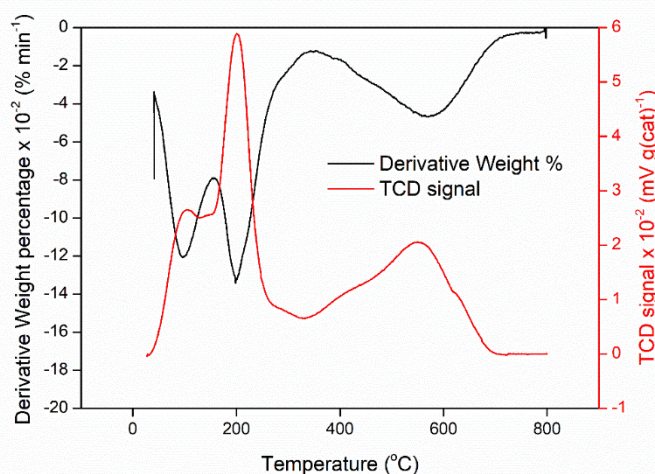
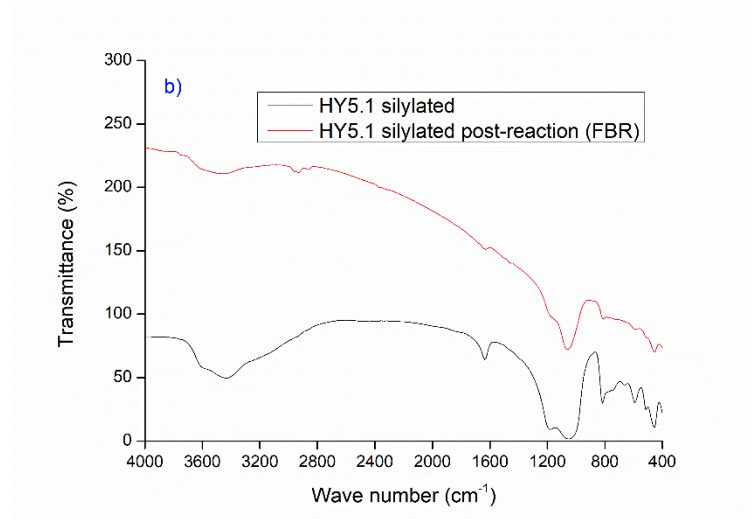
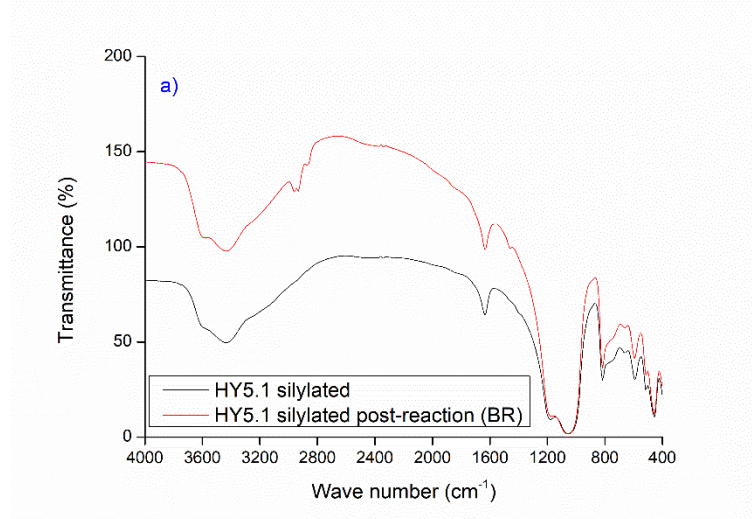


Figure 6.39. TPO and dTG profiles for toluene pre-coked HY5.1 post-reaction during toluene alkylation with 1-heptene at 90 °C, atmospheric pressure, 0.5 g zeolite, TOS of 240 min, T: H ratio is 8: 1, WHSV of 17 h⁻¹, 30 ml min⁻¹ of N₂ flowrate and using FBR.

6.4.5 FTIR spectroscopy results for the post-reaction samples

Figure 6.40 and Figure 6.41 show the FTIR spectra of silylated and pre-coked HY5.1 and HY30 zeolite samples using a BR and a FBR. The FTIR bands of 3000- 2800 cm⁻¹ displays a new branch of aliphatic coke species adsorbed on the catalyst surface whereas, the peaks at 2962-2955, 2870-2862 and 2931-2925 cm⁻¹ represent the asymmetric methyl vibration (aliphatic), the symmetric methyl vibration (aliphatic band) and the asymmetric aliphatic species but with methylene vibration, respectively. These results are in agreement with those that were obtained by Fan and

Watkinson (2006), Epelde *et al.* (2014). Moreover, the type of coke (aliphatic species) confirmed the conclusions given by Zhang *et al.* (2014) who reported that coke formed at low reaction temperatures is usually aliphatic.



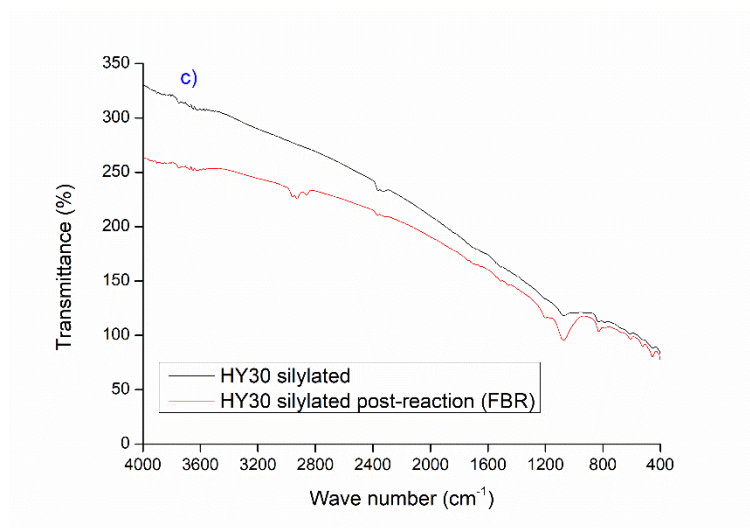
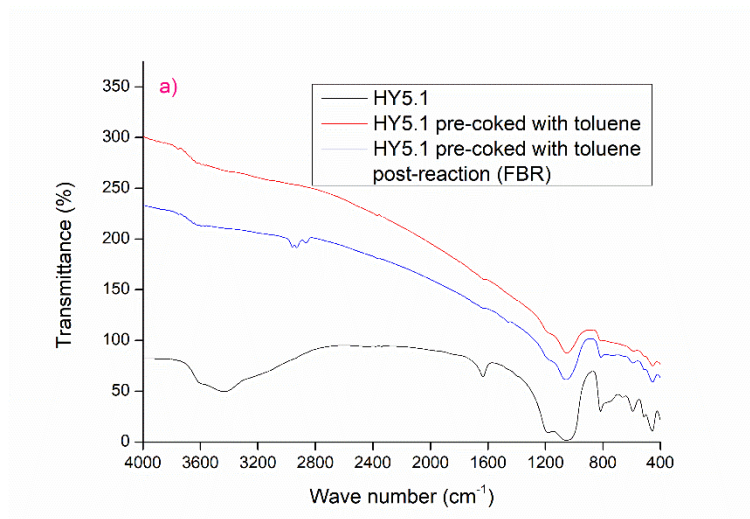


Figure 6.40. The FTIR spectra in the $\nu(\text{CH})$ region for silylated and silylated post-reaction zeolite catalysts of a) HY5.1 (powder); b) HY5.1 (pellet) and c) HY30 (pellet).



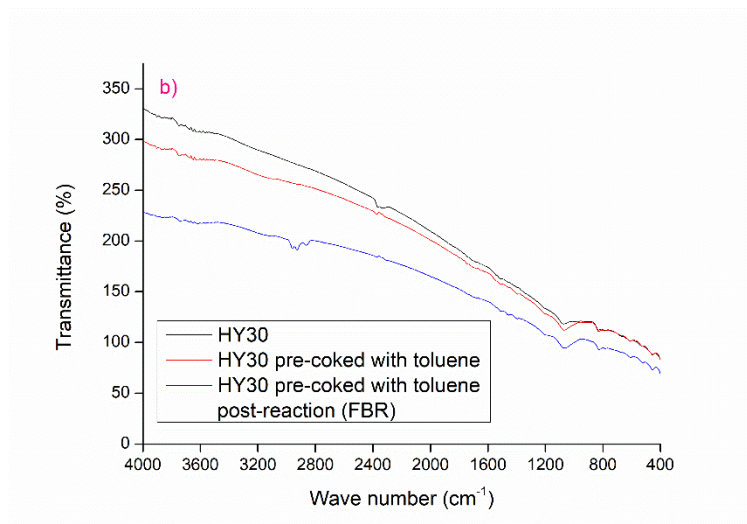
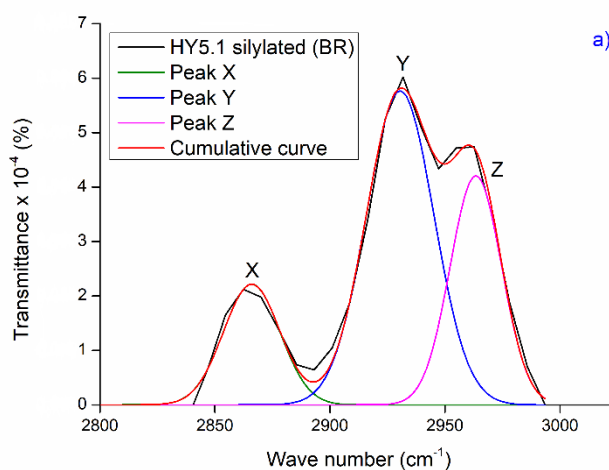


Figure 6.41. The FTIR spectra in the $\nu(\text{CH})$ region for fresh, toluene pre-coked and toluene pre-coked post-reaction zeolite catalysts of a) HY5.1 (pellet) and b) HY30 (pellet).

Origin software (OriginPro 8.5.1) was used to deconvolute the FTIR spectrum of post-reaction zeolite catalyst into three Gaussian peaks (Castaño et al., 2011). Figure 6.42 and Figure 6.43 show the peak deconvolution of silylated and pre-coked spent zeolite at the region between 2800-3000 cm^{-1} for all the samples that were explained above.



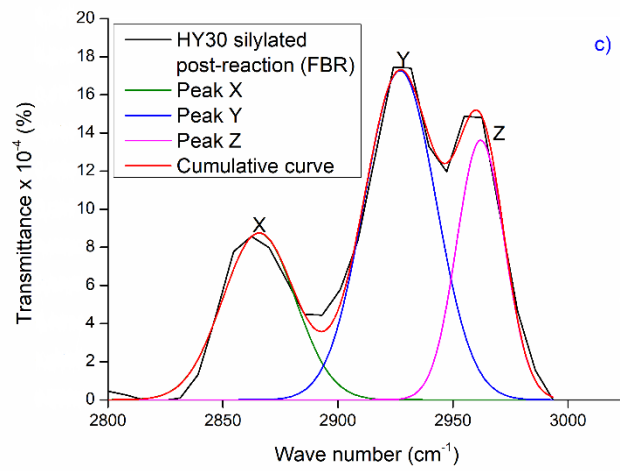
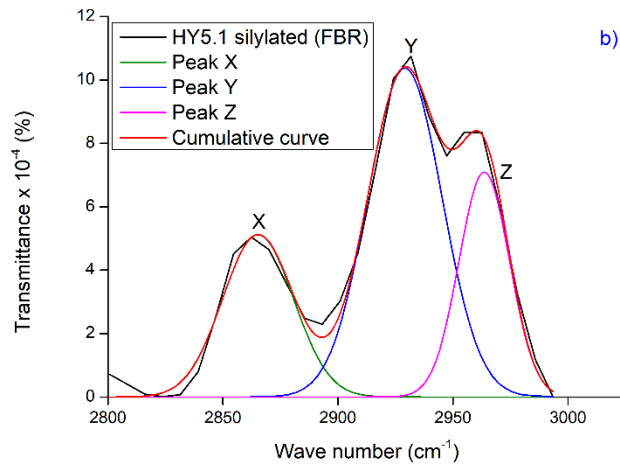
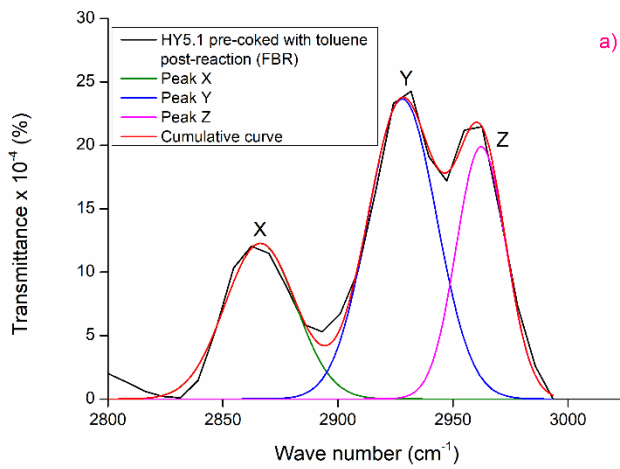


Figure 6.42. Peak deconvolution of FTIR spectra in the $\nu(\text{CH})$ region for silylated spent zeolite catalysts of a) HY5.1 (powder); b) HY5.1 (pellet) and c) HY30 (pellet).



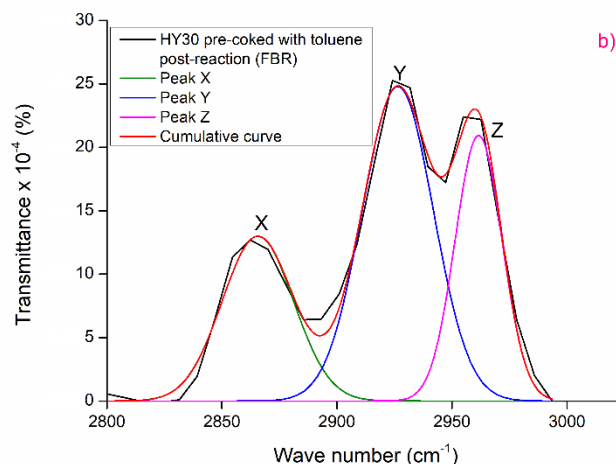


Figure 6.43. Peak deconvolution of FTIR spectra in the $\nu(\text{CH})$ region for toluene pre-coked post-reaction zeolite catalysts of a) HY5.1 (pellet) and b) HY30 (pellet).

Figure 6.44 summarises the results of peak areas at the three different bands. The band of $\nu_{\text{as}} \text{CH}_3$ aliphatic species $\sim 2870 \text{ cm}^{-1}$ was the lowest, whereas the highest appeared at $\sim 2930 \text{ cm}^{-1}$ and refers to $\nu_{\text{as}} \text{CH}_2$ aliphatic species. This indicates that the aliphatic chains of the coke pre-cursor were either naphthenic or longer (Castaño et al., 2011).

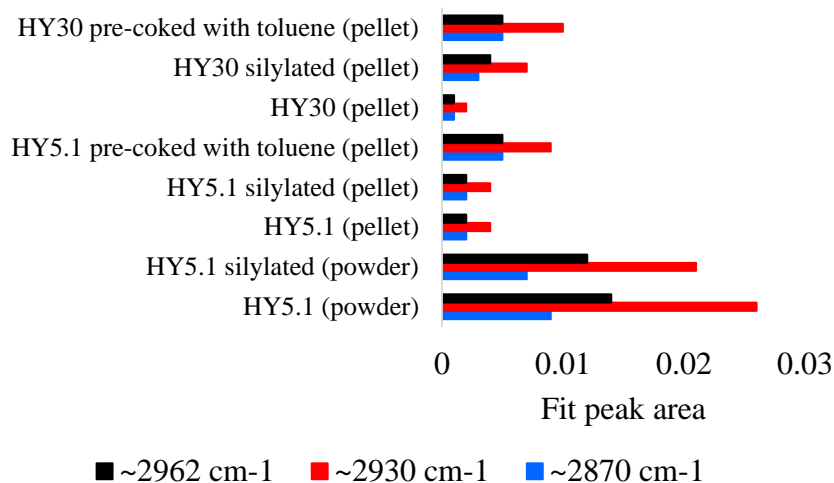


Figure 6.44. The fit peak areas of deconvoluted peaks of FTIR spectra in the $\nu(\text{CH})$ region for fresh, silylated and toluene pre-coked of HY5.1 (powder); HY5.1 (pellet) and HY30 (pellet).

As demonstrated previously in Section 5.6.5, the intensity of the coke for the spent sample that was obtained from the BR was higher than that of FBR. Moreover, the intensities of the modified sample using the FBR were increased compared with the fresh sample which indicates that the nature of the coke was unsaturated (Castaño et al., 2011).

6.5 Conclusions

In this chapter, the influence of the silylation modification as well as pre-coking treatment on the catalytic performance of HY5.1 and HY30 in the toluene alkylation with 1-heptene have been studied. For the silylation treatment, TEOS has been used as a silylation agent while, 1-heptene and toluene were employed as coke pre-cursors during the pre-coking modification.

Zeolite modification by either pre-coking or silylation acts to increase the shape selectivity which contributes to the passivation of unselective catalytic centres. In addition, these modifications work to decrease the diffusion of unwanted products into or out of the zeolite pores through the narrowing of these pores thereby enhancing the selectivity. Generally, pre-coking treatment suffers from activity diminution more than the silylation modification which produces more stable samples than the pre-coking modification. The zeolites which have a lower Si/Al mole ratio (HY5.1) are more appropriate for aromatic pre-coking than those which have a higher Si/Al mole ratio (HY30); they showed an enhancement in the selectivity of the desired products from ~26 % to ~33 % for HY5.1 and from ~33 % to ~39 % for HY30 and a reduction in the coke formation from ~44 % to ~38 % for HY5.1 and from ~47 % to ~46 % for HY30.

TGA results of silylated samples were lower than the fresh samples of the same zeolite catalyst which means that this modification works to cover the external acid sites that are responsible for the production of undesired products and narrows the pores which occurs as a result of TEOS decomposition and prevents the undesired products entering the zeolite pores. Moreover, the elemental analysis and TPO results showed the silylated samples tend to be less aromatic compared with the parent zeolites. The results explain the improved 2-heptyltoluene selectivity after the silylation treatment.

By employing toluene as the pre-coking agent, there was a moderate enhancement in 2-heptyltoluene selectivity from ~26 % to ~33 % for HY5.1 and from ~33 % to ~39 % for HY30. It can be deduced that 1-heptene is the main coke precursor that leads to deactivation of the catalyst through toluene alkylation with 1-heptene. This is because the coke precursor which formed on HY5.1 pre-coked with 1-heptene showed a negative effect on monoheptyltoluene selectivity. This can be traced back to the type of coke formed during this treatment, which was most likely polyromantic coke and deposited in a large amount. The results of the TGA showed that the amount of coke from HY5.1 pre-coked with 1-heptene 11.3 wt. % was higher than that pre-coked with toluene 5.9 wt. %, which means that the carbonaceous species that was formed from 1-heptene was deposited on the internal acid sites and acted to deactivate the zeolite catalyst. However, the distribution of toluene molecules was better because it was more evenly spread between the external and internal acid sites.

Finally, there is significant agreement between the TGA results and coke selectivity for both modifications. In fact, the amount of coke and selectivity of coke that was obtained from silylated post-reaction samples ~7.4 % for HY5.1 and ~10 % for HY30 was lower than that derived from the toluene pre-coking treatment ~10.5 % for HY5.1 and ~11.8 % for HY30. This leads to the conclusion that the size of TEOS prevented it from penetrating inside the zeolite pores, thereby preventing any effect on the internal acid sites. However, both pre-coking agents influenced the internal acid sites because they have small kinetic diameters compared with bulky TEOS molecules.

Chapter 7

*Theoretical study:
reaction kinetic in fixed
bed reactor*

7.1 Introduction

Generally, there are several advantages resulting from kinetic investigations, such as: it helps to identify the most appropriate operating conditions which give high efficiency, select the most appropriate catalyst for a specific reaction and it can describe the conversion of the limiting reactant and selectivity of desired products as well as olefin isomers by using fresh zeolite (Craciun et al., 2012, Aslam et al., 2014).

There are a small number of notable kinetic studies concerning toluene alkylation with olefins (Craciun et al., 2012, Aslam et al., 2015, Kumar et al., 2012, de Almeida et al., 1994). Generally, a few kinetic models in the literature have been used to study both olefin isomerisation and alkylation of aromatics simultaneously. However, there is no kinetic study concerning toluene alkylation with 1-heptene specifically employing a HY5.1 zeolite catalyst.

The kinetics of the alkylation reaction in a fixed-bed reactor ought to be researched separately (Fogler, 2006, Harriott, 2003). The overall rate of toluene alkylation with 1-heptene that contains rate of 1-heptene diffusion into zeolite, adsorbing 1-heptene on the active sites, toluene alkylation reaction step, desorbing the products from active centres and products diffusion from zeolite.

Toluene alkylation with 1-heptene is considered to have pseudo first order kinetics because of the aromatic/olefin ratio is above 5 which makes the concentration of aromatics during the alkylation reaction approximately constant (Sahebdelfar et al., 2002, Querini and Roa, 1997, Siffert et al., 2000, Yuan et al., 2011). Additionally, increasing the aromatic/olefin ratio enhances the selectivity of the alkylated product as well as the life time of the catalyst by increasing the olefin conversion and decreasing the formation of side-products by recycling the unreacted aromatics (Sahebdelfar et al., 2002, Tsai et al., 2003).

In addition to the aromatic/olefin ratio, there are many other factors which affect the alkylation performance, such as: diffusion, catalyst activity, catalyst deactivation and/or zeolite catalyst properties (Craciun et al., 2007). The pore size of the zeolite compared with the diameter of aromatic molecules plays a vital part in the alkylation reaction to identify the most appropriate method to study the reaction kinetics (Smirniotis and Ruckenstein, 1995, Siffert et al., 2000, Corma et al., 2000).

Moreover, temperature and contact time (W/F) are considered important variables that effect the catalytic performance of zeolite catalysts (Sotelo et al., 2005). Contact time W/F (g min mol⁻¹) represents the ratio between W (g), the zeolite catalyst weight, and F (mol min⁻¹), the molar flowrate of feed.

Strictly speaking, the alkylation of aromatics over zeolite catalysts which have large pores, like HY zeolite, tend to use Eley-Rideal kinetic models because the movement of aromatic molecules inside these zeolite pores is easy and is not limited by the zeolite pore dimensions (Craciun et al., 2012, Sahebdehfar et al., 2002, Kirumakki et al., 2004, Corma et al., 2000). Therefore, the reaction rate is measured only as a function of alkene concentration, as shown in the Eley-Rideal mechanism model which represents all of the steps:

$$r_c = \frac{kK_A C_A}{1 + K_A C_A}$$

Where:

r : the reaction rate

C_A : the concentration of 1-heptene

k : rate constant

K_A : equilibrium adsorption constant

The rate constant is calculated using the Arrhenius equation:

$$k = A e^{\left(\frac{-E_a}{RT}\right)}$$

Where:

k : rate constant; mol. g⁻¹. h⁻¹

A : frequency factor

E_a : activation energy; J. mol⁻¹

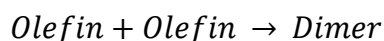
R : molar gas constant; 8.314 J. mol⁻¹. K⁻¹

T : absolute temperature; K

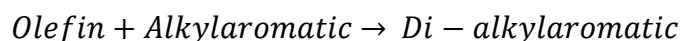
Activation energy (E_a) is considered as a barrier to energy transfer (from kinetic to potential) which must be overcome between reacting molecules for the reaction to take place and products to be formed (Fogler, 2006). In fact, the catalytic reaction acts to reduce the activation energy value contrary to the rate of reaction.

Although the fresh zeolite shows a high activity and selectivity, these swiftly reduce during reaction and this is considered the main drawback of this catalyst (Sahebdehfar et al., 2002, Querini and Roa, 1997). Practically, pore mouth closing has a crucial role in catalyst deactivation (Sahebdehfar et al., 2002). Querini and Roa (1997) revealed that pore plugging is the more likely mechanism than surface deactivation through the alkylation reaction by using Y and mordenite zeolites.

The existence of olefins in the reactant feed leads to deactivation of the external active sites through the formation of coke as a result of olefin dimerisation and oligomerisation which are the most interesting undesired reactions (Sahebdehfar et al., 2002).



These side products act to poison the active sites that are responsible for the alkylation reaction. Increasing the amount of olefin in the feed contributes to the clogging up of the pore mouth of the catalyst. Nevertheless, di- and tri-alkylation are considered as the main reasons for catalyst deactivation (Sahebdehfar et al., 2002, Lei et al., 2003).



Zeolites which have a large pore size and three dimensional structure, like HY zeolite, are more favourable in the alkylation reaction because they facilitate the diffusion of large molecules of alkylated products (Querini and Roa, 1997). In addition, choice of a reasonable temperature, catalyst amount and aromatic/olefin ratio contribute to a decrease in the side products that led to the deactivation of the catalyst during the reaction (Yadav and Doshi, 2002). The length of the olefin chain interestingly contributes to the alkylation reaction rate; any increase in the chain leads to a decrease in the reaction rate.

Despite the fact that double-bond shift is faster than alkylation, the olefins isomers do not reach internal equilibrium distribution (Craciun et al., 2012).

Therefore, both isomerisation and alkylation reactions occur approximately at the same time.

de Almeida *et al.* (1994) investigated the activation energy for the alkylation of benzene with 1-dodecene using a batch reactor with a reaction temperature 100- 150 °C, a pressure of 6-9 bar, a benzene/olefin ratio of 8.7 and an assumption that the kinetics were pseudo first order over HY zeolite. They found the activation energy for the alkylation reaction to be approximately 63 kJ mol⁻¹. Tsai *et al.* (2003) studied the kinetics of benzene alkylation with 1-dodecene over mordenite. They assumed the kinetics were pseudo first order because the benzene/1-dodecene ratio was 9:1. As a result, they concluded the activation energy of alkylation reaction is 71 kJ mol⁻¹. Furthermore, Yadav and Doshi (2002) researched the kinetics of the alkylation of benzene with 1-dodecene using a non-zeolitic catalyst in a batch reactor. They did not take into account the kinetics of olefin isomerisation; so, they only calculated the activation energy of the alkylation reaction, which was approximately 84 kJ mol⁻¹.

Zhang *et al.* (2003) showed the activation energy for the benzene alkylation with 1-dodecene using a fixed bed reactor is between 46-48 kJ mol⁻¹ for 2-, 3-, 4-, 5- and 6-LAB when employing a supported tungstophosphoric acid on a silica catalyst. In the context of this study, Kumar *et al.* (2012) reported that the activation energy of benzene alkylation with 1-dodecene over AlCl₃ supported on SiO₂ catalyst is between 31-40 kJ mol⁻¹ for 2-, 3-, 4-, 5- and 6-LAB.

Aslam *et al.* (2015) described in detail the activation energy of 1-dodecene isomers and benzene alkylation with dodecenes over mordenite zeolite. The authors showed the activation energy of 1- to 2-dodecene is lower than that of 2- to 3-dodecene by 34 and 51 kJ mol⁻¹, respectively. In contrast, the activation energy of benzene alkylation to produce 2-phenyldodecene is 49 kJ mol⁻¹ which is lower than that of 3- phenyldodecene which is 66 kJ mol⁻¹. Moreover, they tended to neglect the concentration of 4-, 5- and 6-phenyldodecanes because they were little compared with other products.

Craciun *et al.* (2012) developed a kinetic model of benzene alkylation with 1- octene using Y zeolite. They obtained the activation energy of olefin protonation as 46 kJ mol⁻¹ whereas it was 70 kJ mol⁻¹ for the alkylation step. Furthermore, Corma *et al.* (2000) explored the kinetics of the alkylation reaction of benzene with propene by

using MCM-22 zeolite. They followed an Eley-Rideal model to illustrate the reaction mechanism and obtained an activation energy of approximately 77 kJ mol⁻¹.

The main conclusion obtained from these studies is that the activation energy varies as a result of the different structures of the catalysts and the different acid site properties as well as the type of reactor. This study focuses on the kinetics of the liquid phase of toluene alkylation with 1-heptene over HY5.1 zeolite catalyst using a FBR. In addition, the kinetics of both 1-heptene isomerisation and toluene alkylation were studied simultaneously. MATLAB 2013a was employed to estimate the parameters of the reaction rate by fitting the predicted and experimental results through minimisation of the mean relative error (MRE).

$$MRE = \frac{1}{N_{exp} \times N_{comp}} \sum_{i=1}^{N_{exp}} \sum_{j=1}^{N_{comp}} \left| \frac{(C_{exp\ i,j} - C_{prde\ i,j})}{C_{exp\ i,j}} \right|$$

7.2 Optimisation and Genetic algorithms

Optimisation techniques are used to solve several problems and to find the optimum solution to a desired differentiable function (Euler, 2014). A problem can consist of either a single optimum or multiple optima, one of which is the global optimum while the others are local optima. A global minimum represents the smallest value of the objective function in a specific region. Several methods are employed to optimise multivariables in simultaneous multi reactions such as: Genetic algorithms (GAs), Particle swarm optimisation (PSO) and Artificial neural network (ANN).

Particle swarm optimisation (PSO) is a heuristic global optimisation paradigm that has become increasingly popular in the last twenty years due to its ease of application to complex multidimensional problems (Sengupta et al., 2018, Hassan et al., 2005). To some extent, it is similar to GAs where evolutionary heuristics work according to population-based stochastic search algorithm methods. However, PSO has some drawbacks: it usually falls at the local optimum with high dimensional space and the convergence rate of the iterative process is often low.

Artificial neural network (ANN) is another evolutionary intelligence computational method; it is employed to study the performance of nonlinear statistical modelling (Tu, 1996). This method has many advantages, such as: it has a sufficient ability to distinguish absolutely between dependent and independent variables in nonlinear processes, it has a considerable capability to generalise and satisfactorily clarify nonlinear systems and it does not require official statistical training. It also has disadvantages, such as: the nature of the method is that of a “black box” where it is difficult to understand why and how the output is produced, it creates a large computational burden and requires more training to use, and it needs an exceptional effort to develop the empirical nature of the model.

In the last four decades, Genetic Algorithms (GAs) have been developed. They are non-traditional search and optimisation techniques which are based on natural phenomena to overcome the problems of traditional techniques. They have been used to find a global minimum for the error function (Von Arx et al., 1998), and to optimise the estimated rate constant of successive reactions by combining them with Tabu Search (Tongcheng et al., 2005). Zhao *et al.* (2006) employed the non-linear least squares regression to find the optimum kinetic profile.

Genetic algorithms (GAs) are a heuristic search and optimisation technique inspired by natural evolution, offering a robust and flexible approach which can be used to solve a wide range of real-world problems of significant complexity (McCall, 2005). For problems which are computationally demanding and where traditional optimisation techniques break down, GAs are particularly suited.

Therefore, in the present work, the GAs are chosen as an evolutionary algorithm to predict the reaction kinetic parameters of nonlinear models during simultaneous multi reactions.

GAs operate on the basis of artificial chromosomes, with each chromosome representing a solution to a problem. It is possible to measure how good a particular solution is to a specific problem with a real number, also known as a *fitness*. GAs work by selecting and recombining chromosomes based on their fitness number to produce a second generation of ‘child’ chromosomes. Over various iterations of this process, the fitness increases until some critical value is achieved and the best solution to the problem is found. In the present study, the main steps of GAs are shown in the Figure 7.1.

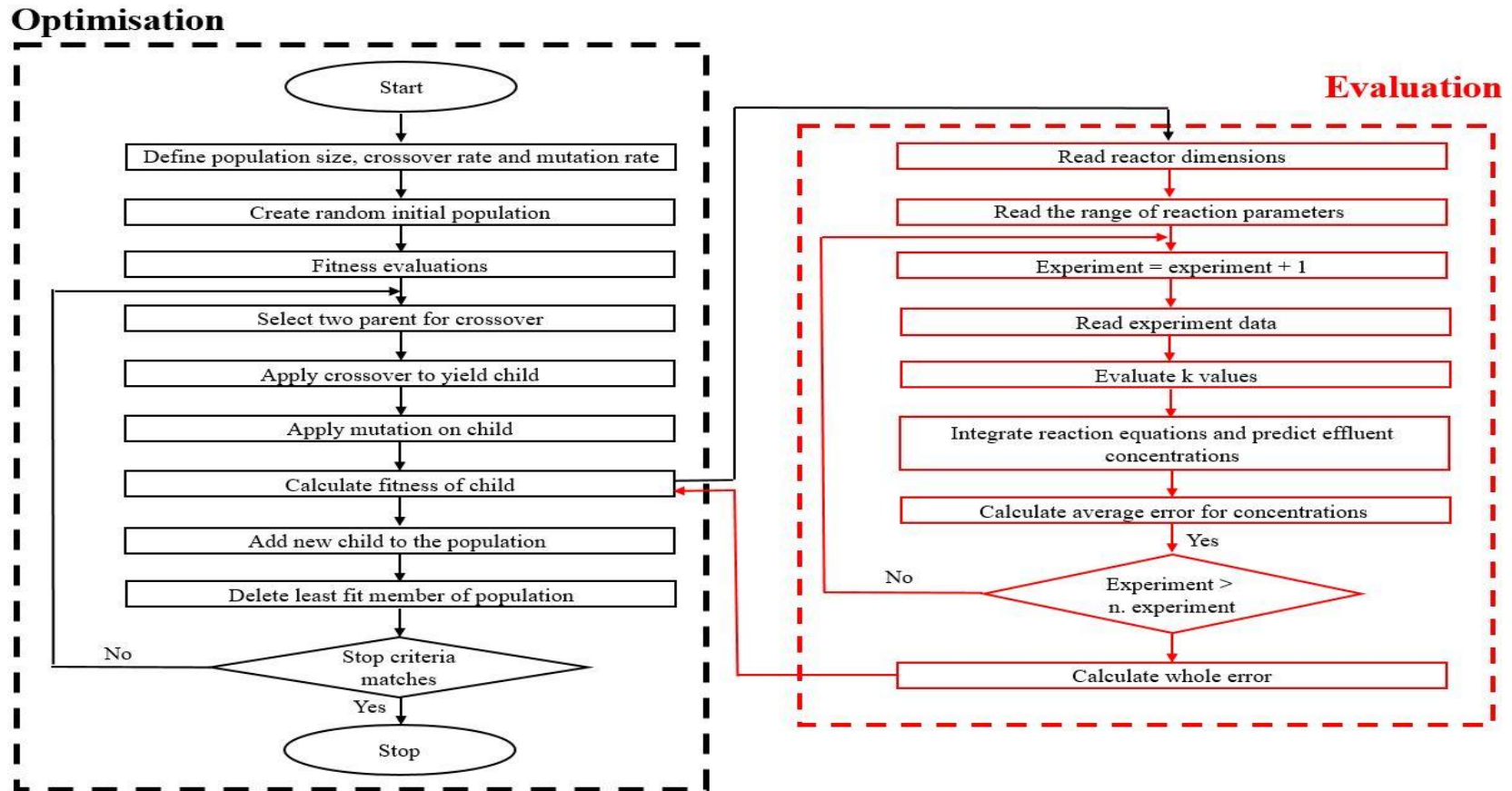


Figure 7.1. The main steps of Genetic optimisation algorithm to calculate Arrhenius constant, activation energy and rate constant.

7.3 Experimental work

Zeolite HY5.1 was loaded in a FBR as a pellet with a size range between 0.3- 0.6 mm and activated at 300 °C as previously described in Section 4.3.2. A total of 24 experiments were conducted for six W/F (1.17, 2.35, 3.52, 4.7, 5.87 and 7.04 g min mol⁻¹), varied by altering the weight of zeolite (0.1, 0.2, 0.3, 0.4, 0.5 and 0.6 g) with a constant flowrate of 10 ml h⁻¹ and at four temperatures (60, 70, 80 and 90 °C). In all these experiments, the toluene/1-heptene ratio was kept constant at 8. To accelerate the reaction to a desired velocity, inert gas (i.e. nitrogen) was employed at a flow rate of 30 ml min⁻¹. In each experiment, fresh zeolite catalyst was employed to investigate the conversion and selectivity and to avoid the deactivation drawbacks. The product was collected after 30 min and analysed employing the GC-FID as explained previously in Section 4.4.2.

Table 7.1 shows the products of toluene alkylation with 1-heptene using various operational conditions over HY zeolite.

7.4 Activity measurements of zeolite catalyst

Essentially, the contact time increased with increases in the weight of catalyst, as shown in Table 7.1. The main products are 2-heptyltoluene, 3-heptyltoluene, 2- heptene and 3-heptene; however, 4-heptyltoluene is the smallest product. Because of the toluene to 1-heptene ratio of 8:1, several undesired products such as 1- heptene dimerisation and dialkylated products did not appear at any of the reaction temperatures. Da *et al.* (1999b) showed that 2- and 3-heptyltoluene isomers of monoheptyltoluene are the main products and diffuse easier than 4-heptyltoluene.

Table 7.1. Experimental data conducted for kinetic study of toluene alkylation with 1-heptene over HY5.1 zeolite by employing the FBR.

T (°C)	Space time W/F (g min mol ⁻¹)	1-heptene (mmol cm ⁻³)	2-heptene (mmol cm ⁻³)	3-heptene (mmol cm ⁻³)	2-heptyltoluene (mmol cm ⁻³)	3-heptyltoluene (mmol cm ⁻³)	4-heptyltoluene (mmol cm ⁻³)
60	1.17	0.426	0.147	0.092	0.150	0.073	0.009
60	2.35	0.360	0.114	0.079	0.253	0.115	0.011
60	3.52	0.227	0.091	0.070	0.348	0.154	0.015
60	4.7	0.117	0.072	0.064	0.445	0.225	0.019
60	5.87	0.093	0.059	0.058	0.470	0.253	0.021
60	7.04	0.052	0.048	0.048	0.504	0.283	0.024
70	1.17	0.331	0.137	0.089	0.210	0.113	0.012
70	2.35	0.222	0.101	0.076	0.357	0.153	0.014
70	3.52	0.158	0.076	0.069	0.411	0.200	0.017
70	4.7	0.081	0.060	0.057	0.479	0.253	0.022
70	5.87	0.064	0.047	0.045	0.496	0.279	0.024
70	7.04	0.037	0.038	0.037	0.524	0.324	0.027
80	1.17	0.262	0.126	0.084	0.258	0.143	0.013
80	2.35	0.197	0.089	0.071	0.373	0.185	0.015
80	3.52	0.143	0.065	0.057	0.435	0.233	0.019
80	4.7	0.061	0.050	0.046	0.514	0.278	0.023
80	5.87	0.046	0.036	0.035	0.527	0.309	0.027
80	7.04	0.029	0.031	0.030	0.550	0.337	0.030
90	1.17	0.213	0.114	0.080	0.298	0.166	0.015
90	2.35	0.173	0.076	0.068	0.385	0.206	0.018
90	3.52	0.116	0.055	0.048	0.465	0.268	0.021
90	4.7	0.047	0.041	0.036	0.535	0.317	0.025
90	5.87	0.032	0.029	0.028	0.555	0.337	0.029
90	7.04	0.023	0.025	0.024	0.570	0.355	0.031

Figure 7.2 indicates the impact of temperature on 1-heptene conversion and selectivity of monoheptyltoluene (MHT) isomers and 2-heptyltoluene at a contact time of $1.17 \text{ g min mol}^{-1}$. The conversion increases linearly with increasing temperature (from ~60 % at 60 °C to ~80 % at 90 °C); this could be because the number of side reactions is decreased at high temperatures when all the zeolite samples have the same Si/Al molar ratio. The selectivity of both MHT isomers and 2-heptyltoluene increases gradually with increases in the reaction temperature from ~18 % at 60 °C to ~28 % at 90 °C for MHT and from ~12 % at 60 °C to ~18 % at 90 °C for 2-heptyltoluene, possibly because the carbonaceous materials that are deposited at high temperatures act to deactivate the acid sites that are responsible mainly for the side reactions and isomerisation reactions in contrast with low temperature where carbonaceous deposits deactivate the acid sites that are responsible for the alkylation reaction. Alternatively, the diffusion limitation is decreased at high temperatures thereby the desorption of bulky monoheptyltoluene molecules becomes easier.

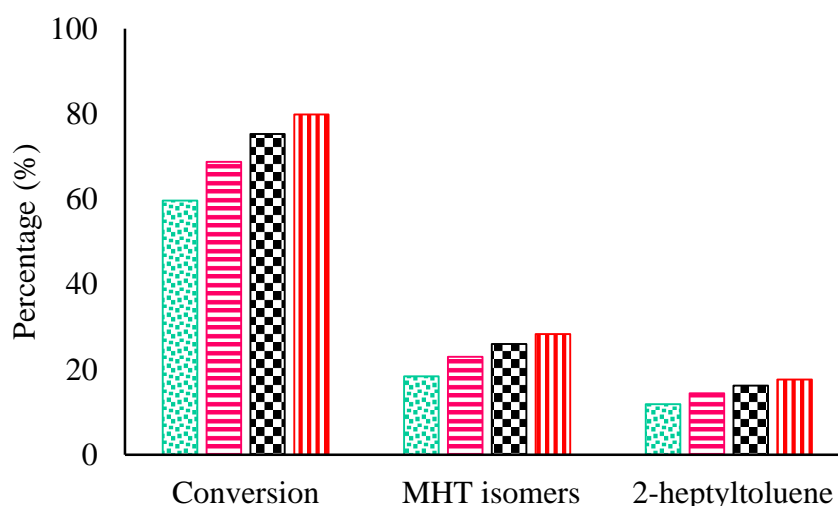


Figure 7.2. Impact of temperature and contact time (W/F) on 1-heptene conversion and selectivity of MHT and 2-heptyltoluene during toluene alkylation with 1-heptene at various temperatures 60 °C (■), 70 °C (■), 80 °C (■) and 90 °C (■) atmospheric pressure, 0.5 g of fresh HY5.1 zeolite, TOS of 30 min, T: H ratio is 8: 1, 30 ml min^{-1} of N_2 flowrate and using FBR.

The influence of W/F values on the conversion of 1-heptene at different temperatures is displayed in Figure 7.3. It shows the conversion increased with increasing W/F presumably because the amount of coke deposited on a small amount of zeolite catalyst was more than that which accumulated on the large amount of the

same zeolite catalyst. And as illustrated previously in Section 4.3.2 and Section 5.4.2.3, the catalyst was loaded vertically in the reactor tube. This leads to the conclusion that the reaction using the large amount of catalyst occurred on the uppermost layers of the catalyst bed, meaning the other lower layers were not affected by the deactivation so a huge number of active sites were still working. Moreover, it can be seen that the 1-heptene conversion at 90 °C is higher than the other three temperatures at W/F of 1.17, 2.35, 3.52, 4.7, 5.87 and 7.04 g min mol⁻¹; however, at the W/F 7.04 g min mol⁻¹, it is exceedingly close to the conversion at 60, 70 and 80 °C. The increase in contact time W/F contributed to the increase of the zeolite catalyst stability. All these results are in agreement with previous studies that showed the conversion is increased by increasing the contact time for a constant reaction temperature during the hydroisomerisation of a hydrocarbon feed and by employing other zeolite catalysts (Jiménez et al., 2003).

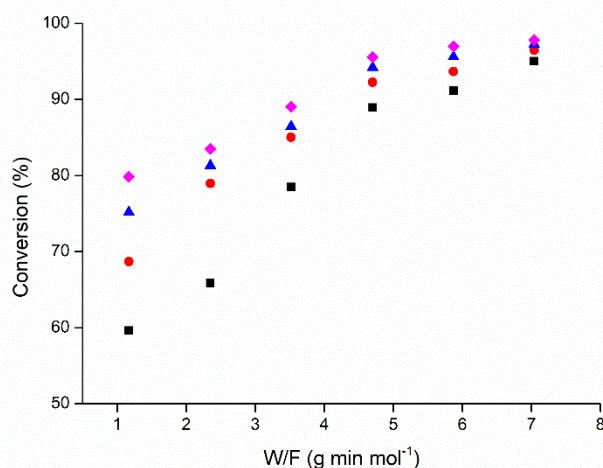


Figure 7.3. Contact time (W/F) effect on 1-heptene conversion during toluene alkylation with 1-heptene at various temperatures 60 °C (■), 70 °C (●), 80 °C (▲) and 90 °C (◆), atmospheric pressure, 0.5 g of fresh HY5.1 zeolite, TOS of 30 min, T: H ratio is 8: 1, 30 ml min⁻¹ of N₂ flowrate and using FBR.

Generally speaking, at high temperatures, the monoheptyltoluene isomers are the predominant species; however, at lower temperatures the heptene isomers are more prevalent. Craciun *et al.* (2007) can be considered as corroborating evidence for these results.

At higher temperatures, the selectivity of 2- and 3-heptyltoluene are slightly increased with increases to the contact time, as shown in Figure 7.4, Figure 7.5, Figure

7.6 and Figure 7.7. On the other hand, the selectivity of monoheptyltoluene dramatically increases from ~28 to ~46 % with rising W/F values at 90 °C (Figure 7.7). In contrast to this, the selectivity of 4-heptyltoluene stays approximately constant ~1 % probably because the pore mouth opening is reduced during the reaction as a result of coke accumulation, thereby the diffusion of bulky molecules becomes more difficult. This conclusion was supported by Da *et al.* (2001) who reported that the pore mouth of the zeolite is constrained; each heptyltoluene isomer faces difficulties moving through the apertures of the zeolite.

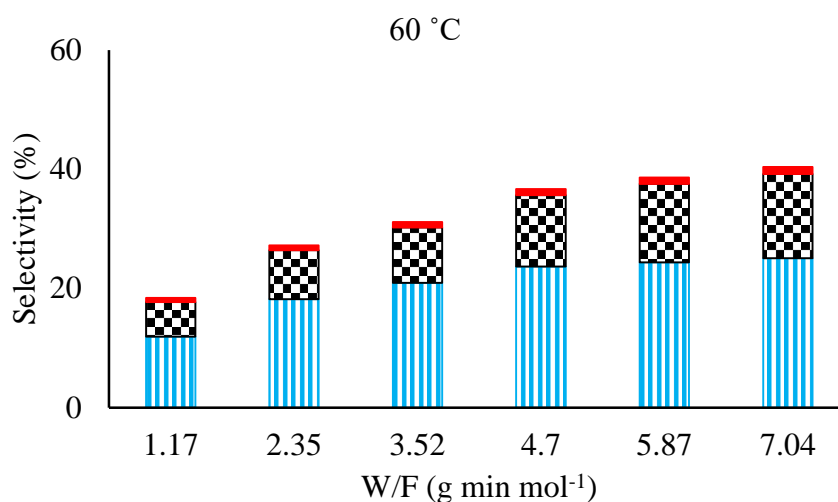


Figure 7.4. Contact time (W/F) effect on 2-heptyltoluene (■), 3-heptyltoluene (■) and 4-heptyltoluene (■) selectivity during toluene alkylation with 1-heptene at 60 °C, atmospheric pressure, 0.5 g of fresh HY5.1 zeolite, TOS of 30 min, T: H ratio is 8:1, 30 ml min⁻¹ of N₂ flowrate and using FBR.

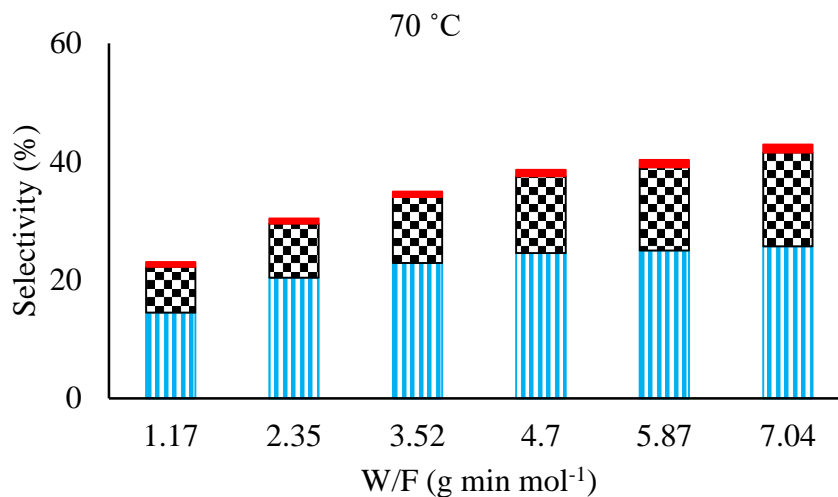


Figure 7.5. Contact time (W/F) effect on 2-heptyltoluene (■), 3-heptyltoluene (■) and 4-heptyltoluene (■) selectivity during toluene alkylation with 1-heptene at 70 °C, atmospheric pressure, 0.5 g of fresh HY5.1 zeolite, TOS of 30 min, T: H ratio is 8:1, 30 ml min⁻¹ of N₂ flowrate and using FBR.

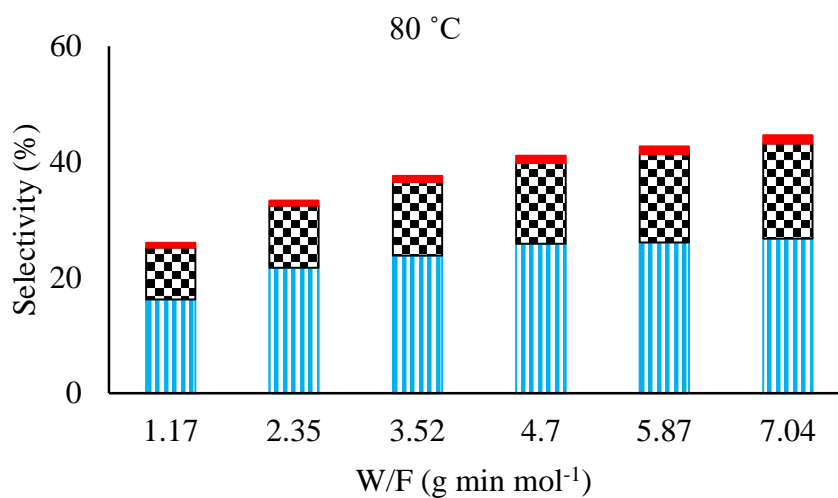


Figure 7.6. Contact time (W/F) effect on 2-heptyltoluene (■), 3-heptyltoluene (■) and 4-heptyltoluene (■) selectivity during toluene alkylation with 1-heptene at 80 °C, atmospheric pressure, 0.5 g of fresh HY5.1 zeolite, TOS of 30 min, T: H ratio is 8:1, 30 ml min⁻¹ of N₂ flowrate and using FBR.

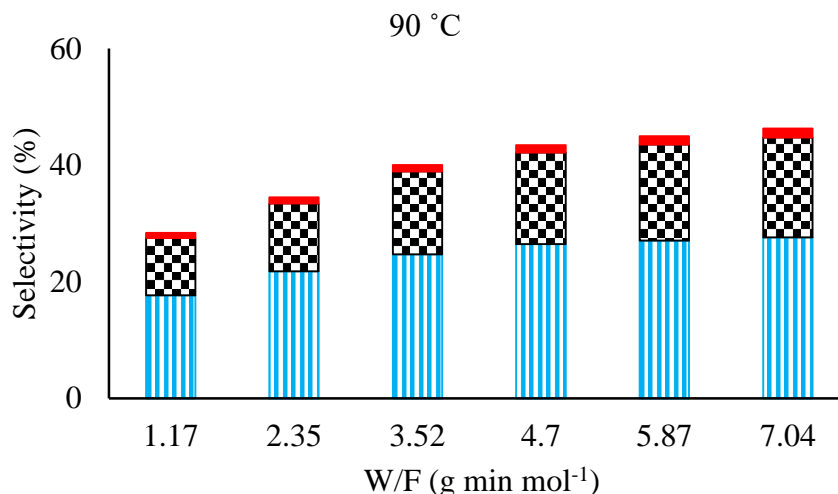


Figure 7.7. Contact time (W/F) effect on 2-heptyltoluene (■), 3-heptyltoluene (■) and 4-heptyltoluene (■) selectivity during toluene alkylation with 1-heptene at 90 °C, atmospheric pressure, 0.5 g of fresh HY5.1 zeolite, TOS of 30 min, T: H ratio is 8:1, 30 ml min⁻¹ of N₂ flowrate and using FBR.

Figure 7.8, Figure 7.9, Figure 7.10 and Figure 7.11 display the selectivity of 2- and 3-heptene as a function of W/F values at different temperatures. The selectivity of 2- and 3-heptene at low temperatures and low W/F values was higher than the selectivity at high temperatures and high space time. For example, the selectivity of 2-heptene at a constant temperature of 60 °C varied from ~23 % at a W/F of 1.17 g min mol⁻¹ to ~5 % when the W/F was increased to 7.04 g min mol⁻¹. This indicates that these isomers were consumed in the alkylation reaction at high temperatures and high W/F values. Aslam and co-worker showed the 2- and 3-dodecane are completely consumed during the alkylation reaction at high temperatures and high W/F values (Aslam et al., 2014). In all these four figures, 2-heptene always has a higher selectivity than 3-heptene because the 2-heptene is formed directly from 1-heptene, however the 3-heptene isomer depends on the 2-heptene formation, as described in Section 2.4.1. This derivation is in agreement with Cao *et al.* (1999) who concluded that the selectivity of 2-heptyltoluene and 2-heptene were the highest from the beginning of the reaction because they are formed from 1-heptene directly.

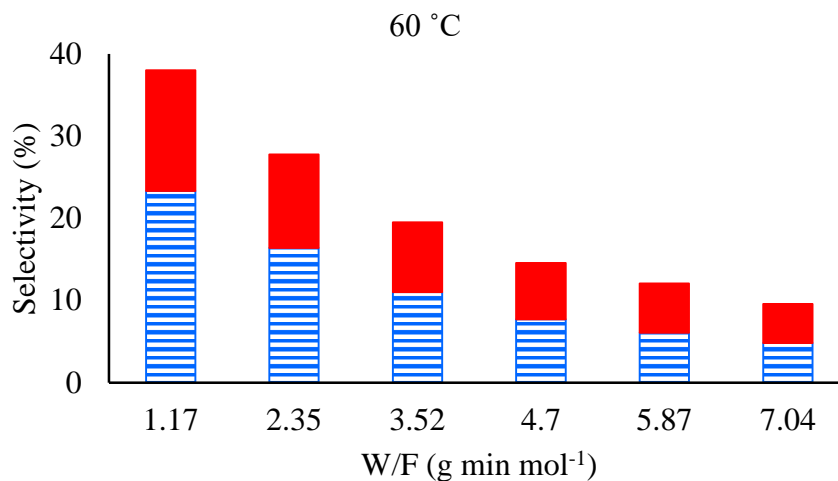


Figure 7.8. Contact time (W/F) effect on selectivity of 2-heptene (■) and 3-heptene (■) isomers during toluene alkylation with 1-heptene at 60 °C, atmospheric pressure, 0.5 g of fresh HY5.1 zeolite, TOS of 30 min, T: H ratio is 8: 1, 30 ml min⁻¹ of N₂ flowrate and using FBR.

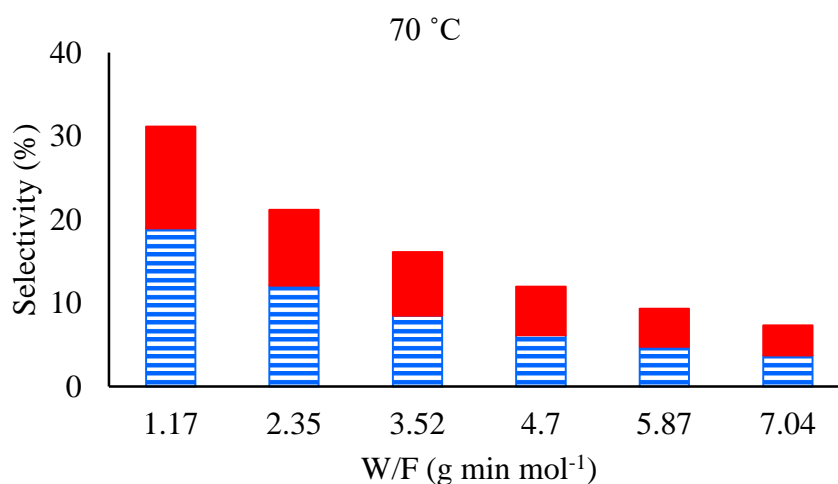


Figure 7.9. Contact time (W/F) effect on selectivity of 2-heptene (■) and 3-heptene (■) isomers during toluene alkylation with 1-heptene at 70 °C, atmospheric pressure, 0.5 g of fresh HY5.1 zeolite, TOS of 30 min, T: H ratio is 8: 1, 30 ml min⁻¹ of N₂ flowrate and using FBR.

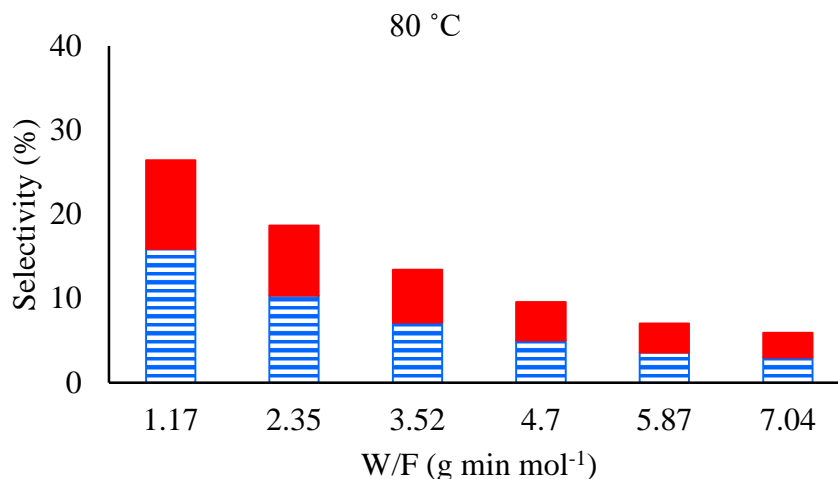


Figure 7.10. Contact time (W/F) effect on selectivity of 2-heptene (■) and 3-heptene (■) isomers during toluene alkylation with 1-heptene at 80 °C, atmospheric pressure, 0.5 g of fresh HY5.1 zeolite, TOS of 30 min, T: H ratio is 8: 1, 30 ml min⁻¹ of N₂ flowrate and using FBR.

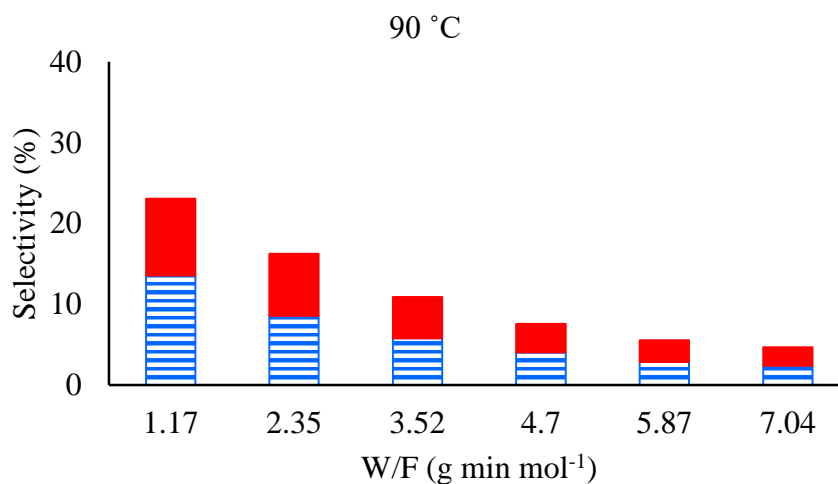


Figure 7.11. Contact time (W/F) effect on selectivity of 2-heptene (■) and 3-heptene (■) isomers during toluene alkylation with 1-heptene at 90 °C, atmospheric pressure, 0.5 g of fresh HY5.1 zeolite, TOS of 30 min, T: H ratio is 8: 1, 30 ml min⁻¹ of N₂ flowrate and using FBR.

Figure 7.12 shows the effect of reaction temperature on the coke selectivity at various contact times (W/F). In general, there was only a slight difference in the coke selectivity with variations in the reaction temperature. The behaviour of the coke formation was different with increasing W/F. When the W/F was 1.17 g min mol⁻¹, the coke formation was increased by increasing the reaction temperature from ~44 % at 60 °C to ~49 % at 90 °C. In contrast, it was decreased with increasing the reaction

temperature at the highest contact time W/F value of $7.04 \text{ g min mol}^{-1}$ from $\sim 50\%$ at 60°C to $\sim 49\%$ at 90°C . This could be owing to the formation of undesired reactions (1-heptene dimerisation and diheptyltoluene) being reduced at high temperatures. TGA results (Figure 7.13) confirm these results by showing that the amount of coke decreases with increasing reaction temperature, at a constant contact time ($7.04 \text{ g min mol}^{-1}$).

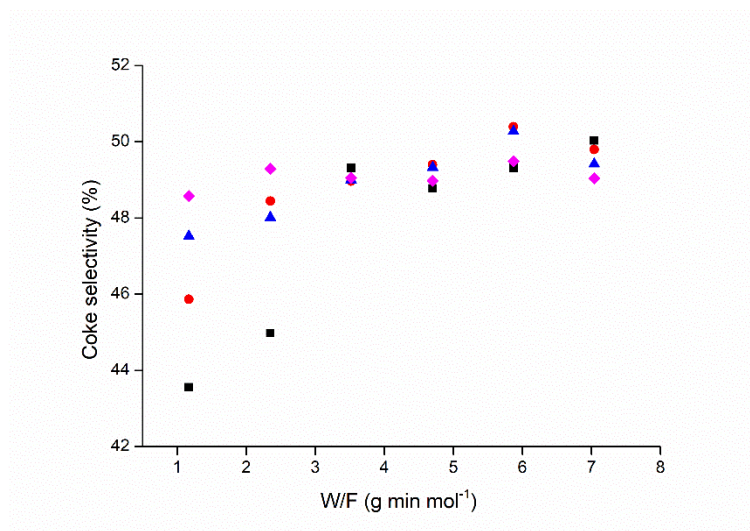


Figure 7.12. Influence of contact time (W/F) on coke selectivity during toluene alkylation with 1-heptene at various reaction temperature 60°C (■), 70°C (●), 80°C (▲) and 90°C (◆), atmospheric pressure, 0.5 g of fresh HY5.1 zeolite, TOS of 30 min, T: H ratio is 8: 1, 30 ml min^{-1} of N_2 flowrate and using FBR.

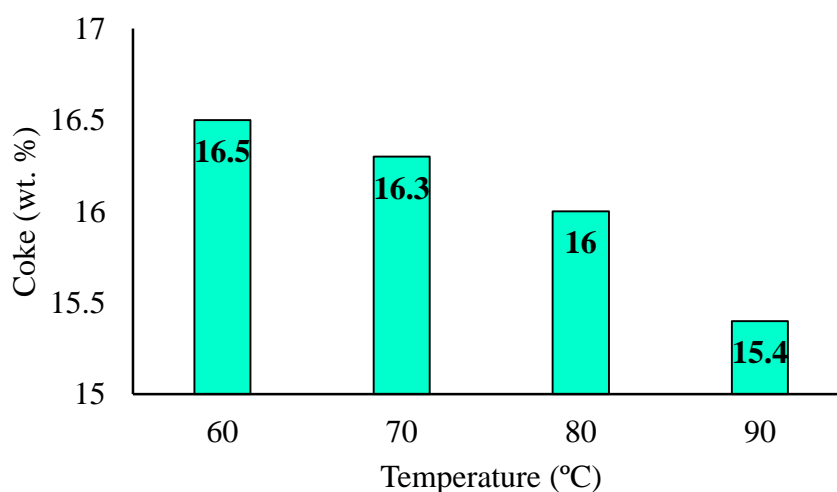


Figure 7.13. Coke % of fresh HY5.1 post-reaction during toluene alkylation with 1-heptene at atmospheric pressure, 0.5 g of fresh HY5.1 zeolite, TOS of 30 min, T: H ratio is 8: 1, 30 ml min^{-1} of N_2 flowrate and using FBR.

7.5 Kinetic study

The kinetics of toluene alkylation with 1-heptene over HY5.1 zeolite are investigated, in the absence of coke accumulation. During the description of kinetics, double bond migration of 1-heptene happens in parallel with toluene alkylation with all isomers of heptene. The reaction rate equations are calculated based on Eley-Rideal kinetics. According to the alkylation of toluene mechanism, as shown in Section 2.4.1, the double bond shift of 1-heptene is supposed to be a reversible reaction. However, the toluene alkylation with heptenes is considered an irreversible reaction (Magnoux et al., 1997).

Several hypotheses are taken in account during the kinetic study, such as: toluene alkylation with 1-heptene is assumed to be a pseudo first order reaction as a result of the molar ratio between toluene and 1-heptene 8:1. As a result of this, the toluene concentration can be assumed negligible thereby, the reaction rate can be measured according to the concentration of 1-heptene only. In addition, as a further result of the high molar ratio, it is presumed, there are no side products produced during this reaction. Fresh catalyst is employed to avoid the effect of coke formation on the other set of reactions. Isothermal conditions are assumed as there is a negligible influence of temperature.

Regrettably, there are no values given in the literature that can be used as a reference to compare the results obtained from the parallel reactions of the double bond isomerisation and toluene alkylation. There are however, a few reports on the kinetics of benzene with 1-dodecene alkylation and dodecene isomerisation as a parallel reaction in the presence of coke formation.

To check out the kinetic parameter prediction, several alkylation experiments have been conducted over HY5.1 zeolite at various reaction temperatures (60-90 °C) and at different W/F values (1.17-7.04 g min mol⁻¹). For this purpose, 144 experimental points were employed to estimate the kinetic parameters.

Figure 7.14, Figure 7.15, Figure 7.16, Figure 7.17, Figure 7.18 and Figure 7.19 show the comparison between the experimental and predicted data for 1-heptene, 2-heptene, 3-heptene, 2-heptyltoluene, 3-heptyltoluene and 4-heptyltoluene concentration (see Appendix D). Most of these results show that the concentration of

the reactant and products predicted by the theoretical study are in good agreement with the experiment results, with a few exceptions. The mean relative error (MRE%) is ~15 %. This error is because of the large number of experiments used during this study and the low concentration of some products such as 3-heptene and 4- heptyltoluene.

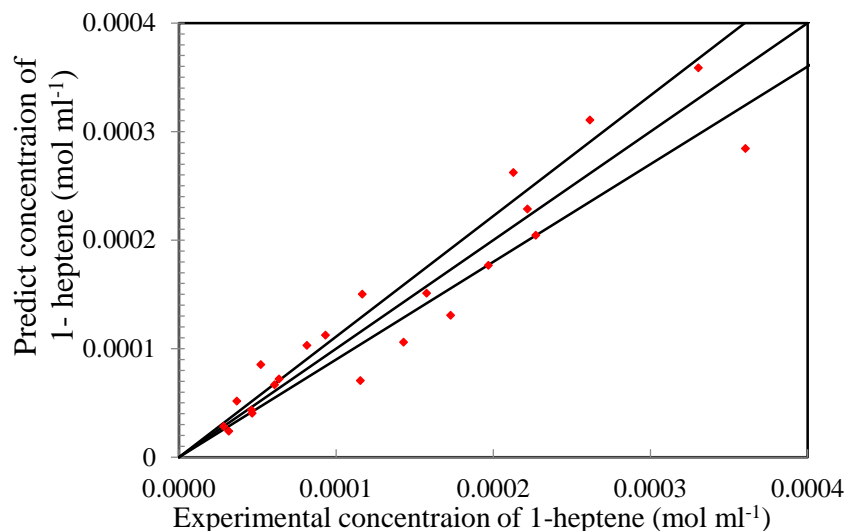


Figure 7.14. Kinetic comparison plot of experimental and predicted concentration of 1-heptene using Eley-Rideal kinetic model during toluene alkylation with 1-heptene at various W/F values and reaction temperatures, atmospheric pressure, 0.5 g of fresh HY5.1 zeolite, TOS of 30 min, T: H ratio is 8: 1, 30 ml min⁻¹ of N₂ flowrate, and using FBR.

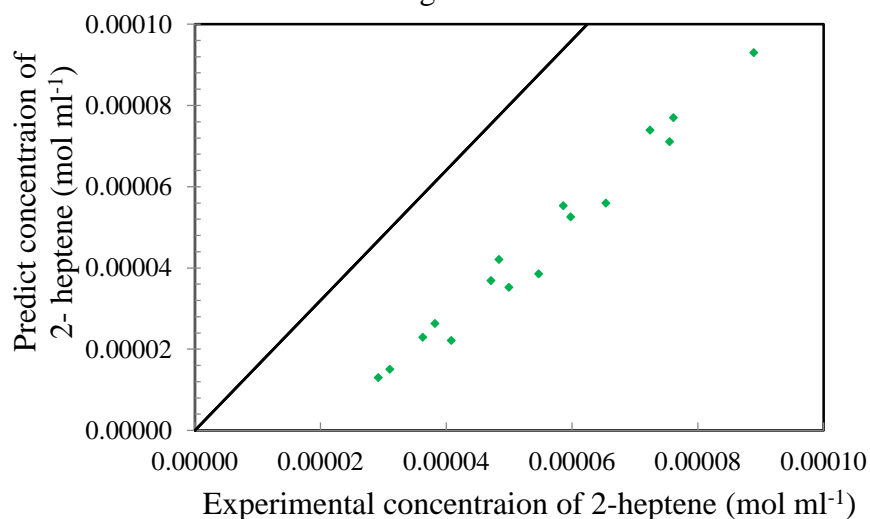


Figure 7.15. Kinetic comparison plot of experimental and predicted concentration of 1-heptene using Eley-Rideal kinetic model during toluene alkylation with 2-heptene at various W/F values and reaction temperatures, atmospheric pressure, 0.5 g of fresh HY5.1 zeolite, TOS of 30 min, T: H ratio is 8: 1, 30 ml min⁻¹ of N₂ flowrate, and using FBR.

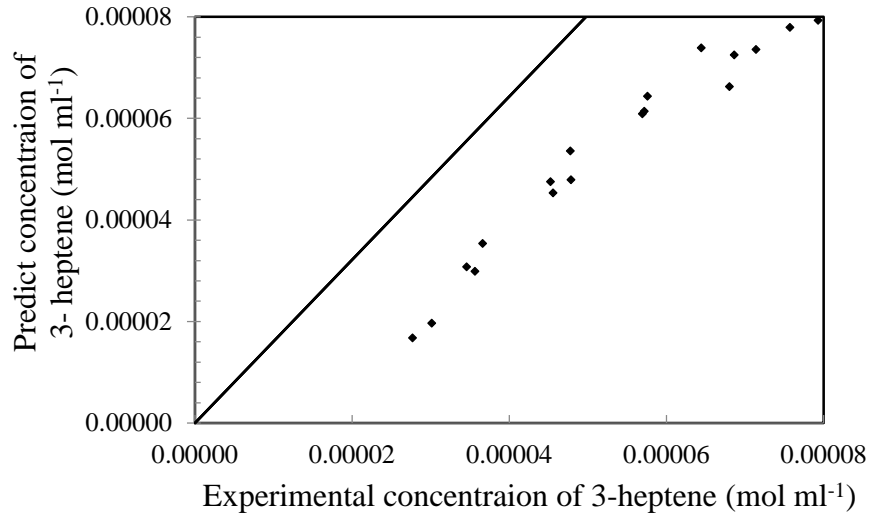


Figure 7.16. Kinetic comparison plot of experimental and predicted concentration of 3-heptene using Eley-Rideal kinetic model during toluene alkylation with 1-heptene at various W/F values and reaction temperatures, atmospheric pressure, 0.5 g of fresh HY5.1 zeolite, TOS of 30 min, T: H ratio is 8: 1, 30 ml min⁻¹ of N₂ flowrate, and using FBR.

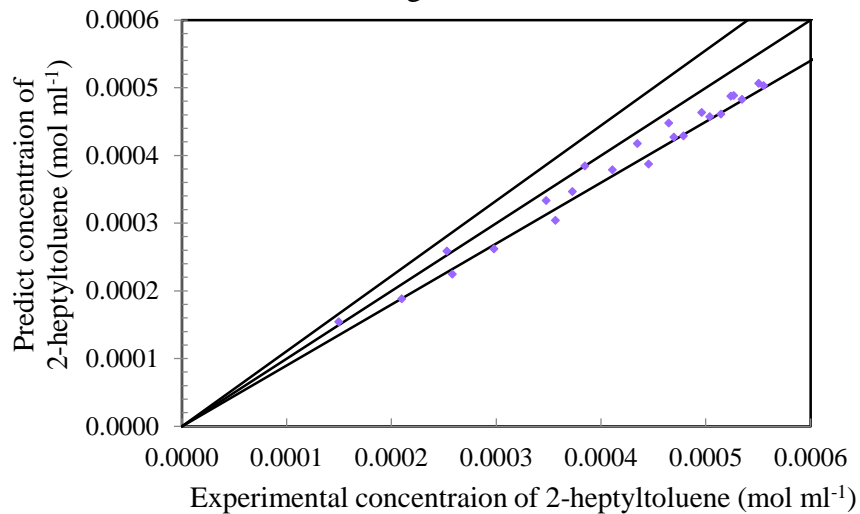


Figure 7.17. Kinetic comparison plot of experimental and predicted concentration of 2-heptyltoluene using Eley-Rideal kinetic model during toluene alkylation with 1-heptene at various W/F values and reaction temperatures, atmospheric pressure, 0.5 g of fresh HY5.1 zeolite, TOS of 30 min, T: H ratio is 8: 1, 30 ml min⁻¹ of N₂ flowrate, and using FBR.

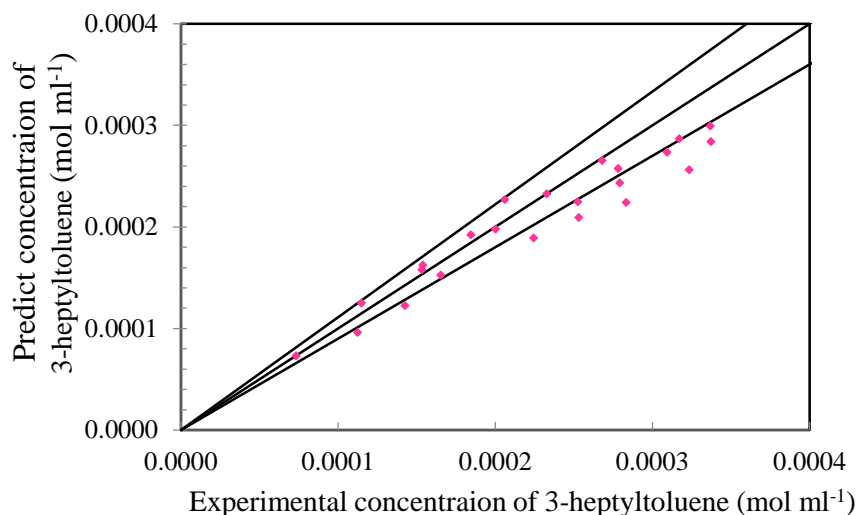


Figure 7.18. Kinetic comparison plot of experimental and predicted concentration of 3-heptyltoluene using Eley-Rideal kinetic model during toluene alkylation with 1-heptene at various W/F values and reaction temperatures, atmospheric pressure, 0.5 g of fresh HY5.1 zeolite, TOS of 30 min, T: H ratio is 8: 1, 30 ml min⁻¹ of N₂ flowrate, and using FBR.

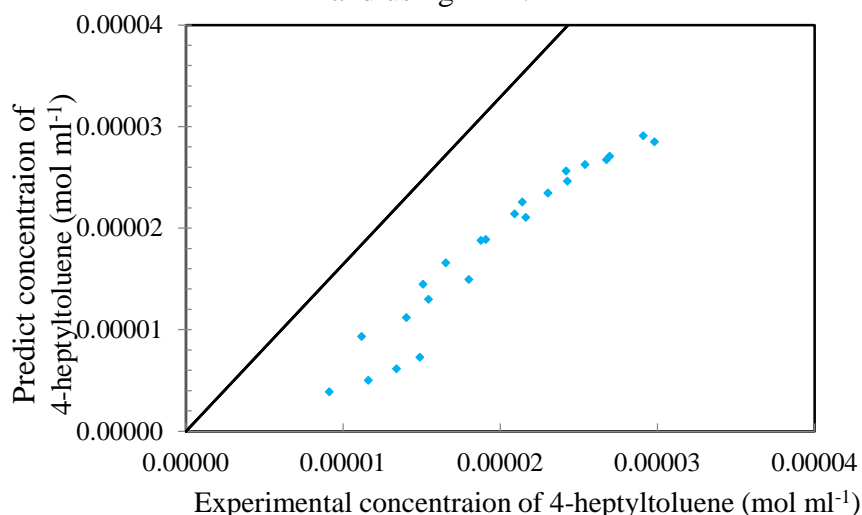








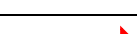
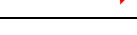







Figure 7.19. Kinetic comparison plot of experimental and predicted concentration of 4-heptyltoluene using Eley-Rideal kinetic model during toluene alkylation with 1-heptene at various W/F values and reaction temperatures, atmospheric pressure, 0.5 g of fresh HY5.1 zeolite, TOS of 30 min, T: H ratio is 8: 1, 30 ml min⁻¹ of N₂ flowrate, and using FBR.

The estimated kinetic parameters for toluene alkylation with 1-heptene are shown in Table 7.2. The estimated activation energy for the conversion of 1-heptene to the 2-heptene isomer is 15.3 kJ mol⁻¹ however, for the double bond migration of 2-heptene to 3-heptene it is 19.5 kJ mol⁻¹. This indicates that the isomerisation of 1-heptene to 2-heptene requires a smaller activation energy compared with that required for the isomerisation of 2-heptene to 3-heptene. These results are identical to

those shown by Aslam *et al.* (2015) who showed that the double bond shift of 1-dodecene to 2-dodecene demanded much less activation energy (34 kJ mol⁻¹) compared with that for converting 2-dodecene to 3-dodecene (51 kJ mol⁻¹). It is clear, that there is a big gap between the present results and those obtained in the previous study by Aslam *et al.* (2015). This gap is reasonable and to be expected because of the difference in chain length between 1-heptene and 1-dodecene, as described by Yadav and Doshi (2002).

Table 7.2. Estimated Arrhenius (min⁻¹) constant and activation energy (kJ mol⁻¹) for each elementary step during the toluene alkylation with 1-heptene.

No.	A _o (min ⁻¹)	E _a (kJ mol ⁻¹)	Elementary step
1	78.3	15.3	1-H  2-H
2	47.4	11.9	2-H  1-H
3	12.1	19.5	2-H  3-H
4	61.5	23.7	3-H  2-H
5	66.2	25.3	1-H+T  2-HT
6	7 * 10 ⁻³	99.0	2-H+T  2-HT
7	218.9	28.5	2-H+T  3-HT
8	3 * 10 ⁻³	99.9	3-H+T  3-HT
9	245.3	30.2	4-H+T  4-HT
10	1305.8 * 10 ⁺⁴	122.2	1-H  Coke
11	137.6	131.7	2-H  Coke
12	2922.1 * 10 ⁺⁶	183.7	3-H  Coke
13	3784.6 * 10 ⁺⁶	182.5	2-HT  Coke
14	467.6	129.2	3-HT  Coke
15	7415.4	40.3	4-HT  Coke

The activation energy values of toluene alkylation to produce 2-heptyltoluene are 25.3 and 99 kJ mol⁻¹ from 1- and 2-heptene, respectively. For 3-heptyltoluene they are 28.5 and 99.9 kJ mol⁻¹ from 2- and 3-heptene, respectively, whilst it is 30.2 kJ mol⁻¹ to produce 4-heptyltoluene from 4-heptene. Indeed, the low values 25.3, 25.5 and 30.2 kJ mol⁻¹ of activation energy pointed out diffusion limitation probably through volatilisation. In contrast, the high activation energy values for 2- and

3- heptyltoluene formation from 2- and 3-heptene (99 and 100 kJ mol⁻¹ respectively), indicated that these reaction steps are less likely to occur than formation from 1- and 2-heptene. These values approach the values of the activation energy (31-40 kJ mol⁻¹) obtained by Kumar *et al.* (2012) during linear alkylbenzene production by benzene alkylation with 1-dodecane over AlCl₃ supported on a silica gel catalyst. In addition, the small difference between the present results and those which were obtained by Kumar *et al.* (2012) seems acceptable because of the variation in the chain length between 1-heptene and 1- dodecene. Decreasing the chain length acts to decrease the activation energy values and increases the reaction rate (Yadav and Doshi, 2002). These estimated values of activation energy are in agreement with the product selectivity from the experimental study which indicates that the product produced in the highest quantity in the toluene alkylation over HY5.1 zeolite is 2- heptyltoluene. The quantity of 3-heptyltoluene is less than 2-heptyltoluene while 4- heptyltoluene is the least produced among these three products, as shown in Table 7.1.

Furthermore, the activation energy values of alkylation reaction are higher than the values of isomerisation reaction. These results are similar to those obtained by Craciun *et al.* (2012), who concluded that the activation energy of benzene alkylation with 1-octene is bigger than that for double bond migration.

Finally, Table 7.2 illustrates that the higher activation energy values are associated with coke formation from several sources, which indicates that the coke formation steps are slower than both the alkylation and isomerisation steps. This could be because either the coke molecules are bigger than the alkylation and isomerisation product molecules and they consist of a large number of carbon atoms, or the coke molecules were formed as a results of side products accumulating *via* trapping the bulky product molecules or a combination of reactants dimerisation or oligomerisation products.

7.6 Conclusions

The main conclusions of the investigation into the kinetics of toluene alkylation with 1-heptene over HY5.1 zeolite. The main product in this reaction is the 2-heptyltoluene, perhaps due to the coke formation which acts to narrow the zeolite pores but could not prevent the diffusion of these small molecules compared with the other heptyltoluene isomers therefore its selectivity was higher than the other products.

The role of temperature and contact time are important in the alkylation reaction, particularly at 90 °C and 7.04 g min mol⁻¹ when the highest selectivity of monoheptyltoluene was seen ~46 %. The selectivity of coke ~49 % and amount of coke by TGA 15.4 wt. % are decreased with increasing reaction temperature and at high contact time W/F of 7.04 g min mol⁻¹.

The activation energy for 1-heptene to 2-heptene isomerisation is lower than that of 2-heptene double bond shift to 3-heptene and this means that the isomerisation of 1-heptene is faster than the 2-heptene isomerisation. The activation energy for toluene alkylation with 1-heptene to produce 2-heptyltoluene was 25.3 kJ mol⁻¹ however, it was 28.5 kJ mol⁻¹ in the production of 3-heptyltoluene from toluene alkylation with 2-heptene and was 30.2 kJ mol⁻¹ in the alkylation of toluene with 3- heptene. These results support the other result from the experimental work which showed that the selectivity of 2-heptyltoluene is higher than both 3- and 4- heptyltoluene. On the other hand, these results indicate the isomerisation steps are faster than the alkylation reaction steps. The activation energies of coke were higher than the those of both alkylation and isomerisation reactions. However, the coke formation was the slowest step during this reaction.

Chapter 8

Conclusions and future works

8.1 Introduction

The objectives of the present thesis were threefold. First was to understand the role of coke formed during the toluene alkylation with 1-heptene over different fresh and modified zeolite catalysts. Second was to evolve a controlled strategy to prepare silylated and/or pre-coked zeolite catalyst to improve the catalytic performance compared with the parent zeolite catalyst. The final objective was to study the kinetics of alkylation of toluene with 1-heptene over HY5.1 zeolite. The following conclusions summarise the main findings and consequences of this thesis, and the future direction has also been discussed.

8.2 Conclusions

8.2.1 Toluene alkylation with 1-heptene over fresh zeolite catalysts

The alkylation of toluene with 1-heptene into heptyltoluene was investigated over a series of fresh HY5.1, HY30, H-mordenite and H-Beta zeolite catalysts with different structures, textures and acidic properties. The reactions were performed using two types of reactors; batch reactor (BR) and fixed bed reactor (FBR). Fresh HY zeolite catalysts showed a conversion ~88 % while fresh H-mordenite illustrated the highest selectivity to 2-heptyltoluene ~49 % when using a BR with a reaction temperature of 90 °C, run at atmospheric pressure, at a reaction time of 120 min, with 0.25 g of zeolite and a toluene to 1-heptene ratio of 3:1.

The operating conditions for the alkylation reaction using the FBR were chosen according to separate studies which showed 90 °C was the most favourable reaction temperature, 0.5 g of zeolite loading was the most appropriate weight to study the role of coke formation and 240 min TOS was the time at which the conversion of 1-heptene reached a stable state. The FBR results showed that the HY30 zeolite catalyst was more stable than HY5.1, especially when the conversion of 1-heptene was approximately constant with increasing TOS at ~98 %. Also, there was a slight enhancement to the selectivity of 2-heptyltoluene by using HY30 ~30 % compared with HY5.1 ~27 %. However, there was no significant change in the selectivity of coke between the two types of HY zeolite catalysts ~45.

Characterisation of the used zeolite catalysts showed there was no appreciable difference in the amount of, the structure or the nature of the coke between HY zeolite catalysts with different Si/Al mole ratios. The rate of coke formation increased rapidly ~9 % of HY5.1 during the first few minutes 20 min of the reaction, but then slowed for the remainder of the reaction ~11 % and ~11.5% for HY5.1 at 120 and 360 min respectively, as the TGA results showed. Additionally, the TPO profile of spent HY5.1 and HY30 demonstrated that there were two types of carbon deposit during the alkylation of toluene with 1-heptene: the first represented the hydrogen-rich carbonaceous deposits and the second was ascribed to the presence of structurally ordered or graphitic-like carbon. In summary, these carbonaceous deposits are believed to play a positive role in the alkylation of toluene with 1-heptene through either deactivation of the acid sites that are responsible for the side reactions or improvement of the selectivity of desired products through enhancement of the shape selectivity of these zeolite catalysts.

8.2.2 Toluene alkylation with 1-heptene over dealuminated and desilicated zeolite catalysts

Acid leaching using aqueous HCl solution acts to decrease the coke formation by decreasing the total acidity through remove of aluminium atoms from the zeolite framework. On the other hand, base leaching employing aqueous NaOH solution works by forming a mesoporous structure which improves the diffusion limitation properties.

Characterisation of dealuminated and desilicated samples showed there was only a slight decrease in the XRD intensity and the structure remained intact. The SEM images confirmed the XRD results by illustrating that there was no significant alteration in the morphology or size of the zeolite particles.

Comparison of the catalytic performance of modified HY30 samples with the fresh zeolite catalysts in the FBR showed an improvement in 2-heptyltoluene selectivity of desilicated HY30 compared with the parent HY30 from ~33 % to ~39 %. The amount of coke for the desilicated sample was increased compared with that obtained from the unmodified HY30 zeolite catalyst from ~10 wt. % to ~11.6 wt. % for HY5.1 and from ~11.8 wt. % to ~13 % for HY30. This confirmed the hypothesis about the desilication treatment which suggested that this modification acts to form

mesopores which leads to additional space being provided for coke to accumulate. This coke played a positive role in enhancing the selectivity of 2-heptyltoluene from ~33 % to ~39 % for HY30 and decreasing the coke selectivity from ~45 % to ~31 % for HY30. In contrast, the coke selectivity of 2-heptyltoluene for the dealuminated HY30 zeolite catalyst was increased from ~31 % to ~36 % as a result of a reduction in the coke selectivity from ~45% to ~35 % because of a significant reduction in the zeolite acidity.

Characterisation of post-reaction modified HY30 zeolite catalysts showed that the amount of coke was reduced for the dealuminated sample from ~11.8 % wt. % to ~11 wt. % whereas, it was increased for the desilicated sample from ~11.8 % wt. % to ~13 wt. % compared with the fresh HY30 zeolite sample. Moreover, the elemental analysis illustrated that the carbonaceous deposits on the spent modified zeolite catalysts were hard coke but that they were softer than that accumulated on the parent zeolite sample H/C was ~0.19 for the fresh HY30 however, it was ~0.28 for HY30 dealuminated and ~0.24 for HY30 desilicated.

8.2.3 Toluene alkylation with 1-heptene over silylated and pre-coked zeolite catalysts

Zeolite modification by either pre-coking or silylation acts to increase the shape selectivity which contributes to passivate unselective catalytic sites. In addition, it works to decrease the diffusion of unwanted products into or out of the zeolite pores by narrowing these pores and thereby enhancing the selectivity. Therefore, silylation and pre-coking of the zeolite catalyst were suggested to be an efficient strategy to enhance selectivity to 2-heptyltoluene in toluene alkylation with 1-heptene, compared with those obtained over the parent zeolite catalyst. TEOS was employed as a silylation agent while toluene and 1-heptene were used as coke pre-cursors.

Characterisation illustrated the total acidity of the silylated samples was extremely reduced when compared with the fresh samples, it was decreased ~33 % for HY5.1 and ~36 % for HY30 which means the TEOS acted to close most of the external acid sites. Moreover, the BET surface area from 577.1 m² g⁻¹ to 503.1 m² g⁻¹ for HY5.1 and from 844.9 m² g⁻¹ to 610.3 m² g⁻¹ for HY30, the pore size distribution of the micropores from 6.96 Å to 6.94 Å for HY5.1 and from 7.53 Å to 7.48 Å for HY30 and the total pore volume from 0.339 m³ g⁻¹ to 0.293 m³ g⁻¹ for HY5.1 and from

0.556 m³ g⁻¹ to 0.405 m³ g⁻¹ for HY30 of the silylated zeolite samples were also slightly reduced however, the pore size distribution of the mesopores was increased from 50.59 Å to 53.61 Å for HY5.1 and from 58.45 Å to 64.63 Å for HY30.

Characterisation of the pre-coked zeolite catalysts showed that the carbonaceous compounds that were derived from different reactant species have a strikingly different effect on the alkylation reaction. The carbonaceous compounds obtained from the aromatic reactants do not induce deactivation and may enhance selectivity from ~26 % to ~33 % and from ~33 % to ~39 % for HY5.1 and HY30 respectively. However, those derived from the alkenes result in a strongly deactivating polyaromatic coke, as the elemental analysis results showed. TGA results showed that the coke formed on HY5.1 zeolite pre-coked with 1-heptene ~11.9 wt. % is more than that formed on HY5.1 zeolite pre-coked with toluene ~11.3 wt. %. However, TPO results showed that the coke formed on HY5.1 zeolite pre-coked with 1-heptene is more polyaromatic coke than that derived from the aromatic pre-cursor which is amorphous or graphitic-like carbon. In addition, the acidity of zeolite pre-coked with toluene explained that the number of acid sites reduced after this modification, it was decreased ~15 % for HY5.1 and ~17 % for HY30. Also, the surface area from 577.1 m² g⁻¹ to 408.5 m² g⁻¹ for HY5.1 and from 844.9 m² g⁻¹ to 377 m² g⁻¹ for HY30 and total pore volume from 0.339 m³ g⁻¹ to 0.25 m³ g⁻¹ for HY5.1 and from 0.556 m³ g⁻¹ to 0.283 m³ g⁻¹ for HY30 decreased after pre-treatment with toluene however, contrastingly, the size distribution of the mesopores was increased from 50.59 Å to 53.7 Å for HY5.1 and from 58.45 Å to 58.78 Å for HY30.

The catalytic performance of the fresh, silylated and pre-coked zeolite catalysts showed that TEOS and toluene molecules acted to cover the acid sites that were located on the external surface or at the pore mouth thereby leading to enhancement of the selectivity of 2-heptyltoluene from ~27 % to ~34 % for HY5.1 silylated and from ~31 % to ~35 % for HY30 silylated and from ~26 % to ~33 % and from ~33 % to ~39 % for HY5.1 toluene pre-coked and HY30 toluene pre-coked respectively accompanied by a significant reduction in the rate of coke formation during the alkylation reaction. However, 1-heptene molecules were able to penetrate through the zeolite pores and attack the internal acid sites, thereby deactivating these zeolites and leading to a reduction in the activity and selectivity of these pre-coked zeolites.

Furthermore, it can be concluded that the 1-heptene is the main coke pre-cursor that leads to deactivation of the zeolite catalysts.

Finally, characterisation of the coke that formed on the silylated zeolite catalysts showed that the amount of coke was reduced compared with that formed on the fresh zeolite, as shown in the TGA results from ~10 % to ~7.4 % for HY5.1 and from ~11.8 % to ~10 % for HY30. The TPO clarified that the structure of the coke deposited after the silylation modification was graphitic-like carbon. On the other hand, the coke formed on the toluene pre-coked HY5.1 and HY30 post reaction showed that the coke was structurally ordered. In addition, the FTIR results demonstrated that the nature of the coke formed was that of aliphatic coke species for both silylated and pre-coked zeolite samples.

To summarise, the investigation of toluene alkylation with 1-heptene over silylated and pre-coked zeolite catalysts illustrated these modifications can be used to enhance the selectivity and decrease the rate of coke formation.

8.2.4 Kinetics study of toluene alkylation with 1-heptene over fresh HY5.1 zeolite catalyst

A kinetic study of toluene alkylation with 1-heptene over HY5.1 was completed using a FBR at various reaction temperatures (60, 70, 80 and 90 °C), different contact times W/F (1.17, 2.35, 3.52, 4.7, 5.87 and 7.04 g min mol⁻¹), atmospheric pressure, 30 ml min⁻¹ of nitrogen flowrate and with a toluene to 1-heptene mole ratio of 8:1. 2-Heptyltoluene was the main product because the size of its molecules is smaller than the other monoheptyltoluene molecules which facilitates desorption of these molecules in spite of any coke formation and the subsequent diffusion limitations.

Temperature and contact time played a vital role during the alkylation of toluene with 1-heptene; the highest selectivity of 2-heptyltoluene ~28 % was obtained at higher temperature 90 °C and contact times 7.04 g min mol⁻¹. Also, the selectivity and amount of coke depend on these two main factors; the highest amount of coke ~16.5 wt. % appears at the lowest temperature 60 °C and highest W/F (7.04 g min mol⁻¹).

The main results of this kinetic study were related to the activation energy and Arrhenius constant. In general, the activation energy of the isomerisation, alkylation and coke formation reactions were in the following order:

$$E_{\text{isomerisation}} < E_{\text{alkylation}} < E_{\text{coke}}$$

8.3 Recommendations for future work

This PhD study provided essential understanding of coke formation and the main ways in which this formation can benefit the yield. The following ideas could contribute to improvements in this area in any future investigations:

- 1- In Chapter 5, the role of coke formation during toluene alkylation with 1-heptene over various zeolite catalysts using a BR and a FBR at a maximum TOS of 12 h was investigated. It was clear that, TOS has a significant impact on the coke depositions. Therefore, performing the alkylation reaction at long times will provide more details on the coke formation.
- 2- The dealumination and desilication modifications contributed to improvements of the catalytic performance and provided a clear understanding of the role of the coke that was formed on these pre-modified zeolite catalysts. The structure of the zeolite suffered from partial or complete collapse during these modifications. Therefore, to develop the zeolite structure, prevent the structure collapse and enhance the activity and stability of zeolite, a successive combination of both previous techniques should be used; either dealumination-desilication or desilication-dealumination treatments (Wei et al., 2015, Möller and Bein, 2013).
- 3- In the present study, EDX and XRF were employed to determine the Si/Al bulk mole ratio, however, there was no information for the framework Si/Al mole ratio. Therefore, either ^{27}Al or ^{29}Si Nuclear Magnetic Resonance (NMR) could provide more specific details about the zeolite structure and to determine the aluminosilicate framework of the zeolite catalyst (Zhou et al., 2017).
- 4- During the current study, TPD was employed to study the acid properties of fresh and modified zeolite samples, as described in Chapter 5 and 6. This

technique provided information on the density and strength of the acid sites but it cannot distinguish between Brønsted and Lewis acid sites. Pyridine (C_5H_5N) FTIR analysis would, therefore, be interesting to provide specific information about Brønsted and Lewis acid sites.

- 5- The influence of surface modification by either silylation or pre-coking treatments on the alkylation of toluene with 1-heptene over HY zeolite catalysts was illustrated. It was remarked that both these treatments enhanced the selectivity of desired products and reduced the coke deposition. Therefore, the main recommendation will be to increase the employment of these treatments to include other reactions such as alcohol alkylation and iso-propylation of naphthalene. On the other hand, other coke pre-cursor agents such as paraffinic or alcoholic materials can be used to enhance the catalytic performance through pre-coking modification.
- 6- In the present work, several thermal and spectroscopic techniques were used to investigate the properties of coke. Nevertheless, some other characterisation techniques (e.g. Nuclear Magnetic Resonance (NMR)) should be used to give more details about the mechanisms of coke deposition. Moreover, ^{13}C NMR could be employed to study the nature and location of carbonaceous deposits (van Donk et al., 2001, Choudhary et al., 1997).
- 7- In the present study, the coke characteristics have been studied employing *ex situ* characterisation techniques. Several problems occurred during contacting the post-reaction zeolite catalyst with the atmosphere such as alteration of the chemical structure and amount of water. Therefore, using *in situ* characterisation techniques would provide more accurate results of the nature, structure and amount of coke deposited. For instance, *in situ* NMR would be helpful to study the mechanisms of coke deposition during the reaction (Cheah et al., 1997).
- 8- Aspects of the toluene alkylation with 1-alkene mechanism have been discussed. Therefore, to elucidate the mechanism and the role of coke precursors that are used as coke agents during the pre-coking modification, ^{13}C -labelled toluene and/or benzene can be potentially used as coke

pre-cursors (Geyer et al., 2005). Adding ^{13}C -labelled aromatic hydrocarbons will help to provide more detail about coke formation.

- 9- In Chapter 7, a kinetic study of toluene alkylation with 1-heptene over HY5.1 using FBR has been completed. Therefore, developing a mathematical model will be the next step which accounts for the effectiveness factor of the catalyst (Szent-Gyergyi, 2006).

References

- Aguado, J. & Serrano, D. P. 1999. *Feedstock Recycling of Plastic Wastes.*, Cambridge, Royal Society of Chemistry.
- Ahmed, R., Sinnathambi, C. M. & Subbarao, D. 2011. Kinetics of De-coking of Spent Reforming Catalyst. *Journal of Applied Sciences*, 11, 1225-1230.
- Airproducts. 2018. *Analytical Laboratories Applications GC with Flame Ionization Detector (GC-FID)* [Online]. Available: <https://www.airproducts.com/industries/Analytical-Laboratories/analytical-lab-applications/product-list/gc-with-flame-ionization-detector-gc-fid-analytical-laboratories.aspx?itemId=D6D6641C668A47139A6F1960D9441B93> [Accessed 14-October 2018].
- Al-Khattaf, S. 2007. Enhancing p-xylene selectivity during m-xylene transformation using mildly pre-coked ZSM-5 catalyst. *Chemical Engineering and Processing: Process Intensification*, 46, 964-974.
- Al-Khattaf, S., D'agostino, C., Akhtar, M. N., Al-Yassir, N., Tan, N. Y. & Gladden, L. F. 2014. The effect of coke deposition on the activity and selectivity of the HZSM-5 zeolite during ethylbenzene alkylation reaction in the presence of ethanol. *Catalysis Science & Technology*, 4, 1017-1027.
- Al-Zaidi, B. Y., Holmes, R. J. & Garforth, A. A. 2012. Study of the Relationship between Framework Cation Levels of Y Zeolites and Behavior during Calcination, Steaming, and n-Heptane Cracking Processes. *Industrial & Engineering Chemistry Research*, 51, 6648-6657.
- Al-Zaidi, B. Y. S. 2011. *The effect of modification techniques on the performance of zeolite-Y catalysts in hydrocarbon cracking reactions*. Doctor of philosophy, The University of Manchester.
- Alonso-Morales, N., Gilarranz, M. A., Heras, F., Rodriguez, J. J. & Eser, S. 2013. Oxidation Reactivity and Structure of LDPE-Derived Solid Carbons: A Temperature-Programmed Oxidation Study. *Energy & Fuels*, 27, 1151-1161.
- Altin, O. & Eser, S. 2001. Analysis of Solid Deposits from Thermal Stressing of a JP-8 Fuel on Different Tube Surfaces in a Flow Reactor. *Industrial & Engineering Chemistry Research*, 40, 596-603.
- Andy, P., Gnep, N. S., Guisnet, M., Benazzi, E. & Travers, C. 1998. Skeletal Isomerization of n-Butenes: II. Composition, Mode of Formation, and Influence of Coke Deposits on the Reaction Mechanism. *Journal of Catalysis*, 173, 322-332.
- AOCS. 2015. *The Future of LAB* [Online]. USA: Clearance Center. Available: <http://www.aocs.org/Membership/FreeCover.cfm?ItemNumber=18059> [Accessed 24 November 2015].

- Argyle, M. & Bartholomew, C. 2015. Heterogeneous Catalyst Deactivation and Regeneration: A Review. *Catalysts*, 5, 145.
- Armor, J. N. 2011. A history of industrial catalysis. *Catalysis Today*, 163, 3-9.
- Ashcroft, A. E. 2015. *An Introduction to Mass Spectrometry* [Online]. United Kingdom: Astbury Centre for Structural Molecular Biology, the University of Leeds. Available: <http://www.astbury.leeds.ac.uk/facil/MStut/mstutorial.htm> [Accessed 30 July 2015].
- Aslam, W., Hossain, M., B. Siddiqui, A., Abussaud, B. & S. Al-Khattaf, S. 2015. *Kinetics modeling of liquid phase alkylation of benzene with dodecene over mordenite*.
- Aslam, W., Siddiqui, M. A. B., Rabindran Jermy, B., Aitani, A., Čejka, J. & Al-Khattaf, S. 2014. Selective synthesis of linear alkylbenzene by alkylation of benzene with 1-dodecene over desilicated zeolites. *Catalysis Today*, 227, 187-197.
- Bae, Y.-S., Yazaydın, A. Ö. & Snurr, R. Q. 2010. Evaluation of the BET Method for Determining Surface Areas of MOFs and Zeolites that Contain Ultra-Micropores. *Langmuir*, 26, 5475-5483.
- Baerlocher, C., L.B. Mccusker & Olson, D. H. 2007. *Atlas of Zeolite Framework Types*, Amsterdam, Elsevier.
- Barrer, R. M. 1978. *Zeolites and clay minerals as sorbents and molecular sieves*, London-New York, Academic Press.
- Barrer, R. M. 1982. *Hydrothermal Chemistry of Zeolites*, London-New York, Academic Press Inc.
- Bauer, F., Bilz, E., Chen, W. H., Freyer, A., Sauerland, V. & Liu, S. B. 2007a. Isomerization of n-butene over pre-coked HZSM-5 and HFER. In: RUREN XU, Z. G. J. C. & WENFU, Y. (eds.) *Studies in Surface Science and Catalysis*. Elsevier.
- Bauer, F., Chen, W.-H., Ernst, H., Huang, S.-J., Freyer, A. & Liu, S.-B. 2004. Selectivity improvement in xylene isomerization. *Microporous and Mesoporous Materials*, 72, 81-89.
- Bauer, F., Chen, W.-H., Zhao, Q., Freyer, A. & Liu, S.-B. 2001. Improvement of coke-induced selectivation of H-ZSM-5 during xylene isomerization. *Microporous and Mesoporous Materials*, 47, 67-77.
- Bauer, F., Chen, W. H., Bilz, E., Freyer, A., Sauerland, V. & Liu, S. B. 2007b. Surface modification of nano-sized HZSM-5 and HFER by pre-coking and silanization. *Journal of Catalysis*, 251, 258-270.

- Bauer, F. & Karge, H. G. 2007. Characterization of Coke on Zeolites. In: KARGE, H. G. & WEITKAMP, J. (eds.) *Characterization II*. Berlin, Heidelberg: Springer Berlin Heidelberg.
- Bayraktar, O. & Kugler, E. L. 2002. Characterization of coke on equilibrium fluid catalytic cracking catalysts by temperature-programmed oxidation. *Applied Catalysis A: General*, 233, 197-213.
- Bellussi, G. & Millini, R. 2007. *Zeoliti. Enciclopedia* [Online]. Available: <http://www.treccani.it/enciclopedia/zeoliti> (*Enciclopedia della Scienza e della Tecnica*) [Accessed 7 July 2015].
- Bhagat, S. D. & Rao, A. V. 2006. Surface chemical modification of TEOS based silica aerogels synthesized by two step (acid–base) sol–gel process. *Applied Surface Science*, 252, 4289-4297.
- Bleken, F. L., Barbera, K., Bonino, F., Olsbye, U., Lillerud, K. P., Bordiga, S., Beato, P., Janssens, T. V. W. & Svelle, S. 2013. Catalyst deactivation by coke formation in microporous and desilicated zeolite H-ZSM-5 during the conversion of methanol to hydrocarbons. *Journal of Catalysis*, 307, 62-73.
- Bogner, A., Jouneau, P. H., Thollet, G., Basset, D. & Gauthier, C. 2007. A history of scanning electron microscopy developments: Towards “wet-STEM” imaging. *Micron*, 38, 390-401.
- BOOMERIA. 2015. *Reaction Rates* [Online]. Available: <http://boomeria.org/chemlectures/rates/rates.html> [Accessed 15 September 2015].
- Borade, R. B. & Clearfield, A. 1996. Preparation of aluminum-rich Beta zeolite. *Microporous Materials*, 5, 289-297.
- Borutskii, P. N., Kozlova, E. G., Podkletnova, N. M., Gil’chenok, N. D., Sokolov, B. G., Zuev, V. A. & Shatovkin, A. A. 2007. Alkylation of benzene with higher olefins on heterogeneous catalysts. *Petroleum Chemistry*, 47, 250-261.
- Bradbury, S., Joy, D. C. & Ford, B. J. 2018. Scanning electron microscope. *Encyclopædia Britannica*.
- Braun, E. I. & Pantano, P. 2014. The importance of an extensive elemental analysis of single-walled carbon nanotube soot. *Carbon*, 77, 912-919.
- Brillis, A. A. & Manos, G. 2003. Coke Formation during Catalytic Cracking of C8 Aliphatic Hydrocarbons over Ultrastable Y Zeolite. *Industrial & Engineering Chemistry Research*, 42, 2292-2298.
- Busca, G. 2014. *Heterogeneous Catalytic Materials*. Amsterdam: Elsevier.

- Butt, J. B. & Peterson, E. E. 1988. *Activation, Deactivation and Poisoning of Catalysts*.
- Byrappa, K. & Yoshimura, M. 2001. *Handbook of Hydrothermal Technology*, New Jersey, Noyes Publications.
- Cadenas, M., Bringué, R., Fité, C., Iborra, M., Ramírez, E. & Cunill, F. 2014. Alkylation of toluene with 1-hexene over macroreticular ion-exchange resins. *Applied Catalysis A: General*, 485, 143-148.
- Cao, Y., Kessas, R., Naccache, C. & Ben Taarit, Y. 1999. Alkylation of benzene with dodecene. The activity and selectivity of zeolite type catalysts as a function of the porous structure. *Applied Catalysis A: General*, 184, 231-238.
- Castaño, P., Elordi, G., Olazar, M., Aguayo, A., Pawelec, B. & Bilbao, J. 2011. *Insights into the coke deposited on HZSM-5, H beta and HY zeolites during the cracking of polyethylene*.
- Cattanach, J., Wu, E. L. & Venuto, P. B. 1968. Stoichiometry of thermochemical transformations of NH₄Y zeolite. *Journal of Catalysis*, 11, 342-347.
- Čejka, J., Bekkum, H. V., Corma, A. & Schüth, F. 2007. *Introduction to Zeolite Science and Practice*, Amsterdam, Elsevier.
- Čejka, J., Filková, N., Wichterlová, B., Eder-Mirth, G. & Lercher, J. A. 1996. Decisive role of transport rate of products for zeolite para-selectivity: Effect of coke deposition and external surface silylation on activity and selectivity of HZSM-5 in alkylation of toluene. *Zeolites*, 17, 265-271.
- Cerqueira, H. S., Ayrault, P., Datka, J. & Guisnet, M. 2000. Influence of coke on the acid properties of a USHY zeolite. *Microporous and Mesoporous Materials*, 38, 197-205.
- Chang, H.-H., Cheng, C.-L., Huang, P.-J. & Lin, S.-Y. 2014. Application of scanning electron microscopy and X-ray microanalysis: FE-SEM, ESEM-EDS, and EDS mapping for studying the characteristics of topographical microstructure and elemental mapping of human cardiac calcified deposition. *Analytical and Bioanalytical Chemistry*, 406, 359-366.
- Chaouati, N., Soualah, A., Chater, M. & Pinard, L. 2017. Beneficial changes in coke properties with alkaline treatment on aluminum-rich mordenite. *Journal of Catalysis*, 353, 28-36.
- Cheah, Y. K., Alexander, P. & Gladden, L. F. 1997. Investigation of coking phenomena in zeolite HY using deuterium NMR. *Applied Catalysis A: General*, 148, 387-403.

- Chen, K., Xue, Z., Liu, H., Guo, A. & Wang, Z. 2013. A temperature-programmed oxidation method for quantitative characterization of the thermal cokes morphology. *Fuel*, 113, 274-279.
- Chen, S. & Manos, G. 2004. Study of Coke and Coke Precursors During Catalytic Cracking of n-Hexane and 1-Hexene over Ultrastable Y Zeolite. *Catalysis Letters*, 96, 195-200.
- Chen, W.-H., Bauer, F., Bilz, E., Freyer, A., Huang, S.-J., Lai, C.-S. & Liu, S.-B. 2004. Acidity characterization of H-ZSM-5 catalysts modified by pre-coking and silylation. In: E. VAN STEEN, M. C. & CALLANAN, L. H. (eds.) *Studies in Surface Science and Catalysis*. Elsevier.
- Choudhary, V. R., Devadas, P., Sansare, S. D. & Guisnet, M. 1997. Temperature Programmed Oxidation of Coked H-Gallosilicate (MFI) Propane Aromatization Catalyst: Influence of Catalyst Composition and Pretreatment Parameters. *Journal of Catalysis*, 166, 236-243.
- Christensen, C. H., Johannsen, K., Schmidt, I. & Christensen, C. H. 2003. Catalytic Benzene Alkylation over Mesoporous Zeolite Single Crystals: Improving Activity and Selectivity with a New Family of Porous Materials. *Journal of the American Chemical Society*, 125, 13370-13371.
- Chromacademy. 2015. *Theory and instrumentation of GC: Introduction to gas chromatography* [Online]. Crawford Scientific. Available: http://www.chromacademy.com/framesetchromacademy.html?fChannel=7&fCourse=66&fSco=394&fPath=sco10/gc_1_1_AimsObj.asp.pdf [Accessed 10 February 2015].
- Chua, L. M., Vazhnova, T., Mays, T. J., Lukyanov, D. B. & Rigby, S. P. 2010. Deactivation of PtH-MFI bifunctional catalysts by coke formation during benzene alkylation with ethane. *Journal of Catalysis*, 271, 401-412.
- Ciec, C. F. I. E. C. 2015. *Zeolites*. [Online]. Catalysis site. Available: http://www.catalysis-ed.org.uk/petrol/petrol3_popup.htm [Accessed 28 August 2015].
- Collett, C. H. & Mcgregor, J. 2015. Things go better with coke: the beneficial role of carbonaceous deposits in heterogeneous catalysis. *Catalysis Science & Technology*.
- Connolly, J. 2007. Introduction to X-ray Powder Diffraction. 1-9.
- Corbin, D. R., Burgess, B. F., Vega, A. J. & Farlee, R. D. 1987. Comparison of analytical techniques for the determination of silicon and aluminum content in zeolites. *Analytical Chemistry*, 59, 2722-2728.

- Corma, A., Martínez-Soria, V. & Schnoefeld, E. 2000. Alkylation of Benzene with Short-Chain Olefins over MCM-22 Zeolite: Catalytic Behaviour and Kinetic Mechanism. *Journal of Catalysis*, 192, 163-173.
- Cowley, M., De Klerk, A. & Nel, R. J. J. 2005. Amylation of Toluene by Solid Acid Catalysis. *Industrial & Engineering Chemistry Research*, 44, 5535-5541.
- Craciun, I., Reyniers, M.-F. & Marin, G. B. 2007. Effects of acid properties of Y zeolites on the liquid-phase alkylation of benzene with 1-octene: A reaction path analysis. *Journal of Molecular Catalysis A: Chemical*, 277, 1-14.
- Craciun, I., Reyniers, M.-F. & Marin, G. B. 2012. Liquid-phase alkylation of benzene with octenes over Y zeolites: Kinetic modeling including acidity descriptors. *Journal of Catalysis*, 294, 136-150.
- Csicsery, S. M. 1984. Shape-selective catalysis in zeolites. *Zeolites*, 4, 202-213.
- Da, Z., Han, Z., Magnoux, P. & Guisnet, M. 2001. Liquid-phase alkylation of toluene with long-chain alkenes over HFAU and HBEA zeolites. *Applied Catalysis A: General*, 219, 45-52.
- Da, Z., Magnoux, P. & Guisnet, M. 1999a. Alkylation of toluene with 1-dodecene over HFAU zeolite. Deactivation and regeneration. *Catalysis Letters*, 61, 203-206.
- Da, Z., Magnoux, P. & Guisnet, M. 1999b. Liquid phase alkylation of toluene with 1-heptene over a HFAU zeolite: evidence for transalkylation between toluene and non-desorbed products. *Applied Catalysis A: General*, 182, 407-411.
- Dann, S. E., Mead, P. J. & Weller, M. T. 1996. Löwenstein's Rule Extended to an Aluminum Rich Framework. The Structure of Bicchulite, $\text{Ca}_8(\text{Al}_2\text{SiO}_6)_4(\text{OH})_8$, by MASNMR and Neutron Diffraction. *Inorganic Chemistry*, 35, 1427-1428.
- De-Silva, M. N., Mcelroy, C. T., Mcgregor, J., York, A. P. E., Zeitler, J. A. & Gladden, A. L. F. 2010. Characterization of Carbon Deposits during Heterogeneous Catalysis using Terahertz Time-Domain Spectroscopy *35th International Conference on Infrared, Millimeter, and Terahertz Waves*. Rome, Italy IEEE.
- De Almeida, J. G., Dufaux, M., Ben Taarit, Y. & Naccache, C. 1994. Effect of pore size and aluminium content on the production of linear alkylbenzenes over HY, H-ZSM-5 and H-ZSM-12 zeolites: Alkylation of benzene with 1-dodecene. *Applied Catalysis A: General*, 114, 141-159.
- De Hoffmann, E. & Stroobant, V. 2007. *Mass Spectrometry Principles and Applications*, England, John Wiley & Sons Ltd.

- De Lucas, A., Canizares, P., Durán, A. & Carrero, A. 1997. Coke formation, location, nature and regeneration on dealuminated HZSM-5 type zeolites. *Applied Catalysis A: General*, 156, 299-317.
- Downard, K. 2004. *Mass Spectrometry*, United Kingdom, The Royal Society of Chemistry.
- Dutrow, B. & Clark, C. 2016. *X-ray Powder Diffraction (XRD)* [Online]. Geochemical Instrumentation and Analysis. Available: http://serc.carleton.edu/research_education/geochemsheets/techniques/XRD.html [Accessed 7/December/2016].
- EESEMI. 2004. *EDX Analysis and WDX Analysis* [Online]. Available: <http://eesemi.com/edxwdx.htm> [Accessed 24/April 2017].
- EKB 2015. *Energy Dispersive Spectroscopy*, Southern Gate, UK, John Wiley & Sons Ltd.
- ENCYCLOPÆDIA BRITANNICA. 2015. *Alkylation* [Online]. Encyclopædia Britannica Online. Available: <http://www.britannica.com/technology/alkylation-petrochemical-process> [Accessed 24 October, 2015].
- Epelde, E., Ibañez, M., Aguayo, A. T., Gayubo, A. G., Bilbao, J. & Castaño, P. 2014. Differences among the deactivation pathway of HZSM-5 zeolite and SAPO-34 in the transformation of ethylene or 1-butene to propylene. *Microporous and Mesoporous Materials*, 195, 284-293.
- Euler, L. 2014. Optimization Techniques: An Overview. In: SERKAN KIRANYAZ, DOC. TURKER INCE & GABBOUJ, M. (eds.) *Multidimensional particle swarm optimization for machine learning and pattern recognition*. Turkey: Springer.
- Fan, Z. & Watkinson, A. P. 2006. Formation and Characteristics of Carbonaceous Deposits from Heavy Hydrocarbon Coking Vapors. *Industrial & Engineering Chemistry Research*, 45, 6428-6435.
- Fiedorow, R., Frański, R., Krawczyk, A. & Beszterda, S. 2004. Carbonaceous deposits on alumina as catalysts and supports. *Journal of Physics and Chemistry of Solids*, 65, 627-632.
- Figueiredo, J. L., Pereira, M. M. & Faria, J. 2008. *Catalysis from theory to application*, Portugal, Imprensa da Universidade de Coimbra.
- Fogler, H. S. 2006. *Elements of chemical reaction engineering*.

- Font-Bardia, M. & Alcobé, X. 2012. X-ray single crystal and powder diffraction: possibilities and applications. *Handbook of instrumental techniques for materials, chemical and biosciences research, Part I. materials technologies (MT)*, MT, 9, 14.
- Fung, S. C. & Querini, C. A. 1992. A highly sensitive detection method for temperature programmed oxidation of coke deposits: Methanation of CO₂ in the presence of O₂. *Journal of Catalysis*, 138, 240-254.
- Galadima, A. & Muraza, O. 2015. Role of zeolite catalysts for benzene removal from gasoline via alkylation: A review. *Microporous and Mesoporous Materials*, 213, 169-180.
- Gerlach, G. & Dotzel, W. 2008. *Introduction to Microsystem Technology: A Guide for Students (Wiley Microsystem and Nanotechnology)*, Wiley Publishing.
- Geyer, R., Peacock, A. D., Miltner, A., Richnow, H. H., White, D. C., Sublette, K. L. & Kästner, M. 2005. In Situ Assessment of Biodegradation Potential Using Biotraps Amended with ¹³C-Labeled Benzene or Toluene. *Environmental Science & Technology*, 39, 4983-4989.
- Golding, C. G., Lamboo, L. L., Beniac, D. R. & Booth, T. F. 2016. The scanning electron microscope in microbiology and diagnosis of infectious disease. *Scientific Reports*, 6, 26516.
- Goldstein, J. I., Newbury, D. E., Echlin, P., Joy, D. C., Jr., A. D. R., Lyman, C. E., Fiori, C. & Lifshin, E. 1992. *Scanning electron microscopy and X-ray microanalysis*. 2nd ed ed. New York, USA: Plenum Press.
- Gomez Sanz, S., Mcmillan, L., Mcgregor, J., Zeitler, J. A., Al-Yassir, N., Al-Khattaf, S. & Gladden, L. F. 2016. The enhancement of the catalytic performance of CrO_x/Al₂O₃ catalysts for ethylbenzene dehydrogenation through tailored coke deposition. *Catalysis Science & Technology*, 6, 1120-1133.
- Gorte, R. J. 1999. What do we know about the acidity of solid acids? *Catalysis Letters*, 62, 1-13.
- Gregg, S. J. & Sing, K. S. W. 1982. *Adsorption, surface area, and porosity*, London; New York, Academic Press.
- Groen, J. C. 2007. *Mesoporous Zeolites Obtained by Desilication*, Netherlands, Ponsen & Looijen B.V.
- Groen, J. C., Moulijn, J. A. & Perez-Ramirez, J. 2006. Desilication: on the controlled generation of mesoporosity in MFI zeolites. *Journal of Materials Chemistry*, 16, 2121-2131.

- Groen, J. C., Moulijn, J. A. & Pérez-Ramírez, J. 2005. Decoupling mesoporosity formation and acidity modification in ZSM-5 zeolites by sequential desilication–dealumination. *Microporous and Mesoporous Materials*, 87, 153-161.
- Gründling, C., Eder-Mirth, G. & Lercher, J. A. 1996. Selectivity Enhancement in Methylamine Synthesis via Postsynthesis Modification of Brønsted Acidic Mordenite: An Infrared Spectroscopic and Kinetic Study on the Reaction Mechanism. *Journal of Catalysis*, 160, 299-308.
- Guisnet, M. 2002. “Coke” molecules trapped in the micropores of zeolites as active species in hydrocarbon transformations. *Journal of Molecular Catalysis A: Chemical*, 182–183, 367-382.
- Guisnet, M., Costa, L. & Ribeiro, F. R. 2009. Prevention of zeolite deactivation by coking. *Journal of Molecular Catalysis A: Chemical*, 305, 69-83.
- Guisnet, M. & Gilson, J.-P. 2002. *Zeolites for Cleaner Technologies*, London, Imperial College Press.
- Guisnet, M. & Magnoux, P. 1989. Coking and deactivation of zeolites: Influence of the Pore Structure. *Applied Catalysis*, 54, 1-27.
- Guisnet, M. & Magnoux, P. 1997. Deactivation by coking of zeolite catalysts. Prevention of deactivation. Optimal conditions for regeneration. *Catalysis Today*, 36, 477-483.
- Guisnet, M. & Magnoux, P. 2001. Organic chemistry of coke formation. *Applied Catalysis A: General*, 212, 83-96.
- Guisnet, M. & Pinard, L. 2018. Characterization of acid-base catalysts through model reactions. *Catalysis Reviews*, 60, 337-436.
- Guisnet, M. & Ribeiro, F. R. 2011. *Deactivation and Regeneration of Zeolite Catalysts*. London: Imperial College Press.
- Guisnet, M. R. 1990. Model reactions for characterizing the acidity of solid catalysts. *Accounts of Chemical Research*, 23, 392-398.
- Guthrie, J. M. 2012. *Overview of X-ray Fluorescence* [Online]. University of Missouri–Columbia. Available: http://archaeometry.missouri.edu/xrf_overview.html [Accessed 30/May 2017].
- Haag, W. O. & Olson, D. H. 1978a. *Selective Disproportionation of Toluene*. United States Patent Office 4097543.
- Haag, W. O. & Olson, D. H. 1978b. *Selective Production of Para Dialkyl Substituted Benzenes*. United States Patent Office 4117026.

- Haag, W. O., Olson, D. H. & Rodewald, P. G. 1985. *Catalytic Conversion Process for Aromatic Feedstocks with Hydrogen Regeneration of Coke-Selectivated Zeolite Catalyst*. United States Patent Office 4508836.
- Hagen, J. 2006. *Industrial Catalysis: a practical approach*, Weinheim, Wiley-VCH.
- Hajimirzaee, S., Ainte, M., Soltani, B., Behbahani, R. M., Leeke, G. A. & Wood, J. 2015. Dehydration of methanol to light olefins upon zeolite/alumina catalysts: Effect of reaction conditions, catalyst support and zeolite modification. *Chemical Engineering Research and Design*, 93, 541-553.
- Harriott, P. 2003. *Chemical Reactor Design*, New York, U.S.A.
- Hassan, R., Cohanin, B., De Weck, O. & Venter, G. 2005. A Comparison of Particle Swarm Optimization and the Genetic Algorithm. *46th AIAA/ASME/ASCE/AHS/ASC Structures, Structural Dynamics and Materials Conference*. American Institute of Aeronautics and Astronautics.
- Hattori, H. 2010. Solid Acid Catalysts: Roles in Chemical Industries and New Concepts. *Topics in Catalysis*, 53, 432-438.
- Hibino, T., Niwa, M. & Murakami, Y. 1991. Shape-selectivity over hzsm-5 modified by chemical vapor deposition of silicon alkoxide. *Journal of Catalysis*, 128, 551-558.
- Holmes, S. M., Garforth, A., Maunders, B. & Dwyer, J. 1997. A solvent extraction method to study the location and concentration of coke formed on zeolite catalysts. *Applied Catalysis A: General*, 151, 355-372.
- Hopkins, P. D., Miller, J. T., Meyers, B. L., Ray, G. J., Roginski, R. T., Kuehne, M. A. & Kung, H. H. 1996. Acidity and cracking activity changes during coke deactivation of ultrastable Y zeolite. *Applied Catalysis A: General*, 136, 29-48.
- Horňáček, M., Horňáčková, M., Lovás, P., Veis, P., Hudec, P., Smiešková, A. & Velebná, K. 2013. *The influence of desilication and dealumination on the activity of mordenite catalysts in alkylation of aromatics with 1-alkenes*.
- Horňáček, M., Hudec, P., Nociar, A., Smiešková, A. & Jakubík, T. 2010a. Activity and regenerability of dealuminated zeolite Y in liquid phase alkylation of benzene with 1-alkene. *Chemical Papers*, 64, 469-474.
- Horňáček, M., Hudec, P., Smiešková, A. & Jakubík, T. 2009a. Alkylation of Benzene with 1-Alkenes over Zeolite Y and Mordenite. *Acta Chimica Slovaca*, 2, 31-45.

- Horňáček, M., Hudec, P., Smiešková, A. & Jakubík, T. 2009b. ALKYLATION OF BENZENE WITH LINEAR 1-ALKENES IN LIQUID PHASE. INFLUENCE OF ZEOLITE TYPE AND CHAIN LENGTH OF 1-ALKENES ON THE ACTIVITY AND SELECTIVITY. *International Petroleum Conference*, 44, 1-12.
- Horňáček, M., Hudec, P., Smiešková, A. & Jakubík, T. 2010b. Alkylation of benzene with 1-alkenes over beta zeolite in liquid phase. *Reaction Kinetics, Mechanisms and Catalysis*, 99, 431-437.
- Ibáñez, M., Gamero, M., Ruiz-Martínez, J., Weckhuysen, B. M., Aguayo, A. T., Bilbao, J. & Castaño, P. 2016. Simultaneous coking and dealumination of zeolite H-ZSM-5 during the transformation of chloromethane into olefins. *Catalysis Science & Technology*, 6, 296-306.
- Imelik, B. & Viedrine, J. C. 1994. *Catalyst Characterization: Physical Techniques for Solid Materials*, FUNDAMENTAL AND APPLIED CATALYSIS.
- Jae, J., Tompsett, G. A., Foster, A. J., Hammond, K. D., Auerbach, S. M., Lobo, R. F. & Huber, G. W. 2011. Investigation into the shape selectivity of zeolite catalysts for biomass conversion. *Journal of Catalysis*, 279, 257-268.
- Jang, K. W., Choi, S. H., Pyun, S. I. & John, M. S. 2001. The Effects of the Water Content, Acidity, Temperature and Alcohol Content on the Acidic Sol-Gel Polymerization of Tetraethoxysilane (TEOS) with Monte Carlo Simulation. *Molecular Simulation*, 27, 1-16.
- Jiang, P., Ma, L., Pan, J., Chun, Y., Xu, Q. & Dong, J. 2009. Preparation of Amphiphilic HZSM-5 Zeolite by Chemical Vapor Deposition of Trimethylchlorosilane. *Chinese Journal of Catalysis*, 30, 503-508.
- JOVE. 2018. *Gas Chromatography (GC) with Flame-Ionization Detection*. [Online]. Cambridge. Available: <https://www.jove.com/science-education/10187/gas-chromatography-gc-with-flame-ionization-detection> [Accessed 14-October 2018].
- Joy, D. C. 1997. Scanning electron microscopy for materials characterization. *Current Opinion in Solid State and Materials Science*, 2, 465-468.
- Kaeding, W. W., Chu, C., Young, L. B., Weinstein, B. & Butter, S. A. 1981. Selective alkylation of toluene with methanol to produce para-Xylene. *Journal of Catalysis*, 67, 159-174.
- Kaneko, K. 1994. Determination of pore size and pore size distribution: 1. Adsorbents and catalysts. *Journal of Membrane Science*, 96, 59-89.

- Kaneko, K. & Ishii, C. 1992. Superhigh surface area determination of microporous solids. *Colloids and Surfaces*, 67, 203-212.
- Karasek, F. W. & Clement, R. E. 1988. *Basic gas chromatography-mass spectrometry: principles and techniques*, Amsterdam, Elsevier.
- Keeley, R. 2000. X-ray Fluorescence Spectrometry—Second Edition by Ron Jenkins, Wiley-Interscience, New York, 1999,. Elsevier.
- Kim, J.-H., Ishida, A., Okajima, M. & Niwa, M. 1996. Modification of HZSM-5 by CVD of Various Silicon Compounds and Generation of Para-Selectivity. *Journal of Catalysis*, 161, 387-392.
- Kim, J., Choi, M. & Ryoo, R. 2010. Effect of mesoporosity against the deactivation of MFI zeolite catalyst during the methanol-to-hydrocarbon conversion process. *Journal of Catalysis*, 269, 219-228.
- Kirumakki, S. R., Nagaraju, N. & Narayanan, S. 2004. A comparative esterification of benzyl alcohol with acetic acid over zeolites H β , HY and HZSM5. *Applied Catalysis A: General*, 273, 1-9.
- Kocal, J. A., Vora, B. V. & Imai, T. 2001. Production of linear alkylbenzenes. *Applied Catalysis A: General*, 221, 295-301.
- Krtil, J., Čejka, J. & Wichterlová, B. 1997. *Zeolite Silylation for the Enhancement of para-Selectivity in Toluene Alkylation with Ethylene*.
- Kulprathipanja, S. 2010. *Zeolites in Industrial Separation and Catalysis*, Weinheim, WILEY-VCH.
- Kumar, R., Kumar, A. & Khanna, A. 2012. Synthesis, characterization and kinetics of AlCl₃ supported on silica superacid catalysts for the formation of linear alkylbenzenes. *Reaction Kinetics, Mechanisms and Catalysis*, 106, 141-155.
- Laforge, S., Martin, D. & Guisnet, M. 2004. m-Xylene transformation over H-MCM-22 zeolite. 2. Method for determining the catalytic role of the three different pore systems. *Microporous and Mesoporous Materials*, 67, 235-244.
- Lange, J. P., Gutsze, A., Allgeier, J. & Karge, H. G. 1988. Coke formation through the reaction of ethene over hydrogen mordenite: III. IR and ¹³C-NMR studies. *Applied Catalysis*, 45, 345-356.
- Lee, C. K., Gladden, L. F. & Barrie, P. J. 2004. TEOM studies on the adsorption of p-xylene in coked FCC catalysts: observation of coke promoting chemical reaction. *Applied Catalysis A: General*, 274, 269-274.

- Lee, K., Lee, S., Jun, Y. & Choi, M. 2017. Cooperative effects of zeolite mesoporosity and defect sites on the amount and location of coke formation and its consequence in deactivation. *Journal of Catalysis*, 347, 222-230.
- Lei, Z., Li, C., Chen, B., Erqiang, W. & Zhang, J. 2003. Study on the alkylation of benzene and 1-dodecene. *Chemical Engineering Journal*, 93, 191-200.
- LENNTECH. 2015. *Zeolites applications* [Online]. Available: <http://www.lenntech.pl/zeolites-applications.htm> [Accessed].
- Li, C. E. & Brown, T. C. 1999. Temperature-Programmed Oxidation of Coke Deposited by 1-Octene on Cracking Catalysts. *Energy & Fuels*, 13, 888-894.
- Li, H., Wang, Y., Fan, C., Sun, C., Wang, X., Wang, C., Zhang, X. & Wang, S. 2018. Facile synthesis of a superior MTP catalyst: Hierarchical micro-meso-macroporous ZSM-5 zeolites. *Applied Catalysis A: General*, 551, 34-48.
- Li, S., Zheng, A., Su, Y., Zhang, H., Chen, L., Yang, J., Ye, C. & Deng, F. 2007. Brønsted/Lewis Acid Synergy in Dealuminated HY Zeolite: A Combined Solid-State NMR and Theoretical Calculation Study. *American Chemical Society*, 129, 11161-11171.
- Liang, W., Jin, Y., Yu, Z., Wang, Z., Han, B., M., H. & E., M. 1996. Alkylation of benzene with dodecene over HY zeolite: Deactivation, regeneration, and product distribution. *Elsevier Science Inc.*, 17, 297-303.
- Liang, W., Zhiqing, Y., Yong, J., Zhanwen, W., Yao, W., Mingyuan, H. & Enze, M. 1995. Synthesis of linear alkylbenzene in a liquid–solid circulating fluidized bed reactor. *Journal of Chemical Technology & Biotechnology*, 62, 98-102.
- Lin, J.-S., Wang, J.-J., Wang, J., Wang, I., Balasamy, R. J., Aitani, A., Al-Khattaf, S. & Tsai, T.-C. 2013. Catalysis of alkaline-modified mordenite for benzene alkylation of diolefin-containing dodecene for linear alkylbenzene synthesis. *Journal of Catalysis*, 300, 81-90.
- LINDE. 2015. *Gas chromatography* [Online]. Germany: Linde Gas Division. Available: http://hiq.linde-gas.com/en/analytical_methods/gas_chromatography/index.html [Accessed 28 July 2015].
- Lisovskii, A. E. & Aharoni, C. 1994. Carbonaceous Deposits as Catalysts for Oxydehydrogenation of Alkylbenzenes. *Catalysis Reviews*, 36, 25-74.
- Liu, S.-B., Wu, J.-F., Ma, L.-J., Tsai, T.-C. & Wang, I. 1991. On the thermal stability of zeolite beta. *Journal of Catalysis*, 132, 432-439.

- Liu, Y., Xu, L., Xu, B., Li, Z., Jia, L. & Guo, W. 2009. Toluene alkylation with 1-octene over supported heteropoly acids on MCM-41 catalysts. *Journal of Molecular Catalysis A: Chemical*, 297, 86-92.
- Lónyi, F. & Valyon, J. 2001. On the interpretation of the NH₃-TPD patterns of H-ZSM-5 and H-mordenite. *Microporous and Mesoporous Materials*, 47, 293-301.
- Lovás, P., Hornáček, M., Hudec, P. & Jorík, V. 2014. Preparation of an active and regenerable catalyst for liquid-phase alkylation of toluene with 1-decene. *Applied Catalysis A: General*, 475, 341-346.
- Lutz, W. 2014. *Zeolite Y: Synthesis, Modification, and Properties—A Case Revisited* [Online]. Available: <http://www.hindawi.com/journals/amse/2014/724248/> [Accessed 2014].
- Magnoux, P., Mourran, A., Bernard, S. & Guisnet, M. 1997. Influence of the acidity and of the pore structure of zeolites on the alkylation of toluene by 1-heptene. In: H.U. BLASER, A. B. & PRINS, R. (eds.) *Studies in Surface Science and Catalysis*. Elsevier.
- Margeta, K., Logar, N. Z., Šiljeg, M. & Farkaš, A. 2013. *Natural Zeolites in Water Treatment – How Effective is Their Use*, Croatia, In Tech.
- Martin, A. J. P. & Synge, R. L. M. 1941. A new form of chromatogram employing two liquid phases: A theory of chromatography. 2. Application to the micro-determination of the higher monoamino-acids in proteins. *Biochemical Journal*, 35, 1358-1368.
- Mccall, J. 2005. Genetic algorithms for modelling and optimisation. *Journal of Computational and Applied Mathematics*, 184, 205-222.
- Mcgregor, J., Canning, A. S., Mitchell, S., Jackson, S. D. & Gladden, L. F. 2010a. The influence of carbon laydown on selectivity in the hydrogenation of pentenenitriles over supported-nickel catalysts. *Applied Catalysis A: General*, 384, 192-200.
- Mcgregor, J. & Gladden, L. F. 2008. The role of carbon deposits in the hydrogenation of C₅ hydrocarbons. *Applied Catalysis A: General*, 345, 51-57.
- Mcgregor, J., Huang, Z., Parrott, E. P. J., Zeitler, J. A., Nguyen, K. L., Rawson, J. M., Carley, A., Hansen, T. W., Tessonier, J.-P., Su, D. S., Teschner, D., Vass, E. M., Knop-Gericke, A., Schlögl, R. & Gladden, L. F. 2010b. Active coke: Carbonaceous materials as catalysts for alkane dehydrogenation. *Journal of Catalysis*, 269, 329-339.
- Mekki-Berrada, A. & Auroux, A. 2012. *Characterization of Solid Materials and Heterogeneous Catalysts*, Wiley-VCH, Weinheim.

- Melkote, R. R. & Jensen, K. F. 1989. Models for catalytic pore plugging: application to hydrodemetallation. *Chemical Engineering Science*, 44, 649-663.
- Menon, P. G. 1990. Coke on catalysts-harmful, harmless, invisible and beneficial types. *Journal of Molecular Catalysis*, 59, 207-220.
- Mériaudeau, P., Ben Taarit, Y., Thangaraj, A., Almeida, J. L. G. & Naccache, C. 1997. Zeolite based catalysts for linear alkylbenzene production: Dehydrogenation of long chain alkanes and benzene alkylation. *Catalysis Today*, 38, 243-247.
- Meunier, F. C., Domokos, L., Seshan, K. & Lercher, J. A. 2002. In Situ IR Study of the Nature and Mobility of Sorbed Species on H-FER during But-1-ene Isomerization. *Journal of Catalysis*, 211, 366-378.
- Mihindou-Koumba, P. C., Comparot, J. D., Laforge, S. & Magnoux, P. 2008. Methylcyclohexane transformation over H-EU-1 zeolite: Selectivity and catalytic role of the acid sites located at the pore mouths. *Journal of Catalysis*, 255, 324-334.
- Milton, R. M. 1989. *Molecular Sieve Science and Technology*, Washington, DC, American Chemical Society.
- Mochizuki, H., Yokoi, T., Imai, H., Namba, S., Kondo, J. N. & Tatsumi, T. 2012. Effect of desilication of H-ZSM-5 by alkali treatment on catalytic performance in hexane cracking. *Applied Catalysis A: General*, 449, 188-197.
- Möller, K. & Bein, T. 2013. Mesoporosity – a new dimension for zeolites. *Royal Society of Chemistry*, 42, 3689-3707.
- Mori, N., Nishiyama, S., Tsuruya, S. & Masai, M. 1991. Deactivation of zeolites in n-hexane cracking. *Applied Catalysis*, 74, 37-52.
- Müller, S., Liu, Y., Vishnuvarthan, M., Sun, X., Van Veen, A. C., Haller, G. L., Sanchez-Sanchez, M. & Lercher, J. A. 2015. Coke formation and deactivation pathways on H-ZSM-5 in the conversion of methanol to olefins. *Journal of Catalysis*, 325, 48-59.
- Nel, R. J. J. & De Klerk, A. 2007. Selectivity Differences of Hexene Isomers in the Alkylation of Benzene over Solid Phosphoric Acid. *Industrial & Engineering Chemistry Research*, 46, 2902-2906.
- Ng, L. V. & McCormick, A. V. 1996. Acidic Sol-Gel Polymerization of TEOS: Effect of Solution Composition on Cyclization and Bimolecular Condensation Rates. *The Journal of Physical Chemistry*, 100, 12517-12531.

- Nishi, Y. & Inagaki, M. 2016. Chapter 11 - Gas Adsorption/Desorption Isotherm for Pore Structure Characterization. *In: INAGAKI, M. & KANG, F. (eds.) Materials Science and Engineering of Carbon*. Butterworth-Heinemann.
- Niwa, M. & Katada, N. 1997. Measurements of acidic property of zeolites by temperature programmed desorption of ammonia. *Catalysis Surveys from Asia*, 1, 215-226.
- Niwa, M., Kato, S., Hattori, T. & Murakami, Y. 1984. Fine control of the pore-opening size of the zeolite mordenite by chemical vapour deposition of silicon alkoxide. *Journal of the Chemical Society, Faraday Transactions 1: Physical Chemistry in Condensed Phases*, 80, 3135-3145.
- Nummi, E. 2016. *Question About XRF and Element Ions* [Online]. Thermo Fisher Scientific. Available: <https://www.thermofisher.com/blog/metals/question-about-xrf-and-element-ions/> [Accessed 31/May 2017].
- O'connor, C. T., Möller, K. P. & Manstein, H. 2007. The Effect of Silanisation on the Catalytic and Sorption Properties of Zeolites. *KONA Powder and Particle Journal*, 25, 230-236.
- Ojha, K., Pradhan, N. C. & Samanta, A. N. 2004. Zeolite from fly ash: synthesis and characterization. *Bulletin of Materials Science*, 27, 555-564.
- Olson, D. H. & Haag, W. O. 1984. Structure-Selectivity Relationship in Xylene Isomerization and Selective Toluene Disproportionation. *Catalytic Materials: Relationship Between Structure and Reactivity*. American Chemical Society.
- Perego, C. & Ingallina, P. 2002. *Combining alkylation and transalkylation for alkylaromatic production* [Online]. Available: <http://www.researchgate.net/publication/260362959> [Accessed].
- Perego, C., Amarillia, S., Bellussia, G., Cappellazzob, O., G., G. & M., S. 2013. *The development of a new zeolite catalyst for the production of cumene: a case history* [Online]. Available: <http://www.researchgate.net/publication/236874011> [Accessed].
- Pérez-Ramírez, J., Verboekend, D., Bonilla, A. & Abelló, S. 2009. Zeolite Catalysts with Tunable Hierarchy Factor by Pore-Growth Moderators. *Advanced Functional Materials*, 19, 3972-3979.
- Petkovic, L. M. & Ginosar, D. M. 2004. The effect of supercritical isobutane regeneration on the nature of hydrocarbons deposited on a USY zeolite catalyst utilized for isobutane/butene alkylation. *Applied Catalysis A: General*, 275, 235-245.

- Pillay, A. E. & Peisach, M. 1991. Zeolite analysis: PIXE, XRF or neutron activation. *Journal of Radioanalytical and Nuclear Chemistry*, 153, 75-84.
- Price, D. 2006. *Thermogravimetry* [Online]. IPTME, Loughborough University: in Available: <http://www.slideshare.net/nimmidalwadi5/tga> [Accessed 2/January/2017].
- Purdue-University. 2014. *Scanning Electron Microscope* [Online]. Available: <https://www.purdue.edu/ehrs/rem/rs/sem.htm> [Accessed 15/April 2017].
- Querini, C. A. 2004. Coke characterization. In: SPIVEY, J. J. & ROBERTS, G. W. (eds.) *Catalysis: Volume 17*. The Royal Society of Chemistry.
- Querini, C. A. & Fung, S. C. 1997. Coke characterization by temperature programmed techniques. *Catalysis Today*, 37, 277-283.
- Querini, C. A. & Roa, E. 1997. Deactivation of solid acid catalysts during isobutane alkylation with C4 olefins. *Applied Catalysis A: General*, 163, 199-215.
- Radwan, M. A., Kyotani, T. & Tomita, A. 2000. *Characterization of coke deposited from cracking of benzene over USY zeolite catalyst*.
- Robson, H. 2001. Preface to the second edition. *Verified Syntheses of Zeolitic Materials*. Amsterdam: Elsevier Science.
- Rojo-Gama, D., Signorile, M., Bonino, F., Bordiga, S., Olsbye, U., Lillerud, K. P., Beato, P. & Svelle, S. 2017. Structure–deactivation relationships in zeolites during the methanol–to–hydrocarbons reaction: Complementary assessments of the coke content. *Journal of Catalysis*, 351, 33-48.
- Rouquerol, J., Rouquerol, F. & Sing, K. 1999. *Adsorption by Powders and Porous Solids*, Academic Press
- Sadowska, K., Wach, A., Olejniczak, Z., Kuśtrowski, P. & Datka, J. 2013. Hierarchic zeolites: Zeolite ZSM-5 desilicated with NaOH and NaOH/tetrabutylamine hydroxide. *Microporous and Mesoporous Materials*, 167, 82-88.
- Sahebdehfar, S., Kazemeini, M., Khorasheh, F. & Badakhshan, A. 2002. Deactivation behavior of the catalyst in solid acid catalyzed alkylation: effect of pore mouth plugging. *Chemical Engineering Science*, 57, 3611-3620.
- Sánchez, B., Gross, M. S., Costa, B. D. & Querini, C. A. 2009. Coke analysis by temperature-programmed oxidation: Morphology characterization. *Applied Catalysis A: General*, 364, 35-41.

- Sandoval-Díaz, L.-E., González-Amaya, J.-A. & Trujillo, C.-A. 2015. General aspects of zeolite acidity characterization. *Microporous and Mesoporous Materials*, 215, 229-243.
- Sengupta, S., Basak, S. & Peters, R. 2018. Particle Swarm Optimization: A Survey of Historical and Recent Developments with Hybridization Perspectives. *Machine Learning and Knowledge Extraction*, 1, 10.
- Shang, Y., Yang, P., Jia, M., Zhang, W. & Wu, T. 2008. Modification of MCM-22 zeolites with silylation agents: Acid properties and catalytic performance for the skeletal isomerization of n-butene. *Catalysis Communications*, 9, 907-912.
- Shehab, A. K. 2018. *The Role of Carbon in the Catalytic Isomerisation-Cracking of n-Alkanes*. PhD, The University of Sheffield.
- Shewale, P. M., Rao, A. V. & Rao, A. P. 2008. Effect of different trimethyl silylating agents on the hydrophobic and physical properties of silica aerogels. *Applied Surface Science*, 254, 6902-6907.
- Sie, S. T. 1980. Catalyst Deactivation by Poisoning and Pore Plugging in Petroleum Processing. In: DELMON, B. & FROMENT, G. F. (eds.) *Studies in Surface Science and Catalysis*. Elsevier.
- Siffert, S., Gaillard, L. & Su, B. L. 2000. Alkylation of benzene by propene on a series of Beta zeolites: toward a better understanding of the mechanisms. *Journal of Molecular Catalysis A: Chemical*, 153, 267-279.
- Silaghi, M.-C. 2014. *Ab initio Molecular Modelling of the Dealumination and Desilication Mechanisms of Relevant Zeolite Frameworks*. University of Lyon.
- Silaghi, M.-C., Chizallet, C. & Raybaud, P. 2014. Challenges on molecular aspects of dealumination and desilication of zeolites. *Microporous and Mesoporous Materials*, 191, 82-96.
- Simonic, P. & Armbruster, T. 2004. *Peculiarity and defect structure of the natural and synthetic zeolite mordenite: A single-crystal X-ray study*.
- Sing, K. 2001. The use of nitrogen adsorption for the characterisation of porous materials. *Colloids and Surfaces A: Physicochemical and Engineering Aspects*, 187-188, 3-9.
- Smirniotis, P. G. & Ruckenstein, E. 1995. Alkylation of Benzene or Toluene with MeOH or C₂H₄ over ZSM-5 or .beta. Zeolite: Effect of the Zeolite Pore Openings and of the Hydrocarbons Involved on the Mechanism of Alkylation. *Industrial & Engineering Chemistry Research*, 34, 1517-1528.

- Sotelo, J. L., Calvo, L., Pérez-Velázquez, A. & Capilla, D. 2005. *Effect of the contact time (W/F) on the coking deactivation process in the transalkylation of diisopropylbenzene with benzene over beta zeolite in sc-CO₂*.
- Storck, S., Bretinger, H. & Maier, W. F. 1998. Characterization of micro- and mesoporous solids by physisorption methods and pore-size analysis. *Applied Catalysis A: General*, 174, 137-146.
- Suwardiyanto, Howe, R. F., Gibson, E. K., Catlow, C. R. A., Hameed, A., Mcgregor, J., Collier, P., Parker, S. F. & Lennon, D. 2017. An assessment of hydrocarbon species in the methanol-to-hydrocarbon reaction over a ZSM-5 catalyst. *Faraday Discussions*, 197, 447-471.
- Szent-Gyergyi, A. 2006. Diffusion and Reaction. In: FOGLER, H. S. (ed.) *Elements of Chemical Reaction Engineering*. United States.
- Thompson, M. 2008. CHNS Elemental Analysers. *The Royal Society of Chemistry*, 29, 1-2.
- Tongcheng, C., Zhongliang, Z., Xiaofeng, H. & Tonghua, L. 2005. *Simultaneous Determination of Reaction Order and Rate Constant of Consecutive Reactions by Union Optimization Algorithm of NGA-TS*.
- Treacy, M. M. J. & Higgins, J. B. 2007. *Collection of Simulated XRD Powder Patterns for Zeolites Fifth (5th) Revised Edition*.
- Triantafillidis, C. S., Vlessidis, A. G. & Evmiridis, N. P. 2000. Dealuminated H–Y Zeolites: Influence of the Degree and the Type of Dealumination Method on the Structural and Acidic Characteristics of H–Y Zeolites. *Industrial & Engineering Chemistry Research*, 39, 307-319.
- Tsai, T.-C., Liu, S.-B. & Wang, I. 1999. Disproportionation and transalkylation of alkylbenzenes over zeolite catalysts. *Applied Catalysis A: General*, 181, 355-398.
- Tsai, T.-C., Wang, I., Li, S.-J. & Liu, J.-Y. 2003. Development of a green LAB process: alkylation of benzene with 1-dodecene over mordenite. *Green Chemistry*, 5, 404-409.
- Tu, J. V. 1996. Advantages and disadvantages of using artificial neural networks versus logistic regression for predicting medical outcomes. *Journal of Clinical Epidemiology*, 49, 1225-1231.
- Uguina, M. A., Serrano, D. P., Van Grieken, R. & Vènes, S. 1993. Adsorption, acid and catalytic changes induced in ZSM-5 by coking with different hydrocarbons. *Applied Catalysis A: General*, 99, 97-113.
- UOP 2007. UOP Linear Alkylbenzene (LAB) Complex.

- Van Bekkum, H., Flanigen, E. M. & Jansen, J. C. 2001. *Introduction to Zeolite Science and Practice*, Amsterdam, Elsevier.
- Van Donk, S., Bitter, J. H. & De Jong, K. P. 2001. Deactivation of solid acid catalysts for butene skeletal isomerisation: on the beneficial and harmful effects of carbonaceous deposits. *Applied Catalysis A: General*, 212, 97-116.
- Verboekend, D. & Pérez-Ramírez, J. 2011. Design of hierarchical zeolite catalysts by desilication. *Catalysis Science & Technology*, 1, 841-1084.
- Vernon-Parry, K. D. 2000. Scanning electron microscopy: an introduction. *III-Vs Review*, 13, 40-44.
- Von Arx, K. B., Manock, J. J., Huffman, S. W. & Messina, M. 1998. Using Limited Concentration Data for the Determination of Rate Constants with the Genetic Algorithm. *Environmental Science & Technology*, 32, 3207-3212.
- Wan, Z., Li, G. K., Wang, C., Yang, H. & Zhang, D. 2018. Relating coke formation and characteristics to deactivation of ZSM-5 zeolite in methanol to gasoline conversion. *Applied Catalysis A: General*, 549, 141-151.
- Wang, B. 2007. *Zeolite Deactivation During Hydrocarbon Reactions: Characterisation of Coke Precursors and Acidity, Product Distribution*. PhD Thesis, University College London.
- Wang, B., Lee, C., Cai, T.-X. & Park, S.-E. 2001a. Benzene Alkylation with 1-Dodecene over H-Mordenite Zeolite. *Catalysis Letters*, 76, 99-103.
- Wang, B., Lee, C. W., Cai, T. X. & Park, S. E. 2001b. *Benzene alkylation with 1-dodecene over Y zeolite*.
- Wang, B. & Manos, G. 2007a. Acid Site Characterization of Coked USHY Zeolite Using Temperature Programmed Desorption with a Component-Nonspecific Detector. *Industrial & Engineering Chemistry Research*, 46, 7977-7983.
- Wang, B. & Manos, G. 2007b. A novel thermogravimetric method for coke precursor characterisation. *Journal of Catalysis*, 250, 121-127.
- Wang, Z., Wang, L., Jiang, Y., Hunger, M. & Huang, J. 2014. Cooperativity of Brønsted and Lewis Acid Sites on Zeolite for Glycerol Dehydration. *ACS Catalysis*, 4, 1144-1147.
- Weber, R. W., Möller, K. P. & O'connor, C. T. 2000. The chemical vapour and liquid deposition of tetraethoxysilane on ZSM-5, mordenite and beta. *Microporous and Mesoporous Materials*, 35-36, 533-543.

- Weber, R. W., Möller, K. P., Unger, M. & O'connor, C. T. 1998. The chemical vapour and liquid deposition of tetraethoxysilane on the external surface of ZSM-5. *Microporous and Mesoporous Materials*, 23, 179-187.
- Weckhuysen, B. M. & Yu, J. 2015. Recent advances in zeolite chemistry and catalysis. *Chemical Society Reviews*, 44, 7022-7024.
- Wei, Y., Parmentier, T. E., De Jong, K. P. & Zečević, J. 2015. Tailoring and visualizing the pore architecture of hierarchical zeolites. Available: <http://pubs.rsc.org/en/content/articlehtml/2015/cs/c5cs00155b> [Accessed 7/September/2015].
- Weitkamp, J. 2000. Zeolites and catalysis. *Solid State Ionics*, 131, 175-188.
- Weitkamp, L. & Puppe, L. 1999. *Catalysis and Zeolites*, New York, Springer-Verlag Berlin Heidelberg.
- Wichterlová, B., Žilková, N., Uvarova, E., Čejka, J., Sarv, P., Paganini, C. & Lercher, J. A. 1999. Effect of Broensted and Lewis sites in ferrierites on skeletal isomerization of n-butenes. *Applied Catalysis A: General*, 182, 297-308.
- Wiedemann, S. C. C., Muñoz-Murillo, A., Oord, R., Van Bergen-Brenkman, T., Wels, B., Bruijninx, P. C. A. & Weckhuysen, B. M. 2015. Skeletal isomerisation of oleic acid over ferrierite: Influence of acid site number, accessibility and strength on activity and selectivity. *Journal of Catalysis*, 329, 195-205.
- Wiedemann, S. C. C., Ristanović, Z., Whiting, G. T., Reddy, M. V. R., Kärger, J., Weitkamp, J., Wels, B., Bruijninx, P. C. A. & Weckhuysen, B. M. 2016. Large Ferrierite Crystals as Models for Catalyst Deactivation during Skeletal Isomerisation of Oleic Acid: Evidence for Pore Mouth Catalysis. *Chemistry – A European Journal*, 22, 199-210.
- Wiedemann, S. C. C., Stewart, J. A., Soulimani, F., Van Bergen-Brenkman, T., Langelaar, S., Wels, B., De Peinder, P., Bruijninx, P. C. A. & Weckhuysen, B. M. 2014. Skeletal isomerisation of oleic acid over ferrierite in the presence and absence of triphenylphosphine: Pore mouth catalysis and related deactivation mechanisms. *Journal of Catalysis*, 316, 24-35.
- Wirth, K. & Barth, A. 2017. *X-Ray Fluorescence (XRF)* [Online]. Available: http://serc.carleton.edu/research_education/geochemsheets/techniques/XRF.html [Accessed 26/May 2017].
- Woodford, C. 2009. *Zeolites. Explainthatstuff* [Online]. Available: <http://www.explainthatstuff.com/zeolites.html> [Accessed].

- Wu, Y., Emdadi, L., Oh, S. C., Sakbodin, M. & Liu, D. 2015. Spatial distribution and catalytic performance of metal–acid sites in Mo/MFI catalysts with tunable meso-/microporous lamellar zeolite structures. *Journal of Catalysis*, 323, 100-111.
- Xia, B., Luo, J., Li, Y., Yang, B., Zhang, S. & Jiang, B. 2017. Preparation of sponge-like porous SiO₂ antireflective coatings with excellent environment-resistance by an acid-catalysed sol–gel method. *RSC Advances*, 7, 26834-26838.
- Yadav, G. D. & Doshi, N. S. 2002. Synthesis of Linear Phenyldecanes by the Alkylation of Benzene with 1-Dodecene over Non-Zeolitic Catalysts. *Organic Process Research & Development*, 6, 263-272.
- Yadav, G. D. & Siddiqui, M. I. N. I. 2009. UDCaT-5: A Novel Mesoporous Superacid Catalyst in the Selective Synthesis of Linear Phenyldecanes by the Alkylation of Benzene with 1-Dodecene. *Industrial & Engineering Chemistry Research*, 48, 10803-10809.
- Yan, Z., Ma, D., Zhuang, J., Liu, X., Liu, X., Han, X., Bao, X., Chang, F., Xu, L. & Liu, Z. 2003. On the acid-dealumination of USY zeolite: a solid state NMR investigation. *Journal of Molecular Catalysis A: Chemical*, 194, 153-167.
- Young, D. A. 1967. *Hydrocarbon conversion process and catalyst comprising a crystalline alumino-silicate leached with sodium hydroxide* United States Patent Office 3326797 patent application.
- Yuan, H.-K., Cao, Z.-Y. & Ren, J. 2011. *Kinetics of Benzene Alkylation with Long Chain Olefin over Solid Acid Catalyst*.
- Yuan, X.-D., Park, J.-N., Wang, J., Lee, C. & Park, S.-E. 2002. Alkylation of benzene with 1- dodecene over usy zeolite catalyst: Effect of pretreatment and reaction conditions. *Korean Journal of Chemical Engineering*, 19, 607-610.
- Yue, Y.-H., Tang, Y., Liu, Y. & Gao, Z. 1996. Chemical Liquid Deposition Zeolites with Controlled Pore-Opening Size and Shape-Selective Separation of Isomers. *Industrial & Engineering Chemistry Research*, 35, 430-433.
- Zachariou, A., Hawkins, A., Lennon, D., Parker, S. F., Suwardiyanto, Matam, S. K., Catlow, C. R. A., Collier, P., Hameed, A., Mcgregor, J. & Howe, R. F. 2019. Investigation of ZSM-5 catalysts for dimethylether conversion using inelastic neutron scattering. *Applied Catalysis A: General*, 569, 1-7.
- Zhang, H., Kim, Y. & Dutta, P. K. 2006. Controlled release of paraquat from surface-modified zeolite Y. *Microporous and Mesoporous Materials*, 88, 312-318.

- Zhang, H., Shao, S., Xiao, R., Shen, D. & Zeng, J. 2014. Characterization of Coke Deposition in the Catalytic Fast Pyrolysis of Biomass Derivates. *Energy & Fuels*, 28, 52-57.
- Zhang, J., Chen, B., Li, C., Zhu, Z., Wen, L. & Min, E. 2003. Kinetics of benzene alkylation with 1-dodecene over a supported tungstophosphoric acid catalyst. *Applied Catalysis A: General*, 249, 27-34.
- Zhang, K., Fernandez, S., O'brien, J., Kobaslija, S. & Ostraat, M. 2017. *Organotemplate-free synthesis of hierarchical beta zeolites*.
- Zhang, K. & Ostraat, M. L. 2016. Innovations in hierarchical zeolite synthesis. *Catalysis Today*, 264, 3-15.
- Zhao, Y., Wang, G., Li, W. & Zhu, Z.-L. 2006. Determination of reaction mechanism and rate constants of alkaline hydrolysis of phenyl benzoate in ethanol–water medium by nonlinear least squares regression. *Chemometrics and Intelligent Laboratory Systems*, 82, 193-199.
- Zheng, S., Heydenrych, H. R., Jentys, A. & Lercher, J. A. 2002. Influence of Surface Modification on the Acid Site Distribution of HZSM-5†. *The Journal of Physical Chemistry B*, 106, 9552-9558.
- Zhou, B., Yu, L., Song, H., Li, Y., Zhang, P., Guo, B. & Duan, E. 2015. Adsorption and oxidation of SO₂ in a fixed-bed reactor using activated carbon produced from oxytetracycline bacterial residue and impregnated with copper. *Journal of the Air & Waste Management Association*, 65, 165-170.
- Zhou, F., Gao, Y., Wu, G., Ma, F. & Liu, C. 2017. Improved catalytic performance and decreased coke formation in post-treated ZSM-5 zeolites for methanol aromatization. *Microporous and Mesoporous Materials*, 240, 96-107.
- Zhou, W., Apkarian, R., Wang, Z. L. & Joy, D. 2006. Fundamentals of scanning electron microscopy (SEM). *Scanning microscopy for nanotechnology*. Springer.

Appendices

Appendix A

TPD calculation

The number of moles of NH₃ that adsorbed on the acid sites of the zeolite catalyst were calculated by injecting a specific volume (5 cm³) of NH₃ gas into the TPD to calibrate the TCD.

$$n = \frac{PV}{RT}$$

Where;

n = number of moles of NH₃

P = atmospheric pressure

V = volume of NH₃ injected

R = gas constant; 8.314 J mol⁻¹ K⁻¹

T = injection temperature; 303.15 K

Therefore:

$$n = \frac{101300 \text{ (pa)} * 5 \times 10^{-6} \text{ (m}^3\text{)}}{303.15 \text{ (K)} * 8.314 \text{ (J mol}^{-1}\text{K}^{-1}\text{)}} = 2.01 \times 10^{-4} \text{ mol}$$

The injection step was repeated several times and each time the signal reading was recorded as shown in Figure A.1.

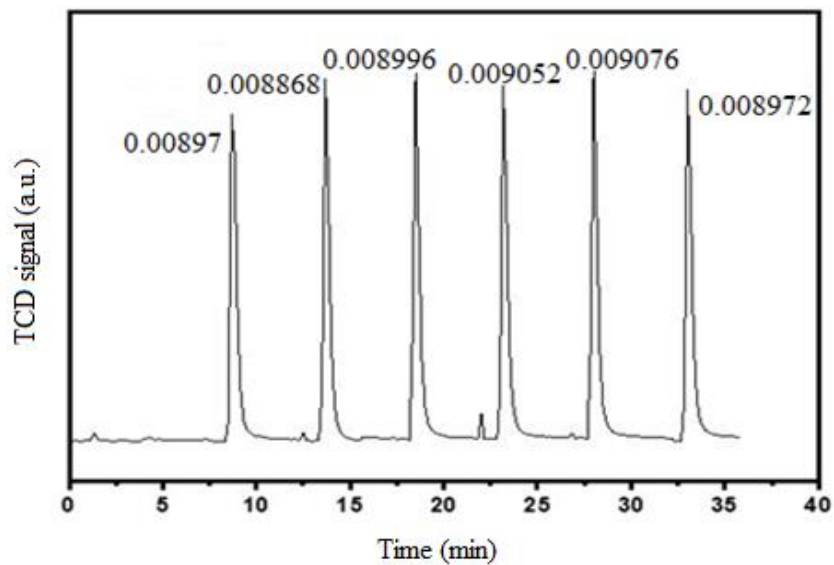


Figure A.1. TPD Calibration curve for NH_3

The acidity can then be calculated from the number of moles of NH_3 and the average of the TCD signal according to:

$$\frac{n}{A_{av}} = \frac{2.01 \times 10^{-4}}{0.008989} = 0.0224$$

Therefore;

$$\text{Acidity} = \frac{\text{Peak area} * 0.0224}{\text{Weight of zeolite catalyst}}$$

Appendix B

Calculation the molarity of acid leaching

The acid aqueous solution that used in the acid leaching modification was hydrochloric acid with purity 37%. In other words, 37 g of hydrochloric acid are dissolved in 100 g of water.

Where the density (ρ) of $\text{H}_2\text{O} = 1 \text{ g cm}^{-3}$; thus, $100 \text{ g}_{\text{H}_2\text{O}} \equiv 100 \text{ ml}_{\text{H}_2\text{O}} = 0.1 \text{ L}_{\text{H}_2\text{O}}$

Molecular weight of hydrochloric acid is $36.46 \text{ g}\cdot\text{mol}^{-1}$; thus, the number of mole of $\text{HCl} = 37 \text{ g} / 36.46 \text{ g}\cdot\text{mol}^{-1} \approx 1.015 \text{ mol}$

The molarity of acid aqueous solution = $1.015 \text{ mol}_{\text{HCl}} / 0.1 \text{ L}_{\text{H}_2\text{O}} = 10.15 \text{ M}$

Molarity of acid solution = Normality (N) = 10.15 N.

To calculate the less concentrated aqueous solution, the equation below can be used to this purpose:

$$C_1 \times V_1 = C_2 \times V_2$$

C_1 = the initial concentration,

V_1 is the initial volume,

C_2 is the final concentration and

V_2 is the final volume.

Therefore, $C_1 = 10.15 \text{ N}$, $C_2 = 10^{-4} \text{ N}$ and $V_2 = 1000 \text{ ml}$.

$10.15 \times V_1 = 0.0001 \times 1000$, Thus $V_1 \approx 0.01 \text{ ml}$.

According to this result, the volume which used from the HCl (10.15 M) to make 1000 ml from acid solution has a 10^{-4} M is:

$$0.01 \times 1000 = 10 \text{ ml}.$$

Appendix C

Calculation the molarity of base leaching

Sodium hydroxide (97%) was used to form alkaline aqueous solution. This means; each 100 g sodium hydroxide has 97 g sodium hydroxide.

Molecular weight of sodium hydroxide is $39.997 \text{ g}\cdot\text{mol}^{-1}$

To calculate molarity of the mixture of 0.5 g of sodium hydroxide with (97%) dissolved with 500 ml water, the following equation can be done this:

$$\text{Molarity} = \frac{\text{amount of NaOH} \times \text{purity of NaOH}}{\text{molecular weight of NaOH} \times \text{amount of water}}$$

$$\text{Molarity} = \frac{0.5 \text{ g}_{\text{NaOH}} \times 0.97}{39.997 \text{ g}\cdot\text{mol}^{-1} \times 0.5 \text{ L}_{\text{H}_2\text{O}}} = 0.0243 \approx 0.025 \text{ M}$$

Appendix D

D.1 Steps of determining of kinetic parameters

- 1- Choosing several rate constant values stochastically as shown in Table D.1 according to the range provided from the previous literature.
- 2- Using the chosen values to calculate the predicted concentrations for all 24 experiments, as shown in Table D.2.
- 3- Comparing the predicted concentrations (Table D.2) and experimental concentrations (Table 7.1) for all experiments as shown in Figure 7.14 to Figure 7.19, then predicting the error percentage for both experimental and predicted according to their concentrations and thereby obtaining the Mean Relative Error (MRE) for all experiments, as shown in Table D.3.
- 4- This process continues by partially changing the rate constant values which were already chosen in Table D.1 and then calculating the MRE for the new values. All the steps above are then repeated until an acceptable range of error is reached.

Table D.1. Reaction constants

No.	A_0 (min^{-1})	E_a (kJ mol^{-1})
1	78.3	15.3
2	47.4	11.9
3	$39 \cdot 10^{+5}$	94.2
4	$77.8 \cdot 10^{+8}$	181.1
5	12.1	19.5
6	61.5	23.7
7	$5 \cdot 10^{-5}$	11.4
8	$55.5 \cdot 10^{+4}$	11.4
9	66.2	25.3
10	$16.2 \cdot 10^{+8}$	136
11	$7 \cdot 10^{-3}$	99
12	$12.7 \cdot 10^{+9}$	110
13	218.9	28.5
14	$62 \cdot 10^{+10}$	186.2
15	$3 \cdot 10^{-3}$	99.9
16	$23 \cdot 10^{+9}$	133.7
17	245.3	30.2
18	$71.4 \cdot 10^{+6}$	23.2
19	$13.1 \cdot 10^{+6}$	122.2
20	$29.1 \cdot 10^{+7}$	59.7
21	137.6	131.7
22	$44.2 \cdot 10^{+10}$	156.9
23	$29.2 \cdot 10^{+8}$	183.7
24	$92.2 \cdot 10^{+8}$	126.5
25	$37.8 \cdot 10^{+8}$	182.5
26	$28.1 \cdot 10^{+6}$	104.4
27	467.6	129.2
28	$36.7 \cdot 10^{+9}$	41.6
29	7415.4	40.3
30	$22.8 \cdot 10^{+14}$	71.4

Table D.2. Predicted Results

No.	1-H	2-H	3-H	2HT	3HT	4HT
1	4.05E-04	1.99E-04	6.23E-05	0.000154	7.32E-05	3.90E-06
2	2.84E-04	1.40E-04	7.93E-05	0.000259	0.000125	9.34E-06
3	2.04E-04	1.01E-04	8.02E-05	0.000333	0.000162	1.45E-05
4	1.50E-04	7.39E-05	7.39E-05	0.000387	0.000189	1.89E-05
5	1.12E-04	5.54E-05	6.44E-05	0.000427	0.000209	2.26E-05
6	8.53E-05	4.21E-05	5.36E-05	0.000457	0.000224	2.56E-05
7	3.59E-04	1.82E-04	6.69E-05	0.000189	9.62E-05	5.03E-06
8	2.29E-04	1.16E-04	7.80E-05	0.000304	0.000158	1.12E-05
9	1.51E-04	7.70E-05	7.25E-05	0.000379	0.000198	1.66E-05
10	1.03E-04	5.26E-05	6.09E-05	0.000429	0.000225	2.11E-05
11	7.21E-05	3.69E-05	4.76E-05	0.000464	0.000243	2.46E-05
12	5.15E-05	2.64E-05	3.54E-05	0.000488	0.000256	2.71E-05
13	3.11E-04	1.63E-04	6.98E-05	0.000225	0.000123	6.17E-06
14	1.77E-04	9.30E-05	7.36E-05	0.000347	0.000192	1.30E-05
15	1.06E-04	5.60E-05	6.14E-05	0.000418	0.000233	1.88E-05
16	6.66E-05	3.52E-05	4.53E-05	0.000461	0.000258	2.35E-05
17	4.32E-05	2.29E-05	3.08E-05	0.000489	0.000274	2.68E-05
18	2.84E-05	1.51E-05	1.97E-05	0.000507	0.000284	2.85E-05
19	2.62E-04	1.42E-04	7.08E-05	0.000262	0.000153	7.31E-06
20	1.31E-04	7.11E-05	6.63E-05	3.85E-04	2.27E-04	1.50E-05
21	7.06E-05	3.85E-05	4.79E-05	4.48E-04	2.65E-04	2.14E-05
22	4.05E-05	2.22E-05	2.99E-05	4.83E-04	2.87E-04	2.63E-05
23	2.38E-05	1.30E-05	1.68E-05	5.03E-04	2.99E-04	2.91E-05
24	1.38E-05	7.55E-06	8.89E-06	5.15E-04	3.07E-04	2.99E-05

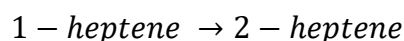
Table D.3. Relative Error

No.	1-H	2-H	3-H	2HT	3HT	4HT
1	4.805	34.646	32.504	3.172	0.460	57.204
2	21.041	21.984	0.109	2.457	8.798	16.251
3	9.927	9.594	13.833	3.965	5.111	3.899
4	28.658	1.799	14.624	12.916	15.946	0.840
5	20.487	5.831	11.595	8.899	17.603	5.774
6	63.424	13.180	11.966	9.092	21.049	6.144
7	8.607	32.166	24.263	9.994	14.747	56.630
8	3.182	14.968	3.013	14.599	2.560	19.875
9	4.217	0.852	5.617	7.641	1.464	0.596
10	26.529	12.260	6.797	10.296	11.305	2.388
11	13.167	21.885	4.816	6.472	13.134	1.688
12	39.522	31.132	3.704	6.736	20.949	0.612
13	18.838	28.775	16.614	12.712	14.122	53.877
14	10.263	4.310	3.042	6.821	3.892	15.545
15	25.839	14.689	7.328	3.845	0.270	0.320
16	9.442	29.633	0.789	10.248	7.620	2.147
17	6.345	36.949	11.444	7.085	11.800	0.180
18	0.490	51.642	35.100	7.785	16.023	4.211
19	23.241	23.956	11.716	11.912	8.097	50.788
20	24.374	6.141	2.558	0.158	9.792	16.679
21	38.802	29.695	0.034	3.479	1.227	2.672
22	13.006	45.783	16.486	9.547	9.780	3.699
23	25.311	55.469	39.836	9.182	11.366	0.247
24	39.851	69.660	62.711	9.516	13.843	3.227

Mean Relative Error (MRE) = 15.074 %

D.2 Sample of calculation of pseudo-first order reaction

In order to calculate the activation energy, Arrhenius constant and reaction rate, the following equations can be commonly utilised to describe the irreversible alkylation and isomerisation kinetics of the toluene with olefin. The following reaction is chosen as a sample of calculation for one reaction step:



$$R_{re} = k \cdot C_A = -\frac{dC_A}{d\tau} \quad \dots\dots (D.1)$$

By integrating Equation D.1; the following Equation is obtained:

$$-\ln(1 - x) = k \cdot \left(\frac{W}{F}\right) \quad \dots\dots (D.2)$$

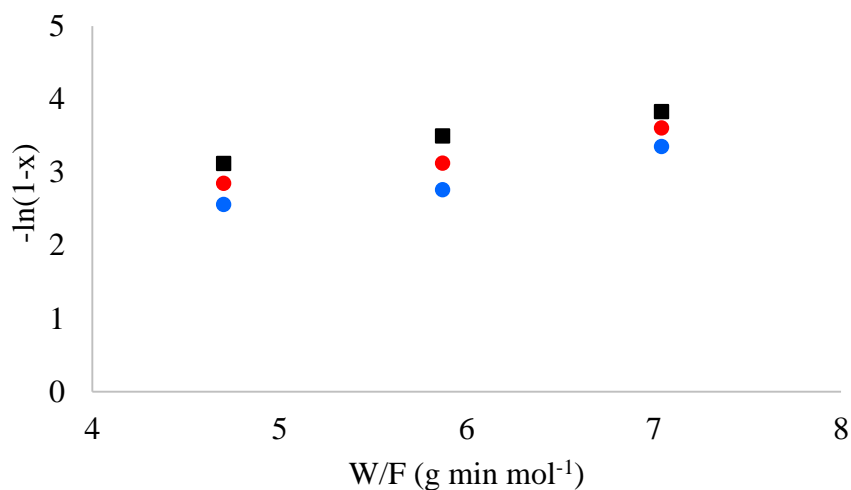


Figure D.1. First order plots for 1-heptene isomerisation to 2-heptene reactions over HY5.1 zeolite catalysts at (●) 70 and (●) 90 °C.

The rate constant (k) is determined from the slope that obtained from Figure D.1:

$$\text{Rate constant } (k) \text{ at } 70 \text{ } ^\circ\text{C} = 0.0051 \text{ mol g}^{-1} \text{ h}^{-1}$$

$$\text{Rate constant } (k) \text{ at } 90 \text{ } ^\circ\text{C} = 0.0056 \text{ mol g}^{-1} \text{ h}^{-1}$$

Using Arrhenius equation:

$$k = A \cdot \exp\left(\frac{-E_a}{RT}\right)$$

Where; $R=8.314 \text{ J mol}^{-1} \text{ K}^{-1}$, both the value of E_a and A could be determined.

Or by plotting the following equation:

$$\ln(k) = \left(\frac{-E_a}{R}\right) \cdot \frac{1}{T} + \ln(A)$$

Temperature (°C)	Temperature (K)	1000/T
70	343	2.915452
80	353	2.832861
90	363	2.754821

Where; $R=8.314 \text{ J mol}^{-1} \text{ K}^{-1}$, from the slope: E_a could be determined.

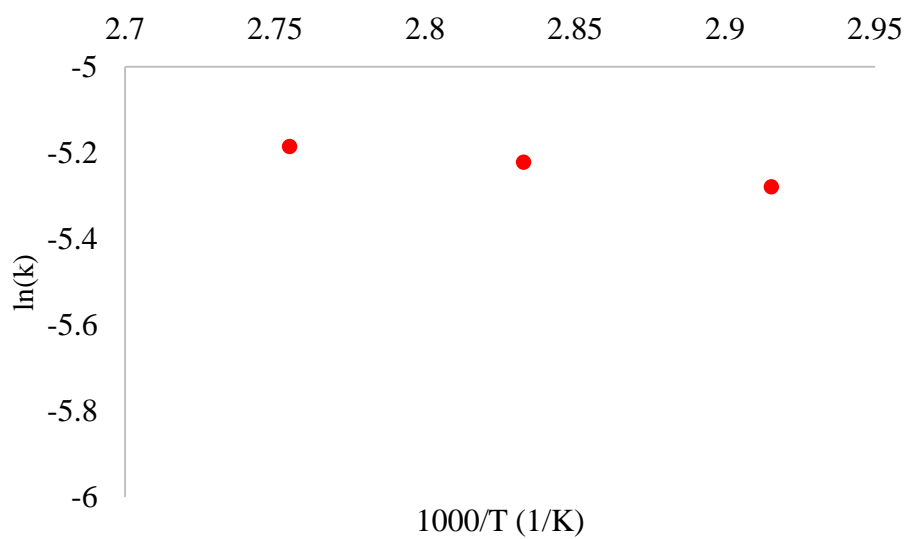


Figure D.2. Arrhenius plots of the isomerisation of 1-heptene to 2-heptene over HY5.1 zeolite catalysts

Appendix E

Conference presentations

Oral presentations

- Postgraduate Research Conference at Chemical and Biological Engineering, *Modified Zeolites for Catalytic Alkylation*, Department, June 2017, The University of Sheffield.
- 25th Canadian Symposium on Catalysis, *Toluene alkylation with 1-heptene: the influence on reaction selectivity of different coke pre-cursors*, May 2018, University of Saskatchewan.

Poster presentations

- Catalysis Day, Chemical and Biological Engineering Department, June 2016, University of Sheffield.
- Postgraduate Research Conference, Chemical and Biological Engineering Department, June 2016, University of Sheffield.

Catalysis and Reaction Engineering Symposium, Department of Chemical and Biological Engineering, May 2017, University of Sheffield.



Toluene alkylation with 1-heptene: the influence on reaction selectivity of different coke pre-cursors

Ali Al-Shathr* and James McGregor

University of Sheffield, Department of Chemical and Biological Engineering,
Sheffield, S1 3JD, UK

*aral-shathr1@sheffield.ac.uk

Introduction

The petrochemical industry relies on heterogeneous catalysts to improve the activity of its processes and selectivity to key products [1]. Although these solid catalysts are applied in several processes, a significant limitation is the formation of heavy by-products, such as coke. However, in addition to coke deposits having a negative impact, recent studies show that different structures of coke can play different roles ranging from deactivation through to enhancing both catalyst activity and selectivity [2]. Pre-coking is an effective method to modify the catalyst surface through the deposition of hydrocarbonaceous material. Through pre-coking with the individual reactant species it is possible to determine the differing influences that coke derived from these pre-cursors has on the reaction and hence gain a greater insight into catalyst operation. Additionally, the use of pre-coking to enhance catalyst selectivity is well-established in petrochemical processing [3].

The aim of present study is to employ reactant pre-coking to understand deactivation and potentially process enhancement in the alkylation of toluene with 1-heptene for the selective production of heptyltoluene over zeolite catalysts. Alkylation reactions are an important class of industrial reactions being used in the production of surfactants and other products.

Materials and Methods

The alkylation of toluene (C₇H₈) with 1-heptene (C₇H₁₄) was carried out in a fixed bed reactor (FBR) at 90 °C for 240 min 0.5 g of zeolite-HY (SiO₂/Al₂O₃=5.1:1), or pre-coked HY, was employed. WHSV was 17 hr⁻¹ and the toluene to 1-heptene ratio was 8:1. Liquid-phase reactants were introduced to the FBR via a peristaltic pump. Pre-coking was conducted by adsorbing 1-heptene and toluene as coke precursors. Toluene was introduced at flowrate of 10 ml hr⁻¹ at 90 °C for 2 h, 1-heptene was introduced at the same temperature and flowrate for 1 h. In all cases an inert nitrogen flow at 30 ml min⁻¹ was used. Various characterisation techniques have been employed to study the fresh and post-reaction catalysts, including: TPO, TGA, FTIR, elemental analysis (CHNS), SEM-EDX, XRD, XRF and nitrogen adsorption measurements.

Results and Discussion

Fig. 1 shows (a) the conversion and (b) the selectivity to 2-heptyltoluene as a function of time-on-stream for the fresh HY catalyst and the catalysts pre-coked with either toluene or 1-heptene. Table 1 details the coke content on the pre- and post-reaction catalysts. TGA data shows that toluene pre-coking deposits significant (~6 wt.%) coke on the catalyst however as Fig. 1 shows this coke has no appreciable effect on conversion of 1-heptene and indeed results in a slight enhancement in selectivity to the desired product. Pre-coking with 1-heptene however shows radically different behavior. The alkene pre-coked catalyst has approximately



the same coke content as the fresh catalyst after 240 min of reaction, however while the fresh catalyst is still active at that time no appreciable conversion is achieved over the pre-coked catalyst it is not selective towards 2-heptyltoluene. The nature of the coke formed from the two reactants is very different. Elemental analysis shows that coke derived from 1-heptene is more polyaromatic (H/C = 0.18) than that derived from the aromatic precursor (H/C = 1.2).

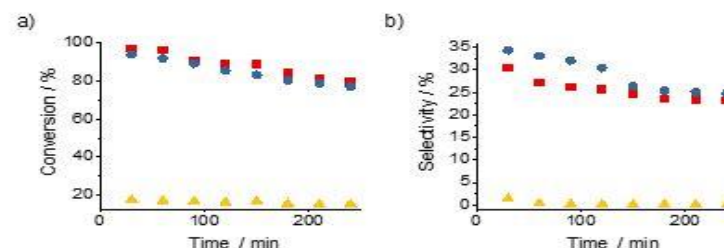


Figure 1. (a) Conversion of 1-heptene, and (b) selectivity to 2-heptyltoluene as a function of time-on-stream for toluene alkylation with 1-heptene over HY (■), HY pre-coked with toluene (●) and HY pre-coked with 1-heptene (▲). Reaction conditions: T=90 °C, liquid flow=10 ml h⁻¹, WHSV=17 h⁻¹, N₂ flowrate =3 0 ml min⁻¹ and zeolite mass= 0.5 g.

Table 1. Elemental analysis indicating H/C mass ratio and TGA showing the coke % after pre-coking via toluene and 1-heptene over 0.5 gm of Y zeolite at 90 °C for 2 and 1 h.

Zeolite	Fresh-HY post-reaction (240 min)	Toluene pre-coked HY (120 min)	Toluene pre-coked HY post reaction (240 min)	1-heptene pre-coked HY (60 min)	1-heptene pre-coked HY post-reaction (240 min)
Coke %	9.8 ± 0.28	5.9 ± 0.26	7.8 ± 0.3	10.2 ± 0.28	9 ± 0.31
H/C	0.23 ± 0	1.2 ± 0.28	0.2 ± 0.01	0.18 ± 0	0.16 ± 0.01

These data clearly show that coke derived from different reactant species has a strikingly different effect on the alkylation reaction. That derived from the aromatic reactant does not induce deactivation and may enhance selectivity, while that derived from the alkene results in a strongly deactivating polyaromatic coke.

References

- VAN BEKKUM, H., FLANIGEN, E. M. & JANSEN, J. C. 2001. *Introduction to Zeolite Science and Practice*, Amsterdam, Elsevier.
- COLLETT, C. H. & MCGREGOR, J. 2015. *Catalysis Science & Technology*.
- BAUER, F., CHEN, W.-H., ZHAO, Q., FREYER, A. & LIU, S.-B. 2001. *Microporous and Mesoporous Materials*, 47, 67-77.